uOttawa

L'Université canadienne
Canada's university

FACULTÉ DES ÉTUDES SUPÉRIEURES ET POSTOCTORALES

uOttawa

L'Université canadienne
Canada's university

FACULTY OF GRADUATE AND POSDOCTORAL STUDIES

Jaime Blais

AUTEUR DE LA THÈSE / AUTHOR OF THESIS

Ph.D. (Biochemistry)

GRADE / DEGREE

Department of Biochemistry, Microbiology and Immunology

FACULTÉ, ÉCOLE, DÉPARTEMENT / FACULTY, SCHOOL, DEPARTMENT

Regulation of Translation during Hypoxic Stress: An Integrated Stress Response

TITRE DE LA THÈSE / TITLE OF THESIS

John Bell

DIRECTEUR (DIRECTRICE) DE LA THÈSE / THESIS SUPERVISOR

CO-DIRECTEUR (CO-DIRECTRICE) DE LA THÈSE / THESIS CO-SUPERVISOR

EXAMINATEURS (EXAMINATRICES) DE LA THÈSE / THESIS EXAMINERS

Douglas Gray

Luc Sabourin

Hoyun Lee

Michael Ohh

Gary W. Slater

Le Doyen de la Faculté des études supérieures et postdoctorales / Dean of the Faculty of Graduate and Postdoctoral Studies

Regulation of Translation during Hypoxic Stress: An Integrated Stress Response

Jaime D. Blais

Thesis submitted to the Department of Biochemistry, Microbiology and Immunology in partial fulfillment of the requirements for the degree of Doctor of Philosophy

University of Ottawa

Ottawa, Ontario, Canada

Your file Votre référence
ISBN: 978-0-494-25857-6
Our file Notre référence
ISBN: 978-0-494-25857-6

The Paradox of Life:

A bit beyond perception's reach
I sometimes believe I see
that Life is two locked boxes,
Each containing the other's key.

Piet Hein

ACKNOWLEDGEMENTS

This thesis could not have been accomplished without the support and guidance from several significant people.

I would first like to thank my supervisor, Dr. John Bell, who has afforded me so many opportunities over the course of my research in his lab. His outlook on science, life, and friendship has been an inspiration. Over the hurdles and small victories experienced throughout this journey, he has taught me to persist even in the face of opposition.

To my committee, Dr. Martin Holcik, Dr. Christina Addison, and Dr. Bruce McKay for your guidance throughout the course of this research. In times of doubt, you believed, for that I am indebted to you all.

To Grace, Kelley, and Jenn, I thank you for your support and friendship. We have shared so much of our lives with each other; for that I will be eternally grateful. All three of you are strong, compassionate, and talented women, do not stop dreaming and you will undoubtedly realize every aspiration.

To Theresa for your amazing animal skills, this thesis could never have been completed without your assistance. Your hard work and attention to detail are not only recognized, they are applauded.

To my Mom for being a strong female role model in my life. You have instilled in me the drive to excel, the curiosity to try new things, and the desire to succeed.

To my family who have shared this journey with me and for their perpetual encouragement.

To my loving husband Steven who has lived and breathed my PhD whether he was willing to or not. If ever an award of support should be offered, he would be the most gracious recipient. Thank you for your encouragement to follow my dreams wherever they might take us. I can't wait to see what the future has in store for us next, what an adventure it's already been.

ABSTRACT

Oxygen supports the life of all aerobic organisms and virtually every cell type is capable of sensing decreased tissue oxygenation, known as hypoxia. Hypoxic microenvironments have been detected within developing solid tumors as a result of insufficient host vascular delivery of oxygen and nutrients. Consequently, the formation of solid tumors requires the coordination of angiogenesis: the recruitment of blood vessels for the purpose of tumor vascularization. Furthermore, clinical and experimental evidence have demonstrated that hypoxic cells in solid tumors can limit the efficacy of standard anticancer therapeutics including radiotherapy and chemotherapy. Low oxygenation can also accelerate malignant progression and metastasis resulting in poorer prognosis irrespective of the chosen treatment regiment.

It is the focus of our research to improve our understanding of the molecular events that support the development of tumor cell resistance to hypoxia as a tool for the discovery of effective therapeutics that can specifically and effectively target hypoxic tumors. Understanding exactly how tumor cells adapt to transient hypoxia could lead to the identification of novel therapeutic targets that in combination therapy with current anticancer treatments could help reduce the incidence of morbidity and mortality from cancer.

TABLE OF CONTENTS

LIST OF FIGURES

CHAPTER 1: INTRODUCTION

CHAPTER 2: Activating Transcription Factor 4 is Translationally Regulated by Hypoxic Stress

CHAPTER 3: Perk-dependent translational regulation promotes tumor cell adaptation and angiogenesis in response to hypoxic stress

LIST OF TABLES

LIST OF ABBREVIATIONS

ActD	Actinomycin D
ANOVA	Analysis of variance
APAF-1	Apoptotic protease activating factor 1
ARNT	aryl hydrocarbon receptor nuclear translocator
ATF4	activating transcription factor 4
ATF6	activating transcription factor 6
ATP	Adenosine Triphosphate
βgal	beta-galactosidase
bHLH/PAS	basic helix-loop-helix-containing PER-ARNT-SIM
BiP/Grp78	Immunoglobin binding protein of B cells /Glucose regulated protein 78
bZIP	basic leucine zipper protein
C/EBP	CCAAT/enhancer binding protein
CA12	Carbonic anhydrase 12
CA9	Carbonic anhydrase 9
CAT	Chloramphenicol actyl transferase
CHOP	C/EBP homologous protein
CHX	cycloheximide
COOH	Carboxyl terminus
DBS	Donor bovine serum
DKO	double knock out
DMEM	Dulbecco's modified media
DNA	deoxyribonucleic acid
DRB	5, 6-dichloro-1-beta-D-ribofuranosylbenzimidazole
ECL	Enhanced chemiluminescence
eIF	eukaryotic initiation factor
eIF2α ^{S51D}	phophomimetic mutant of eIF2a
eIF2α^{S51A}	unphosphorylatable knock-in mutant of Eif2a
ELISA	enzyme-linked immunosorbent assay
EMCV	Encephalomyocarditis virus
ER	endoplasmic reticulum
ERO1α	ER oxidase 1-alpha
ERSE	ER stress element
FCS	fetal calf serum
FGF2	Fibroblast growth factor 2
GADD34	growth arrest and DNA damage inducible protein 34
GAPDH	Glyceraldehyde-3-phosphate dehydrogenase
GDP	Guanice diphosphate
Glut-1	glucose transporter gene
GTP	Guanine triphosphate
Hdmec	Human microdermal endothelial cells
Huvec	Human umbilical vessel endothelial cells
HIF1	Hypoxia Inducible Factor 1
HLH/PAS	helix-loop-helix/PER-ARNT-SIM
HRE	Hypoxia regulatory element
IGFBP4	insulin growth factor binding protein 4
IRES	internal ribosome entry sequence
ISR	integrated stress response

MEF	mouse embryonic fibroblast
Met-tRNA	methionyl-initiator tRNA
MMP13	matrix melloproteinase 13
mRNA	messenger RNA
mTOR	mammalian target of rapamycin
OD	optical density
ODC	Ornithine decarboxylase
ODD	oxygen degradation domain
PARP	poly(ADP-ribosyl)ation protein
PBS	phosphate buffered solution
PCR	polymerase chain reaction
PDGF	Platlet Derived Growth Factor
PERK/PEK	pancreatic ER kinase or PKR-like ER kinase
PERKΔC	Catalytically inactive COOH-truncated mutant of PERK
PHD	prolyl hydroxylase
pO_2	partial pressure of oxygen
PP1	protein phosphatase 1
Puro	puromycin
pVHL	von Hippel Lindau protein
Q-PCR	quantitative PCR
RA	Rheumatoid Arthritis
RNA	ribonucleic acid
RT-PCR	Reverse transcription PCR
S.E.M.	Standard error of the mean
SCID	severe combined immuno deficiency
SDS	sodium dodecyl sulfate
Tg	thapsigargin
Tn	tunicamycin
tRNA	transfer RNA
uORF	upstream open reading frame
UPR	unfolded protein response
UTR	untranslated region
UV	ultraviolet
VCIP	VEGF and Collagen type I inducible protein
VEGF	Vascular Endothelial Growth Factor
VSV	Vesicular stomatitis virus
XBP1	X-box binding protein1
XIAP	X-linked inhibior of apoptosis

1. INTRODUCTION

1.1 Tumor Hypoxia

Tumor hypoxia, regions of low oxygen tension within the tumor microenvironment, results from an imbalance in oxygen supply and consumption. Tumor hypoxia was postulated over 50 years ago by Thomlinson and Gray, who made the observation of the distribution of necrosis relative to blood vessels [1]. Since the late 1980's, the introduction of a commercially available oxygen electrode (Eppendorf), has facilitated the accurate measurement of oxygen levels within the tumor microenvironment. A convincing body of evidence now reveals that reduced oxygen tensions are a common feature of human solid tumors [2]. In a study of human breast cancer the median tumor oxygen partial pressure (pO_2) was measured at 28mmHg vs 65mmHg reported within normal breast tissue. One-third of these patients had pO_2 measurements in the range considered severe hypoxia (<2.5mmHg). Regions of severe hypoxia have been reported in numerous cancer types including, head and neck cancer, breast cancer, cervical cancer, soft tissue sarcoma, and melanoma. It is now considered the most significant factor in explaining poor patient prognosis [3].

The calculated distance that oxygen diffuses as it passes from the capillary into the cells before being completely metabolized is 180μm. Solid tumors larger than $1mm^3$ must therefore rely on the development of new blood vessels to support the energy and nutrient demands of a developing tumor. Limited oxygen diffusion within the tumors is termed "chronic" hypoxia, as the uncontrolled proliferation causes tumors to outgrow the available blood supply and hence their source of oxygen and nutrients. As a result, the angiogenic stimulus in tumors results in the outgrowth of new blood vessels from the

existing vasculature, with the consequence of developing aberrant blood vessels. Whereas normal vasculature is organized in a hierarchical manner with vessels close enough to allow for adequate nutrient and oxygen supply to all cells, tumor vessels are chaotic, dilated, and torturous resulting in sluggish and insufficient blood flow. In addition to "chronic" hypoxia, temporary occlusions or reduced blood flow in certain vessels results in "acute" or perfusion limited hypoxia, however closed vessels can be reopened, leading to reperfusion of hypoxic tissue with oxygenated blood.

1.2 Hypoxia Induced Resistance to Standard Anti-Cancer Therapeutics

1.2.1 Radiation Resistance in Hypoxic Cells

It has been appreciated for over 50 years that severe hypoxia can protect cells from killing by radiotherapy and recent studies have demonstrated that this does indeed, impact on clinical outcome: better oxygenated tumors respond better to radiation therapy [4-6].

Radiation resistance of hypoxic cells is due primarily to the role of oxygen in radiation damage. Ionizing radiation, such as that used in radiotherapy, induces cell death mainly through the production of DNA damage due to its ability to form free radicals in DNA. An oxidizing environment, primarily determined by the presence of oxygen, rapidly reacts with the free electron. This acts to "fix" the DNA damage, making the radiation damage permanent. In the absence of an oxidizing environment, free radicals are likely to be neutralized by the donation of a hydrogen atom from a sulfhydryl-containing compound allowing time for DNA repair, avoiding cell death. Thus the dose of radiation required to cause the same amount of cell death under hypoxic stress relative to aerobic conditions is on

average 2- to 3-fold higher. Radiation resistance in cells begins when oxygen levels are less than 10mmHg, however levels below 3mmHg give rise to extreme resistance to radiation therapy. The results of numerous studies have now unequivocally demonstrated that the extent of tumor hypoxia has a negative impact on the ability of radiotherapy to locally control tumors, because of the resistance of hypoxic cells to killing by radiation [4, 5].

Recently, in a study of 397 cases of head and neck cancer, Nordsmark *et al.,* demonstrated that tumor hypoxia below 2.5mmHg was the most significant factor in explaining poor patient prognosis. Furthermore, their prognostic model demonstrated that patients with severely hypoxic tumors (<2.5mmHg) had a 5-year survival rate between 0-20%, approaching 0% in cases reported to contain the most severe hypoxic tumors [3].

1.2.2 Hypoxia Induced Resistance to Chemotherapy

Studies using both animal tumor spheroids and human tumor xenographs support that chemoresistance is in part mediated by tumor hypoxia despite the absence of any clinical studies that report the correlation between tumor hypoxia and resistance to chemotherapy. A number of factors associated either directly or indirectly with tumor hypoxia have been demonstrated to contribute to resistance to anti-cancer drugs.

i) Chemotherapeutic drugs are delivered through the blood stream. Due to their increased distance from the vasculature, hypoxic cells are not adequately exposed to some types of anticancer drugs [7, 8]. Additionally, the action of some anticancer agents requires oxygen to increase their cytotoxicity, including bleomycin and neocarzinostatin [9, 10].

ii) A combination of hypoxia and nutrient deprivation causes cells to slow their rate of proliferation through the cell cycle or stop cell cycle progression altogether, most commonly at G_1/S [11]. Since most anticancer drugs are more effective against rapidly proliferating cells then slowly or non-proliferation cells, hypoxic cells are insufficiently targeted by these agents [12-14]. Thus as the cell cycle slows, and distance from the vasculature increases, the efficiency of cell killing by chemotherapy drugs decreases.

iii) Genes involved in drug resistance are up-regulated in response to hypoxic stress, including p-glycoprotein. This protein, localized to the cell membrane, is able to actively pump many drugs including anti-cancer agents out of the cell, thereby, decreasing the therapeutic dose delivered to the cell and increasing resistance to other anticancer therapeutics [15].

iv) Hypoxic stress provides a physiological pressure that selects for cells that have lost their apoptotic potential; in particular for cells acquiring mutations to p53 [16], predisposing them to a more malignant phenotype.

1.2.3 Tumor Hypoxia Increases Malignant Progression and Metastasis

Genetic instability is a hallmark of malignant progression. Large deletions, insertions, translocations and recombinations at the chromosome level and point mutations including simple frameshift mutations at the DNA level can be attributed to the progression of the disease. Hypoxic stress and the tumor microenvironment have been demonstrated to initiate genetic instability. Reynolds *et al.*, using a tumorigenic cell line expressing a chromosomally located lambda phage shuttle vector, reported that cells cultured under hypoxic stress or as

xenograft tumors in nude mice had a 5-fold higher frequency in their mutation rate than cells cultured under normoxic conditions [17]. Moreover, hypoxia is an independent and highly significant prognostic factor, predisposing tumors to metastatic spread. In a study of 103 patients with advanced cancers of the uterine cervix, 50% of patients were diagnosed with hypoxic tumors with pO_2 levels <10mmHg. Patients with hypoxic tumors had significantly lower disease free and overall survival probabilities with increased occurrence of metatastic spread irrespective of their treatment regiment [18].

Resistance to radiation and chemotherapy manifested by hypoxic stress means that neither form is uniformly effective against a significant population of solid tumor cells, demonstrating the necessity for novel anti-cancer therapeutics that can exploit the unique physiology of hypoxic tumors.

1.3 Cellular Adaptation to Hypoxic Stress

Accumulating evidence implicates the biological response to hypoxia and the development of hypoxia tolerance as an important contributor to malignant progression. It appears that the key to cellular survival and adaptation to hypoxia, a stress that results in the impairment of ATP production by the lack of oxidative phosphorylation, includes reallocating the available cellular energy from non-essential to essential processes. This process, known as oxygen conformance involves reducing the energy demand of the cell in response to a decline in oxygen while minimally affecting the intracellular concentration of ATP. In the hypoxic cell, this is accomplished by several mechanisms including the regulation of energy homeostasis by switching from aerobic metabolism to anaerobic glycolysis. Additionally, tumor cells respond to hypoxic stress by stimulating

angiogenesis to increase tumor oxygenation. This process, named the "angiogenic switch" has been suggested as one of the key six hallmarks of cancer [19]. Lastly, a major biological response to hypoxia includes the inhibition of energy demanding processes including protein translation, RNA/DNA synthesis, and cell proliferation.

1.3.1 HIF-1α and the Regulation of Gene Expression

The transcriptional response to hypoxia is mediated in large part by a single oxygen regulated transcription factor, HIF-1, which modulates the expression of a large number of genes critical to the adaptive response to hypoxic stress. These pathways include the induction of glycolytic enzymes and glucose transporters which mediate the switch to energy saving glycolysis, while angiogenic genes, including Vascular Endothelial Growth Factor (VEGF) and Platelet Derived Growth Factor (PDGF), are induced to promote improved oxygen delivery to regions of low oxygen. To further counteract the detrimental effect of a low oxygen environment, vasodilators like nitric oxide synthase and genes involved in erythrocyte production, including erythropoietin and transferrin receptors, are induced by HIF-1 to enhance the oxygen carrying capacity of the blood.

The HIF-1 transcription factor is a heterodimer of two proteins; the constitutively expressed HIF-1β/ARNT and the oxygen regulated HIF-1α; both belong to the basic helix-loop-helix (HLH/PAS) family of transcription factors. Although HIF-1α mRNAs are stable under normoxic conditions, the protein is rapidly degraded by the proteasome in the presence of oxygen. This regulation is imparted by a highly conserved binding domain, the oxygen-dependent degradation domain (ODD), that is recognized by an E3 ubiquitin ligase, von

Hippel-Lindau protein (pVHL), which is responsible for the ubiquitination of HIF-1α; an act that targets the protein for proteasomal degradation. This interaction is regulated by the hydroxylation of two conserved proline residues (Pro-402 and Pro-564) within the ODD of HIF-1α by specific HIF-1α prolyl hydroxylases (PHD) [20, 21]. Since oxygen is required for prolyl hydroxylation, hypoxia prevents this modification impairing the ability of VHL to bind and ubiquitinate HIF-1α. As a consequence, HIF-1α is stabilized and translocates into the nucleus, where it dimerizes with HIF-1β/ARNT and binds the core DNA sequence 5'-RCGTG-3', known as the hypoxia response element (HRE) leading to the transcriptional regulation of up to 60 putative genes.

Complete deficiency of HIF-1α results in embryonic lethality at mid-gestation, a consequence of dramatic vascular regression due to extensive endothelial cell death [22, 23]. The importance of HIF-1α in tumor development is underscored by the observation that HIF-1α$^{-/-}$ tumors, when injected into nude mice, display impaired vascular development and delayed growth when compared to wild type tumors[24, 25]. Moreover, HIF-1α is overexpressed in a broad range of human cancers [26-28], and is furthermore associated with poor patient prognosis. HIF-1α overexpression has been correlated with tumor grade and increased metastatic potential [29-31].

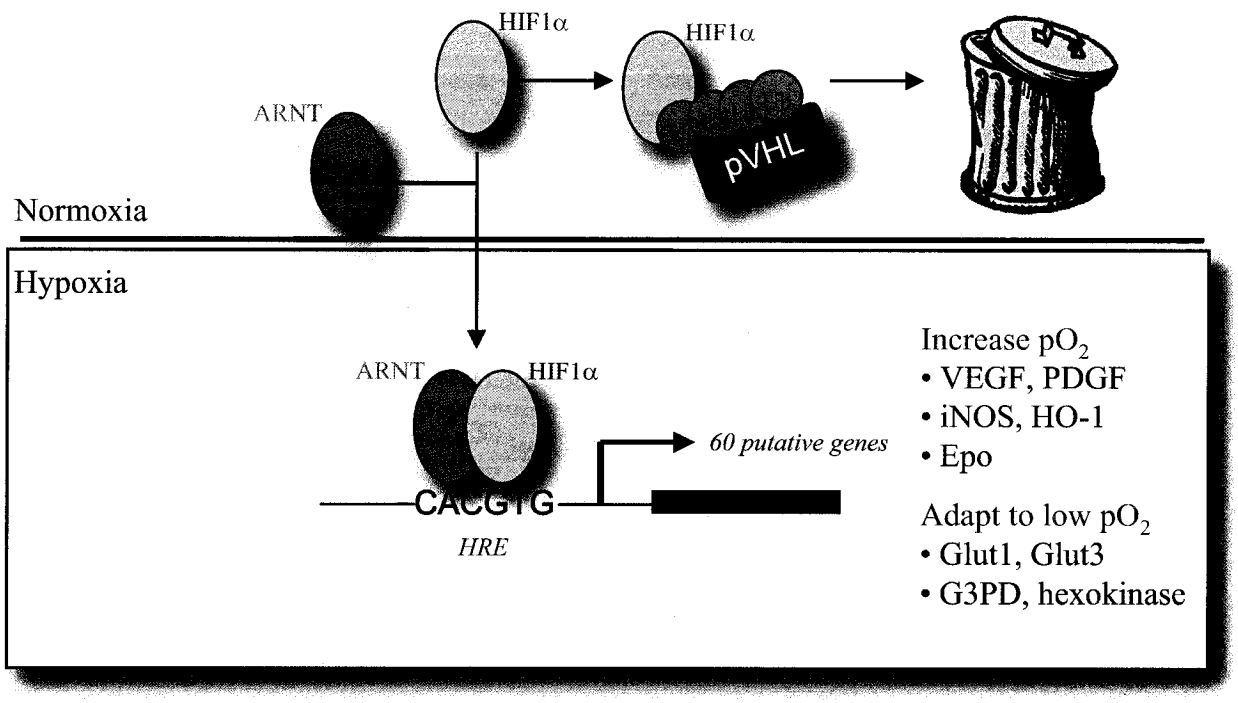
HIF1α
HIF1α
ARNT
pVHL
Normoxia
Hypoxia
ARNT
HIF1α
60 putative genes
CACGTG
HRE
Increase pO_2
• VEGF, PDGF
• iNOS, HO-1
• Epo
Adapt to low pO_2
• Glut1, Glut3
• G3PD, hexokinase

Figure 1: Regulation of HIF1α

Under normoxic conditions (top), two proline residues within the ODD of HIF1α are hydroxylated by the PHD family of prolyl hydroxylases, allowing for recognition by the E3 ubiquitin ligase, pVHL. Ubiquitination promotes the proteasomal degradation of the HIF1α subunit. Under conditions of hypoxic stress (bottom) prolyl hydroxylases are blocked, promoting the stabilization of the HIF1α subunit which translocates to the nucleus and heterodimerizes with the constitutively expressed ARNT subunit to form the active transcription factor HIF1. Together, HIF1 promotes transcriptional regulation through the recognition of an HRE consensus sequence proximal to the promoter of target genes. To date approximately 60 putative HIF1 target genes have been identified. Target genes induced by HIF1 are involved in the adaptive response to hypoxic stress through the upregulation of critical metabolic gene products including glycolytic enzymes and glucose transporters that mediate the switch from aerobic metabolism to anaerobic glycolysis. While other genes are involved in escaping the hostile hypoxic microenvironment by increasing oxygen delivery to the cells through increased angiogenesis, vasodilation, and red blood cell development.

Although oxygen is the principal regulator of HIF-1α, this protein can also be activated in response to oncogenic pathways. A classic genetic lesion in hemangioblastoma and clear cell renal carcinoma is the functional inactivation of the tumor suppressor VHL. Von Hippel Lindau syndrome, which is characterized by highly angiogenic tumors, results in the defective ubiquitination of HIF-1α under normoxic conditions, leading to aberrant HIF-1α expression and its target genes (**Figure 1**). Such mutations increase the potential for angiogenesis likely through continuous synthesis of pro-angiogenic proteins like VEGF. Studies where exogenous wild-type VHL were restored in 786-O renal cell carcinomas, resulted in re-established oxygen-dependent degradation of HIF-1α and significantly slower tumor growth in a xenograft model [32].

In addition to the various biological processes that are influenced by the transcriptional regulation of HIF-1, one target in particular is critical to tumor growth and angiogenesis. VEGF is capable of inducing endothelial cell proliferation and is therefore one of the most important angiogenic growth factors relevant to tumor growth and metastasis. It has been proposed that hypoxia-induced VEGF expression precedes an invasive phenotype based on observations that VEGF expression increases through the neoplastic progression of colon carcinoma [33]. This concept is further supported by findings that VEGF expression in metastatic melanomas is higher than in the primary lesion [34]. The importance of VEGF expression during tumor development is revealed by its mechanisms of regulation. The presence of an HRE within the promoter of VEGF ensures its transcriptional activation by HIF-1α during hypoxic stress. However,

elements within its 5' and 3' untranslated regions (UTRs) mediate its post-transcriptional regulation. Within its 3'UTR, five AU-rich elements have been identified. The RNA binding protein, HuR, has been demonstrated to bind and stabilize the VEGF mRNA, however others have demonstrated that elements within the 5'UTR may contain additional elements that lead to the hypoxia induced stability of VEGF mRNAs [35, 36]. The presence of an internal ribosome entry site (IRES) has been identified within the 5'UTR of VEGF, thereby providing a translational advantage to VEGF mRNAs when translation is inhibited and competition for initiation factors is high [37-39].

1.3.2 Regulation of Translation

The rapid and sustained inhibition of protein translation is a less well understood biological response to hypoxic stress. In response to extreme hypoxia, protein synthesis is decreased by 60-70% within 1 hr [40], remains significantly repressed for up to 24 hrs of hypoxia [41], and is completely reversible upon re-oxygenation. In addition to the promotion of hypoxia tolerance through the conservation of energy, the control of mRNA translation is increasingly being viewed as a means of rapidly changing the cellular proteome by controlling the translational efficiency of individual mRNAs essential for the development of hypoxia tolerance. The control of translation is critical in regulating numerous other physiological processes including, growth stimulation [42], cell cycle progression [43], differentiation [44], ER stress [45], oncogenic signaling [46], and viral infection [47]. The importance of translational regulation on gene expression during oncogenic transformation was demonstrated recently by Rajasekhar *et al.* using microarray analysis of polysome-associated mRNAs upon the activation of

Ras and AKT pathways. Their analysis revealed that larger translational changes resulted from activation of oncogenic pathways than transcriptional changes in gene expression. Translational regulation can occur during any of the three stages of translation including initiation, elongation, and termination. However, translation initiation is by far the most complex and highly regulated process in protein synthesis.

1.3.3 Translation Initiation

The majority of translation initiation requires the assembly of an active eukaryotic initiation factor 4F (eIF4F) complex at the m^7GpppN cap structure present at the 5'terminus of the mRNA, a process referred to as "cap-dependent" translation initiation. Formation of the eIF4F complex is a major control point in the regulation of translation initiation and involves the concerted recruitment of numerous initiation factors for the formation of the 48S pre-initiation complex. The eIF4F complex includes the m^7GpppN binding protein, eIF4E, an ATP dependent RNA helicase, eIF4A, and a modular scaffolding protein, eIF4G, that bridges the mRNA to the ribosome. Assembly of the eIF4F complex facilitates recruitment of the 43S pre-initiation complex to form the 48S pre-initiation complex. The 43S pre-initiation complex is composed of the small 40S ribosome, the initiation factor eIF3, and the ternary complex which consists of eIF2/GTP and the methionine-loaded initiator tRNA (Met-tRNA). Once formed, the 48S pre-initiation complex is believed to scan the 5'UTR searching for a start codon (AUG). Upon encountering a start codon, in the proper context, eIF5 stimulates the hydrolysis of eIF2/GTP to GDP promoting the release of all initiation factors and

recruitment of the large 60S ribosome. Formation of the 80S ribosome represents the beginning of the elongation step of protein translation (**Figure 2**).

1.4 Translational Control during Hypoxic Stress

Formation of eIF4F and the ternary complex constitute the two major regulatory control points during the initiation of translation. In cancer, alterations in signaling pathways that result in the stimulation of translation have been extensively studied [48]. Over-expression of either eIF4E or an unphosphorylatable mutant of eIF2α (eIF2α^{S51A}), results in malignant transformation likely as a result of deregulated translation of oncogenic mRNAs [48-51].

1.4.1 Regulation of eIF4F

The formation of the eIF4F complex during 'cap-dependent' translation initiation is dependent on the rate-limiting availability of the cap-binding protein, eIF4E. Competitive binding of eIF4E to a family of eIF4E binding proteins (4E-BP1, 4E-BP2, and 4E-BP3) is regulated by sequential phosphorylation of 4E-BPs on five known phosphorylation sites. Upon hyperphosphoryation, 4E-BPs lose their affinity for eIF4E, which preferentially binds eIF4G to induce translation initiation. This mechanism is controlled in large part by the mammalian target of rapamycin (mTOR). In response to hypoxic stress, inhibition of mTOR results in the hypophosphorylation of 4E-BPs which increases their affinity for eIF4E resulting in decreased eIF4E:eIF4G complex formation, and explains in part, the inhibition in translation initiation (**Figure 2**) [52]. Moreover, in response to hypoxic stress, the 4E-T nuclear transporter was demonstrated to mediate re-

localization of eIF4E into the cell nucleus, thereby reducing the availability of eIF4E for the formation of active initiation complexes [41].

1.4.2 Cap-Independent Translational Regulation

IRES (internal ribosome entry site) mediated cap-independent translation can direct ribosome binding proximal or adjacent to the start codon of a given mRNA in the absence of the cap binding protein, eIF4E. IRES mediated translation initiation was first described in picornavirus infection, naturally uncapped mRNAs that are efficiency translated despite a strong inhibition in host mRNA translation [53]. The successive identification of IRES activity in numerous viral genomes pioneered the exploration for IRES activity in cellular mRNAs as well. A study by Johannes *et al.,* in response to poliovirus infection, calculated that as many as 3-5% of cellular mRNAs are translated in a cap-independent mechanism. To date, the list of identified IRES elements in cellular mRNAs is growing exponentially. However, despite this recent progress, comparative analysis of the identified cellular IRES elements has not revealed any consensus sequence or structural similarities that might expedite this process. Instead, the identification of novel IRES elements remains largely empirical. Traditionally, IRES elements have been identified in mRNAs harboring unusually long 5'UTRs (>100bp) or containing a high GC content, however the true test for IRES activity relies on the gold standard bicistronic assay. Numerous studies have identified hypoxia responsive genes that employ IRES elements to maintain their translational priority during translational inhibition, specifically, HIF1α [54], VEGF [37], BiP [55], TIE-2 [56], and ODC [57]. Moreover, a possible connection between eIF2α

phosphorylation and IRES translation has also been proposed. The activities of cat1, PDGF2, VEGF and c-myc have been shown to increase either during differentiation or in response to various cellular stresses that increase the phosphorylation of eIF2α [58, 59]. The importance of IRES mediated translation is revealed by the observation that mRNAs that contain IRES elements encode proteins that play important roles in cell growth, proliferation, differentiation, and in the regulation of apoptosis; cellular programs that are often usurped by malignant cells [60]. This suggests that IRES mediated translation may be an important mechanism utilized by the cell to maintain and induce gene expression in order to mediate cellular adaptation and cell viability when faced with stressful microenvironments.

1.4.3 Regulation of eIF2α

Formation of the ternary complex constitutes the second major control point for the cell in the regulation of translation initiation and is tightly regulated through phosphorylation of the eIF2α subunit on Ser51. Prior to eIF2 binding to Met-tRNA, the inactive eIF2/GDP must be converted to the active eIF2/GTP complex, a reaction that is mediated by the guanine nucleotide exchange factor eIF2B. Upon phosphorylation of eIF2α, eIF2/GDP and eIF2B form a tight inhibitory complex, impeding the exchange of GDP for GTP. As levels of eIF2B are rate limiting, even small amounts of phosphorylated eIF2α result in a significant impairment to eIF2 recycling and 43S pre-initiation complex formation (**Figure 2**). Four different eIF2α kinases, regulated by diverse physiological signals, have been identified in mammalian cells. They include (i) PKR, an

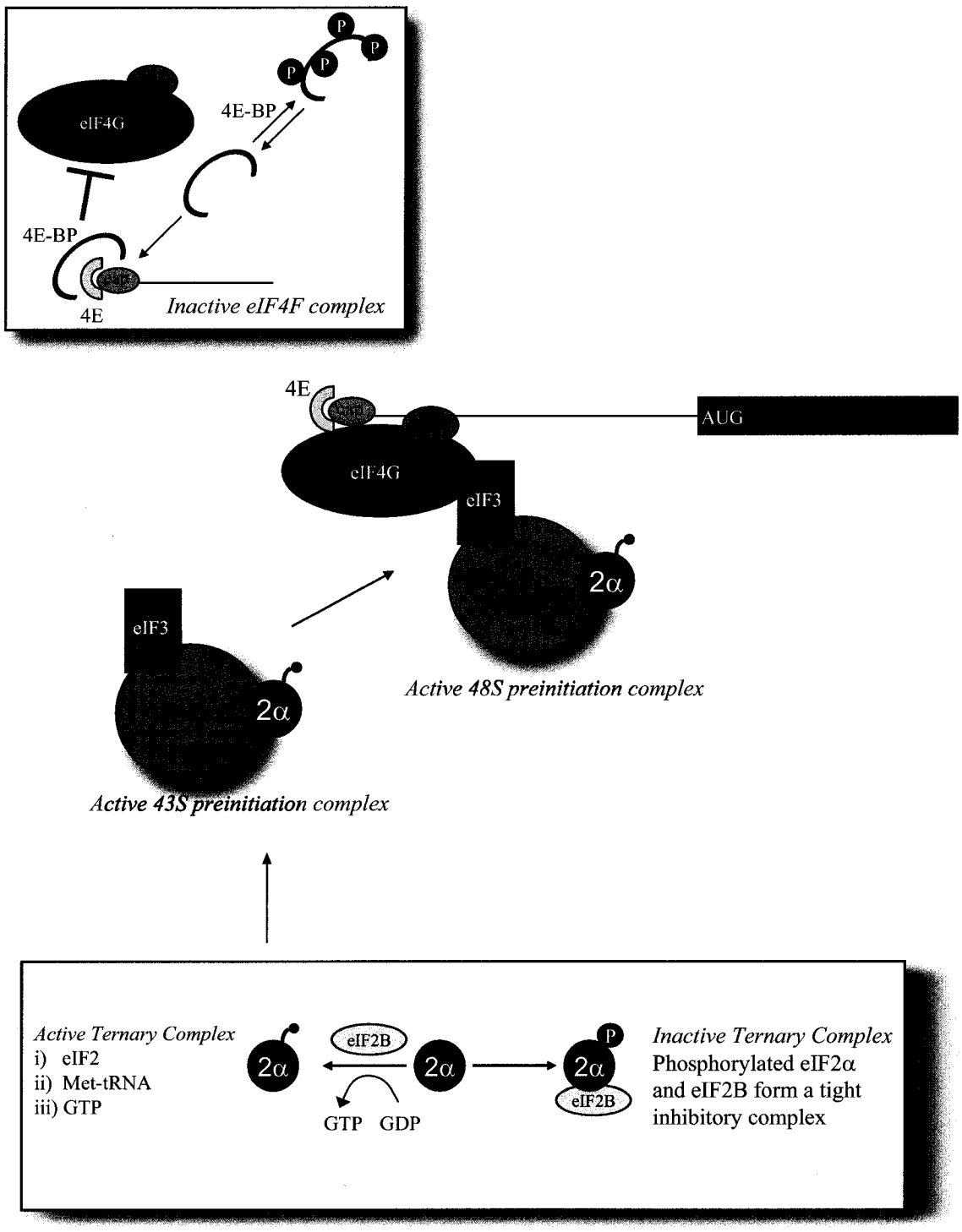
P
P
P
eIF4G
4E-BP
4E-BP
4E
Inactive eIF4F complex
4E
AUG
eIF4G
eIF3
2α
eIF3
2α
Active 48S preinitiation complex
Active 43S preinitiation complex
Active Ternary Complex
i) eIF2
ii) Met-tRNA
iii) GTP
2α
eIF2B
2α
GTP GDP
P
2α
eIF2B
Inactive Ternary Complex
Phosphorylated eIF2α
and eIF2B form a tight
inhibitory complex

Figure 2: Regulation of Translation Initiation

Translation initiation begins following assembly of the eIF4F complex (containing the cap binding protein eIF4E, the RNA helicase eIF4A, and the scaffold protein eIF4G) at the m^7GpppN "cap" structure at the 5'end of the mRNA. Interaction of the 43S preinitiation complex (eIF3, eIF2, Met-tRNA, GTP, 40S ribosomal subunit) with the eIF4F complex through eIF3 and eIF4G binding facilitates recruitment of the 40S ribosomal subunit and formation of the 48S preinitiation complex. This complex scans through the 5'UTR until it reaches the AUG start site. Here GTP bound to eIF2α is hydrolyzed by eIF5 resulting in release of eIF2 and recruitment of the large 60S ribosomal subunit. Regulation of initiation occurs primarily at two steps. The first is through the phophorylation of eIF2α at Ser51 resulting in the formation of an inhibitory complex with the GDP/GTP exchange factor eIF2B. The second is through the inhibition of the eIF4F complex as a result of competitive binding of the 4E-BPs to eIF4E in their hypophosphorylated state resulting in the inhibition of "cap-dependent" translation initiation.

interferon inducible kinase that is activated by double stranded RNA produced in virus-infected cells [61]; (ii) GCN2, a kinase originally identified in yeast, which is activated by nutrient deprivation [62]; (iii) HRI, a kinase that is found predominantly in erythroid cells that is activated by heme deprivation [63]; and (iv) PERK, an ER resident kinase that is activated by accumulated unfolded proteins in the endoplasmic reticulum (ER), and participates in a conserved pathway known as the unfolded protein response (UPR) [64]. Activation of any of these kinases results in high levels of eIF2α phosphorylation and activation of a signaling pathway referred to as the integrated stress response (ISR) which is sufficient to inhibit general translation initiation and induce the expression of genes that play a key role in the adaptation to hostile environments. The cellular response to hibernation serves as an outstanding example of adaptation. Frerichs *et al.* measured a remarkable inhibition in protein translation to 0.04% of active animals in the absence of any measurable cell death [65]. Furthermore, this inhibition in translation was not only completely reversible upon completion of the hibernating state, but was additionally found to require the phosphorylation of eIF2α [65], thus demonstrating the importance of eIF2α regulation in harsh environmental conditions when energy supplies are limited.

1.5 Unfolded Protein Response

Protein folding, export, and post-translational modification of secretory and membrane proteins occur within the ER. When an imbalance occurs between the load of client proteins and the ability of the ER to process that load, unfolded proteins

accumulate and a signaling pathway referred to as the UPR is activated. This stress response serves to decrease the influx of client proteins by inhibiting protein translation, increase the expression of molecular chaperones to mediate protein folding, and induce ER-associated protein degradation to eliminate unfolded proteins from the ER. UPR-mediated stress signals can be induced by different pathophysiological conditions including tissue ischemia [66], tumor hypoxia [67, 68], viral infection [69, 70], and genetic mutations in proteins that impair client folding (eg: Pelizaeus-Merzbacher disease; [71]), as well as by agents that inhibit various molecular functions in the ER including, protein glycosylation (tunicamycin) [72, 73], ER/Golgi transport (brefeldin A) [73], and calcium homeostasis (thapsigargin) [73, 74]. Three unique ER transmembrane proteins, PERK, IRE1, and ATF6, respond to perturbations in the protein folding environment of the cell [75, 76]. Each has an N-terminal luminal domain that is regulated by the ER chaperone protein BiP/Grp78. When unfolded proteins accumulate, BiP dissociates from PERK, IRE1, and ATF6, to promote folding, resulting in the oligomerization of PERK and IRE1, transautophosphorylation of their serine/threonine kinase domains and to the translocation of ATF6 to the Golgi apparatus (**Figure 3**).

1.5.1 IRE-1

The type 1 transmembrane serine/threonine protein kinase, IRE1, contains a site specific endoribonuclease that cleaves its own mRNA [77], 28S rRNA [78], and the mRNA encoding the bZIP transcription factor Xbox binding protein 1 (XBP1) [79-81]. IRE1 is activated by oligomerization and autophosphorylation upon increased unfolded proteins in the ER. IRE1 uses its endoribonuclease activity to excise an intron from XBP-1 mRNA [81, 82] resulting in a translational frame-shift that produces a functional XBP1 transcription factor that translocates

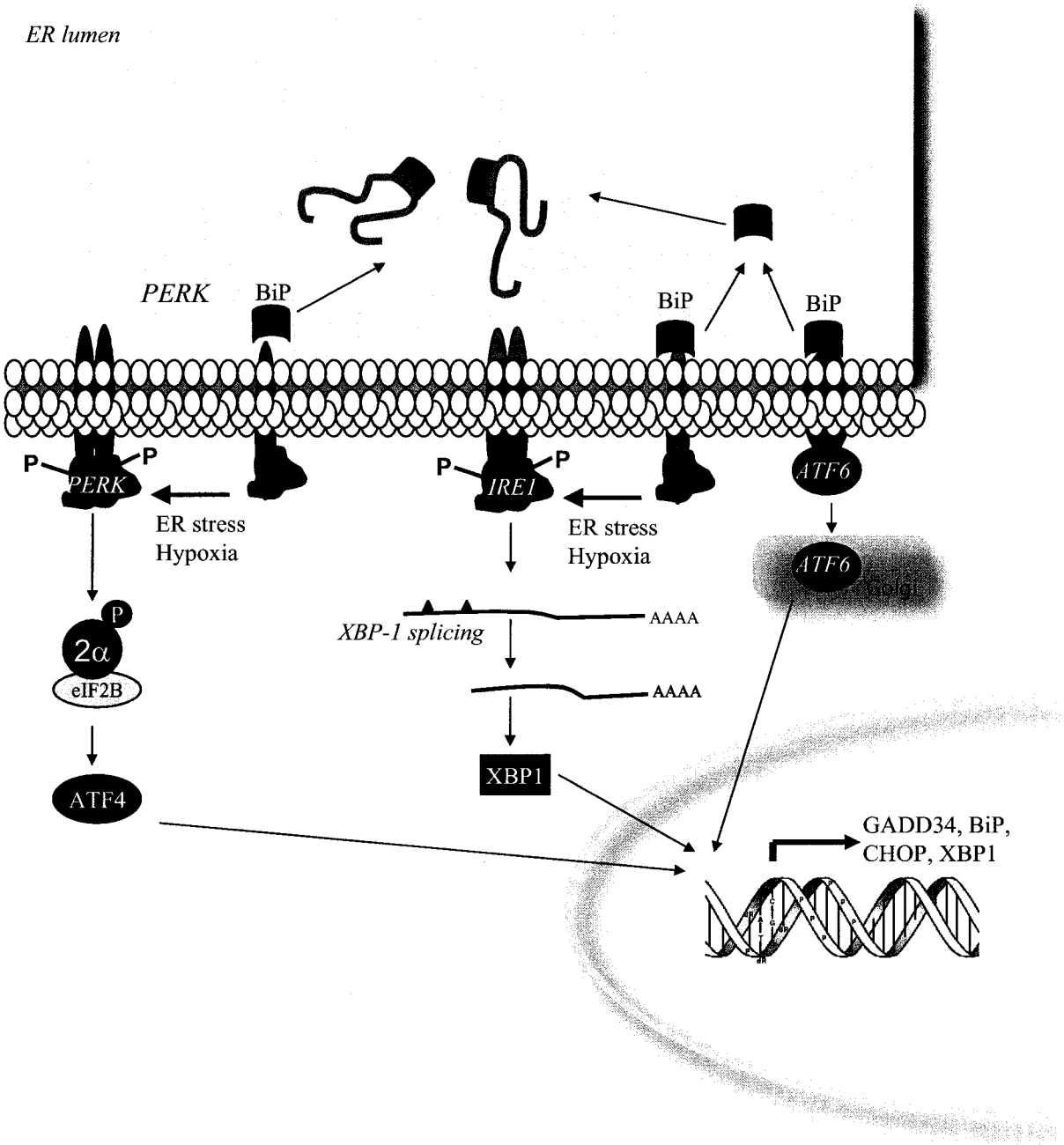
ER lumen
PERK
BiP
BiP
BiP
P
P
PERK
P
P
IRE1
ATF6
ER stress
Hypoxia
ER stress
Hypoxia
ATF6
Golgi
P
2α
eIF2B
XBP-1 splicing
AAAA
AAAA
XBP1
ATF4
GADD34, BiP,
CHOP, XBP1

Figure 3: Regulation of the Unfolded Protein Response

Three critical ER transmembrane proteins, PERK, IRE1, and ATF6, are responsible for activating three main signaling pathways of the UPR. Activation of PERK and the subsequent phosphorylation of eIF2α, leads to a general inhibition in protein synthesis while paradoxically increasing the translational efficiency of a subset of proteins including ATF4. IRE1 endoribonuclease activity splices a 26-nucleotide region of the XBP-1 mRNA resulting in the formation of a potent transcription factor. ATF6 is cleaved by two site specific proteases, processed in the golgi, and translocated to the nucleus where it acts as a stress-induced transcription factor.

into the nucleus, binds and activates the transcription of several chaperone genes containing the ER stress response element (ERSE: CCAAT-9bp-CCACG) [83], including BiP/Grp78 and XBP1 [84].

1.5.2 ATF6

ATF6, a type II transmembrane protein, was first identified in a screen for factors that bind the bipartite ERSE. Upon ER stress, ATF6 translocates to the golgi where it is cleaved first by a site-1 protease and subsequently by a site-2 protease, thereby, liberating the cytosolic transactivation domain from the membrane. ATF6 then translocates to the nucleus where it binds and activates the transcription of genes containing the ERSE consensus sequence [85, 86].

1.5.3 PERK

Exposing cells to conditions that promote ER stress, activates the eIF2α kinase PERK, resulting in the rapid phosphorylation of eIF2α and adaptive modulation of protein synthesis and gene expression through a signal transduction pathway referred to as the ISR [87]. PERK is necessary and sufficient to inhibit translation initiation in response to ER stress, as $Perk^{-/-}$ cells lose their ability to phosphorylate eIF2α and control protein synthesis [88]. Interestingly, this inhibition paradoxically leads to the increased expression of several proteins including the transcription factor 4 (ATF4), a member of the ATF/CREB subfamily of basic-region leucine zipper (bZIP) proteins that is preferentially translated in an eIF2α-phosphorylation-dependent manner [89, 90]. Its 5'UTR contains two conserved upstream open reading frames (uORFs), the second of which overlaps with the ATF4 reading frame. In unstressed cells, scanning

ribosomes initiate translation efficiently at both uORFs, and ribosomes that have translated uORF1, efficiently reinitiate translation at uORF2, thus preventing translation of ATF4. In stressed cells, high levels of eIF2α phosphorylation delay ribosome reinitiation at uORF2 and favors reinitiation at the authentic AUG of ATF4, resulting in its enhanced translation [89, 90]. ATF4 plays an important role in regulating the ER stress response by inducing the expression of genes which encode proteins that help to attenuate the ER stress response including, growth arrest and DNA damage gene 34 (GADD34), Immunoglobin binding protein of B cells (BiP), and C/EBP homologous protein (CHOP) [91, 92].

The activation of PERK and induction of the ISR arm of the UPR are critical to the cellular adaptation to stress, as $PERK^{-/-}$ cells are markedly impaired in their ability to survive exposure to conditions that promote protein malfolding in the ER [88]. Moreover, induction of CHOP and GADD34 is completely blocked in cells harboring an unphosphorylatable mutant of $eIF2\alpha^{S51A}$, or in $PERK^{-/-}$ cells, and BiP expression is attenuated 2-fold [91].

1.5.4 Physiological roles of PERK

$PERK^{-/-}$ mice are indistinguishable from their wildtype litermates at birth, but develop a hypersenstitivity to physiological levels of ER stress over time. This sensitivity is most notable in highly secretory cells, including the endocrine and exocrine cells of the pancreas and collagen I-secreting osteoblasts [93, 94]. The development of diabetes mellitus, malabsorption and sever bone defects eventually result due to the inability to modulate the stress response. Similar observations have been made in patients suffering from Wolcott-Rallison syndrome, a rare

autosomal-recessive disease resulting from mutations in the human PERK gene (EIF2AK3) [95].

1.5.5 GADD34

The carboxyl terminus of GADD34 encodes a regulatory subunit of an eIF2α specific phosphatase complex (PP1) that participates in a negative feedback loop to attenuate ISR signaling by increasing the cellular phosphatase activity that dephosphorylates eIF2α [96, 97]. This negative feedback loop is necessary for cellular recovery during ER stress, as cells expressing a truncated COOH deletion mutant of GADD34 or a phosphomimetic of eIF2α^{S51D}, demonstrate decreased survival in response to ER stress [97, 98]. Conversely, a non-phosphorylatable mutant of eIF2α^{S51A} partially protects cells from ER stress induced apoptosis.

1.5.6 BiP

In addition to its role in the activation of the UPR through its dissociation from PERK, IRE1, and ATF6, BiP is an ER chaperone that mediates protein folding. In response to ER stress, its transcriptional induction is positively regulated by the UPR through at least three independent signaling pathways [99, 100], one of which involves ATF4 [91]. BiP is also translationally regulated by a cap-independent mechanism during stress as an active IRES element has been identified within its 5'UTR [55]. BiP plays a critical role in the resolution of the UPR due to its ability to bind and inactivate oligomerized/activated IRE1 and PERK [101] and inhibition of BiP expression has severe consequences on cell survival in response to ER stress and to chronic hypoxia [102, 103].

1.5.7 CHOP

Also known as Gadd153, CHOP is a transcription factor that binds and activates the promoters of target genes believed to play a role in programmed cell death [104]. Although the identities of these target genes and the manner by which they might be related to the death of ER stressed cells remain unknown, deregulated CHOP activity compromises cell viability [105, 106], and CHOP deletion protects both the kidney and cultured fibroblasts against various inducers of ER stress [107, 108]. One mechanism by which CHOP may sensitize cells to ER stress induced cell death is through the transcriptional activation of ER oxidoreductin 1α (ERO1α). By activating ERO1α, CHOP promotes an oxidizing environment within the ER which favors protein malfolding [109] and contributes to cell death due to the accumulation of reactive oxygen species (ROS) [87]

1.5.8 Role of the UPR in cancer

Accumulating evidence supports the notion that the UPR is not only an important physiological response to temporal and developmental variations in the ER, but additionally plays a critical role in tumor development and adaptation. The over-expression of BiP has been observed in numerous human cancers and its enhanced expression correlates with malignant progression [110, 111] [112]. In one study of primary melanoma, Korabiowska *et al.* reported elevated GADD34 and CHOP expression in 73% and 80% of patients tested, respectively. Remarkably, 3 out of the 26 cases of primary melanoma tested, demonstrated deleterious mutations in the CHOP gene, and a further 6 cases reported polymorphisms within the CHOP gene that significantly decreased CHOP expression in these patients [113].

Transformed cells are constitutively exposed to low levels of ER stress, due in part to their higher rates of proliferation and elevated demands on transcriptional and translational machinery within the cell. The necessity of the UPR for tumor cell adaptation and cell viability can be exploited as a novel molecular target for the development of innovative anti-cancer treatment modalities. This approach is supported by findings that inhibiting major signaling pathways within the UPR results in increased sensitivity to hypoxic stress and anti-cancer agents and delays or inhibits tumor growth. Transformed cells stably expressing amplified anti-sense BiP expression vectors did not develop tumors when injected in nude mice [114]. Transformed MEFs derived from $XBP1^{-/-}$ animals, when injected into nude mice displayed similar results due in part to their increased sensitivity to hypoxic stress. Data presented herein reveal a role for PERK in the adaptive response to hypoxia. In response to hypoxic stress, cells stimulate the translation of numerous UPR genes including ATF4 and its downstream targets BiP, GADD34, and CHOP **(Chapter 2 and Appendix A)**. Moreover, cells derived from $PERK^{-/-}$ animals and cells expressing a non-phosphorylatable mutant of $eIF2\alpha^{S51A}$ display enhanced sensitivity to hypoxic stress and result in the growth of smaller tumors than their wild-type counterparts due in part to their increased sensitivity to hypoxic stress and in part to disrupted angiogenic signals that result in less vascularized tumors **(Chapter 3 and Appendix A)**.

Combined these studies suggest that all three arms of the UPR are activated during hypoxia. Disruption of either PERK or IRE1 signaling sensitizes cells to hypoxia and impairs the cellular adaptive response to hypoxic stress resulting in the inhibition of tumor growth and development. Together these findings provide

the impetus to explore the possibility of targeting these molecular pathways for the treatment of cancer in the future.

1.6 Aim of Thesis

The primary objective of this thesis was to identify and characterize the cohort of genes that are translationally regulated during hypoxic stress by microarray analysis of polysome-associated mRNAs. We hypothesized that genes necessary for the cellular adaptation to hypoxic stress would be preferentially translated in hypoxia treated cells and could be identified from translationally inhibited transcripts due to their increased association with polysomes during stress. Our analysis revealed a critical role for PERK in the activation of the ISR and translational regulation of ATF4 during severe hypoxic stress (**Chapter 2**). Follow-up studies in our lab and in active collaboration with Dr. Koumenis have delineated the importance of PERK signaling to the cellular adaptation to hypoxic stress both *in vitro* and *in vivo* (**Appendix A and Chapter 3**), and reveal a role for PERK in the translational regulation of pro-angiogenic genes. Fruitful collaborations with the labs of Dr. Pelletier and Dr. Holcik have demonstrated the importance of cap-independent translational regulation during hypoxia (**Appendix B**) and UV-irradiation (**Appendix C**) and describe a role for PERK in the negative-regulation of pro-apoptotic protein, APAF-1 (**Appendix C**) Combined, these studies demonstrate that the regulation of translation is a critical player not only to the oncogenic phenotype but also in the response to cellular stress.

2. ACTIVATING TRANSCRIPTION FACTOR 4 IS TRANSLATIONALLY REGULATED BY HYPOXIC STRESS

Contribution of Collaborators

The contents of this manuscript were written by J. Blais and edited by J. Bell prior to submission. All of the experiments performed and figures presented in this manuscript are the work of J. Blais with the exception of Figures 6 and 7 which were accomplished with the technical assistance of Vasilisa Filipenko (Co-op student, 2004). Dr. Costas Koumenis and his technician provided us with the HT29-Puro and HT29-A1 cell lines. Drs. David Ron and Heather Harding provided us with the $PERK^{-/-}$ SV40 transformed MEFs. Dr. Bradly Wouters provided assistance in dissecting the microarray data presented within this manuscript.

Summary

Using microarray analysis of polysome-bound mRNAs in aerobic and hypoxic HeLa cells, we demonstrate that a subset of transcripts are preferentially translated during hypoxia, including numerous genes involved in the unfolded protein response. One of theses genes, ATF4, is translationally induced upon PERK activation and eIF2α phosphorylation during hypoxic stress. The overexpression of a C-terminal fragment of GADD34 that constitutively dephosphorylates eIF2α, attenuates eIF2α phosphorylation and severely inhibits the induction of ATF4 in response to hypoxic stress demonstrating its role in a negative feedback loop initiated by ATF4. Together, this study supports that activation of the integrated response likely facilitates the cellular adaptation to hypoxic stress.

Activating Transcription Factor 4 is Translationally Regulated by Hypoxic Stress

Running Title: Translational Regulation During Hypoxia

Jaime D. Blais[1,2], Vasilisa Filipenko[2], Meixia Bi[3], Heather P Harding[4], David Ron[4], Costas Koumenis[3], Bradly G. Wouters[5], and John C. Bell[1*]

[1]Ottawa Regional Cancer Center, Ontario K1H 2C4

[2]Department of Biochemistry, University of Ottawa

[3]Department of Radiation Oncology, Wake Forest University School of Medicine, Winston-Salem, North Carolina 27157

[4]Skirball Institute, New York University School of Medicine, New York, NY 10016

[5]Department of Radiotherapy, University of Maastricht, 6200MD Maastricht, The Netherlands

key words: Hypoxia, translation, polysome, ATF4, UPR, eIF2-alpha

*Corresponding author:

Dr. John Bell
503 Smyth Rd.
3rd Floor ORCC
Ottawa ON
K1H 1C4
Work: 613-737-7700 ext 6893
Fax: 613-247-3524
e-mail: jbell@ohri.ca

Total word count of Materials and Methods: 1354

Total word count of Intro, Results and Discussion: 4268

Abstract

Hypoxic stress results in a rapid and sustained inhibition of protein synthesis that is at least partially mediated by eIF2α phosphorylation by the endoplasmic reticulum kinase PERK. Here we show through microarray analysis of polysome-bound RNA in aerobic and hypoxic HeLa cells that a subset of transcripts are preferentially translated during hypoxia including ATF4, an important mediator of the unfolded protein response. Changes in mRNA translation during the UPR are mediated by PERK phosphorylation of the translation initiation factor eIF2α at Ser 51. Similarly, PERK is activated and is responsible for translational regulation under hypoxic conditions, while inducing the translation of ATF4. The overexpression of a C-terminal fragment of GADD34 that constitutively dephosphorylates eIF2α, was able to attenuate the phosphorylation of eIF2α and severely inhibit the induction of ATF4 in response to hypoxic stress. These studies demonstrate the essential role of ATF4 in the response to hypoxic stress, define the pathway for its induction, and reveal that GADD34, a target of ATF4 activation, negatively regulates the eIF2α-mediated inhibition of translation. Taken with the concomitant induction of additional ER-resident proteins identified by our microarray analysis, this study suggests an important integrated response between ER signaling and the cellular adaptation to hypoxic stress.

Introduction

Mammalian cells have the ability to alter their gene expression in order to adapt to a variety of environmental stresses including nutrient depletion, oxidative stress, UV irradiation, reductive stress, exposure to toxins, and hypoxia, although the exact molecular events controlling the stress response have not been fully elucidated.

Hypoxic stress plays a pivotal role in normal human development and physiology including embryogenesis and wound repair, and is well studied for its importance in the pathogenesis of several human diseases, namely heart disease, stroke, diabetes, and cancer (for a detailed review, (53)). Hypoxia results when oxygen availability does not meet the demand of the surrounding tissue, resulting in decreased oxygen tension. In cancer this is initiated by the rapid proliferation of tumour cells, which gives rise to abnormal and chaotic vasculature, leading to the development of occlusions, blind ends, and vesicular shunts (4). The presence of hypoxic cells in solid tumors is well documented and both clinical and experimental evidence suggests that the hypoxic microenvironment of a tumour helps to produce a more aggressive phenotype (63) by functioning as a selective pressure for the clonal expansion of apoptotically insensitive cells (16). The presence of hypoxic regions in solid tumours also correlates with a poor prognosis and has been shown to limit the efficacy of standard anticancer treatments, such as radiotherapy and chemotherapy (5). A key element to cellular survival and adaptation during hypoxia is the transcription factor HIF-1, the master regulator of oxygen homeostasis. Numerous critical genes are tightly regulated by HIF-1, including growth factors, oncoproteins, transcription factors, and glycolytic enzymes (Wouters, submitted), which mediate a shift in cellular metabolism toward energy conserving anaerobic glycolysis (54).

Other mechanisms of gene regulation are important to the cellular response to stress, such as the control of translation initiation. The importance of translational control on gene expression was originally proposed to play a fundamental role during development (48) and has subsequently been proven critical in regulating numerous physiological processes in the cell including: growth stimulation (40), cell cycle progression (49), differentiation (56), ER stress, (17), and oncogenic signaling in cancer (47). Translational control provides a rapid and reversible mechanism of expression, whereas transcriptional induction can take hours to occur.

Regulation of eukaryotic protein translation occurs mainly at the level of translation initiation. Most mRNAs recruit ribosomes through the m^7G-cap structure by the eIF4F complex followed by binding of the 43S pre-initiation complex, consisting of the 40S ribosomal subunit, eIF1A, eIF3 and eIF2-GTP bound to the initiator tRNA, before scanning downstream to the initiating AUG (30). Successful translation initiation is only achieved when eIF2α binds GTP and (Met) tRNA, thereby forming the ternary complex. Formation of this complex is dependent on the exchange factor eIF2B, which exchanges the GDP bound eIF2α for GTP. This can be inhibited by the phosphorylation of eIF2α at Ser 51 by an active eIF2α kinase. Mammalian cells have several eIF2α kinases that are activated in response to a variety of cellular stresses. PKR is activated by double-stranded RNA as a result of viral infection, whereas the Endoplasmic Reticulum (ER) resident kinase, PERK, is activated by malfolded proteins in response to ER stress (20). The transcriptional effects during hypoxia and the result of HIF-1 signaling on cellular survival and adaptation are a well studied phenomenon, while the contribution of translational control on hypoxia responsive gene expression remains unclear. PERK has been implicated in the phosphorylation of eIF2α and

the resulting attenuation of protein translation in response to hypoxic stress (29). Despite a profound inhibition of translation initiation that occurs in response to hypoxia, several discrete transcripts remain efficiently translated, including VEGF (59), HIF-1α (32), BiP (37), and ODC (46). These cellular mRNAs are able to recruit ribosome binding to internal ribosome entry sites (IRES) without the need of cap-recognition from the eIF4F complex.

We have focused on identifying novel hypoxia regulated genes with the use of microarray analysis of polysomal and total mRNA populations in order to gain insight into both the transcriptional and translational changes that occur in response to hypoxic stress. Our studies reveal the preferential translation of numerous hypoxia-induced genes namely, eIF5, ATF3, ATF4, ATF6, VEGF, FGF2 and IGFBP4. One of these, activating transcription factor 4 (ATF4) is an important mediator of the unfolded protein response (UPR), supporting the possibility of an integrated response between the UPR and hypoxia through the translational regulation of ATF4.

Materials and Methods

Cell Culture. HeLa cells and 293T cells were maintained in alpha-modified Eagle's medium supplemented with a 10% mixture of DBS (Donor Bovine Serum) and FCS (Fetal Calf Serum) (3:1). Wild-type, PERK-/-, PKR-/-, and PERK-/- PKR-/- mouse embryonic fibroblasts were maintained in alpha-modified Eagle's medium supplemented with 10% FCS. The constitutively active GADD34 C-terminal protein fragment was expressed in cells by transduction of the A1 retrovirus as previously described (41). HT-29 cells stably transfected with the GADD34 C-terminal fragment (HT29-A1) and control HT-29 cells transfected with the parent plasmid (HT29-Puro) were maintained in McCoys media supplemented with 10% FCS, β-mercaptoethanol (0.55μM), non-essential amino acids (10μM), and puromycin (1μg/ml). Cells were treated with thapsigargin (100nM), cycloheximide (100mM) and Actinomycin D (100μM) where indicated.

Hypoxic Treatments. All experiments were performed with exponentially growing cells. For all experiments except for polysome fractionation, cells were plated in 60-mm glass culture dishes at a density of ~1 x 10^6 cells/plate. After approximately 20hr, the culture dishes were placed in a hypoxic culture chamber (MACS VA500 miroaerophillic workstation [Don Whitley Scientific, Shipley, United Kingdom]). Hypoxic conditions were achieved with 90% N_2, 5% CO_2, 5% H_2 (anaerobic grade gas) and palladium catalysts to scavenge trace oxygen.

Isolation of Polysomes and RNA. HeLa cells were plated on 150-mm glass culture dishes at a density of ~7 x 10^6 cells/plate. Cells were left untreated for approximately 32hr prior to hypoxic exposure (16hr) or they were left untreated (0hr). For the isolation of intact polysomes, cells were first treated with 0.1mg/ml cycloheximide (CHX) for 3min (37°C)

prior to cell lysis. Cell extracts were prepared at 4°C; the cells were washed twice with PBS containing CHX (0.1mg/ml) and lysed in RNA lysis buffer (1% Triton X-100, 0.3M NaCl, 15mM $MgCl_2$, 15mM Tris (pH 7.4), 0.1mg/ml CHX, 100U/ml RNAsin [Ambion, Austin TX]). Lysed HeLa cells were stained with Hoechst 33342 (5μg/mL) to ensure nuclei were intact during lysis. Nuclei were subsequently removed by centrifugation (3000rpm, 5min, 4°C) and the supernatant was centrifuged again to remove cellular debris (14,000rpm, 5min, 4°C). The lysate was layered onto 10ml continuous sucrose gradients (10-50% sucrose in 15mM $MgCl_2$, 15mM Tris (pH 7.4), 0.3M NaCl). Approximately 20% of the total volume of the cytoplasmic lysate was employed as a source for total RNA using phenol/chloroform extraction and ethanol precipitation. After 90min of centrifugation at 39,000 rpm in an SW41-Ti rotor at 4°C, the absorbance at 254nm was measured continuously as a function of gradient depth. Each fraction was digested with proteinase K and RNA was recovered from individual fractions by phenol-chloroform extraction and ethanol precipitation.

Microarray Analysis. Following polysome fractionation and RNA isolation, RNA from the high molecular weight polysomes (fractions 7-10 or 11) were pooled from the normoxic samples (hereafter called 0hr poly) and from the hypoxic samples (hereafter called 16hr poly). Prior to Microarray analysis RNA from the polysome fractions and the total RNA from the cytoplasmic lysates (0hr Total and 16hr Total) was purified using the RNeasy kit (Qiagen, Mississauga, Canada), as per manufacturer's instructions. Twenty micrograms of each RNA sample was processed according to manufacture's standard protocol (Affymetrix; Santa Clara CA, USA) and hybridized to an Affymetrix HGU95Av2 chip. Three independent 16hr poly and 0hr poly samples were obtained and two independent 16hr Total and 0hr Total samples were obtained. Data from three independent experiments were

analyzed using the Affymetrix Mass 5.0 software and Genespring software (Silicon Genetics; Redwood City CA, USA).

Total Cellular Changes and Polysome Analysis. Prior to the assessment of gene changes in response to hypoxic stress, data was filtered in order to decrease the number of irrelevant unchanging genes. Genes classified as absent (Affymetrix MAS 5.0) across all gene chips were removed from the analysis as were genes whose mean signal intensity for one or more samples was not greater than 600 (This number reflects the background noise of the microarray and would not result in a meaningful interpretation of the data generated). To identify total cellular changes in gene expression we used a mean cut off of 2-fold when comparing the 0hr Total gene chips to the 16hr Total gene chips. Genes were further categorized based on Molecular Function and sorted on Fold-Change (only previously corroborated and interesting gene changes have been reported in this publication). To identify genes that are preferentially translated during hypoxic stress we compared the mean signal intensities of the 0hr poly gene chips to the 16hr poly gene chips using a mean cut-off of 2-fold. In order to identify purely translationally regulated candidates we removed genes from this list that demonstrated a concomitant increase in total mRNA expression (>3-fold change in the 16hr total gene chip relative to the 0hr total gene chip). Using Genespring software (Silicon Genetics), we used Venn Diagrams in order to subtract genes induced by the hypoxic stress and genes that were preferentially mobilized into the polysome fractions during hypoxic stress. Genes were further categorized based on Molecular Function and sorted on the ratio of 16hr poly signal/ 0hr poly signal, used as a basis for interpreting the efficiency of translation during hypoxic stress. ANOVA was used to assess the statistical significance of the polysomal changes.

Quantitative RT-PCR. The aforementioned total and polysomal RNA from hypoxic and normoxic treated HeLa cells was reverse transcribed (500ng RNA) in the presence of 250pg of VSV-M RNA (a viral transcript used as a control for RT efficiency and Q-PCR). Quantitative PCR was performed in triplicate to amplify all targets using the FastStart DNA Master SYBR Green I kit (Roche Diagnostics, Laval Canada, as per manufacturer's instructions) and the Roche Lightcycler thermocycler. Crossing points were converted to absolute quantities based on standard curves generated for each target amplicon. All target signals were subsequently normalized to VSV-M in order to correct for RT-PCR efficiency. Primers used are listed below

hATF4: left 5'-CTTACGTTGCCATGATCCCT-3'; right 5'-CTTCTGGCGGTACCTAGTGG-3', mATF4: left 5'- TCCTGAACAGCGAAGTGTTG-3'; right 5'- ACCCATGAGGTTTCAAGTGC-3', eIF5: left 5'-TTGAAGGAGGCAGAGGAAGA-3'; right 5'-ACATGTTGCACTTCTGGCTG-3', txbp151: left 5'-CCAAAGGCTCCAAAAACAAA-3'; right 5'-CATTTCACAGACTTGCCCCT-3', hsCDC6: left5'- 5'-TTGTTGTTGTTTTTGAGGCG-3'; right 5'-CCTGGCCAACATGGTAAAAC-3', VSV-M: Astart 5'-ACGAATTCAAATTAGGGATCGCACCACC-3', Bend 5'-ACGGATCCCGTGATACTCGGGTTGACCT-3', ATF3: left 5'-TAGGCTGGAAGAGCCAAAGA-3', right 5'- TTCTCACAGCTGCAAACACC-3', Prolyl-4 Hydroxylase: left 5'-CCCATGTCAACGTGACAGAC-3', right 5'-GCAGCCACTTTGATCCTAGC-3', ATF6: forward 5'- AGCAGGAACTCAGGGAGTGA -3', reverse 5'- GGAGGTAAGGAGGAACCGAC -3', BiP: forward 5'-CCACCAAGATGCTGACATTG-3', reverse 5'- GAAAAGCAGTAAACAGCCGC-3',

Cyclin D3: forward 5'- AGGCTGATGGGACAGAATTG-3', reverse 5'-AGCTGAGCAGAAAGCAAAGC-3'

Q-PCR results are presented as either the number of transcripts in Total RNA or as the polysomal RNA per cell. Results from each transcript were normalized to an exogenous control (VSV-M), multiplied by 100 and transformed to log scale prior to plotting.

Immunoblotting. Following treatments, cells were placed on ice and washed with PBS and lysed on ice in 2X WB buffer (5mM Trix [pH 6.8], 0.5% SDS, 2% glycerol, 2mM DTT, supplemented Complete mini protease inhibitor cocktail tablets (Roche Diagnostics, Susex, UK), NaPPi (2mM) and NaF(2mM) for Western analysis. Protein concentrations of each sample were determined by the modified Bradford assay as recommended by the manufacturer (Bio-Rad, Hercules, Calif.). Proteins were resolved on sodium dodecyl sulfate 10% polyacrylamide gels and transferred onto Hybond ECL nitrocellulose membrane (Amersham, Arlington Heights, Ill.) with a wet transfer system (Bio-Rad). Membranes were stained with 0.15% Ponceau red (Sigma) to ensure equal loading and transfer and then blocked with 5% (wt/vol) dried nonfat milk in TBST buffer (10mM Tris base, 150mM NaCl, 0.5% Tween-20).

Primary antibodies for anti-rabbit ser51 phosphorylated eIF2α (1:500) and anti-mouse eIF2α (1:500; recognizes both the unphosphorylated and phosphorylated forms of eIF2α) were obtained from Cell Signaling Technologies (Cell Signaling Technologies, Beverly, Mass) Primary antibody for anti-mouse HIF1α (1:1000) was obtained from Transduction Labs (H72320, Transduction Labs, Lexington, KY). Primary antibody for anti-rabbit ATF4 (1:250) was obtained from Santa Cruz (sc-200, Santa Cruz, CA). Primary antibody for anti-mouse Actin (1:10,000) was obtained from Sigma (A-5316, St. Louis MO) Primary antibody

for anti-rabbit GADD34 (1:1000) was a kind gift from Dr. David Ron (Skirball Institute NY). Primary antibody for BiP (1:1000) was a kind gift from Dr. Martin Holcik (CHEO, ON). Anti-rabbit secondary antibody was obtained from Jackson ImmunoResearch (1:10,000) and anti-mouse secondary antibody was obtained from BioRad (1:3000). Horseradish peroxidase-coupled secondary antibodies were detected by enhanced-chemiluminescence (ECL-Plus) reagent kit in accordance with the recommendations by the manufacturer (Amersham Biosciences, Piscataway, NJ).

Results

Protein translation is inhibited by hypoxic stress

In this study, we used HeLa cervical carcinoma cells to study the preferential translation of messages following severe hypoxic stress (O_2<0.01%). Microarray analysis was used to analyze gene expression profiles from total cellular mRNAs and polysome associated mRNAs in HeLa cells grown in a hypoxic or normoxic environment.

Polysomal mRNA was isolated from total cellular mRNA by fractionation through a 10%-50% sucrose gradient. The optical density (OD) profiles of the sucrose gradients are shown in Figure 1. In each gradient, the top fractions (1-4) represent ribosomal complexes (40S, 60S and 80S) and free mRNAs, whereas the bottom fractions (5-10 or 11) represent transcripts associated with polysomes. In order to verify the proper identification of the polysomal peaks, cells were treated with puromycin, an inhibitor that causes release of nascent peptides and mRNAs from ribosomes. The resulting polysome profile demonstrated a shift of the mRNAs from the polysomes into the free mRNA, 40S and 60S ribosomal complexes and monosome peaks (data not shown). Following hypoxic stress, there is a significant inhibition in protein translation, as seen by the accumulation of free mRNA and rRNAs, with a considerable increase in the monosome peak. HeLa cells remained >98% viable throughout the 16hr of hypoxic stress (data not shown). For microarray analysis, mRNA associated with more than 2 ribosomes were pooled. These messages are thus indicative of highly expressed transcripts that undergo preferential translation in an environment that favors the overall inhibition of protein translation. Total RNA was also obtained from 16hr hypoxic lysates and normoxic lysates, hereafter named 16hr total and 0hr total respectively, treated identically to the polysomal RNA prior to sucrose gradient

fractionation. Affymetrix MAS 5.0 software was used to compare steady state changes and polysomal changes in gene expression between the 16hr and 0hr lysates.

Microarray analysis of total and polysomal RNA

We compared the 0hr and 16hr total mRNA species to identify changes in overall gene expression following hypoxic stress. We found that 11.6% and 10.3% of the accurately measured genes (see Materials and Methods for a description of this interpretation) were induced or repressed more than 2-fold, respectively (Figure 2A). Interestingly, of the induced genes, only 58% of them were found to be enhanced in the polysomes, whereas the remaining 42% were either translationally unchanged or repressed, signifying that all transcripts are not translated with equal efficiency. These genes were functionally clustered and are displayed in Table 1. Many of the genes listed have been previously identified in the literature indicating that our microarray analysis provided an accurate representation of known hypoxia induced gene expression. The previously corroborated hypoxia induced genes are referenced, including genes involved in: glucose metabolism (Glut3, PGK, G6PD), angiogenesis (VEGF, HO-1, PAI, angiogenin), pH regulation (CA9, CA12), cell stress response (CHOP, ORP150, BiP), and cell death (NIP3, BIK).

Although changes in overall transcripts were conservative, hypoxic stress is known to cause a remarkable inhibition in protein translation. Indeed 88.5% of genes demonstrated no increase in translation or were subjected to a substantial decrease in translation following hypoxia. By comparing the expression profiles of the 0hr poly and 16hr poly microarray chips, we were able to deduce that 2.5% of genes demonstrated increased translational efficiency by more than 2-fold during hypoxia (Figure 2C), as determined by their increased polysomal association without a concomitant increase in total cellular

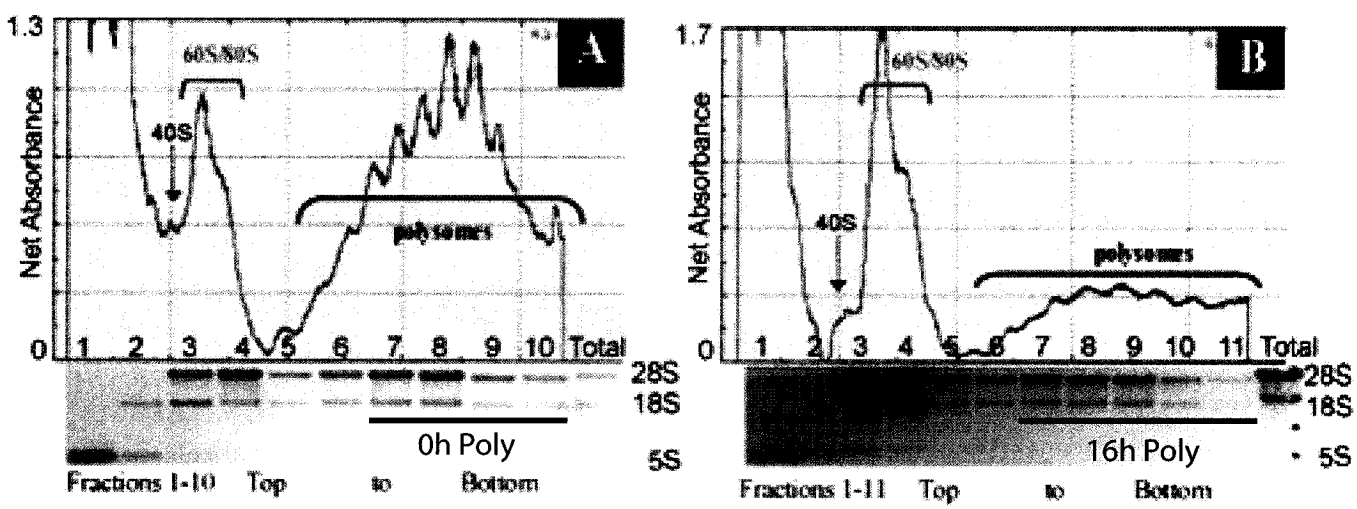
A
B
Net Absorbance
1.3
0
1.7
0
60S/80S
40S
polysomes
1 2 3 4 5 6 7 8 9 10 Total
1 2 3 4 5 6 7 8 9 10 11 Total
28S
18S
5S
0h Poly
16h Poly
Fractions 1-10 Top to Bottom
Fractions 1-11 Top to Bottom

Figure 1: Hypoxic stress results in global inhibition of protein translation

Polysome Profiles (Abs at 254nm) in cell lysates fractionated by sucrose density ultracentrifugation. HeLa cells were exposed to hypoxic stress for 16hrs (B) or left untreated (A). Cells were treated with cycloheximide (100μg/mL) (37°C, 3min) and lysed in a Triton X-100 buffer (4°C). Cell lysates were layered on a 10ml continuous sucrose gradient (10-50%), ultracentrifuged in an SW-41 rotor 39K for 90min. The position of the polysomes and ribosomal subunits is indicated. The increase in monosome-bound transcripts and ribosomal subunits combined with the decrease in polysomes apparent in the hypoxia treated cells is indicative of decreased protein translation. RNA extracted from the polysome gradient fractions was applied to a 1% agarose gel and electrophoresed. The abundant 28S, 18S and 5S rRNAs were directly visualized by ethidium bromide staining. staining. The polysome fractions isolated for microarray analysis, named 0h poly and 16h poly, are indicated.

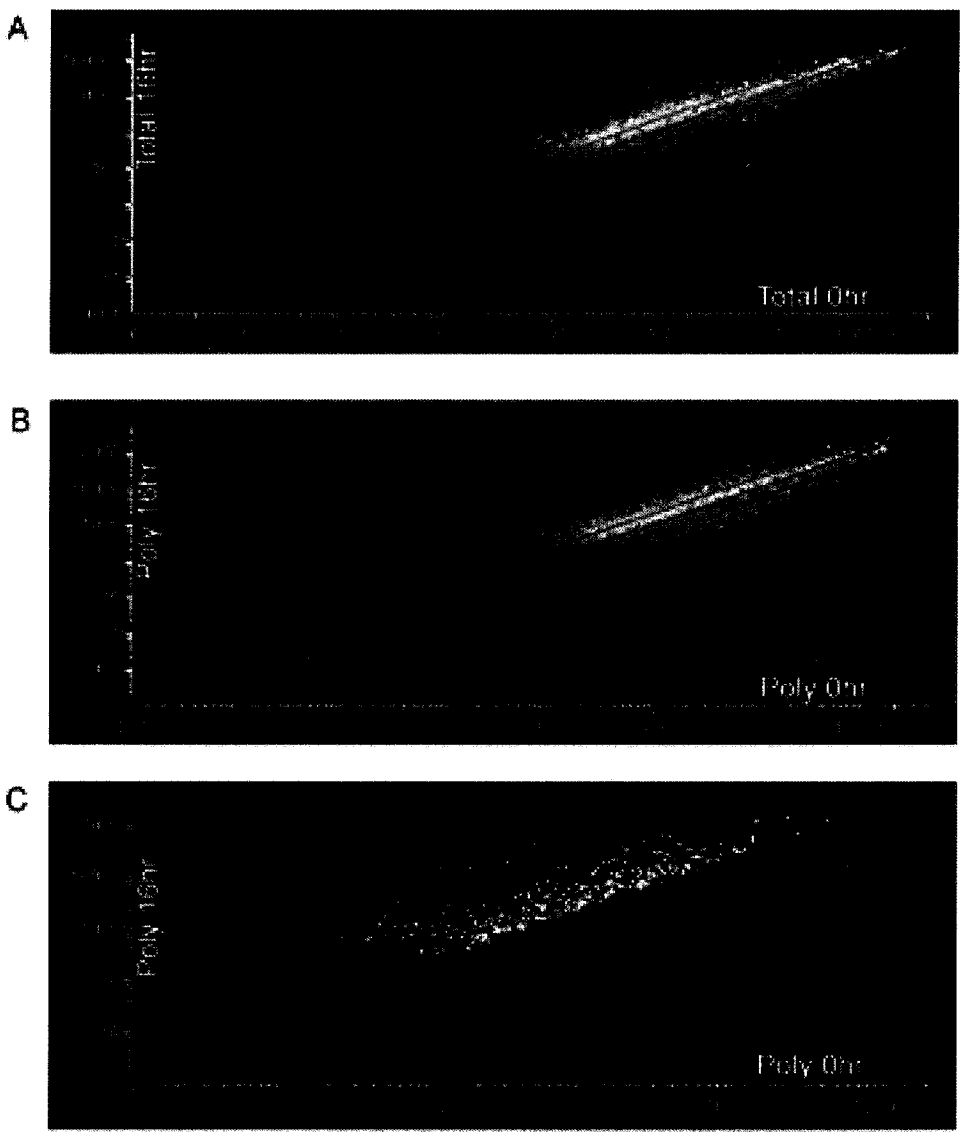
A
Total 1/hr
Total On
B
Poly 1/hr
Poly On
C
Poly 1/hr
Poly On

Figure 2: Scatter Plots of Oligo Probes as Affected by Hypoxic Stress

Total and polysomal RNAs were hybridized to the Affymetrix Human Genome U95A (HG-U9Av2) oligonucleotide microarray chip. Relative gene probe intensities (X-axis) of total RNA (A), and polysomal mRNA (B and C) of aerobic cells (0hr) were plotted against the corresponding gene probe intensities (Y-axis) of hypoxia treated cells (16hr). Gene probes above the top green line represent genes induced greater than 2-fold, gene probes below the bottom green line represent genes repressed greater than 2-fold. (C) Gene probes in green represent those genes that were induced more than 2-fold in the polysomes but whose total mRNA was not induced more than 2-fold. A short list of these translational candidates is presented in Table 2. Gene probes in yellow represent genes whose expression was induced greater than 2-fold in both the total RNA and polysomal mRNA profiles.

Table 1: Steady State Changes In Gene Expression

probe set	*Fold Change*	*poly16/0hr*	*GenBank*	*Descriptions*	*Reference*
Energy Generation and Metabolism					
40193_at	19	12.9	X51956	ENO2 gene for neuron specific (gamma) enolase	43
37188_at	14	12.7	X92720	phosphoenolpyruvate carboxykinase	42
1586_at	11	18.8	M35878	Human insulin-like growth factor-binding protein-3	102
32331_at	6	7.4	X60673	adenylate kinase3 (AK3)	103
31488_s_at	5	2.3	S81916	phosphoglycerate kinase {alternatively spliced}	43
40107_at	3	5.5	AF054987	aldolase C	43
38042_at	2.4	1.6	X03674	glucose-6-phosphate dehydrogenase (G6PD)	
36979_at	2.4	3.1	M20681	glucose transporter-like protein-III (GLUT3)	103
35938_at	**-12**	**-10**	M72393	calcium-dependent phospholipid-binding protein (PLA2)	
262_at	**-3.8**	**-3.6**	M21154	S-adenosylmethionine decarboxylase	
Angiogenesis/Vessel Dynamics					
1103_at	9.2	15	M11567	angiogenin	47
34777_at	8.7	17.4	D14874	adrenomedullin precursor	104
36606_at	5.9	2.9	X51405	carboxypeptidase E	
36100_at	4	5.4	AF022375	vascular endothelial growth factor (VEGF)	105, 43, 44
Matrix Metabolism and pH Regulation					
40309_at	83	85.6	X66839	Carbonic Anhydrase IX	39, 50
926_at	20	8.8	J03910	metallothionein-IG (MT1G)	
34390_at	20	20.4	U90441	Human prolyl 4-hydroxylase alpha (II) subunit	51
38637_at	17.3	20.5	L16895	Human lysyl oxidase (LOX)	
33127_at	13.5	11.9	U89942	Human lysyl oxidase-related protein (WS9-14)	
37037_at	10.2	14.9	M24486	Human prolyl 4-hydroxylase alpha subunit	51
41750_at	8.1	8.6	D49489	protein disulfide isomerase-related protein P5	
34795_at	7.8	5.4	U84573	Lysyl hydroxylase isoform 2 (PLOD2) mRNA	
36454_at	5.8	9.6	AF037335	carbonic anhydrase precursor (CA 12)	50
36666_at	5.7	5.1	M22806	prolyl 4-hydroxylase beta-subunit	51
Cell Stress Response/DNA Repair					
442_at	12.2	15.8	X15187	tra1 mRNA	
36614_at	11.3	9.4	X87949	BiP	28
38986_at	6.3	7.2	Z49835	protein disulfide isomerase (glucose related protein 58)	
1955_s_at	**-6.1**	**-10.6**	AF035528	Smad6 mRNA	
1104_s_at	**-5**	**-3.8**	M11717	Human heat shock protein (hsp 70)	
36785_at	**-3.3**	**-2.5**	Z23090	28 kDa heat shock protein	
Cell Death and Proliferation					
37168_at	16.5	20.7	AB013924	TSC403 protein	
39436_at	15.1	8.3	AF079221	BCL2/adenovirus E1B 19kDa-interacting protein 3a	
654_at	15.3	12.5	L07648	Human MXI1 mRNA	
2011_s_at	11.9	3.8	U34584	Human Bcl-2 interacting killer (BIK)	15
38010_at	10.8	10.4	AF002697	Homo sapiens E1B 19K/Bcl-2-binding protein Nip3	54
37028_at	3.4	6	U83981	apoptosis associated protein (GADD34)	55
37228_at	**-4.6**	**-5.9**	U01038	pLK mRNA	
Cell Cycle					
1913_at	3.5	2.9	U47414	cyclin G2	
1206_at	**-7.3**	**-2.3**	X66364	PSSALRE for serine/threonine protein kinase	
38414_at	**-5.3**	**-3.6**	U05340	p55CDC	
1945_at	**-4.7**	**-7**	M25753	cyclin B	
1794_at	**-3.9**	**-3.9**	M92287	cyclin D3 (CCND3)	56
1943_at	**-3.3**	**-2.4**	X51688	cyclin A	
35699_at	**-3**	**-4.4**	AF053306	mitotic checkpoint kinase Mad3L	
1803_at	**-2.3**	**-2.7**	X05360	CDC2	
RNA Splicing/Transcription					
36618_g_at	**-23**	**-12**	X77956	Id1 mRNA	106
351_f_at	**-4**	**-2.4**	D28423	pre-mRNA splicing factor SRp20	

Table 1: Total Cellular mRNA Changes in Gene Expression During Hypoxia.

Results of Affymetrix HGU95A-V2 microarray analysis used to identify steady state changes in gene expression during hypoxia. Affymetrix MAS5.0 software and Genespring 5.0 were used to compare 16total to 0total RNA to determine gene changes induced or repressed >2-fold. Genes were functionally clustered and referenced if previously identified in the literature. Only named genes are included in this list, ESTs were omitted. Analysis is representative of two independent microarray analyses performed with RNA isolated from two independent experiments.

Table 2: Hypoxia Induced Translationally Regulated Genes

Function	poly 16/0	ANOVA	total16/0	genbank	Gene Name
Anti-Apoptosis/Apoptosis	4.1	0.179	2.2	U33821	TXBP151: Tax1-binding protein
	2.7	0.243	1.3	X75861	TEGT:testis enhanced gene transcript (BAX inhibitor 1)
	2.7	0.015	1.8	S81914	IER3: immediate early response 3
	2.3	0.100	1.5	Z15108	PRKCZ: protein kinase C, zeta
	2.3	0.007	1.9	AB020680	BAG5: BCL2-associated athanogene 5
	2.0	0.063	1.8	AF099935	GG2-1: TNF-induced protein
Cell Cycle Regulator	2.0	0.040	1.8	U22398	KIP2: Cdk-inhibitor p57KIP2
DNA Repair	2.4	0.126	1.7	D83702	CRY1: cryptochrome 1
	2.3	0.113	1.4	D21089	XPC: xeroderma pigmentosum
Metabolism	5.0	0.023	1.2	AF061741	SDR1: short-chain dehydrogenase/reductase 1
	3.5	0.052	1.6	AA873266	PDK3: pyruvate dehydrogenase kinase
	2.9	0.148	1.9	Y10275	PHKG1: phosphorylase kinase
	2.1	0.205	1.2	X69433	IDH2: isocitrate dehydrogenase 2
	1.9	0.064	1.1	M15182	GUSB: glucuronidase
	1.6	0.288	1.6	X15573	PFKL: phosphofructokinase
Stress Response/UPR	9.0	0.013	2.7	L19871	ATF3: Activating Transcription Factor 3
	5.0	0.037	1.2	AL022312	ATF4: activating transcription factor 4
	2.4	0.129	1.7	D83702	casein kinase 1, epsilon
	2.0	0.336	1.8	AB017642	OSR1: oxidative-stress responsive 1
	2.0	0.250	1.0	X68277	DUSP1: dual specificity phosphatase 1
	1.9	0.054	0.9	AF005887	ATF6: activating transcription factor 6
	1.9	0.080	1.0	U09759	MAPK9: mitogen-activated protein kinase 9
Regulation of Transcription	3.1	0.257	2.5	U49020	MEF2A: MADS box transcription enhancer factor 2
	3.0	0.181	0.5	AB015051	DAXX: death-associated protein 6
	2.8	0.010	1.3	AB000468	RNF4: ring finger protein 4
	2.6	0.033	1.9	U11861	G10: maternal G10 transcript
	2.5	0.168	1.0	AF069733	TADA3L: transcriptional adaptor 3
	2.3	0.017	2.0	X51345	JUNB: jun B proto-oncogene
	2.3	0.113	1.6	M95929	PMX1: paired mesoderm homeo box 1
	2.2	0.216	1.5	X91648	PURA: purine-rich element binding protein A
	2.2	0.068	1.9	AF038177	FHX: FOXJ2 forkhead factor
	2.1	0.022	1.4	M34539	FKBP1A: FK506 binding protein 1A
	2.1	0.500	1.1	M25077	SSA2: Sjogren syndrome antigen A2
	2.0	0.025	1.2	Z35278	RUNX3: runt-related transcription factor 3
	2.0	0.027	1.1	AF078096	FOXC1: forkhead box C1
	2.0	0.004	1.6	U71300	SNAPC3: small nuclear RNA activating complex
	1.9	0.097	0.9	M16801	NR3C2: nuclear receptor
	1.8	0.480	1.9	M27691	CREB1: cAMP responsive element binding protein 1
	1.8	0.702	1.5	AF019214	HBP1: HMG-box containing protein 1
Signal Transduction	4.0	0.070	1.4	L11284	MAP2K1: mitogen-activated protein kinase kinase 1
	2.2	0.167	1.6	M62403	IGFBP4: insulin-like growth factor binding protein 4
	2.0	0.154	1.3	M97815	CRABP2: cellular retinoic acid binding protein 2
Protein Biosynthesis	2.8	0.004	1.7	X94754	MARS: methionine-tRNA synthetase
	2.5	0.014	2.0	AL050281	NAG: neuroblastoma-amplified protein
Regulation of Translation	3.4	0.459	1.7	U49436	EIF5: eukaryotic translation initiation factor 5
Angiogenesis	2.2	0.032	1.3	U43368	VEGFB: vascular endothelial growth factor B
	2.0	0.053	0.7	M27968	FGF2: fibroblast growth factor 2
Iron Ion Transport	5.5	0.000	1.3	L20941	FTH1: ferritin, heavy polypeptide 1
Proteolysis	3.5	0.048	1.9	AB029027	PITRM1: pitrilysin metalloproteinase 1

Table 2: Hypoxia Induced Translationally Regulated Genes

Results of microarray analysis to identify transcripts that were specifically associated with high molecular weight polysomes in hypoxia treated cells. Genespring 5.0 software was used to compare the relative expression of polysome-bound mRNAs in hypoxic (16poly) and normoxic cells (0poly). Genes that were induced >2-fold in the polysomes (poly 16/0) and induced <3-fold in the total cellular mRNA (Total 16/0) were considered for further analysis. ANOVA was used to assess the statistical significance of the changes in mRNA found in polysomal fractions. In this analysis, reported P values between 0 and 0.1 represent highly significant changes with little variance in the data set. P values between 0.1 and 0.3 represent changes that have a higher degree of variation between replicate experiments but are maintained as biologically relevant changes. There is a high probability that differences observed between hypoxic and normoxic samples are due to chance when Anova P values exceed 0.5. A subset of the genes identified by this analysis were functionally clustered and are represented in this table.

mRNA. It is important to stress that this portion of the differentially regulated genes would have been missed if only the total cellular transcript profiling had been performed. Data comparing gene expression of the polysome-associated transcripts from 0hr and 16hr hypoxia treated HeLa cell extracts were used to generate a list of translational candidates. The genes listed in Table 2 were chosen based on high levels of mRNA in the polysomes at 16hr versus at 0hr (poly 16/0) and were grouped based on cellular function. One example, ATF4, has been described in the literature as being translationally induced in response to ER stress and amino acid starvation (18).

Patterns of Gene Expression During Hypoxia

Two predominant patterns of gene expression emerged throughout the analysis of the microarray data, these being changes in the steady state mRNA and translationally mediated changes. Changes in the steady state levels of mRNA could be a result of changes in transcription or may involve changes in mRNA stability. These were marked by an increase in total mRNA expression and may or may not correlate with their presence in the polysomes, since not all cellular transcripts are translated with equal efficiency. In contrast, genes that are regulated exclusively at the translational level display a higher efficiency of translation, as seen by their presence in the polysomes, but do not demonstrate any change in their gene expression at the level of total mRNA. We used quantitative real-time PCR (Q-PCR) to verify the translational regulation of 6 candidate genes identified by our microarray analysis (Figure 3). Q-PCR values were normalized to an internal control, vesicular stomatitis virus RNA encoding the M protein (VSV-M), added exogenously to each RT reaction. All data was converted to the number of transcripts per cell for a more meaningful interpretation of the data sets. Hypoxia causes numerous changes in gene

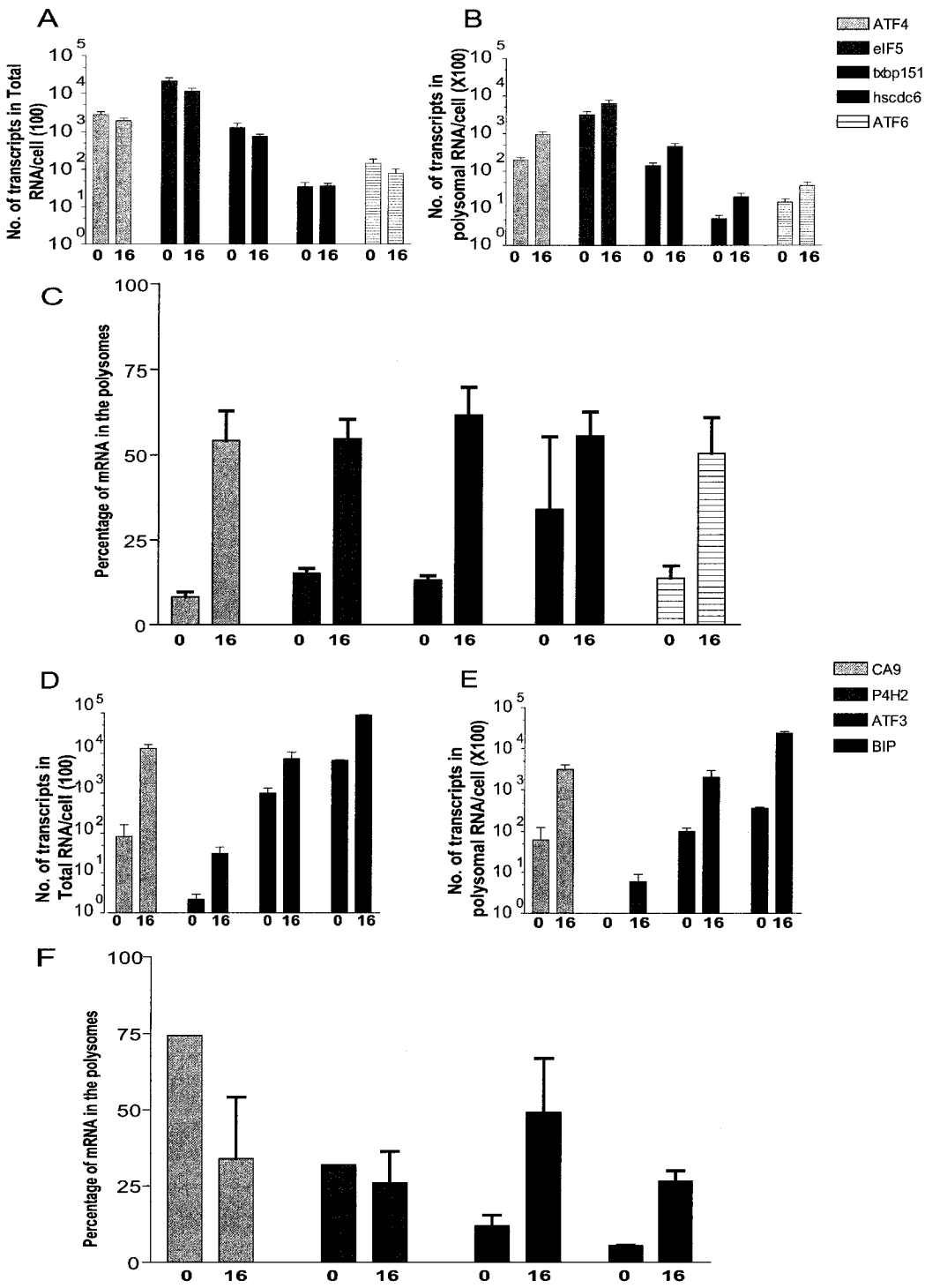
A
B
C
D
E
F
No. of transcripts in Total RNA/cell (100)
No. of transcripts in polysomal RNA/cell (X100)
Percentage of mRNA in the polysomes
ATF4
eIF5
bbp151
hscdc6
ATF6
CA9
P4H2
ATF3
BIP
0 16

Figure 3: ATF4 mRNA is more efficiently translated during hypoxia

(A) *Translational Candidates: Total mRNA expression does not change during hypoxia.* Total RNA was isolated prior to sucrose gradient fractionation from hypoxia treated (16hr) or normoxic (0hr) HeLa cells, reverse transcribed and quantified by real-time PCR. The quantities of each transcript are described as the number of transcripts isolated from total RNA per cell. Each sample was independently normalized to a spiked internal control. Q-PCR analysis was replicated in triplicate. Results are representative of the average ± S.E.M of at least five independent experiments.

(B) *Translational Candidates: Transcripts are enriched in the polysomes during hypoxia.* High molecular weight polysomes from hypoxia treated (16hr) or normoxic (0hr) HeLa cells were pooled (fraction 7-11), reverse transcribed and quantified by real-time PCR. The quantities of each transcript are described as the number of transcripts isolated from polysomal RNA per cell. Each sample was independently normalized to a spiked internal control. Q-PCR analysis was repeated in triplicate. Results are representative of the average ± S.E.M of at least five independent experiments.

(C) *Translation efficiency increases for translationally regulated genes.* The efficiency of translation during hypoxic treatment (16hr) and normoxia (0hr) was plotted as the percentage of total mRNA associated with polysomes.
(quantity poly $mRNA_{time\ x}$ /quantity of total $mRNA_{time\ x}$)*100%

(D) *Hypoxia Induced Genes: Total mRNA expression is induced during hypoxia.* Total RNA was isolated prior to sucrose gradient fractionation from hypoxia treated (16hr) or normoxic (0hr) HeLa cells, reverse transcribed and quantified by real-time PCR. The quantities of each transcript are described as the number of transcripts isolated from total RNA per cell. Each sample was independently normalized to a spiked internal control. Q-PCR analysis was replicated in triplicate. Results are representative of the average ± S.E.M of at least three independent experiments.

(E) *Hypoxia Induced Genes: Transcripts are enriched in the polysomes during hypoxia.* High molecular weight polysomes from hypoxia treated (16hr) or normoxic (0hr) HeLa cells were pooled (fraction 7-11), reverse transcribed and quantified by real-time PCR. The quantities of each transcript are described as the number of transcripts isolated from polysomal RNA per cell. Each sample was independently normalized to a spiked internal control. Q-PCR analysis was repeated in triplicate. Results are representative of the average ± S.E.M of at least three independent experiments.

(F) *Changes in Translation efficiency for hypoxia induced genes.* The efficiency of translation during hypoxic treatment (16hr) and normoxia (0hr) was plotted as the percentage of total mRNA associated with polysomes.
(quantity poly $mRNA_{time\ x}$ /quantity of total $mRNA_{time\ x}$)*100%

expression, including those of housekeeping genes such as actin and GAPDH. Thus using a spiked viral mRNA as an internal control not only allows for the control of gene expression differences between normoxic and hypoxic samples, it also allows us to control for differences in the efficiency of each RT reaction.

Data from the translationally regulated candidates and transcriptionally regulated genes are illustrated in Figure 3. Translationally active transcripts demonstrate a re-distribution onto the polysomes without a concomitant increase in the amount of mRNA in the total lystate (Figure 3A and 3B) therefore translationally regulated genes are more efficiently translated in response to hypoxia (Figure 3C). Even genes that appeared to be statistically insignificant by ANOVA (TXBP151 and eIF5) demonstrated consistent increases in their translational efficiency as determined by Q-PCR analysis. On the contrary, transcriptionally induced genes exhibit a substantial increase in both the total lysate and polysomal fractions (Figure 3D and 3E). Examples of this regulation are the HIF-1 responsive genes, carbonic anhydrase 9 (CA9) and prolyl-4-hydroxylase-2 (P4H2). These genes however, do not increase their overall translation efficiency (Figure 3F). The detection of BiP in the high molecular weight polysomes substantiates the possibility of identifying a third expression profile, a transcriptional and translational-coupled response. BiP is both transcriptionally induced by hypoxia and preferentially translated perhaps due to an IRES element in its 5'UTR, as such there is an increase in the efficiency of BiP translation in response to hypoxia. ATF3 demonstrated a similar expression pattern to BiP under hypoxic stress, exhibiting a transcriptional induction in the total lysate and mobilization of the transcript onto the polysomes (Figure 3D and 3E). The increase in translational efficiency of ATF3 in response to hypoxia (Figure 3F) indicates the likelihood of a combined transcriptional and translation induction of ATF3, a possibility to be further determined.

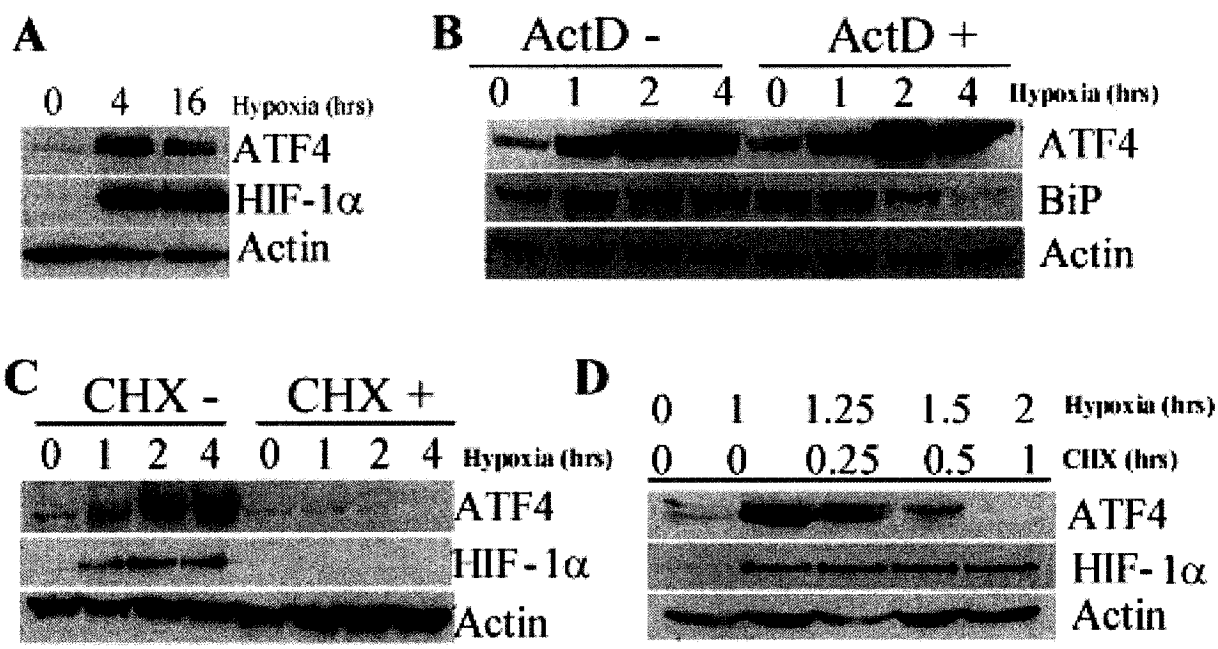
A
0 4 16 Hypoxia (hrs)
ATF4
HIF-1α
Actin
B
ActD -
ActD +
0 1 2 4 0 1 2 4 Hypoxia (hrs)
ATF4
BiP
Actin
C
CHX -
CHX +
0 1 2 4 0 1 2 4 Hypoxia (hrs)
ATF4
HIF-1α
Actin
D
0 1 1.25 1.5 2 Hypoxia (hrs)
0 0 0.25 0.5 1 CHX (hrs)
ATF4
HIF-1α
Actin

ATF4 Protein Expression Is Induced During Hypoxia

Previous reports have established a regulatory mechanism for the translational control of ATF4 in response to ER stress and amino acid starvation (19). The 5'UTR of human ATF4 encodes three short open reading frames (uORFs), two of which are conserved in all known species. These mediate the repression of ATF4 expression in unstressed cells. Under conditions of eIF2α phosphorylation successful re-initiation at the authentic start codon results in the efficient translation of ATF4. Our observation that hypoxia results in the mobilization of ATF4 mRNA onto the polysomes made us question whether ATF4 is preferentially translated during hypoxic stress. Both the microarray and Q-PCR analysis suggest a post-transcriptional induction of ATF4 during hypoxia. This was further corroborated by the induction of the ATF4 protein following both 4hr and 16hr of hypoxia (Figure 4A), with maximal ATF4 induction by 4hr. The translational regulation of ATF4 was further supported by the observation that treatment with the transcriptional inhibitor Actinomycin D (ActD) did not prevent the accumulation of ATF4 protein during hypoxia (Figure 3B). Similar observations were found with a second transcriptional inhibitor, DRB (data not shown). To refute the possibility that ATF4 protein expression was mediated by increased protein stability during translation, HeLa cells were treated with the translational inhibitor cycloheximide (CHX) before treatment with hypoxia and following 1hr of hypoxia (Figure 4C and 4D). Cells treated with CHX before hypoxic stress do not induce ATF4 protein during 4hr of hypoxia, and do not further induce ATF4 if treated with CHX following 1hr of hypoxic stress. ATF4 has a short half-life between 30min and 1hr (33),

A

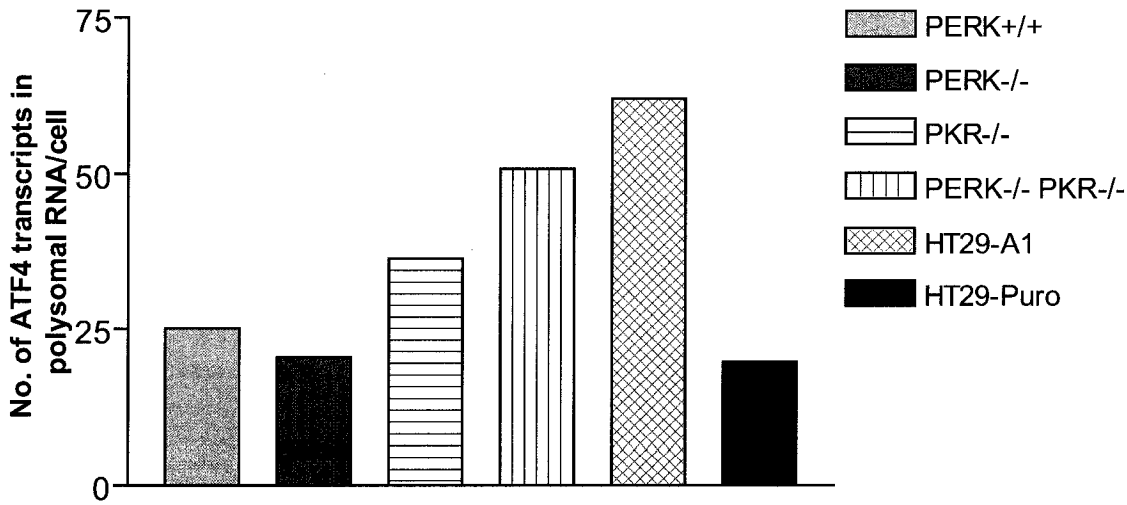
No. of ATF4 transcripts in polysomal RNA/cell
75
50
25
0
PERK+/+
PERK-/-
PKR-/-
PERK-/- PKR-/-
HT29-A1
HT29-Puro

B

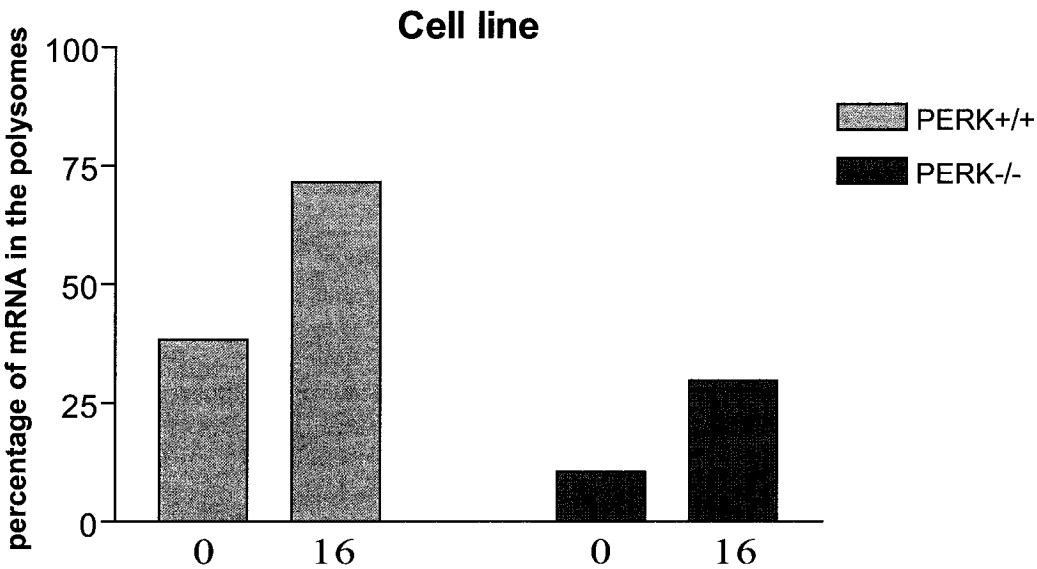
Cell line
percentage of mRNA in the polysomes
100
75
50
25
0
0
16
0
16
PERK+/+
PERK-/-

C

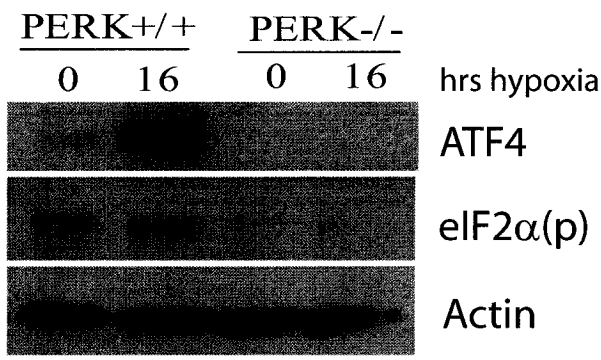
PERK+/+
PERK-/-
0
16
0
16
hrs hypoxia
ATF4
eIF2α(p)
Actin

Figure 4: ATF4 is translationally induced following hypoxic stress

(A) Immunoblot analysis of ATF4 and HIF1α protein content in HeLa cells exposed to hypoxia or left untreated for the indicated period of time. Actin serves as a loading control

(B) Immunoblot of ATF4 and BiP in HeLa cells treated with hypoxia for the indicated period of time in the presence or absence of the transcriptional inhibitor actinomycin D (100μM) added 5 min before treatment. Similar results were obtained using another transcriptional inhibitor, DRB (100μM), data not shown. Actin serves as a loading control

(C) Immunoblot of ATF4 and HIF1α in HeLa cells treated with hypoxia for the indicated period of time in the presence or absence of the translational inhibitor cycloheximide (100μM). Actin serves as a loading control.

(D) Immunoblot of ATF4 and HIF1α in HeLa cells exposed to hypoxia for the indicated period of time. Cells were first treated with hypoxia followed by the addition of the translational inhibitor cycloheximide for 15min, 30min, or 1hr. Actin serves as a loading control.

which supports the observed immediate degradation of ATF4 following CHX treatment. These findings are consistent with the previously reported translational regulation of ATF4 during ER stress and amino acid deprivation (19).

Phosphorylation of eIF2α by PERK is necessary for ATF4 translation during hypoxia.

The activation of eIF2α kinases and phosphorylation of eIF2α has been shown to be essential for the selective translational induction of ATF4 in response to both ER stress and amino acid starvation (19). The importance of PERK in the phosphorylation of eIF2α during hypoxic and anoxic stress has been reported (29).

Parallel analysis of ATF4 mRNA in the polysomes of PERK+/+ and PERK-/- Mouse Embryonic Fibroblasts (MEFs) revealed that in the absence of PERK there was a significant decrease in the amount of ATF4 mRNA recruited to polysomes and translated under both normoxic and hypoxic conditions (Figure 5B and 5C). As expected, eIF2α phosphorylation was induced in response to hypoxic stress only in PERK+/+ MEFs (Figure 5C). In a previous study, analysis of PKR knockout (PKR-/-) MEFs during hypoxic stress was not shown to have any impact on the levels of eIF2α phosphorylation (29). Our analysis of MEFs derived from wild type (wt), PKR knockout (PKR-/-), and PERK/PKR double knockout (PERK-/-, PKR-/-) mice confirmed these findings (Figure 6). However, we sought to examine directly the effects of disrupting both the PKR and the PERK signaling pathways on ATF4 expression during hypoxia.

As expected, hypoxia increased the levels of eIF2α phosphorylation and the induction of ATF4 in the wt and PKR-/- MEFs. Under normoxic conditions all MEFs exhibited very little expression of ATF4. Within 1hr of hypoxic stress, ATF4 expression was induced in

A

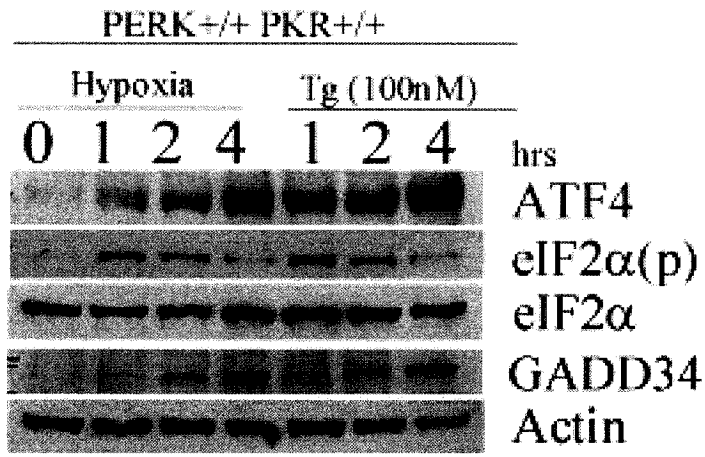
PERK+/+ PKR+/+
Hypoxia
Tg (100nM)
0 1 2 4 1 2 4
hrs
ATF4
eIF2α(p)
eIF2α
GADD34
Actin

B

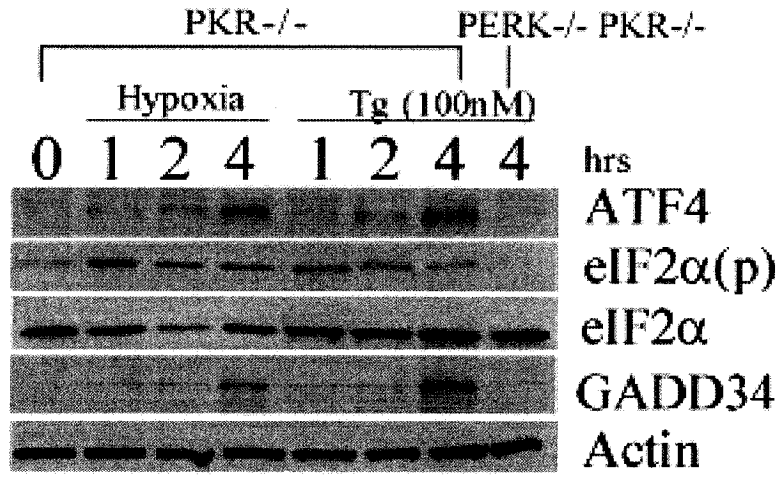
PKR-/-
PERK-/- PKR-/-
Hypoxia
Tg (100nM)
0 1 2 4 1 2 4 4
hrs
ATF4
eIF2α(p)
eIF2α
GADD34
Actin

C

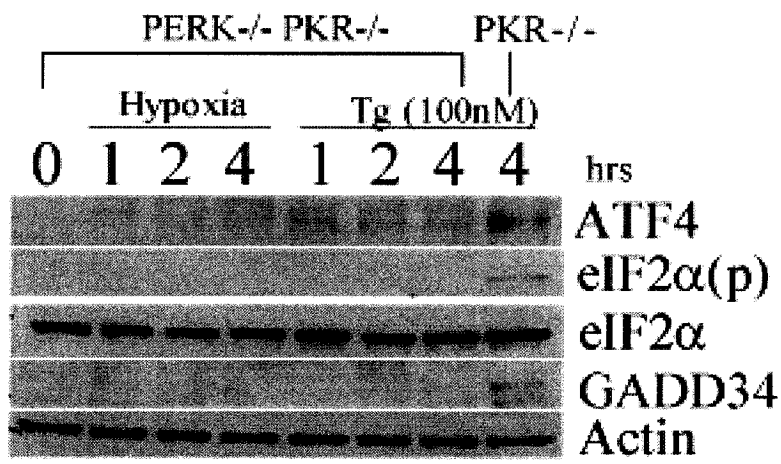
PERK-/- PKR-/-
PKR-/-
Hypoxia
Tg (100nM)
0 1 2 4 1 2 4 4
hrs
ATF4
eIF2α(p)
eIF2α
GADD34
Actin

Figure 5: PERK is required for induction of ATF4 in response to hypoxic stress

(A) High molecular weight polysomes from normoxic cells (PERK+/+, PERK-/-, PKR-/-, PERK-/- PKR-/-, HT29-A1, HT29-Puro) were pooled (fraction 7-11), reverse transcribed, and quantified by real-time PCR. The quantity of ATF4 is described as the number of ATF4 transcripts isolated from polysomal RNA per cell. Each sample was independently normalized to a spiked internal control. Q-PCR analysis was repeated in triplicate.

(B) High molecular weight polysomes from hypoxia treated (16hr) or normoxic (0hr) PERK+/+ and PERK-/- cells were pooled (fraction 7-11), reverse transcribed and quantified by real-time PCR. The efficiency of ATF4 translation during hypoxic treatment (16hr) and normoxia (0hr) was plotted as the percentage of total mRNA associated with polysomes.
(quantity poly $mRNA_{time\ x}$ /quantity of total $mRNA_{time\ x}$)*100%.
Each sample was independently normalized to a spiked internal control. Q-PCR analysis was repeated in triplicate.

(C) Immunoblot of ATF4, eIF2a(p) in PERK+/+ and PERK-/- MEFs for the indicated period of time following hypoxic stress. Actin serves as a loading control.

both the wild-type and PKR-/- MEFs (Figure 6A and 6B). Although the magnitude of this induction appears lower in the PKR-/- cells relative to wild-type, the consequence of this on the eIF2α signaling pathway remain to be elucidated. Similar results were obtained with cells treated with thapsigargin. Treatment of DKO (PERK-/- PKR-/-) MEFs with either hypoxia or thapsigargin failed to induce phosphorylation of eIF2α or increase translation of ATF4 (Figure 6C), whereas the PKR-/- thapsigargin treated control demonstrated a phosphorylated eIF2α signal as well as induced ATF4 protein expression.

GADD34 Expression Antagonizes the Induction of ATF4 during hypoxia.

GADD34 protein can directly interact and activate the catalytic subunit of type 1 protein serine/threonine phosphatase (PP1), which in turn functions to dephosphorylate eIF2α to allow protein translation to resume, (41), (9), (42). Recently, ATF4 was found to bind and activate a conserved ATF site in the promotor sequence of GADD34, providing a model for a negative feedback loop that might control protein translation during ER stress (36). To date there is no evidence that GADD34 is induced during hypoxia. Data obtained with the wild-type, PKR-/- and DKO MEFs during hypoxic stress revealed that the induction of GADD34 was abrogated when the PERK signaling pathway was repressed (Figure 7, 6B, 6C). To determine whether GADD34 expression can antagonize eIF2α phosphorylation and ATF4 induction during hypoxia, HT29 cells stably expressing a C-terminal truncated mutant of GADD34 (HT-29 A1) were treated with hypoxia and thapsigargin. These cells express the insert of a retroviral clone A1, which encodes the COOH-terminal 299 amino acids (aa 292-590) of the hamster GADD34 protein (41), which causes the constitutive dephosphorylation of eIF2α. Treatment of HT-29 A1 cells with hypoxia severely inhibited the phosphorylation of eIF2α and induction of ATF4, however HT-29 cells expressing the parental plasmid (HT-

29 Puro) exhibited the same expression profile as wild-type and PKR-/- MEFs in response to hypoxia. Similar results were obtained when these cells were treated with thapsigargin. These findings suggest that ATF4 regulates the expression of GADD34, which in turn can abrogate the ATF4 signaling pathway during hypoxia. Q-PCR analysis verified that reduced levels of ATF4 protein expression observed in the knockout MEFs and the HT29-GADD34 truncated mutant was not the product of decreased ATF4 mRNA levels (Figure 5A). Interestingly, the PKR-/- and DKO MEFs express higher basal levels of ATF4 mRNA than wild-type MEFs. Similarly, higher ATF4 mRNA levels are expressed in HT29 cells expressing the COOH-terminal truncated GADD34.

A

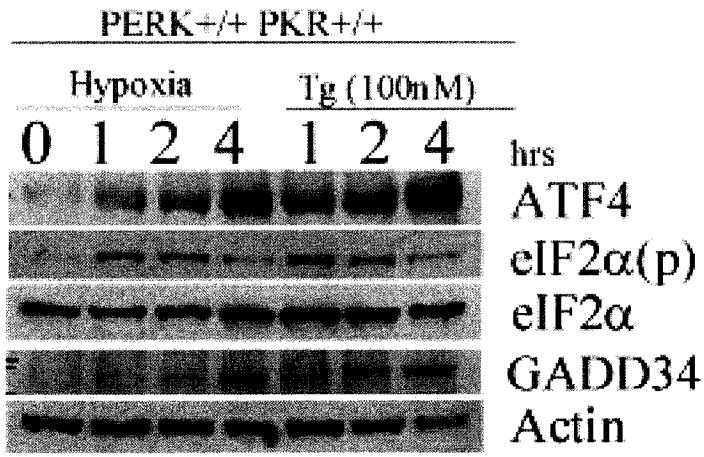
PERK+/+ PKR+/+
Hypoxia
Tg (100nM)
0 1 2 4 1 2 4
hrs
ATF4
eIF2α(p)
eIF2α
GADD34
Actin

B

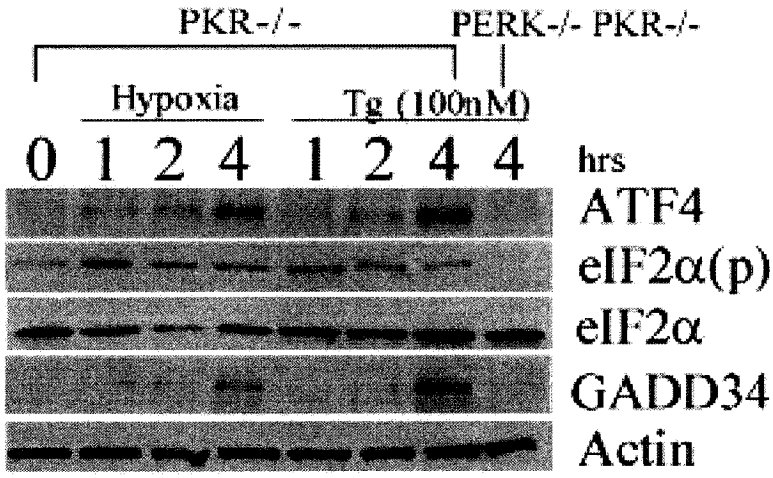
PKR-/-
PERK-/- PKR-/-
Hypoxia
Tg (100nM)
0 1 2 4 1 2 4 4
hrs
ATF4
eIF2α(p)
eIF2α
GADD34
Actin

C

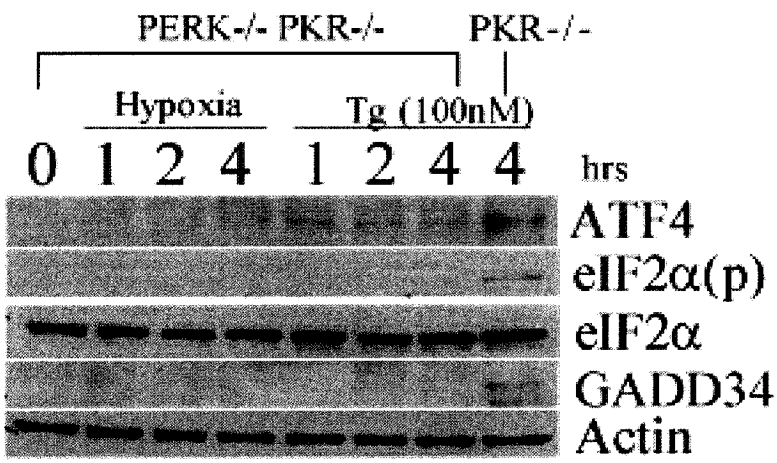
PERK-/- PKR-/-
PKR-/-
Hypoxia
Tg (100nM)
0 1 2 4 1 2 4 4
hrs
ATF4
eIF2α(p)
eIF2α
GADD34
Actin

Figure 6: PERK is necessary for ATF4 signal transduction during hypoxic stress

Immunoblot of ATF4, eIF2α phosphorylated on serine 51 [eIF2α (p)], total eIF2α and GADD34 from hypoxia and thapsigargin (Tg 100nM) treated wild-type , PKR-/- and PKR-/- PERK-/- double knock-out mouse embryonic fibroblasts for the indicated period of time. Actin serves as a loading control.

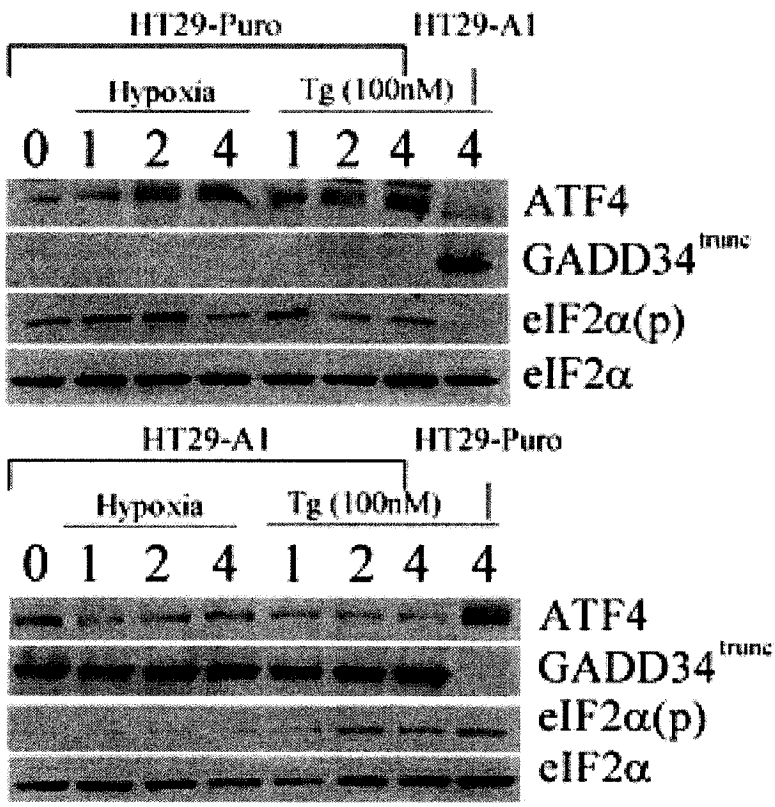
HT29-Puro
HT29-A1
Hypoxia
Tg (100nM)
0 1 2 4 1 2 4 4
ATF4
GADD34trunc
eIF2α(p)
eIF2α
HT29-A1
HT29-Puro
Hypoxia
Tg (100nM)
0 1 2 4 1 2 4 4
ATF4
GADD34trunc
eIF2α(p)
eIF2α

Figure 7: Overexpression of GADD34 can antagonize ATF4 signaling during hypoxia

Immunoblot of ATF4, eIF2α phosphorylated on serine 51 [eIF2α (p)], total eIF2α and GADD34 from hypoxia treated or thapsigargin (Tg 100nM) treated HT29-Puro (Parental) cells or HT29-A1 cells expressing a C-terminal fragment of GADD34 that constitutively dephosphorylates eIF2α ($GADD34^{trunc}$) (41). Actin serves as a loading control.

Discussion

Adaptation to environmental stress is essential for long-term cell survival. Mechanisms that control cellular responses to stress are often exploited by tumor cells, allowing them to survive and to thrive in unfavorable environments. As an example, metabolic changes that provide a growth advantage to tumor cells exposed to a hypoxic microenvironment are mediated in large part by the heterodimeric transcription factor HIF-1. The shift in cellular metabolism toward the energy conserving anaerobic glycolysis is facilitated by the HIF-1 regulated glycolytic enzymes (phosphoglycerate kinase-1, and aldolase-A) and glucose transporters (GLUT-1 and GLUT-3) (14, 55, 57). Tolerance to hypoxia is also promoted through changes in protein translation. Translation is the second largest consumer of ATP (23) in the cell and its coordinated shutdown may be one strategy to ensure energy conservation in the cell when ATP levels are limiting. It has been well established that hypoxic stress results in a profound inhibition in translation (44, 34, 31) thereby causing the majority of mRNA transcripts to experience diminished translational efficiencies. Our microarray analysis revealed that 95% of cellular mRNA species that do not change or decrease in abundance during hypoxia, experience a decrease in their translational efficiency. PERK has been implicated in the inhibition of translation during hypoxia through the phosphorylation of eIF2α at Ser51 (29). However, despite PERK mediated inhibition, the translation of some genes remains unaffected while others are translated more efficiently, examples being HIF-1α and its downstream gene products (32). Consequently, cells must be capable of maintaining and inducing gene expression in order to mediate cellular adaptation and cell viability during hypoxia.

A collective analysis of data generated by microarray and Q-PCR facilitated the identification of three classes of gene expression that likely contribute to this strategy. The first category includes mRNAs that are transcriptionally induced and are more efficiently translated under hypoxic stress; both BiP and ATF3 are examples of this method of gene regulation (Figure 3: D, E, F; additional candidate genes are listed in Table 1). A second category includes genes that are transcriptionally induced and whose translational efficiencies are either unchanged or diminished in response to hypoxia. Carbonic Anhydrase IX (CA9) and Prolyl-4-hydroxylase-2 (P4H2), both HIF-1 regulated gene products, demonstrate a decrease in their translational efficiencies during hypoxia (Figure 3: D, E, F; additional candidate genes are listed in Table 1). The third class of gene expression includes genes that are more efficiently translated during hypoxia without an associated transcriptional induction in total mRNA. Genes that correspond to this category include eIF5, txbp151, ATF6 and ATF4 (Figure 3: A, B, C; additional candidate genes are listed in Table 2). Similar analyses have been previously employed to identify translationally regulated genes involved in host cell response to poliovirus infection (27), T-cell activation (39), VHL expression (15), and most recently in oncogenic signalling through Ras and Akt (47). Thus a combination of changes in steady state mRNA and translational changes in gene expression can modulate the cellular responses to stress.

The selective inhibition of cap-dependent translation could regulate the translational expression of important hypoxia responsive genes with internal ribosome entry sites (IRES). IRES mediated initiation was first discovered in picornaviruses such as poliovirus (26). Many cellular IRES elements function under stress conditions when rates of protein synthesis via cap-dependent translation are reduced, namely: PDGF2 (2), c-sis (52), APAF-1 (8), c-myc (60), and XIAP (24). Specifically, VEGF (59), HIF-1α (32), BiP (37), and ODC (46)

have demonstrated functional IRES activity during hypoxic stress. The importance of IRES expression as a key regulator of translation during hypoxia currently remains undetermined. We are undertaking efforts to determine which, if any, of the translationally regulated transcripts reported possess functional IRESes.

ATF4, an important mediator of the UPR, is ubiquitously expressed at low basal levels, though poorly translated in unstressed cells due to the presence of three uORFs in its 5'UTR (19). This regulatory mechanism resembles that of the yeast protein GCN4. In yeast, global inhibition of translation occurs upon amino acid depletion. Active GCN2 phosphorylates eIF2α and preferentially promotes the synthesis of GCN4, a transcription factor that controls the expression of genes involved in amino acid biosynthesis (22).

Translation of ATF4 rapidly follows eIF2α phosphorylation during times of ER stress, arsenite treatment, and amino acid starvation (17). During hypoxia PERK activation results in the phosphorylation of eIF2α (29); taken together this suggests an important UPR-integrated response to hypoxic stress. Microarray analysis of total cellular mRNAs revealed the transcriptional induction of many other ER-resident proteins including: GADD34, GRP58, HSP70, Grp78/BiP, and HSP28 (Table 1), as well as CHOP/Gadd153, ORP150, Gadd45 (C. Koumenis, personal communication) further supporting the connection between hypoxia and the UPR.

Our studies with PERK-/- MEFs have shown that this kinase is absolutely required for ATF4 translation (Figure 5C). Interestingly, even in the absence of efficient translation, ATF4 mRNA is still recruited, to some extent, into the polysome fraction. Since we and others have shown that the initiation of translation at the authentic start codon of ATF4 is dependent on PERK phosphorylation of eIF2α (18, 29), our results (Figure 5B) suggest that ATF4 mRNA

can be recruited to the polysome fraction in the absence of PERK activity through initiation and translation of upstream open reading frames.

While others have suggested that anoxic induction of ATF4 is regulated at the level of protein stability (1), our experiments with cycloheximide treatment of HeLa cells (Figure 4) suggest a requirement for *de novo* protein synthesis. Although we cannot exclude that increased protein stability of ATF4 may contribute to its post-translational regulation, our data demonstrate that ATF4 is regulated, at least in part, by an increase in its translational efficiency during hypoxic stress.

Our microarray analysis revealed an induction of GADD34 gene expression in the total cellular mRNA by 3.4-fold accompanied by a 6.1-fold increase in its translational efficiency. GADD34 directs the catalytic subunit of protein phosphatase 1 to eIF2 (41, 9, 36) leading to its dephosphorylation and promoting resolution of the translational repression stage of the UPR (42). ATF4 is known to directly bind and activate an ATF site upstream of the GADD34 promoter (36), however the role of GADD34 expression in the attenuation of hypoxia-induced eIF2α phosphorylation has not been addressed. Phosphorylation of eIF2α occurs upon acute exposure to hypoxic stress yet eIF2α phosphorylation appears to subside by 8h (29). Our data demonstrates that induction of GADD34 begins after 2hr of hypoxic stress and is strongly induced by 4hr (Figure 7). Furthermore, over expression of a COOH-truncated GADD34, which constitutively dephosphorylates eIF2α, demonstrated a severe inhibition in the induction of ATF4 during hypoxia (Figure 7). This suggests an important role for GADD34 as a negative feedback regulator, mediating eIF2α dephosphorylation and abrogating ATF4 expression during hypoxic stress (Figure 8). Protein synthesis inhibition and phosphorylation of eIF2α are transient in response to ER stress (45). Sustained eIF2α

phosphorylation is lethal both in cultured cells and in the in vivo neuronal response to ischemic stress (11). It has been suggested that the GADD34 negative feedback loop is necessary for cellular recovery following ER stress (42), as seen by a decrease in cell survival in cells expressing a GADD34 mutant lacking the COOH-terminal domain necessary for PP1 activation and eIF2α dephosphorylation. Additionally, it has been demonstrated that expression of a non-phosphorylatable eIF2α partially protects cells from apoptosis. Conversely, the expression of an eIF2α phosphormimetic (S51D) increased apoptotic cell death (58). The observation that the mechanism of translational inhibition during prolonged hypoxic exposure changes from a global inhibition through eIF2α phosphorylation to a selective inhibition of cap-dependent translation by preventing the formation of eIF4F complexes (Wouters, unpublished observations), presents the possibility of a molecular switch responsible for this response. The attenuation of eIF2α phosphorylation by GADD34 during hypoxia may play a role in this molecular switch.

Our experiments show that in response to severe hypoxic stress, the result of translational inhibition promotes the selective translation of several hypoxia responsive genes. The increase in translational efficiency of these genes at a time of global protein synthesis inhibition indicates the importance of rapid and reversible gene expression in response to hypoxic stress. The preferential translation of ATF4 and the analogous translational and transcriptional induction of other ER-resident proteins, suggests an integrated stress response involving an ER-generated signal and the cellular adaptation to hypoxia (Figure 8). Furthermore, induction of GADD34 and its role in the dephosphorylation of eIF2α

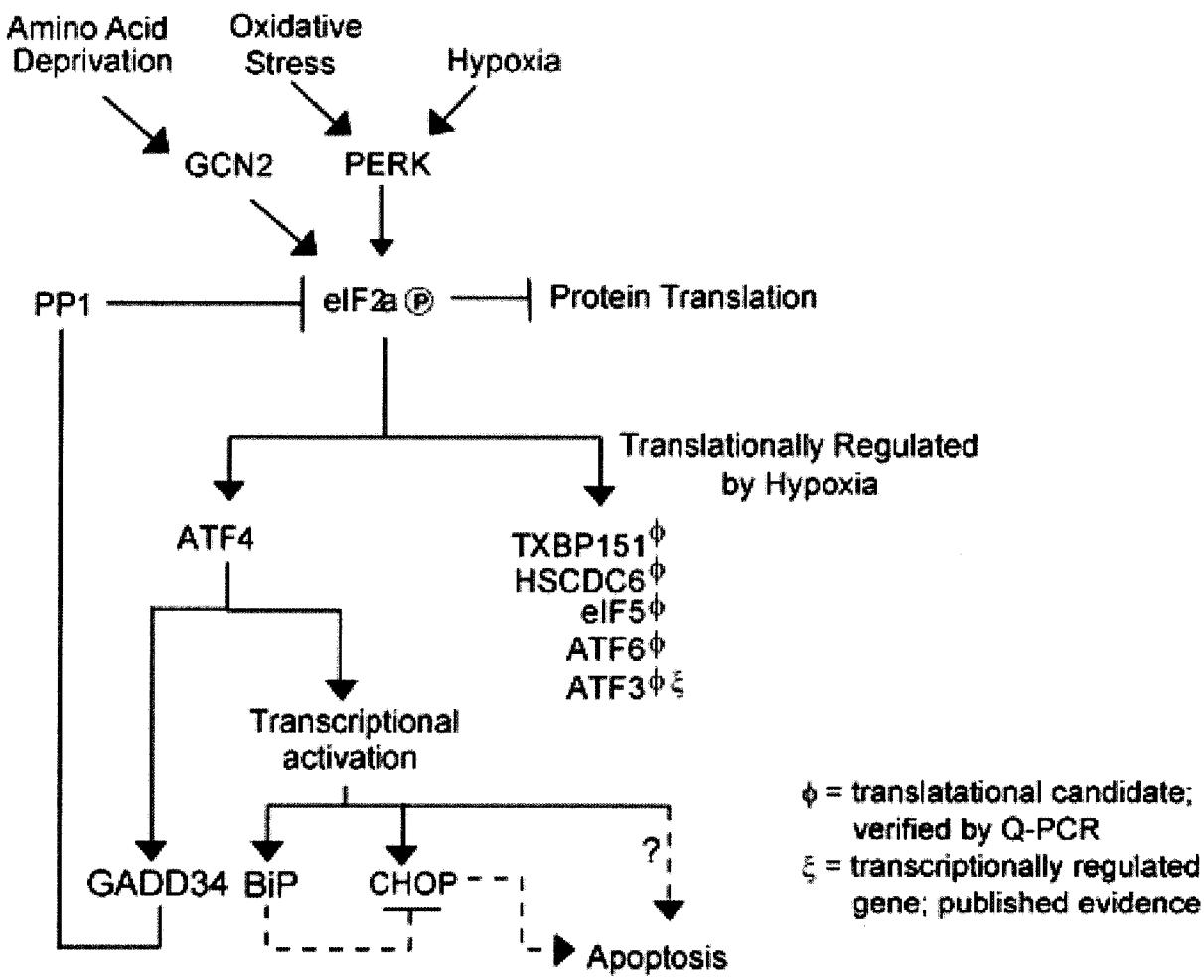
Amino Acid Deprivation
Oxidative Stress
Hypoxia
GCN2
PERK
PP1
eIF2a Ⓟ
Protein Translation
Translationally Regulated by Hypoxia
ATF4
TXBP151ϕ
HSCDC6ϕ
eIF5ϕ
ATF6ϕ
ATF3ϕξ
Transcriptional activation
GADD34
BiP
CHOP
?
Apoptosis
ϕ = translatational candidate; verified by Q-PCR
ξ = transcriptionally regulated gene; published evidence

Figure 8: Model depicting the role of ATF4 during Hypoxic stress

Hypoxia and Oxidative stress activate the eIF2α kinase PERK. Phosphorylation of eIF2α results in the global inhibition of protein translation. Some transcripts are able to escape this general control mechanism, such as ATF4, ATF6 and eIF5. Transcriptional induction of GADD34 results in the activation of PP1 and the dephosphorylation of eIF2α after prolonged exposure to hypoxia. Microarray data also support the notion that numerous ER-resident proteins are induced in response to hypoxic stress suggesting that cellular adaptation to hypoxic stress may rely on a integrated ER-generated stress signal.

may be an essential intermediate signal for the switch from the inhibition of global translation to a more selective inhibition of cap-dependent translation.

Understanding the molecular events that support the development of tumor cell resistance to hypoxia is imperative for the discovery of effective therapies. The ability of hypoxic tumor cells to simultaneously promote angiogenesis, metastasis, and glycolysis, substantiates the need of cellular adaptation for continued cell viability. Whether the ATF4 signaling pathway is a key element that promotes cell survival during hypoxia still needs to be determined. Interestingly, the over-expression of a novel hypoxia regulated gene, SKIP3, has been implicating in destabilization of ATF4 protein in multiple primary human tumors (3). The occurrence of deregulated ATF4 expression in primary cancers therefore implicates ATF4 signaling in tumor progression.

Acknowledgments

JB was supported by OGGST with funds raised from the Ottawa Regional Cancer Center Foundation. This work was supported by a grant from the National Cancer Institute of Canada (to JCB). Work done by DR and HPH was supported by NIH grants ES08681 and DK47119.

We thank Dr. D Stojdl for the critical reading of this manuscript.

References

1. **Ameri, K., C. E. Lewis, M. Raida, H. Sowter, T. Hai, and A. L. Harris.** 2003. Anoxic induction of ATF-4 via HIF-1 independent pathways of protein stabilization in human cancer cells. Blood.

2. **Bernstein, J., O. Sella, S. Y. Le, and O. Elroy-Stein.** 1997. PDGF2/c-sis mRNA leader contains a differentiation-linked internal ribosomal entry site (D-IRES). J Biol Chem **272:**9356-62.

3. **Bowers, A. J., S. Scully, and J. F. Boylan.** 2003. SKIP3, a novel Drosophila tribbles ortholog, is overexpressed in human tumors and is regulated by hypoxia. Oncogene **22:**2823-35.

4. **Brown, J. M., and A. J. Giaccia.** 1998. The unique physiology of solid tumors: opportunities (and problems) for cancer therapy. Cancer Res **58:**1408-16.

5. **Brown, J. M., and Q. T. Le.** 2002. Tumor hypoxia is important in radiotherapy, but how should we measure it? Int J Radiat Oncol Biol Phys **54:**1299-301.

6. **Bruick, R. K.** 2000. Expression of the gene encoding the proapoptotic Nip3 protein is induced by hypoxia. Proc Natl Acad Sci U S A **97:**9082-7.

7. **Carmeliet, P., Y. Dor, J. M. Herbert, D. Fukumura, K. Brusselmans, M. Dewerchin, M. Neeman, F. Bono, R. Abramovitch, P. Maxwell, C. J. Koch, P. Ratcliffe, L. Moons, R. K. Jain, D. Collen, E. Keshert, and E. Keshet.** 1998. Role of HIF-1alpha in hypoxia-mediated apoptosis, cell proliferation and tumour angiogenesis. Nature **394:**485-90.

8. **Coldwell, M. J., S. A. Mitchell, M. Stoneley, M. MacFarlane, and A. E. Willis.** 2000. Initiation of Apaf-1 translation by internal ribosome entry. Oncogene **19:**899-905.

9. **Connor, J. H., D. C. Weiser, S. Li, J. M. Hallenbeck, and S. Shenolikar.** 2001. Growth arrest and DNA damage-inducible protein GADD34 assembles a novel signaling complex containing protein phosphatase 1 and inhibitor 1. Mol Cell Biol **21:**6841-50.

10. **Cormier-Regard, S., S. V. Nguyen, and W. C. Claycomb.** 1998. Adrenomedullin gene expression is developmentally regulated and induced by hypoxia in rat ventricular cardiac myocytes. J Biol Chem **273:**17787-92.

11. **DeGracia, D. J., R. Kumar, C. R. Owen, G. S. Krause, and B. C. White.** 2002. Molecular pathways of protein synthesis inhibition during brain reperfusion: implications for neuronal survival or death. J Cereb Blood Flow Metab **22:**127-41.

12. **Douglas, R. M., T. Xu, and G. G. Haddad.** 2001. Cell cycle progression and cell division are sensitive to hypoxia in Drosophila melanogaster embryos. Am J Physiol Regul Integr Comp Physiol **280:**R1555-63.

13. **Feldser, D., F. Agani, N. V. Iyer, B. Pak, G. Ferreira, and G. L. Semenza.** 1999. Reciprocal positive regulation of hypoxia-inducible factor 1alpha and insulin-like growth factor 2. Cancer Res **59:**3915-8.

14. **Firth, J. D., B. L. Ebert, C. W. Pugh, and P. J. Ratcliffe.** 1994. Oxygen-regulated control elements in the phosphoglycerate kinase 1 and lactate dehydrogenase A genes: similarities with the erythropoietin 3' enhancer. Proc Natl Acad Sci U S A **91:**6496-500.

15. **Galban, S., J. Fan, J. L. Martindale, C. Cheadle, B. Hoffman, M. P. Woods, G. Temeles, J. Brieger, J. Decker, and M. Gorospe.** 2003. von Hippel-Lindau protein-mediated repression of tumor necrosis factor alpha translation revealed through use of cDNA arrays. Mol Cell Biol **23:**2316-28.

16. **Graeber TG, O. C., Jacks T, Housman DE, Koch CJ, Lowe SW, Giaccia AJ.** 1996. Hypoxia-mediated selection of cells with diminished apoptotic potential in solid tumours. Nature **379:**88-91.

17. **Harding, H. P., M. Calfon, F. Urano, I. Novoa, and D. Ron.** 2002. Transcriptional and translational control in the Mammalian unfolded protein response. Annu Rev Cell Dev Biol **18:**575-99.

18. **Harding HP, N. I., Zhang Y, Zeng H, Wek R, Schapira M, Ron D.** 2000. Regulated translation initiation controls stress-induced gene expression in mammalian cells. Mol Cell **6:**1099-108.

19. **Harding, H. P., I. Novoa, Y. Zhang, H. Zeng, R. Wek, M. Schapira, and D. Ron.** 2000. Regulated translation initiation controls stress-induced gene expression in mammalian cells. Mol Cell **6:**1099-108.

20. **Harding HP, Z. Y., Ron D.** 1999. Protein translation and folding are coupled by an endoplasmic-reticulum-resident kinase. nature **397:**271-4.

21. **Hartmann, A., M. Kunz, S. Kostlin, R. Gillitzer, A. Toksoy, E. B. Brocker, and C. E. Klein.** 1999. Hypoxia-induced up-regulation of angiogenin in human malignant melanoma. Cancer Res **59:**1578-83.

22. **Hinnebusch, A. G.** 1997. Translational regulation of yeast GCN4. A window on factors that control initiator-trna binding to the ribosome. J Biol Chem **272:**21661-4.

23. **Hochachka, P. W., L. T. Buck, C. J. Doll, and S. C. Land.** 1996. Unifying theory of hypoxia tolerance: molecular/metabolic defense and rescue mechanisms for surviving oxygen lack. Proc Natl Acad Sci U S A **93:**9493-8.

24. **Holcik, M., C. Lefebvre, C. Yeh, T. Chow, and R. G. Korneluk.** 1999. A new internal-ribosome-entry-site motif potentiates XIAP-mediated cytoprotection. Nat Cell Biol **1:**190-2.

25. **Iyer, N. V., L. E. Kotch, F. Agani, S. W. Leung, E. Laughner, R. H. Wenger, M. Gassmann, J. D. Gearhart, A. M. Lawler, A. Y. Yu, and G. L. Semenza.** 1998. Cellular and developmental control of O2 homeostasis by hypoxia-inducible factor 1 alpha. Genes Dev **12:**149-62.

26. **Jang, S. K., H. G. Krausslich, M. J. Nicklin, G. M. Duke, A. C. Palmenberg, and E. Wimmer.** 1988. A segment of the 5' nontranslated region of encephalomyocarditis virus RNA directs internal entry of ribosomes during in vitro translation. J Virol **62:**2636-43.

27. **Johannes, G., M. S. Carter, M. B. Eisen, P. O. Brown, and P. Sarnow.** 1999. Identification of eukaryotic mRNAs that are translated at reduced cap binding complex eIF4F concentrations using a cDNA microarray. Proc Natl Acad Sci U S A **96:**13118-23.

28. **Koong, A. C., N. C. Denko, K. M. Hudson, C. Schindler, L. Swiersz, C. Koch, S. Evans, H. Ibrahim, Q. T. Le, D. J. Terris, and A. J. Giaccia.** 2000. Candidate genes for the hypoxic tumor phenotype. Cancer Res **60:**883-7.

29. **Koumenis C, N. C., Koritzinsky M, Rastani S, Diehl A, Sonenberg N, Koromilas A, Wouters BG.** 2002. Regulation of protein synthesis by hypoxia via activation of

the endoplasmic reticulum kinase PERK and phosphorylation of the translation initiation factor eIF2alpha. Mol Cell Biol **22:**7405-16.

30. **Kozak, M.** 1999. Initiation of translation in prokaryotes and eukaryotes. Gene **234:**187-208.

31. **Kraggerud, S. M., J. A. Sandvik, and E. O. Pettersen.** 1995. Regulation of protein synthesis in human cells exposed to extreme hypoxia. Anticancer Res **15:**683-6.

32. **Lang, W. H., and R. H. Reeder.** 1993. The REB1 site is an essential component of a terminator for RNA polymerase I in Saccharomyces cerevisiae. Mol Cell Biol **13:**649-58.

33. **Lassot, I., E. Segeral, C. Berlioz-Torrent, H. Durand, L. Groussin, T. Hai, R. Benarous, and F. Margottin-Goguet.** 2001. ATF4 degradation relies on a phosphorylation-dependent interaction with the SCF(betaTrCP) ubiquitin ligase. Mol Cell Biol **21:**2192-202.

34. **Lefebvre, V. H., M. Van Steenbrugge, V. Beckers, M. Roberfroid, and P. Buc-Calderon.** 1993. Adenine nucleotides and inhibition of protein synthesis in isolated hepatocytes incubated under different pO2 levels. Arch Biochem Biophys **304:**322-31.

35. **Liebermann, D. A., and B. Hoffman.** 2002. Myeloid differentiation (MyD)/growth arrest DNA damage (GADD) genes in tumor suppression, immunity and inflammation. Leukemia **16:**527-41.

36. **Ma, Y., and L. M. Hendershot.** 2003. Delineation of a negative feedback regulatory loop that controls protein translation during endoplasmic reticulum stress. J Biol Chem **278:**34864-73.

37. **Macejak, D. G., and P. Sarnow.** 1991. Internal initiation of translation mediated by the 5' leader of a cellular mRNA. Nature **353:**90-4.

38. **Maxwell, P. H., C. W. Pugh, and P. J. Ratcliffe.** 2001. Activation of the HIF pathway in cancer. Curr Opin Genet Dev **11:**293-9.

39. **Mikulits, W., B. Pradet-Balade, B. Habermann, H. Beug, J. A. Garcia-Sanz, and E. W. Mullner.** 2000. Isolation of translationally controlled mRNAs by differential screening. Faseb J **14:**1641-52.

40. **Nielsen, F. C., L. Ostergaard, J. Nielsen, and J. Christiansen.** 1995. Growth-dependent translation of IGF-II mRNA by a rapamycin-sensitive pathway. Nature **377:**358-62.

41. **Novoa, I., H. Zeng, H. P. Harding, and D. Ron.** 2001. Feedback inhibition of the unfolded protein response by GADD34-mediated dephosphorylation of eIF2alpha. J Cell Biol **153:**1011-22.

42. **Novoa, I., Y. Zhang, H. Zeng, R. Jungreis, H. P. Harding, and D. Ron.** 2003. Stress-induced gene expression requires programmed recovery from translational repression. Embo J **22:**1180-7.

43. **O'Rourke, J. F., C. W. Pugh, S. M. Bartlett, and P. J. Ratcliffe.** 1996. Identification of hypoxically inducible mRNAs in HeLa cells using differential-display PCR. Role of hypoxia-inducible factor-1. Eur J Biochem **241:**403-10.

44. **Pettersen, E. O., N. O. Juul, and O. W. Ronning.** 1986. Regulation of protein metabolism of human cells during and after acute hypoxia. Cancer Res **46:**4346-51.

45. **Prostko, C. R., M. A. Brostrom, E. M. Malara, and C. O. Brostrom.** 1992. Phosphorylation of eukaryotic initiation factor (eIF) 2 alpha and inhibition of eIF-2B

in GH3 pituitary cells by perturbants of early protein processing that induce GRP78. J Biol Chem **267:**16751-4.

46. **Pyronnet, S., L. Pradayrol, and N. Sonenberg.** 2000. A cell cycle-dependent internal ribosome entry site. Mol Cell **5:**607-16.

47. **Rajasekhar, V. K., A. Viale, N. D. Socci, M. Wiedmann, X. Hu, and E. C. Holland.** 2003. Oncogenic Ras and Akt signaling contribute to glioblastoma formation by differential recruitment of existing mRNAs to polysomes. Mol Cell **12:**889-901.

48. **Richter, J. D.** 1993. Translational control in development: a perspective. Dev Genet **14:**407-11.

49. **Rosenwald, I. B., N. A. Setkov, V. N. Kazakov, J. J. Chen, A. G. Ryazanov, I. M. London, and O. I. Epifanova.** 1995. Transient inhibition of protein synthesis induces expression of proto-oncogenes and stimulates resting cells to enter the cell cycle. Cell Prolif **28:**631-44.

50. **Ruzinova, M. B., R. A. Schoer, W. Gerald, J. E. Egan, P. P. Pandolfi, S. Rafii, K. Manova, V. Mittal, and R. Benezra.** 2003. Effect of angiogenesis inhibition by Id loss and the contribution of bone-marrow-derived endothelial cells in spontaneous murine tumors. Cancer Cell **4:**277-89.

51. **Ryan, H. E., J. Lo, and R. S. Johnson.** 1998. HIF-1 alpha is required for solid tumor formation and embryonic vascularization. Embo J **17:**3005-15.

52. **Sella, O., G. Gerlitz, S. Y. Le, and O. Elroy-Stein.** 1999. Differentiation-induced internal translation of c-sis mRNA: analysis of the cis elements and their differentiation-linked binding to the hnRNP C protein. Mol Cell Biol **19:**5429-40.

53. **Semenza, G. L.** 2000. HIF-1 and human disease: one highly involved factor. Genes Dev **14:**1983-91.

54. **Semenza, G. L.** 1998. Hypoxia-inducible factor 1: master regulator of O2 homeostasis. Curr Opin Genet Dev **8:**588-94.

55. **Semenza, G. L., P. H. Roth, H. M. Fang, and G. L. Wang.** 1994. Transcriptional regulation of genes encoding glycolytic enzymes by hypoxia-inducible factor 1. J Biol Chem **269:**23757-63.

56. **Sheets, M. D., C. A. Fox, T. Hunt, G. Vande Woude, and M. Wickens.** 1994. The 3'-untranslated regions of c-mos and cyclin mRNAs stimulate translation by regulating cytoplasmic polyadenylation. Genes Dev **8:**926-38.

57. **Sivitz, W. I., D. D. Lund, B. Yorek, M. Grover-McKay, and P. G. Schmid.** 1992. Pretranslational regulation of two cardiac glucose transporters in rats exposed to hypobaric hypoxia. Am J Physiol **263:**E562-9.

58. **Srivastava, S. P., K. U. Kumar, and R. J. Kaufman.** 1998. Phosphorylation of eukaryotic translation initiation factor 2 mediates apoptosis in response to activation of the double-stranded RNA-dependent protein kinase. J Biol Chem **273:**2416-23.

59. **Stein, I., A. Itin, P. Einat, R. Skaliter, Z. Grossman, and E. Keshet.** 1998. Translation of vascular endothelial growth factor mRNA by internal ribosome entry: implications for translation under hypoxia. Mol Cell Biol **18:**3112-9.

60. **Stoneley, M., S. A. Chappell, C. L. Jopling, M. Dickens, M. MacFarlane, and A. E. Willis.** 2000. c-Myc protein synthesis is initiated from the internal ribosome entry segment during apoptosis. Mol Cell Biol **20:**1162-9.

61. **Takahashi, Y., S. Takahashi, Y. Shiga, T. Yoshimi, and T. Miura.** 2000. Hypoxic induction of prolyl 4-hydroxylase alpha (I) in cultured cells. J Biol Chem **275:**14139-46.

62. **Wood, S. M., M. S. Wiesener, K. M. Yeates, N. Okada, C. W. Pugh, P. H. Maxwell, and P. J. Ratcliffe.** 1998. Selection and analysis of a mutant cell line defective in the hypoxia-inducible factor-1 alpha-subunit (HIF-1alpha). Characterization of hif-1alpha-dependent and -independent hypoxia-inducible gene expression. J Biol Chem **273:**8360-8.

63. **Wouters, B. G., M. Koritzinsky, R. K. Chiu, J. Theys, J. Buijsen, and P. Lambin.** 2003. Modulation of cell death in the tumor microenvironment. Semin Radiat Oncol **13:**31-41.

64. **Wykoff, C. C., N. J. Beasley, P. H. Watson, K. J. Turner, J. Pastorek, A. Sibtain, G. D. Wilson, H. Turley, K. L. Talks, P. H. Maxwell, C. W. Pugh, P. J. Ratcliffe, and A. L. Harris.** 2000. Hypoxia-inducible expression of tumor-associated carbonic anhydrases. Cancer Res **60:**7075-83.

APPENDIX A:
ER STRESS-REGULATED TRANSLATION INCREASES TOLERANCE TO EXTREME HYPOXIA AND PROMOTES TUMOR GROWTH

Contribution to the Collaboration

Our contribution to this manuscript included providing data from our microarray analaysis of polysome-associated transcripts from 16hr hypoxia-treated HeLa cells. Our microarray analysis and identification that multiple UPR induced genes are induced during hypoxia supported Dr. Koumenis's findings that hypoxic stress activates the UPR, and that this activation has important consequences for cellular adaptation and continued cell viability. The written contribution to this manuscript was completed by J. Blais, including a northern blot analysis of polysome-fractionated RNAs that was removed from the final draft of the manuscript.

Summary

The authors of this paper demonstrate that severe hypoxic stress activates the ISR, one branch of the UPR, both in cultured cells and in xenograft tumor models in nude mice. Cells harboring mutations that result in the inactivation of the UPR, including $PERK^{-/-}$ MEFs, and cells that constitutively express dn-PERKΔC and $eIF2\alpha^{S51A}$ demonstrate an overt sensitivity to hypoxic stress. Moreover the observation that tumors derived from these mutant cell lines are smaller and display higher levels of apoptosis suggests that activation of the ISR is required for tumor cell adaptation to hypoxic stress.

The EMBO Journal (2005) 24, 3470–3481 | © 2005 European Molecular Biology Organization | All Rights Reserved 0261-4189/05
www.embojournal.org

THE
EMBO
JOURNAL

ER stress-regulated translation increases tolerance to extreme hypoxia and promotes tumor growth

Meixia Bi[1], Christine Naczki[1], Marianne Koritzinsky[2], Diane Fels[1,3], Jaime Blais[4], Nianping Hu[1], Heather Harding[5], Isabelle Novoa[5], Mahesh Varia[6], James Raleigh[6], Donalyn Scheuner[7], Randal J Kaufman[7], John Bell[4], David Ron[5], Bradly G Wouters[2] and Constantinos Koumenis[1,3,8,*]

[1]Department of Radiation Oncology, Wake Forest University School of Medicine, Winston-Salem, NC, USA, [2]Department of Radiation Oncology, GROW Research Institute, University of Maastricht, Maastricht, The Netherlands, [3]Department of Cancer Biology, Wake Forest University School of Medicine, Winston-Salem, NC, USA, [4]Ottawa Regional Cancer Center, Ontario, Canada, [5]Skirball Institute of Biomolecular Medicine, New York University School of Medicine, New York, NY, USA, [6]Department of Radiation Oncology, University of North Carolina School of Medicine, Chapel Hill, NC, USA, [7]Howard Hughes Medical Institute and Department of Biological Chemistry, University of Michigan Medical Center, Ann Arbor, MI, USA and [8]Department of Neurosurgery, Wake Forest University School of Medicine, Winston-Salem, NC, USA

Tumor cell adaptation to hypoxic stress is an important determinant of malignant progression. While much emphasis has been placed on the role of HIF-1 in this context, the role of additional mechanisms has not been adequately explored. Here we demonstrate that cells cultured under hypoxic/anoxic conditions and transformed cells in hypoxic areas of tumors activate a translational control program known as the integrated stress response (ISR), which adapts cells to endoplasmic reticulum (ER) stress. Inactivation of ISR signaling by mutations in the ER kinase PERK and the translation initiation factor eIF2α or by a dominant-negative PERK impairs cell survival under extreme hypoxia. Tumors derived from these mutant cell lines are smaller and exhibit higher levels of apoptosis in hypoxic areas compared to tumors with an intact ISR. Moreover, expression of the ISR targets ATF4 and CHOP was noted in hypoxic areas of human tumor biopsy samples. Collectively, these findings demonstrate that activation of the ISR is required for tumor cell adaptation to hypoxia, and suggest that this pathway is an attractive target for antitumor modalities.

The EMBO Journal (2005) 24, 3470–3481. doi:10.1038/sj.emboj.7600777; Published online 8 September 2005
Subject Categories: proteins; molecular biology of disease
Keywords: apoptosis; ATF4; endoplasmic reticulum; hypoxia; PERK

*Corresponding author. Departments of Radiation Oncology, Cancer Biology and Neurosurgery, NRC, Room 411, Wake Forest University School of Medicine, Medical Center Blvd., Winston-Salem, NC 27157, USA. Tel.: +1 336 713 7637; Fax: +1 336 713 7639; E-mail: ckoumeni@wfubmc.edu

Received: 24 March 2005; accepted: 19 July 2005; published online: 8 September 2005

Introduction

The development of fluctuating hypoxic and anoxic regions in tumors has profound consequences for malignant progression, response to therapy and overall patient survival (Hockel and Vaupel, 2001). Elucidating the processes that enable tumor cells to adapt to the unfavorable conditions of hypoxia is critical for understanding malignant progression and for developing more effective antitumor modalities. The hypoxia-inducible factor 1 (HIF-1) plays a key role in tumor cell adaptation to hypoxia by regulating the expression of over 60 genes involved in angiogenesis, anaerobic glycolysis and cell survival (Ratcliffe *et al*, 1998; Semenza, 2000). Loss-of-function studies indicate that, in most cases, HIF-1 promotes overall tumor growth (Maxwell *et al*, 1997; Ryan *et al*, 2000). However, the role of HIF-1 is complex and may be dependent on the tumor microenvironment (Carmeliet *et al*, 1998; Blouw *et al*, 2003).

The hypoxic cell also elicits additional, HIF-1-independent adaptive responses that contribute to increased survival under low oxygen conditions. An immediate reaction to hypoxia is a reduction in the rates of global protein synthesis that is thought to reduce energy demands when oxygen and ATP levels are low (Hochachka *et al*, 1996). This translational inhibition appears to occur in distinct phases and to involve multiple pathways. We have previously shown that hypoxia rapidly increases phosphorylation of the translation initiation factor eIF2α through activation of the endoplasmic reticulum (ER) kinase PERK (Koumenis *et al*, 2002; Blais *et al*, 2004). These events serve two major functions in a cell experiencing ER stress. The first is to rapidly downregulate protein synthesis, which reduces the ER protein load and leads to lower energy expenditure, since both protein synthesis and protein folding are ATP-requiring processes (Dorner *et al*, 1990; Shi *et al*, 1998; Harding *et al*, 2000b). The second is to upregulate genes that promote amino-acid sufficiency and redox homeostasis (Harding *et al*, 2003), thereby further promoting cell survival. Some, but not all of the effects of PERK are mediated by the transcription factor ATF4, which is translationally upregulated by ER stress in an eIF2α phosphorylation-dependent manner (Harding *et al*, 2000a, 2003). This pathway, known as the integrated stress response (ISR) (Ron, 2002), constitutes one arm of a larger coordinated program called the unfolded protein response (UPR), which facilitates the cell to adapt to ER stress. Cells with compromised PERK and eIF2α signaling are substantially more sensitive to ER-induced cell death than wild-type cells (Harding *et al*, 2000b, 2001; Scheuner *et al*, 2001; Zhang *et al*, 2002).

Recently, it was reported that hypoxia upregulates ATF4 in a PERK-dependent manner (Blais *et al*, 2004) and that ATF4 levels are increased by anoxic stress and in human tumors (Ameri *et al*, 2004). These findings prompted us to investigate the physiological role for the ISR in cellular adaptation to hypoxia *in vitro* and in tumor development *in vivo*. We report that hypoxia/anoxia activates the ISR pathway *in vitro* and

in vivo, and that several proteins previously implicated in the UPR are also upregulated by hypoxia. Expression of ATF4 and CHOP colocalizes with hypoxic areas of primary human tumors and animal xenografts, and inactivation of the ISR compromises cell survival during hypoxia *in vitro* and *in vivo* and significantly impairs tumor growth. These findings establish the ISR as an important mediator of hypoxia tolerance and tumor growth, and raise the possibility that the ISR may be an attractive target for antitumor modalities.

Results

Hypoxic/anoxic stress induces expression of ISR genes in a PERK- and eIF2α-phosphorylation-dependent manner

To investigate the effects of hypoxia on the expression of ISR-related genes, mouse embryonic fibroblasts (MEFs) from $PERK^{+/+}$ and $PERK^{-/-}$ animals were exposed to extreme hypoxia ($\leqslant 0.02\%$) or were treated with thapsigargin, an inhibitor of the SERCA (Ca^{2+}-ATPase) pump and potent ER stressor (*Note*: for brevity, hypoxia in the text denotes extreme hypoxia unless otherwise noted). Consistent with previous findings (Koumenis *et al*, 2002), hypoxia and thapsigargin caused a time-dependent increase in PERK autophosphorylation and eIF2α phosphorylation in $PERK^{+/+}$ MEFs (results not shown). Phosphorylation of eIF2α stimulates translational upregulation of ATF4, which activates the expression of downstream targets involved in the UPR, such as CHOP. As shown in Figure 1A, ATF4 levels increased by hypoxia and thapsigargin in the $PERK^{+/+}$ MEFs, whereas this increase was transient and considerably attenuated in $PERK^{-/-}$ MEFs. Induction of CHOP did not occur until after 16 h of hypoxia, reflecting a requirement for ATF4 accumulation. BiP was not significantly increased by hypoxia. Hypoxia-induced ATF4 accumulation occurred primarily at the post-transcriptional level, because ATF4 mRNA levels were not upregulated in hypoxic $PERK^{+/+}$ MEFs (Figure 1B). CHOP and BiP mRNA levels were substantially increased by hypoxia and by thapsigargin in $PERK^{+/+}$ and $PERK^{-/-}$ MEFs. The increase in CHOP was higher after 16 h of hypoxia in the $PERK^{+/+}$ cells, consistent with the higher levels of ATF4 protein in these cells, but PERK status had no effect on the increase in BiP mRNA levels.

Although hypoxia induced a largely PERK-independent increase in CHOP mRNA, there was a strong PERK dependence on CHOP protein accumulation, suggesting that the translational efficiency of CHOP mRNA might be regulated in a PERK-dependent manner. Thus, we analyzed the levels of both overall and gene-specific translation in the $PERK^{+/+}$ and $PERK^{-/-}$ cell lines. We have previously shown that inhibition of global translation during hypoxia is dependent on PERK at early times after hypoxia (<8 h), but, after longer

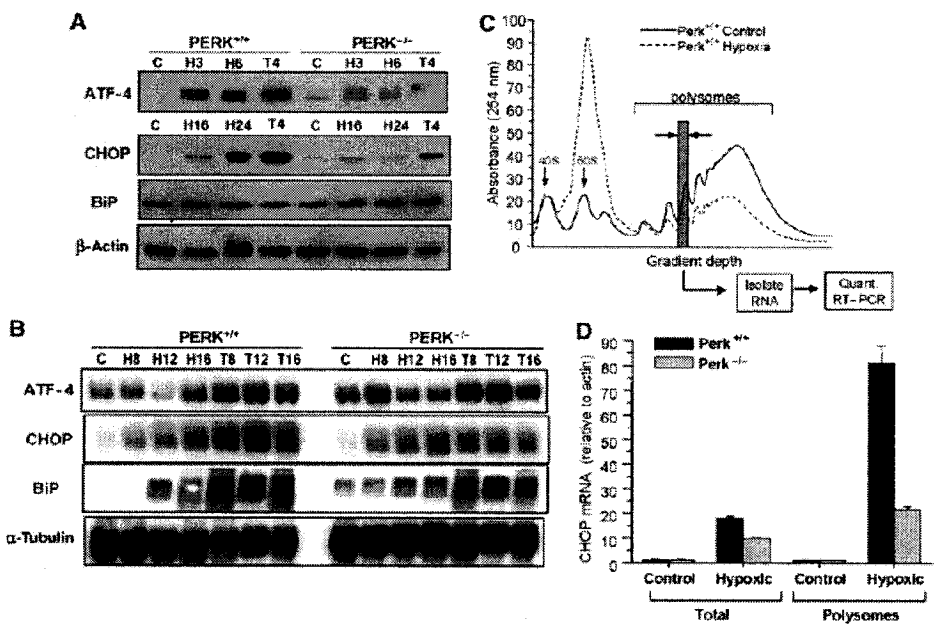

Figure 1 Extreme hypoxia induces ATF4 and CHOP upregulation in a PERK-dependent manner. $PERK^{+/+}$ and $PERK^{-/-}$ MEFs were exposed to $\leqslant 0.02\%$ O_2 or treated with 1 μM thapsigargin for the times indicated. (**A**) Immunoblots with anti-ATF4, anti-CHOP, anti-BiP and anti-β-actin (loading control). Different time points are used since induction of ATF4 occurs much earlier than CHOP or BiP. (**B**) Northern blot analysis of UPR mRNAs following hypoxia and thapsigargin treatments. $PERK^{+/+}$ and $PERK^{-/-}$ MEFs were treated as in (**A**). Blotting for α-tubulin was used as a loading control. (**C**) Translation efficiency of CHOP mRNA following hypoxia. $PERK^{+/+}$ and $PERK^{-/-}$ MEFs were treated as in (**A**) and lysates were subjected to sucrose gradient sedimentation. Polysome profiles shown are from cell lysates of aerobic and hypoxic $PERK^{+/+}$ cells. The positions of the 40S and 60S subunits as well as the polysomal RNA are indicated. (**D**) The amounts of CHOP, β-actin and 18S mRNA were determined by real-time quantitative PCR in each of the polysome fractions. The gray column indicates the polysome fraction used for quantitative PCR. Values plotted represent the total amount of CHOP mRNA found within the polysomes relative to β-actin. Also shown is the total cellular amount of CHOP found in the $PERK^{+/+}$ and $PERK^{-/-}$ MEFs normalized to β-actin as determined by quantitative RT–PCR.

periods of hypoxia translation, is inhibited in both PERK$^{+/+}$ and PERK$^{-/-}$ cells (Koumenis *et al*, 2002). As shown in Figure 1C, 16 h of hypoxia caused a strong inhibition of translation initiation in the PERK$^{+/+}$ cells, as evident by a reduction in polysomal RNA and an increase in free monosome and ribosome subunits. A similar inhibition was observed in PERK$^{-/-}$ cells after 16 h of hypoxia; however, following 2 h hypoxia, translation was inhibited much more strongly in the PERK$^{+/+}$ compared to PERK$^{-/-}$ cells (data not shown). To explore potential PERK-dependent differences in specific CHOP mRNA translation following prolonged hypoxia, polysome fractions were collected and individually analyzed by quantitative RT–PCR for the levels of 18S, actin and CHOP. In both PERK$^{+/+}$ and PERK$^{-/-}$ cells, the levels of actin associated with polysomes decreased during hypoxia in accordance with the drop in overall translation. In contrast, CHOP mRNA levels increased substantially within the polysomes. Notably, the relative increase in CHOP mRNA within the polysomes was approximately four times higher in the PERK$^{+/+}$ cells than in the PERK$^{-/-}$ cells (Figure 1D). Thus, in addition to an increase in CHOP mRNA, there is a significant PERK dependence on polysome association of CHOP mRNA during hypoxia.

Similarly, by coupling ribosome fractionation with microarray gene analysis, we identified changes in steady-state gene expression and translation-mediated changes in HeLa cells following 16 h of extreme hypoxia. We found that the mRNA levels of genes associated with the UPR (including ORP150, heme oxygenase; HO-1 and MIF1) were not only substantially induced by hypoxia but also remained efficiently translated, as indicated by their association with high-molecular-weight polysomes (Figure S1). Conversely, the free total and polysome-bound mRNA levels of genes associated with other types of stress, such as the heat-shock response (HSF2, HSP70) or of constitutively synthesized genes (ribosomal protein S20 and HSC70), were either only weakly upregulated or substantially downregulated by hypoxia.

Prolonged hypoxia induces apoptosis in a PERK-dependent manner

Cells with a compromised UPR are more susceptible to ER stress-induced apoptosis compared to cells with an intact UPR (Kaufman, 2002; Ma and Hendershot, 2004). We previously reported that PERK$^{-/-}$ cells exhibit reduced clonogenic survival under extreme hypoxia compared to PERK$^{+/+}$ cells (Koumenis *et al*, 2002). To determine whether the difference in clonogenic survival was due to differential apoptotic sensitivity, we assayed for cleavage of caspase-12, caspase-3 and PARP following exposure to extreme hypoxia. Caspase-12, associated with the ER, is cleaved during ER stress and this event can be used as an indicator of UPR activation (Nakagawa *et al*, 2000; Rao *et al*, 2001). Exposure of PERK$^{-/-}$ cells to hypoxia resulted in higher levels of caspase-12 cleavage (as evident by the disappearance of the procaspase-12 form) by 9 h of hypoxia compared to PERK$^{+/+}$ cells (Figure 2A). However, caspase-12$^{-/-}$ MEFs were as sensitive as caspase-12$^{+/+}$ MEFs under hypoxia (results not shown), indicating that, while caspase-12 processing is a marker of hypoxia-induced ER stress, it cannot account for the higher sensitivity of PERK$^{-/-}$ cells to hypoxia. Activation of caspase-3, a terminal caspase and proteolytic processing of PARP, a marker for late-stage apoptosis, followed a similar

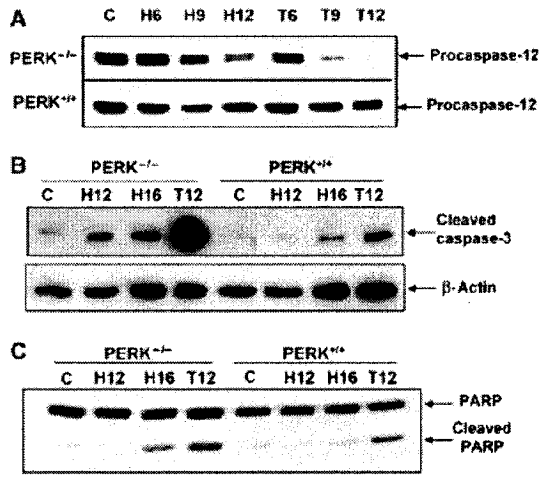

Figure 2 PERK confers resistance to hypoxia-induced apoptosis. (A–C) PERK$^{+/+}$ and PERK$^{-/-}$ MEFs were exposed to $\leqslant$0.02% O_2 or treated with 500 nM thapsigargin for the indicated times before immunoblotting with antibodies specific for procaspase-12 (A), cleaved caspase-3 or anti-β-actin (B), or cleaved and uncleaved PARP (C).

pattern with higher levels of cleaved caspase-3 and PARP in the PERK$^{-/-}$ compared to PERK$^{+/+}$ cells (Figure 2B and C) following treatments with hypoxia and thapsigargin. These results indicate that PERK contributes to cellular survival under prolonged hypoxia.

PERK contributes to tumor growth in vivo

The increased sensitivity of PERK$^{-/-}$ cells to hypoxic stress *in vitro* suggested that PERK might play a role in tumor growth *in vivo*. To investigate this possibility, PERK$^{+/+}$ and PERK$^{-/-}$ MEFs were immortalized with SV40 large/small T-antigen and transformed with oncogenic Ki-RasV12. This transformation did not cause any overt morphological differences between the two cell lines (data not shown). Phosphorylation of ERK1 and ERK2 was analyzed in PERK$^{+/+}$ and PERK$^{-/-}$ MEFs with or without Ki-RasV12. As expected, expression of Ki-RasV12 increased ERK phosphorylation without affecting the levels of total ERK1 and ERK2. The extent of this phosphorylation was comparable in PERK$^{+/+}$ and PERK$^{-/-}$ MEFs (Figure 3A), suggesting that PERK does not influence Ki-RasV12 signaling. Further experiments demonstrated that PERK status did not affect the *in vitro* growth kinetics or the ability of the Ki-RasV12-transformed cell lines to grow colonies in soft agar (Figures 3B and C).

Equal numbers of these transformed MEFs were injected in the flanks of nude mice and tumor growth was monitored over a period of 3–4 weeks. Tumors from PERK$^{+/+}$.RasV12 MEFs grew faster and larger compared to those from the PERK$^{-/-}$.RasV12 MEFs (Figures 3D and E). Several PERK$^{-/-}$ tumors displayed an opaque morphology with apparent necrosis of the skin when the experiment was terminated (Figure 3D, top). Analysis of eIF2α phosphorylation status in homogenized tissue revealed markedly higher levels of phosphorylated eIF2α in PERK$^{+/+}$ tumors compared to PERK$^{-/-}$

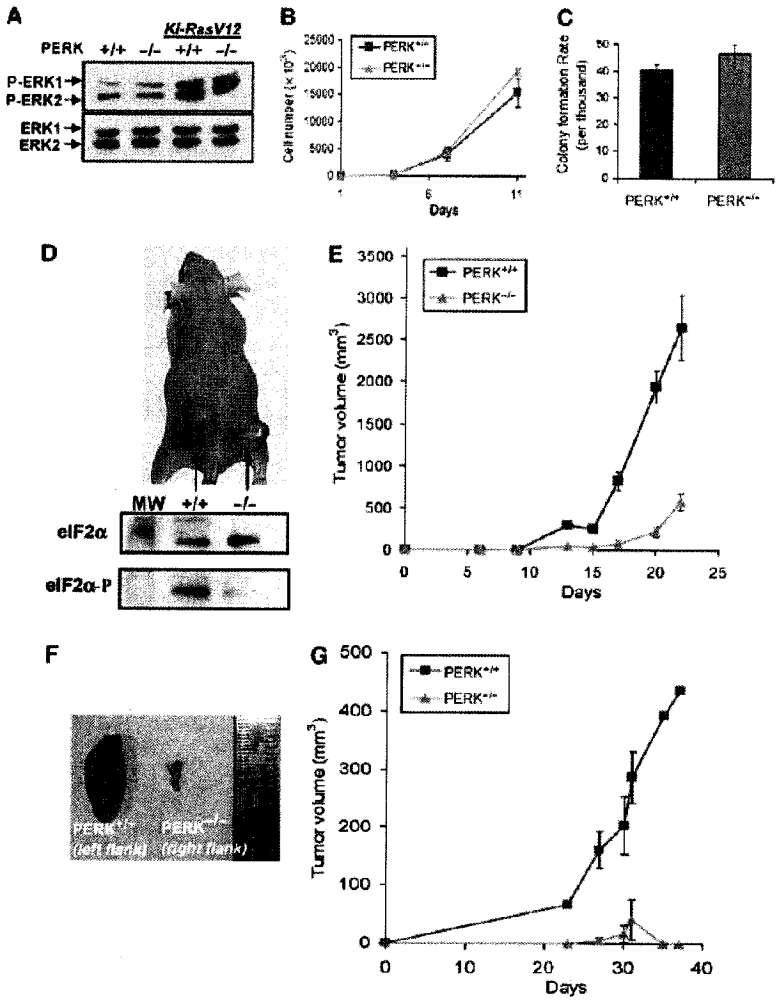

Figure 3 PERK affects the rate of tumor growth *in vivo*. (A) Immunoblot of untransformed PERK$^{+/+}$ and PERK$^{-/-}$ MEFs, and MEFs stably transformed with Ki-RasV12, using a phospho-specific anti-ERK1/2 antibody (top), or an antibody against total ERK1 and ERK2 (bottom). (B) Growth rates of Ki-RasV12-transformed PERK$^{+/+}$ and PERK$^{-/-}$ MEFs *in vitro*. (C) PERK$^{+/+}$.Ki-RasV12 and PERK$^{-/-}$.Ki-RasV12 MEFs form colonies in soft agar at similar rates. (D) Top, picture of a representative nude mouse injected with PERK$^{+/+}$.Ki-RasV12 MEFs (left flank) and PERK$^{-/-}$.Ki-RasV12 MEFs (right flank) with 3×10^6 cells/site at 22 days following injection. The bottom panel shows eIF2α phosphorylation levels from the excised tumors shown in the top panel. Tumor sections were homogenized and immunoblotted for phospho-eIF2α and total-eIF2α. (E) PERK$^{+/+}$ (blue line and squares) and PERK$^{-/-}$ (green line and triangles) tumor volumes from seven animals monitored over a period of 22 days following inoculation (mean±s.e.). (F) Tumors from a mouse injected with clone #2 PERK$^{+/+}$.Ki-RasV12 MEFs (left) or clone #2 PERK$^{-/-}$.Ki-RasV12 MEFs (right). (G) Growth of PERK$^{+/+}$.Ki-RasV12#2 (blue line and rectangles) and PERK$^{-/-}$.Ki-RasV12#2 (green line and triangles) tumors ($N=4$) monitored over a period of 37 days (mean±s.e.).

tumors, indicating PERK-dependent eIF2α phosphorylation caused by the tumor microenvironment (Figure 3D, bottom). On average, PERK$^{+/+}$ tumors grew approximately six times larger than PERK$^{-/-}$ tumors after 22 days (average 2647±573 versus 391±101 mm^3, $N=7$) (Figure 3E). Similar results were obtained when Ha-RasV12 instead of Ki-RasV12 was used to transform PERK$^{+/+}$ and PERK$^{-/-}$ MEFs (data not shown).

To minimize the effect of random clonal variation in this experimental system, we also examined the *in vivo* growth of individual clones of Ki-RasV12-transfected cells. Although the growth kinetics of PERK$^{+/+}$.Ki-RasV12.#2 and PERK$^{-/-}$.Ki-RasV12.#2 MEFs were indistinguishable *in vitro* (results not shown), the PERK$^{-/-}$ tumors failed to grow beyond a few mm in size (Figures 3F and G). Collectively, these results indicate that PERK status affects tumor growth in a manner that is independent of *in vitro* growth characteristics, suggesting that the differential response of these cells to the tumor microenvironment must play a critical role in tumor development.

PERK confers resistance to hypoxia-induced apoptosis in vivo

The compromised ability of PERK$^{-/-}$ cells to tolerate hypoxic conditions *in vitro* and the slower growth of PERK$^{-/-}$ tumors suggested that the presence of PERK increased the ability of

transformed MEFs to survive tumor hypoxia, resulting in tumors with larger hypoxic areas. We therefore studied the patterns of cell death in relation to areas of hypoxia within $PERK^{+/+}$ and $PERK^{-/-}$ tumor sections. The hypoxia marker EF-5 is metabolized and forms macromolecular adducts preferentially in hypoxic areas that can be visualized using a Cy3-labeled anti-EF5 adduct antibody. Nude mice with $PERK^{+/+}$.Ki-RasV12 and $PERK^{-/-}$.Ki-RasV12 flank tumors were injected with EF-5 and sections were co-stained with Cy3-labeled anti-EF5 antibody and with an anti-cleaved caspase-3 antibody. The patterns of EF-5 and caspase-3 staining in the $PERK^{+/+}$ and $PERK^{-/-}$ tumors were quite distinct. In $PERK^{-/-}$ tumors, areas of hypoxia were fewer and smaller compared to the $PERK^{+/+}$ tumors (Figure 4A). Image analysis revealed that ~70% of apoptotic cells in four distinct fields colocalized with hypoxic areas (Figure 4B). In contrast, $PERK^{+/+}$ tumors exhibited more extensive areas of hypoxia that were largely devoid of apoptotic cells, with only ~22% apoptotic cells being within the hypoxic areas. Strong staining for cleaved caspase-3 was observed only in areas surrounded by a 'hypoxic ring', which is indicative of a necrotic tumor area. Similar results were obtained from two independent tumors of each cell line. These results suggest that $PERK^{+/+}$.Ki-RasV12 MEFs can better tolerate hypoxia *in vivo*, resulting in larger tumors with extensive hypoxic areas. In contrast, $PERK^{-/-}$.Ki-RasV12 MEFs, which are more sensitive to hypoxia, form smaller tumors with fewer hypoxic areas. Since hypoxic areas *in vivo* are usually accompanied by conditions of low pH and/or growth factor levels, it is possible that the sensitivity of the $PERK^{-/-}$ cells *in vivo* may be due not only to low oxygen levels but also to these factors as well.

Cells with a nonphosphorylatable 'knock-in' mutation of eIF2α display attenuated induction of ISR genes under hypoxia, and are sensitive to hypoxic stress

Although eIF2α phosphorylation is a primary target of activated PERK, it has been suggested that PERK phosphorylation may activate additional targets (Cullinan *et al*, 2003). To further study the role of the ISR in tumor cell adaptation to hypoxic stress, we used MEFs in which the endogenous eIF2α gene has been genetically replaced by a nonphosphorylatable (S51A) allele. These cells display dramatically reduced downstream effector responses to ER stress and other stresses that induce eIF2α phosphorylation (Scheuner *et al*, 2001). Exposure of these cells to hypoxia failed to induce eIF2α

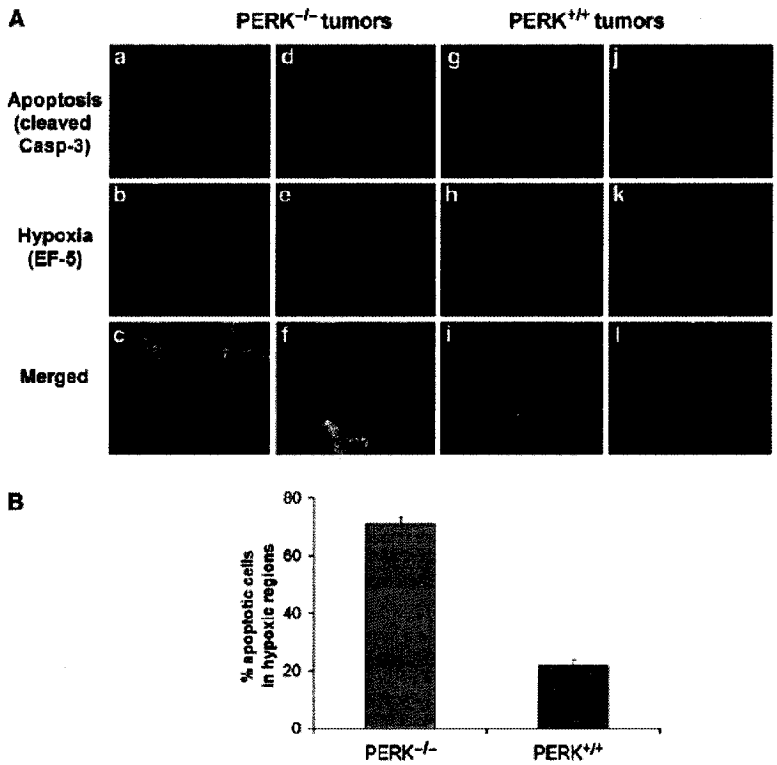

Figure 4 Hypoxic areas in $PERK^{-/-}$ but not in $PERK^{+/+}$ tumors overlap with areas of apoptosis. (A) Sections of $PERK^{-/-}$ tumors (a–f) or $PERK^{+/+}$ tumors (g–l) were incubated with a Cy3-conjugated antibody to EF-5 adducts (hypoxia, red) (b, e and h, k), followed by incubation with a FITC-conjugated anti-cleaved caspase-3 antibody (apoptosis, green) (a, d and g, j). Panels c, f and i, l are merged images showing both apoptotic and hypoxia areas. Two different $PERK^{-/-}$ (a–c and d–f) and $PERK^{+/+}$ (g–i and j–l) tumor sections are shown. Bar = 15 μm (a–i) and 60 μm (j–l). (B) Quantitation of four independent field images from $PERK^{+/+}$ or $PERK^{-/-}$ tumors. The number of apoptotic cells in hypoxic (EF-5 positive) and normoxic (EF-5 negative) areas of each image were automatically counted and expressed as a percentage of the total number of apoptotic cells in the image. Error bars represent s.e. values.

phosphorylation (Figure 5A) and induction of ISR proteins ATF4 and CHOP by hypoxia was significantly attenuated (Figure S2A). At the mRNA level, hypoxia again failed to induce a significant upregulation of ATF4 (Figure S2B), further confirming that the induction of ATF4 by hypoxia is post-transcriptional (Blais *et al*, 2004).

The S51A knock-in mice display striking phenotypic similarities with the PERK knockout mice, particularly in the sensitivity of cells with specialized and increased secretory capacity to endogenous ER stress (Harding *et al*, 2001; Scheuner *et al*, 2001). To determine whether similar parallels exist in the response of $PERK^{-/-}$ and S51A cells to hypoxic stress, we transformed S51A and wild-type MEFs (WT-MEFs) with SV40 large/small T-antigen and mutant Ha-RasV12 and tested their survival under hypoxia. S51A cells exhibited progressively higher apoptotic sensitivity to hypoxia compared to WT-MEFS (Figure 5B). Furthermore, exposure of WT-MEFs to 24 and 48 h of hypoxia resulted in 16 and 60% decreases in clonogenic survival, respectively, whereas S51A-transformed MEFs were significantly more sensitive, exhibiting 60 and 100% decreases in survival, respectively (Figure 5C and D). The increased levels of cell death in the S51A cells were accompanied by higher levels of cleaved caspase-3 and PARP at 16 and 24 h of hypoxia compared to WT-MEFs (Figure 5E). Thus, the higher sensitivity of S51A cells to hypoxia compared to WT cells is similar to that of the $PERK^{-/-}$ cells and parallels the sensitivity of S51A cells to other ER stressors like thapsigargin (Harding *et al*, 2000b).

Phosphorylation of eIF2α affects tumor growth and ISR signaling in vivo

As was the case with $PERK^{-/-}$ and $PERK^{+/+}$ transformed MEFs, *in vitro* growth rates of SV40/Ha-RasV12-transformed WT and S51A MEFs were very similar (Figure S2C). However, when injected into nude mice, the S51A tumors grew slower during the first 14 days following inoculation, and, between days 14 and 21, the majority of S51A tumors developed areas of apparent necrosis (Figure 6A) and the animals had to be euthanized. At that time, the average weight of S51A tumors was approximately half of that of WT tumors (179 ± 26 versus 318 ± 77 mg, respectively; $P < 0.05\%$) (Figure 6B). Similar to the $PERK^{-/-}$ tumors, the S51A tumors exhibited extensive colocalization of apoptotic and hypoxic areas (Figure S3A, a–f and m, n), whereas hypoxic areas of WT tumors were largely devoid of apoptotic cells and apoptosis was confined to necrotic areas (Figure S3A, g–l and o, p). Quantitative image analysis showed that in WT tumors only 17% of apoptotic cells were in hypoxic regions, compared to 80% in tumors from the S51A cells (Figure S3B). Furthermore, the difference in tumor weight was not due to differences in the angiogenic response to hypoxia, since secretion of VEGF was not statistically different between the two cell types (Figure 6C). To determine whether the induction of the ISR *in vivo* is eIF2α-dependent, we analyzed the induction of ATF4 in the two tumor types. WT tumors displayed areas of ATF4 expression that colocalized with hypoxia, whereas the S51A tumors were devoid of any significant staining for ATF4 (Figure 6D). We failed to detect any significant expression of ATF4 in 6/6 S51A sections obtained from three different mouse tumors. These results indicate that eIF2α phosphorylation is required for hypoxic induction of ATF4 *in vivo*. Thus, the phenotype of S51A tumors paralleled that of the

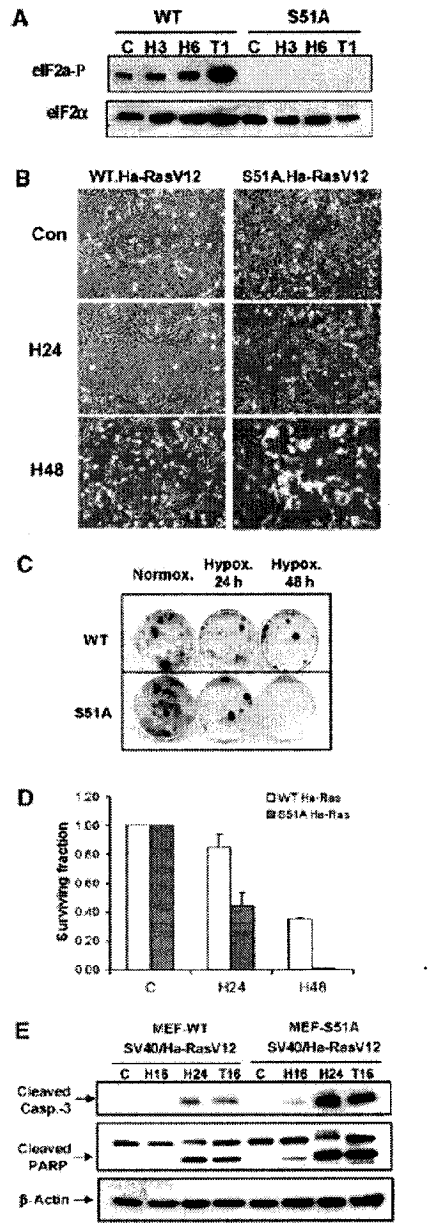

Figure 5 MEFs with nonphosphorylatable eIF2α mutant are more sensitive to extreme hypoxia than WT MEFs. (A) WT and S51A MEFs were exposed to $\leqslant 0.02\%$ O_2 or treated with 1 μM thapsigargin before immunoblotting with anti-phospho-eIF2α or anti-total-eIF2α antibodies. (B) WT and S51A MEFs transformed with SV40/Ha-RasV12 were exposed to extreme hypoxia ($\leqslant 0.02\%$ O_2) and then photographed using phase-contrast microscopy. (C) Reduced clonogenic survival of S51A MEFs after hypoxia compared to WT MEFs. (D) Reduced survival of S51A MEFs after hypoxia compared to WT MEFs, as measured by clonogenic survival assay. Cells were treated as in (C). Experiments were performed in triplicate and error bars represent standard errors. (E) WT and S51A MEFS transformed with SV40/Ha-RasV12 were exposed to hypoxia or treated with 500 nM thapsigargin before immunoblotting for cleaved caspase-3, PARP or β-actin.

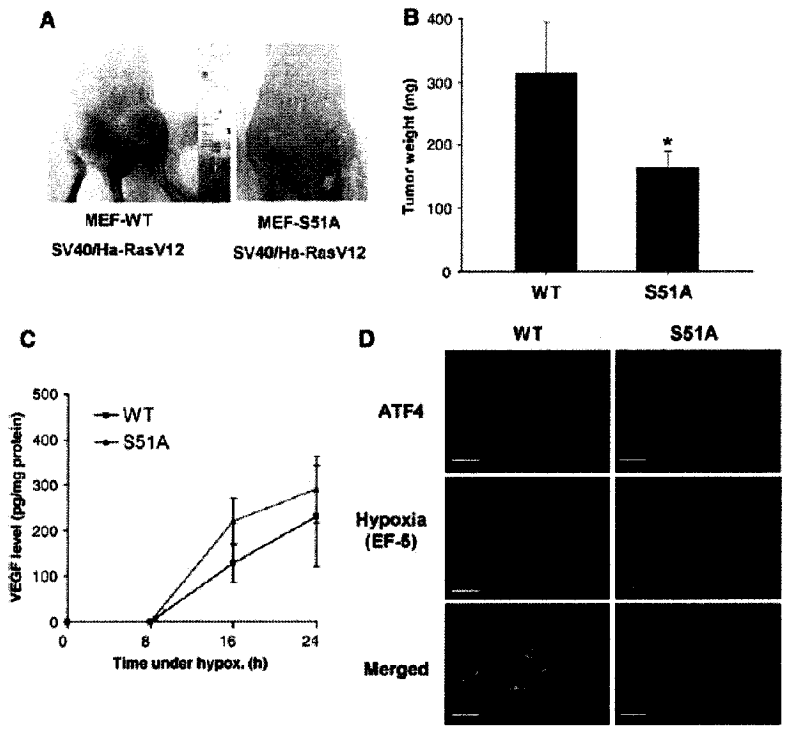

Figure 6 Inhibition of eIF2α phosphorylation affects the rate of tumor growth *in vivo*. (A) Nu/Nu mice were injected on each side with 1×10^6 cells/site, with either WT.Ha-RasV12 MEFs (left panel) or S51A.Ha-RasV12 MEFs (right panel). Necrotic areas on the skin and opaque morphology are evident in the S51A.Ha-RasV12 tumors. (B) Tumor growth after 3 weeks. At the end of the experiment, tumors were excised and weighed (mean ± s.e., $N=7$, $^*P<0.05$, one-tailed Student's *t*-test). (C) VEGF levels following hypoxia in WT and S51A MEFs. Ras-transformed MEFs were treated as in Figure 5A and secreted VEGF levels in the media were analyzed at the times indicated. Experiments were performed in triplicate and error bars represent s.e. values. (D) ATF4 upregulation in hypoxic areas is dependent on eIF2α phosphorylation. Tumor xenografts from Ha-RasV12-transformed WT and S51A cells were stained for ATF4 expression. Staining for ATF4 was observed only in WT tumors and localized within hypoxic regions. No significant staining was seen in 6/6 sections from three different S51A tumors. Bar = 15 μm.

$PERK^{-/-}$ tumors, indicating that the PERK-eIF2α component of the ISR is required for *in vivo* resistance to hypoxic stress and tumor growth.

Expression of a dominant-negative PERK (dn-PERK) allele in human tumor cells reduces hypoxia tolerance and inhibits tumor growth

The results presented so far were obtained using minimally transformed MEFs, a useful and informative isogenic system, but one that may not be representative of human tumor cells of epithelial origin. To examine the role of the PERK-eIF2α pathway *in vitro* and *in vivo*, we used a dn-PERK construct to block the activity of endogenous PERK in an established human cancer cell line. This dn-allele, PERKΔC, lacks the C-terminal kinase domain, has a myc-tag epitope and was shown to inhibit the ability of endogenous PERK to phosphorylate eIF2α following various stresses, including hypoxia (Brewer and Diehl, 2000; Koumenis *et al*, 2002). HT29 colorectal carcinoma cells stably expressing the dn-PERK construct (HT29.PERKΔC), or the empty vector (HT29.Puro) were exposed to normoxia or 6 h of extreme hypoxia. HT29.PERKΔC cells failed to increase eIF2α phosphorylation after 6 h of hypoxia, confirming that this construct exerts a dominant-negative function by inhibiting endogenous PERK activity (Figure 7A). We next tested the apoptotic sensitivity of these cells to hypoxia and thapsigargin. After 32 h of extreme hypoxia, substantially higher levels of cleaved PARP were observed in the HT29.PERKΔC cells compared to the HT29.Puro cells (Figure 7B, top). The HT29.PERKΔC cells also displayed morphology consistent with swollen ER, indicative of ER stress (Figure 7B, bottom). The *in vitro* growth of the control and PERKΔC cell lines was not significantly different over a period of 12 days in culture (data not shown) and HIF-1α was induced to comparable levels in both cell lines (Figure 7C), confirming that HIF-1 regulation is not dependent on PERK status. To test the role of PERK in HT29 tumor growth, cells were injected into the flanks of nude mice and tumor volume was followed for up to 25 days. Tumors obtained from HT29.PERKΔC cells grew significantly smaller compared to those obtained from the HT29.Puro cells (Figure 7D and E), providing additional evidence that inhibition of PERK activity hinders tumor growth *in vivo*. Immunoblot analysis from homogenized tumors showed that expression of the dn-PERKΔC allele was retained for the duration of tumor growth and correlated with inhibition of eIF2α phosphorylation in the HT29.PERKΔC tumors (Figure 7F). Also, similar to the $PERK^{-/-}$ MEF tumors, the HT29.PERKΔC tumors displayed extensive colocalization of

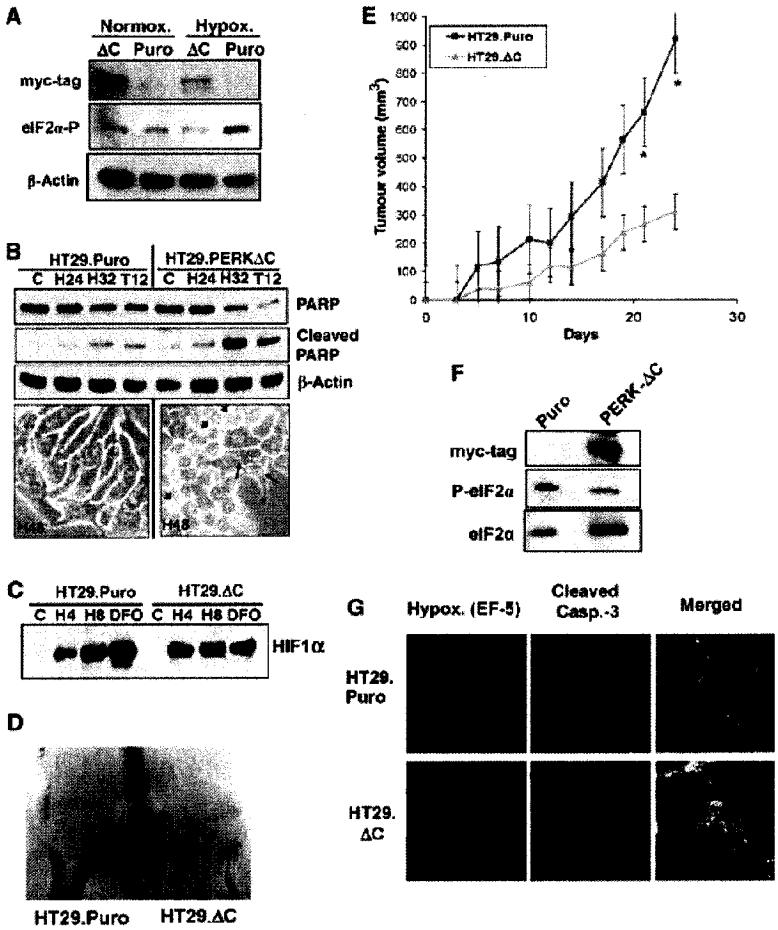

Figure 7 Expression of a dn-PERK allele in human tumor cells decreases hypoxia tolerance and inhibits tumor growth. (A) Immunoblot of myc-tagged PERKΔC, eIF2α phosphorylation and β-actin (loading control). Exposure of HT29.Puro cells to extreme hypoxia induces an increase in eIF2α phosphorylation, which is blocked in HT29.PERKΔC cells. (B) Immunoblot of uncleaved and cleaved PARP in HT29.Puro and HT29.PERKΔC cells following hypoxia or 12 h treatment with 500 nM thapsigargin (top). β-Actin was used as a loading control. Apoptotic morphology following extreme hypoxia for 48 h at ×40 magnification (bottom). Arrowheads indicate cells with membrane blebbing and arrows indicate cells exhibiting vacuoles, a sign of ER stress. (C) PERK status does not affect induction of HIF-1α levels. HT29.Puro and HT29.PERKΔC cells were treated with extreme hypoxia or DFO. HIF-1α levels were determined by immunoblotting using nuclear extracts. (D) Tumor xenografts from HT29.Puro cells (left mouse) grow larger compared to tumors from HT29.PERKΔC cells (right mouse). (E) Growth measurements of HT29.Puro xenografts (blue line and squares) and HT29.PERKΔC xenografts (green line and triangles). Growth from six tumors was monitored over a period of 25 days following injection (mean ± s.e.) (*$P < 0.05$). (F) Immunoblot analysis of PERKΔC expression, eIF2α phosphorylation status or total eIF2α levels from excised and homogenized tumors shown in (D, E). (G) Sections from HT29.Puro and HT29.PERKΔC xenografts were stained for regions of hypoxia using a Cy-3-labeled anti-EF-5 antibody and apoptosis using an anti-cleaved caspase-3, FITC-labeled antibody. The merged images are shown on the right.

apoptosis with areas of hypoxia. In contrast, the HT29.Puro tumors had larger hypoxic areas that were largely devoid of apoptotic cells (Figure 7G). Collectively, these results provide further evidence that inhibition of PERK activity compromises hypoxia tolerance of tumor cells *in vitro* and *in vivo*.

Cells lacking ATF4 are sensitive to hypoxic stress and expression of the ISR proteins ATF4 and CHOP is upregulated in hypoxic areas of primary human tumors

Since both $PERK^{-/-}$ and S51A MEFs were more sensitive to hypoxia compared to the corresponding WT-MEFs, we wished to determine whether lack of the downstream target ATF4 would result in a similar phenotype. Extreme hypoxia resulted in significant levels of apoptosis in the $ATF4^{-/-}$ MEFs but not in $ATF4^{+/+}$ MEFs, which was evident both morphologically (Figure 8A) and by cleaved caspase-3 and cleaved PARP analysis (Figure 8B). The sensitivity of $ATF4^{-/-}$ cells to hypoxia also occurred at more moderate hypoxic levels. Exposure of the MEFs to 1% O_2 resulted in a 55% decrease in survival in $ATF4^{-/-}$ cells compared to 25% in $ATF4^{+/+}$ cells as assayed by MTT assay, whereas the sensitivity of the two cell types to a different stress, ionizing radiation, was the same (Figure 8C).

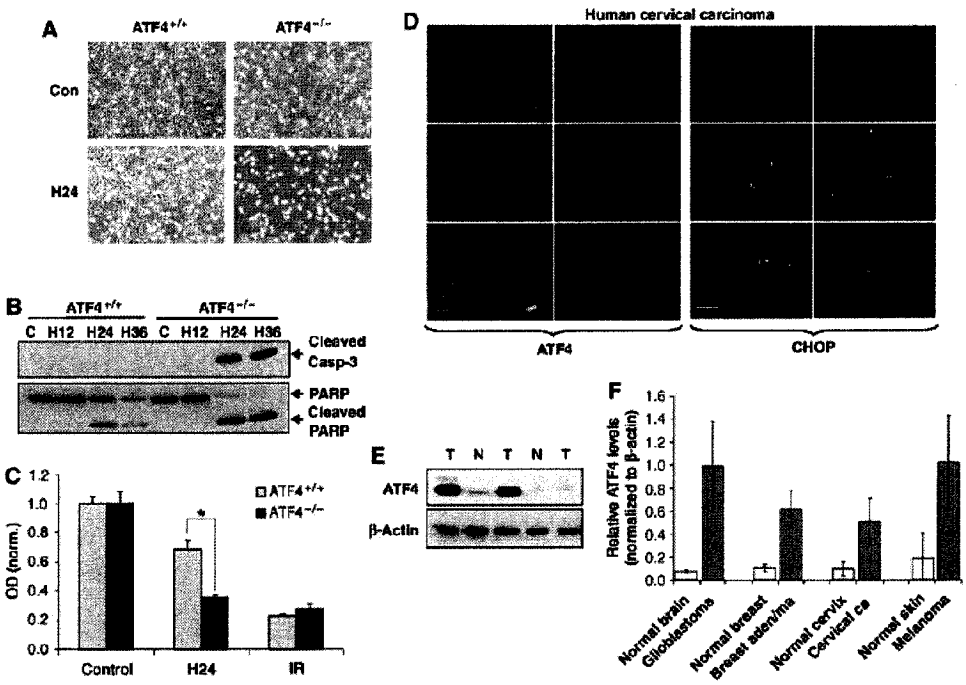

Figure 8 ATF4 contributes to hypoxia tolerance, and ATF4 and CHOP are upregulated in hypoxic areas of primary human tumors. (A) Cells were exposed to extreme hypoxia for 24 h and photographed for apoptotic morphology at × 100 magnification. (B) Immunoblot of cleaved caspase-3 (top) or uncleaved and cleaved PARP (bottom) following hypoxia. (C) MTT assay of $ATF4^{+/+}$ and $ATF4^{-/-}$ MEFs following exposure to moderate hypoxia (1% O_2) or treatment with a 4 Gy dose of IR. Experiments were performed in triplicate and results are normalized to control levels. Error bars represent s.e. values ($^*P<0.05$). No significant difference in survival was observed between untreated $ATF4^{+/+}$ and $ATF4^{-/-}$ MEFs. (D) Immunofluorescence for ATF4 and hypoxia (a–f), or CHOP and hypoxia (g–l) in primary human cervical tumors. Sections were stained with anti-ATF4 (a, d) or anti-CHOP (g, j) polyclonal antibodies followed by a FITC-conjugated secondary antibody, and with a Cy-3-labeled anti-Pimonidazole antibody (b, e, h, k). Panels c, f, i and l are combined images of (a + b), (d + e), (g + h), (j + k), respectively. Bar = 15 μm (a–c, g–i) and 30 μm (d–f, j–l). (E) Immunoblot of ATF4 in lysates from human GBMs and normal human brain tissue. (F) Analysis of ATF4 levels (normalized to levels of β-actin) in normal and malignant tissues obtained from human patients. Error bars represent s.e. values. Brain, $N=6$ normal and 6 glioblastoma; breast, $N=3$ normal and 3 adenocarcinoma; cervix, $N=4$ normal and 6 carcinoma; skin, $N=2$ normal and 2 melanoma.

To investigate whether the induction of the ISR also occurs in primary human tumors, we analyzed ATF4 and CHOP levels in human cervical tumor sections obtained from patients that had been injected with the hypoxia-sensitive dye pimonidazole (Varia *et al*, 1998). Immunohistochemical staining showed significant intra- and intertumoral variations of ATF4 and CHOP expression. However, expression of both proteins colocalized with either hypoxic areas or areas adjacent to hypoxic regions. ATF4 expression showed stronger association with highly hypoxic areas (pimonidazole-positive staining, Figure 8D), whereas CHOP expression was associated with highly hypoxic and surrounding areas (Figure 8D). Similar results were obtained in four different sections obtained from two distinct cervical tumors (Figure S4A). We also examined ATF4 expression in several normal and malignant tissues obtained from patients with brain, breast, cervical and skin cancers. The expression of ATF4 was significantly higher in all malignant tissues compared to the corresponding normal tissues (Figures 8E and F and Figure S4B). The results with ATF4 are in agreement with a previously reported study in which ATF4 expression was found to be higher in breast tumors than in normal breast tissue, and to be present near necrotic areas (Ameri *et al*, 2004).

Discussion

We have presented evidence that the ISR arm of the UPR is activated by hypoxic/anoxic stress *in vitro* and in hypoxic/anoxic areas of solid tumors, and that failure of tumor cells to mount an effective ISR in response to low oxygen results in increased apoptosis, reduced overall cell survival and inhibition of tumor growth. Recently, a study by Chen *et al* showed that XBP1, the target of IRE1, is essential for cell survival under hypoxic conditions and that XBP1 is required for tumor growth (Romero-Ramirez *et al*, 2004). Together, these studies suggest that the full UPR is activated under hypoxia/anoxia and contributes to cellular adaptation to this stress.

The induction of gene expression under conditions of global translational repression is reminiscent of other stress responses (e.g., heat-shock response), during which select groups of genes are upregulated in a background of repressed gene expression to help in the recovery from the stress. Thus, it is noteworthy that several genes with important roles in the

hypoxic response, including VEGF and HIF-1α, harbor unusually long 5′ UTRs with extensive secondary structures that presumably enable them to be efficiently translated under hypoxic conditions (Akiri *et al*, 1998; Lang *et al*, 2002). Conversely, our screen for genes whose mRNAs are efficiently translated under hypoxic conditions revealed that several mRNAs of UPR genes, including BiP, CHOP and ORP150, are among the most efficiently translated mRNAs (Figure S1). It is tempting to speculate that the hypoxic/anoxic response and the UPR may share common post-translational regulation mechanisms.

The complex picture of tumor hypoxia, composed of significant intra- and intertumoral variations in oxygen levels that can change dynamically in time, prompted the investigation of UPR gene expression in hypoxic areas of tumors. We show that at least two ISR target genes, ATF4 and CHOP, are highly expressed in hypoxic areas of tumors. Previously, we demonstrated that induction of eIF2α phosphorylation (a requirement for significant ATF4 and CHOP accumulation as shown in Figure S2) can occur at more moderate hypoxic levels—as high as 1% O_2—albeit with slower kinetics (Koumenis *et al*, 2002), suggesting that the ISR can be elicited over a wide range of hypoxic conditions.

What is the physiological role for these proteins in hypoxia tolerance? ATF4 activates the induction of downstream UPR genes, but has also been implicated in antioxidant cellular defense processes (Fawcett *et al*, 1999; Harding *et al*, 2003; Lu *et al*, 2004). Recent mechanistic studies on HIF-1α induction appear to support a model of increased oxidative stress in the cytosol due to release of reactive oxygen species from the mitochondria (Guzy *et al*, 2005; Mansfield *et al*, 2005). Furthermore, reoxygenation following hypoxia produces oxidative stress severe enough to activate DNA damage response pathways (Hammond *et al*, 2003). We hypothesize that induction of ATF4 by hypoxia serves to upregulate antioxidant-related genes to ameliorate oxidative stress. CHOP, itself a target of ATF4, is a transcription factor with proapoptotic properties (Zinszner *et al*, 1998; McCullough *et al*, 2001). While CHOP may promote apoptosis under prolonged/severe hypoxia, it is evident—as is also the case for induction of CHOP by pharmacological agents (Harding *et al*, 2000a)—that the consequences of PERK ablation are significantly more severe in terms of apoptosis than an reduced CHOP expression. Thus, the significance of CHOP induction by hypoxia at present remains unclear and will have to be elucidated by using cells with abrogated CHOP expression.

Cells with a compromised ISR pathway show significant sensitivity to ER stress due to the deleterious effects of accumulated misfolded proteins in the ER (Harding *et al*, 2000b; Scheuner *et al*, 2001). Our results showing PERK-dependent activation of caspase-12 provide further evidence of ER stress under hypoxic stress. However, caspase-12$^{-/-}$ MEFs display equal sensitivity to prolonged hypoxia compared to their WT-MEFs (data not shown), suggesting that caspase-12 is not required for hypoxia-induced cell death. Recently, the BH3-only proapoptotic proteins Bax and Bak have been localized in the ER membrane and shown to mediate stress-induced release of ER Ca^{2+} (Scorrano *et al*, 2003; Zong *et al*, 2003), raising the possibility that they could play a critical role in hypoxia-induced, ER-dependent apoptosis.

An interesting question not addressed by these studies is the nature of the signal for induction of the UPR by hypoxia/anoxia. Activation of PERK, IRE1 and ATF6 by ER stress is negatively regulated by BiP. Under physiological conditions, BiP binds to the ER-lumenal portion of the proteins and keeps them in an inactive state (Bertolotti *et al*, 2000; Shen *et al*, 2002), and this binding is perturbed during ER stress. One can envision a scenario in which low oxygen perturbs the pro-oxidant environment of the ER lumen causing misfolding of labile proteins, thereby triggering BiP-dependent PERK activation. This model is supported by the findings that (a) in yeast, molecular oxygen is the final electron acceptor in protein disulfide isomerase-dependent protein folding, (b) BiP expression is upregulated by hypoxia (Gazit *et al*, 1999) and (c) downregulation of BiP by antisense cDNA decreases the survival of tumor cells (Koong *et al*, 1994). Further validation of this model will require careful examination of the interactions between BiP and the initiators of the UPR under normoxic and hypoxic conditions. Based on the findings presented here, we propose that, in addition to HIF-1-dependent processes, the induction of the UPR by hypoxia represents an encompassing and critical aspect of hypoxia resistance and tumor development. Since stringent hypoxic conditions do not normally exist outside a tumor microenvironment, targeting UPR processes could provide an alternative or complementary approach for therapeutic exploitation of tumor hypoxia.

Materials and methods

Cell culture and generation of the stable cell lines

PERK$^{+/+}$, PERK$^{-/-}$, S51A, ATF4$^{-/-}$ and WT MEFs, and HeLa cells were cultured in DMEM. HT29 colorectal carcinoma cells (ATCC) were cultured in McCoy's 5A medium. All media were supplemented with penicillin, streptomycin, 10% fetal calf serum and L-glutamine. S51A mutant and ATF4$^{-/-}$ MEFs and HT.29PERKΔC cells were also supplemented with 20% FBS, 1 × MEM non-essential amino-acid mix and 55 μM 2-mercaptoethanol. Cell transformation and establishment of HT29.PERKΔC cells are described in Supplementary data.

Hypoxia treatments

Cells were placed in either a Bactron 1 Anaerobic Chamber (Sheldon Manufacturing) or an InVivo$_2$ 400 Hypoxia Workstation (Biotrace, Inc.), for the time(s) indicated. The oxygen concentration in the anaerobic chamber was maintained at ⩽0.02% and monitored with a polarographic, membrane-covered oxygen sensor (Animas Corp.).

Animals

Athymic Nu/Nu mice (Charles River Labs) were subcutaneously injected with 3×10^6 transformed PERK$^{+/+}$ and PERK$^{-/-}$ MEFs or transformed MEF-WT and S51A MEFs or 1.5×10^6 HT29.Puro or HT.29PERKΔC cells in 150 μl of PBS. Tumors were monitored daily until they became cumbersome or necrotic. Tumor volumes were measured every other day based on the formula $V = \text{length}^2 \times \text{width}$, where length was always the longest dimension. For hypoxia visualization, mice were injected with 300 μl of 3 mg/ml EF-5 (University of Pennsylvania) i.p. 1 h before euthanization, tumors were immediately excised, frozen and embedded in OCT freezing medium.

Human tumors

Human cervical squamous cell carcinoma tumors were obtained at the UNC-CH School of Medicine. Patients were injected with pimonidazole prior to surgical resection of tumors. Tumors were flash frozen in liquid nitrogen, embedded in OCT and stored at −80°. Human tumor and normal tissues were obtained through the WFU Comprehensive Cancer Center Tissue Procurement Core Lab. Collection and processing of human specimens was performed in accordance to UNC-CH and WFUSM IRB regulations.

Immunohistochemistry

Frozen tissue was sectioned in 5 μm and fixed to glass slides in 4% formaldehyde solution for 10 min. For detection of hypoxic areas using EF-5, sections were further fixed with 100% methanol for 10 min, blocked in 3% BSA in PBS for 30 min and incubated with a Cy3-conjugated ELK 3–51 (75 μg/ml) monoclonal antibody (University of Pennsylvania) that recognizes EF-5 adducts, followed by incubation with a FITC-conjugated anti-cleaved caspase-3 antibody (Cell Signaling). Fluorescence was detected using Olympus IX70 Epifluoroscope and photographed at several magnifications. For detection of hypoxia/ATF4 and hypoxia/CHOP colocalization, mouse and human cervical tumor sections were fixed in 95, 75 and 50% ethanol, blocked in 3% BSA in PBS and hypoxia adducts detected with either ELK 3-51 antibody for mouse tumors or Cy3-conjugated anti-pimonidazole monoclonal antibody (2 μg/ml) (UNC-CH) for human tumors. Sections were incubated with anti-CHOP or anti-ATF4 polyclonal antibodies, followed with a FITC-conjugated secondary antibody.

Immunoblotting

Immunoblotting was performed as previously described (Koumenis *et al*, 2002). For primary antibodies used, please see Supplementary data.

Supplementary data

Supplementary data are available at *The EMBO Journal* Online.

Acknowledgements

We thank Chris Counter and Peter Howley for the Ha-RasV12 and Ki-RasV12 expression plasmids, Alan Diehl for the PERKAC expression vector, Andrew Thorburn and John Connor for critically reading the manuscript, Albert Koong for helpful discussions and Lori Hart, Dawn Eads and Jack Smallwood for expert technical help. This work was supported by NIH grants CA94214 (CK), ES08681 (DR) and DK42394 (RJK).

References

Akiri G, Nahari D, Finkelstein Y, Le SY, Elroy-Stein O, Levi BZ (1998) Regulation of vascular endothelial growth factor (VEGF) expression is mediated by internal initiation of translation and alternative initiation of transcription. *Oncogene* 17: 227–236

Ameri K, Lewis CE, Raida M, Sowter H, Hai T, Harris AL (2004) Anoxic induction of ATF-4 through HIF-1-independent pathways of protein stabilization in human cancer cells. *Blood* 103: 1876–1882

Bertolotti A, Zhang Y, Hendershot LM, Harding HP, Ron D (2000) Dynamic interaction of BiP and ER stress transducers in the unfolded-protein response. *Nat Cell Biol* 2: 326–332

Blais JD, Filipenko V, Bi M, Ron D, Koumenis C, Wouters BG, Bell JC (2004) Transcription factor 4 is translationally regulated by hypoxic stress. *Mol Cell Biol* 24: 7469–7482

Blouw B, Song H, Tihan T, Bosze J, Ferrara N, Gerber HP, Johnson RS, Bergers G (2003) The hypoxic response of tumors is dependent on their microenvironment. *Cancer Cell* 4: 133–146

Brewer JW, Diehl JA (2000) PERK mediates cell-cycle exit during the mammalian unfolded protein response. *Proc Natl Acad Sci USA* 97: 12625–12630

Carmeliet P, Dor Y, Herbert JM, Fukumura D, Brusselmans K, Dewerchin M, Neeman M, Bono F, Abramovitch R, Maxwell P, Koch CJ, Ratcliffe P, Moons L, Jain RK, Collen D, Keshert E, Keshet E (1998) Role of HIF-1alpha in hypoxia-mediated apoptosis, cell proliferation and tumour angiogenesis. *Nature* 394: 485–490

Cullinan SB, Zhang D, Hannink M, Arvisais E, Kaufman RJ, Diehl JA (2003) Nrf2 is a direct PERK substrate and effector of PERK-dependent cell survival. *Mol Cell Biol* 23: 7198–7209

Dorner AJ, Wasley LC, Kaufman RJ (1990) Protein dissociation from GRP78 and secretion are blocked by depletion of cellular ATP levels. *Proc Natl Acad Sci USA* 87: 7429–7432

Fawcett TW, Martindale JL, Guyton KZ, Hai T, Holbrook NJ (1999) Complexes containing activating transcription factor (ATF)/cAMP-responsive-element-binding protein (CREB) interact with the CCAAT/enhancer-binding protein (C/EBP)-ATF composite site to regulate Gadd153 expression during the stress response. *Biochem J* 339 (Part 1): 135–141

Gazit G, Hung G, Chen X, Anderson WF, Lee AS (1999) Use of the glucose starvation-inducible glucose-regulated protein 78 promoter in suicide gene therapy of murine fibrosarcoma. *Cancer Res* 59: 3100–3106

Guzy RD, Hoyos B, Robin E, Chen H, Liu L, Mansfield KD, Simon MC, Hammerling U, Schumacker PT (2005) Mitochondrial complex III is required for hypoxia-induced ROS production and cellular oxygen sensing. *Cell Metab* 1: 401–408

Hammond EM, Dorie MJ, Giaccia AJ (2003) ATR/ATM targets are phosphorylated by ATR in response to hypoxia and ATM in response to reoxygenation. *J Biol Chem* 278: 12207–12213

Harding HP, Novoa I, Zhang Y, Zeng H, Wek R, Schapira M, Ron D (2000a) Regulated translation initiation controls stress-induced gene expression in mammalian cells. *Mol Cell* 6: 1099–1108

Harding HP, Zeng H, Zhang Y, Jungries R, Chung P, Plesken H, Sabatini DD, Ron D (2001) Diabetes mellitus and exocrine pancreatic dysfunction in perk−/− mice reveals a role for translational control in secretory cell survival. *Mol Cell* 7: 1153–1163

Harding HP, Zhang Y, Bertolotti A, Zeng H, Ron D (2000b) Perk is essential for translational regulation and cell survival during the unfolded protein response. *Mol Cell* 5: 897–904

Harding HP, Zhang Y, Zeng H, Novoa I, Lu PD, Calfon M, Sadri N, Yun C, Popko B, Paules R, Stojdl DF, Bell JC, Hettmann T, Leiden JM, Ron D (2003) An integrated stress response regulates amino acid metabolism and resistance to oxidative stress. *Mol Cell* 11: 619–633

Hochachka PW, Buck LT, Doll CJ, Land SC (1996) Unifying theory of hypoxia tolerance: molecular/metabolic defense and rescue mechanisms for surviving oxygen lack. *Proc Natl Acad Sci USA* 93: 9493–9498

Hockel M, Vaupel P (2001) Tumor hypoxia: definitions and current clinical, biologic, and molecular aspects. *J Natl Cancer Inst* 93: 266–276

Kaufman RJ (2002) Orchestrating the unfolded protein response in health and disease. *J Clin Invest* 110: 1389–1398

Koong AC, Chen EY, Lee AS, Brown JM, Giaccia AJ (1994) Increased cytotoxicity of chronic hypoxic cells by molecular inhibition of GRP78 induction. *Int J Radiat Oncol Biol Phys* 28: 661–666

Koumenis C, Naczki C, Koritzinsky M, Rastani S, Diehl A, Sonenberg N, Koromilas A, Wouters BG (2002) Regulation of protein synthesis by hypoxia via activation of the endoplasmic reticulum kinase PERK and phosphorylation of the translation initiation factor eIF2alpha. *Mol Cell Biol* 22: 7405–7416

Lang KJ, Kappel A, Goodall GJ (2002) Hypoxia-inducible factor-1alpha mRNA contains an internal ribosome entry site that allows efficient translation during normoxia and hypoxia. *Mol Biol Cell* 13: 1792–1801

Lu PD, Jousse C, Marciniak SJ, Zhang Y, Novoa I, Scheuner D, Kaufman RJ, Ron D, Harding HP (2004) Cytoprotection by pre-emptive conditional phosphorylation of translation initiation factor 2. *EMBO J* 23: 169–179

Ma Y, Hendershot LM (2004) The role of the unfolded protein response in tumor development: friend or foe? *Nat Rev Cancer* 4: 966–977

Mansfield KD, Guzy RD, Pan Y, Young RM, Cash TP, Schumacker PT, Simon MC (2005) Mitochondrial dysfunction resulting from loss of cytochrome *c* impairs cellular oxygen sensing and hypoxic HIF-[alpha] activation. *Cell Metab* 1: 393–399

Maxwell PH, Dachs GU, Gleadle JM, Nicholls LG, Harris AL, Stratford IJ, Hankinson O, Pugh CW, Ratcliffe PJ (1997) Hypoxia-inducible factor-1 modulates gene expression in solid tumors and influences both angiogenesis and tumor growth. *Proc Natl Acad Sci USA* 94: 8104–8109

McCullough KD, Martindale JL, Klotz LO, Aw TY, Holbrook NJ (2001) Gadd153 sensitizes cells to endoplasmic reticulum stress by down-regulating Bcl2 and perturbing the cellular redox state. *Mol Cell Biol* 21: 1249–1259

Nakagawa T, Zhu H, Morishima N, Li E, Xu J, Yankner BA, Yuan J (2000) Caspase-12 mediates endoplasmic-reticulum-specific apoptosis and cytotoxicity by amyloid-beta. *Nature* 403: 98–103

Rao RV, Hermel E, Castro-Obregon S, del Rio G, Ellerby LM, Ellerby HM, Bredesen DE (2001) Coupling endoplasmic reticulum stress to the cell death program. Mechanism of caspase activation. *J Biol Chem* 276: 33869–33874

Ratcliffe PJ, O'Rourke JF, Maxwell PH, Pugh CW (1998) Oxygen sensing, hypoxia-inducible factor-1 and the regulation of mammalian gene expression. *J Exp Biol* 201 (Part 8): 1153–1162

Romero-Ramirez L, Cao H, Nelson D, Hammond E, Lee AH, Yoshida H, Mori K, Glimcher LH, Denko NC, Giaccia AJ, Le QT, Koong AC (2004) XBP1 is essential for survival under hypoxic conditions and is required for tumor growth. *Cancer Res* 64: 5943–5947

Ron D (2002) Translational control in the endoplasmic reticulum stress response. *J Clin Invest* 110: 1383–1388

Ryan HE, Poloni M, McNulty W, Elson D, Gassmann M, Arbeit JM, Johnson RS (2000) Hypoxia-inducible factor-1alpha is a positive factor in solid tumor growth. *Cancer Res* 60: 4010–4015

Scheuner D, Song B, McEwen E, Liu C, Laybutt R, Gillespie P, Saunders T, Bonner-Weir S, Kaufman RJ (2001) Translational control is required for the unfolded protein response and *in vivo* glucose homeostasis. *Mol Cell* 7: 1165–1176

Scorrano L, Oakes SA, Opferman JT, Cheng EH, Sorcinelli MD, Pozzan T, Korsmeyer SJ (2003) BAX and BAK regulation of endoplasmic reticulum Ca^{2+}: a control point for apoptosis. *Science* 300: 135–139

Semenza GL (2000) Surviving ischemia: adaptive responses mediated by hypoxia-inducible factor 1. *J Clin Invest* 106: 809–812

Shen J, Chen X, Hendershot L, Prywes R (2002) ER stress regulation of ATF6 localization by dissociation of BiP/GRP78 binding and unmasking of Golgi localization signals. *Dev Cell* 3: 99–111

Shi Y, Vattem KM, Sood R, An J, Liang J, Stramm L, Wek RC (1998) Identification and characterization of pancreatic eukaryotic initiation factor 2 alpha-subunit kinase, PEK, involved in translational control. *Mol Cell Biol* 18: 7499–7509

Varia MA, Calkins-Adams DP, Rinker LH, Kennedy AS, Novotny DB, Fowler Jr WC, Raleigh JA (1998) Pimonidazole: a novel hypoxia marker for complementary study of tumor hypoxia and cell proliferation in cervical carcinoma. *Gynecol Oncol* 71: 270–277

Zhang P, McGrath B, Li S, Frank A, Zambito F, Reinert J, Gannon M, Ma K, McNaughton K, Cavener DR (2002) The PERK eukaryotic initiation factor 2 alpha kinase is required for the development of the skeletal system, postnatal growth, and the function and viability of the pancreas. *Mol Cell Biol* 22: 3864–3874

Zinszner H, Kuroda M, Wang X, Batchvarova N, Lightfoot RT, Remotti H, Stevens JL, Ron D (1998) CHOP is implicated in programmed cell death in response to impaired function of the endoplasmic reticulum. *Genes Dev* 12: 982–995

Zong WX, Li C, Hatzivassiliou G, Lindsten T, Yu QC, Yuan J, Thompson CB (2003) Bax and Bak can localize to the endoplasmic reticulum to initiate apoptosis. *J Cell Biol* 162: 59–69

3. PERK-DEPENDENT TRANSLATIONAL REGULATION PROMOTES TUMOR CELL ADAPTATION ND ANGIOGENESIS IN RESPONSE TO HYPOXIC STRESS

Contribution of Collaborators

The contents of this manuscript were written by J. Blais and edited by J. Bell prior to submission. All of the experiments performed and figures presented in this manuscript are the work of J. Blais. All animal work was completed with the technical assistance of Theresa Falls. The Bgal/VCIP/CAT bicistronic construct and the various 5'UTR VCIP deletion constructs were created by Robert Edge. Dr. Christina Addison and her technician Huijun Zhao provided reagents, protocol, and technical assistance for the mouse model of angiogenesis. Dr. Costas Koumenis provided Kras transformed $PERK^{+/+}$ and $PERK^{-/-}$ MEFs. Drs. David Ron and Heather Harding provided us with the $PERK^{-/-}$ SV40 transformed MEFs.

Summary

Here we demonstrate evidence with *in vivo* tumor models that tumors with a compromised ISR are smaller, exhibit less angiogenesis, and promote a tumor microenvironment that favors the formation of non-functional microvessels. Using microarray analysis of polysome-bound RNA from aerobic (0h) and hypoxic (4h) $Perk^{+/+}$ and $Perk^{-/-}$ MEFs, we corroborated our *in vivo* observations by revealing a subset of pro-angiogenic transcripts are preferentially translated, in a Perk-dependent manner. Included in this cohort of angiogenic genes was VCIP, an adhesion molecule that promotes cellular adhesion, integrin binding, and capillary morphogenesis. We demonstrate that VCIP is preferentially regulated, as least in part, due to an IRES element within its highly conserved 5'UTR. This study suggests that Perk plays a role in tumor cell adaptation to hypoxic stress by regulating the translation of angiogenic factors necessary for the development of functional microvessels

Perk-dependent translational regulation promotes tumor cell adaptation and angiogenesis in response to hypoxic stress

Running Title: Perk mediates tumor cell adaptation to hypoxia

Jaime D. Blais[1,2], Christina L. Addison[1], Robert Edge[1,2], Theresa Falls[1], , Huijun Zhao[1], Kishore Wary[4] , Costas Koumenis[5], Heather P Harding[6], David Ron[6], Martin Holcik[3], and John C. Bell[1*]

[1]Ottawa Health Research Institute, 501 Smyth Rd., Ottawa, Ontario K1H 8L6

[2]Department of Biochemistry, University of Ottawa

[3]Apoptosis Research Centre, Children's Hospital of Eastern Ontario, 401 Smyth Rd., Ottawa, Ontario K1H 8L1, Canada

[4]Department of Pharmacology, University of Illinois at Chicago, 835 S. Wolcott, Room E403, Chicago, IL 60612

[5] Department of Radiation Oncology, University of Pennsylvania School of Medicine, 185 John Morgan Building, 3620 Hamilton Walk, Philadelphia, PA 19104-6072

[6]Skirball Institute, New York University School of Medicine, New York, NY 10016

key words: Hypoxia, translation, polysome, ISR, Perk, eIF2α, angiogenesis

*Corresponding author:

Dr. John Bell
503 Smyth Rd.
3rd Floor ORCC
Ottawa ON
K1H 1C4
Work: 613-737-7700 ext 70439
Fax: 613-247-3524
e-mail: jbell@ohri.ca

Total word count of Materials and Methods: 1265

Total word count of Intro, Results and Discussion: 5547

Abstract

It has been well established that the tumor microenvironment can promote tumor cell adaptation and survival. However, the mechanisms that influence malignant progression have not been clearly elucidated. We have previously demonstrated that cells cultured under hypoxic/anoxic conditions and transformed cells in hypoxic areas of tumors activate a translational control program known as the integrated stress response (ISR). Here we show that tumors derived from k-ras transformed $Perk^{-/-}$ MEFs are smaller and exhibit less angiogenesis compared to tumors with an intact ISR. Furthermore, Perk promotes a tumor microenvironment that favors the formation of functional microvessels. These observations were corroborated by a microarray analysis of polysome-bound RNA in aerobic (0h) and hypoxic (4h) $Perk^{+/+}$ and $Perk^{-/-}$ MEFs. This analysis revealed that a subset of pro-angiogenic transcripts are preferentially translated, in a Perk-dependent manner, including VCIP, an adhesion molecule that promotes cellular adhesion, integrin binding, and capillary morphogenesis. Taken with the concomitant Perk-dependent translational induction of additional pro-angiogenic genes identified by our microarray analysis, this study suggests that Perk plays a role in tumor cell adaptation to hypoxic stress by regulating the translation of angiogenic factors necessary for the development of functional microvessels and further supports the contention that the Perk pathway could be an attractive target for novel anti-tumor modalities.

Introduction

The presence of hypoxic cells in solid tumors is well documented and both clinical and experimental evidence suggests that the hypoxic microenvironment of a tumor promotes a more aggressive phenotype by selecting for the clonal expansion of apoptotically insensitive cells (28). Growing tumors are often exposed to heterogeneous environments with regions of solid tumors containing microenvironmental niches deficient of critical metabolites including oxygen and glucose (11). Indeed, low oxygenation can accelerate malignant progression and metastasis resulting in a poorer prognosis irrespective of the chosen treatment regimen (38). The ability of tumor cells to survive and adapt to hypoxic microenvionments can be attributed to the regulation of several key mechanisms. These mechanisms include the loss of pathways that can induce cell death (28), the stimulation of angiogenesis to increase tumor oxygenation (87), and the capability to strictly regulate energy homeostasis (37). Energy conservation is crucial to cellular survival as ATP production is diminished by the lack of oxidative phosphorylation. Thus, hypoxic stress results in a rapid metabolic shift that favors anaerobic glycolysis and the inhibition of high energy consuming processes including protein translation (75).

The control of mRNA translation is emerging as an important cellular response to stress that can assert significant influence on individual gene expression (9, 22, 31, 48, 50, 65, 79). Hypoxia results in a rapid and reversible inhibition in global protein synthesis to help alleviate energy demands when oxygen and ATP levels are low; however, the exact mechanisms controlling translational regulation are not fully understood. While early responses to hypoxia involve the activation of Perk and transient phosphorylation of eIF2α (7, 9, 51), translational inhibition appears to occur in distinct phases and to involve

multiple pathways (16, 50, 59). Exposure to hypoxia activates the ER resident kinase Perk, resulting in the phosphorylation of eIF2α and adaptive modulation of protein synthesis and gene expression through a signal transduction pathway referred to as the Integrated Stress Response (ISR) (35), an arm of the unfolded protein response (UPR), that facilitates the cellular adapatation to ER stress. Translational repression is mediated by phosphorylation of serine 51 of the alpha subunit of translation initiation factor 2 (eIF2α) resulting in decreased ternary complex formation and subsequently decreased translation initiation. An important function of the UPR is to reduce demand on the protein-folding machinery within the ER to protect the cell from ER stress. Inhibiting translation not only conserves ATP, it additionally helps to decrease the client load in the ER. Translational inhibition paradoxically leads to the selective translation of several mRNAs necessary for the survival and adaptation of cells to cellular stress including the transcription factor ATF4 (9, 31). ATF4 transcriptionally activates stress responsive genes which encode proteins that are necessary to resolve the UPR including Gadd34, BiP, and CHOP (31, 61). The physiological significance of Perk signaling is underscored by the observation that $Perk^{-/-}$ mice are viable at birth but die quickly due to early onset diabetes caused by the rapid destruction of secretory cells as a result of accumulated unfolded proteins (32). Furthermore, cells with compromised Perk and eIF2α signaling are significantly more sensitive to ER-induced cell death than wild-type cells (32, 33, 84, 102). The critical role for Perk in tumor cell adaptation to hypoxic stress is underscored by our observation that in its absence, cells are incapable of initiating the integrated stress response during oxygen deprivation, thus leading to a loss in tumour cell viability (7). Moreover, $Perk^{-/-}$ tumours are substantially smaller than $Perk^{+/+}$ tumours, and exhibit decreased survival in response to hypoxic stress (7). In this study we demonstrate

that tumors derived from k-ras-transformed $Perk^{-/-}$ mouse embryonic fibroblasts (MEFs) are not only smaller than wildtype tumors, but appear to have severe limitations in their ability to stimulate angiogenesis. Using a mouse model of angiogenesis we assessed the significance of Perk within the tumor microenvironment on vessel formation and maturation. We demonstrate that $Perk^{+/+}$ tumors facilitated endothelial cell survival and functional vessel formation, whereas $Perk^{-/-}$ tumors formed more non-functional, irregularly structured vessels that lead to hemorrhaging within the tumor matrix. These findings are supported by a microarray analysis of polysome-bound mRNAs, which demonstrated that Perk affects the translation of numerous angiogenic genes during hypoxic stress. Included in the cohort of genes identified was an adhesion protein, VEGF and type-1-Collagen Inducible Protein (VCIP), that promotes cell adhesion, spreading, and integrin binding within tumour endothelium (41, 42). These findings help to establish that Perk is a key post-transcriptional regulator that is capable of inducing the expression of a collection of genes necessary for the cellular adaptation to hypoxic stress. This work further supports the notion that the ISR represents an attractive target for novel anti-tumor therapies that may help overcome the development of hypoxia tolerance in tumors.

Materials and Methods

Cell culture and generation of stable cell lines

SV40 immortalized and k-ras transformed $Perk^{+/+}$ and $Perk^{-/-}$ MEFs were maintained in DMEM supplemented with 10% FCS (Fetal Calf Serum), 55uM β-Mercaptoethanol and 10μM Non-Essential Amino Acids (NEAA). HDMECs were cultured in microvascular endothelial cell growth medium (EGM-2MV; Cambrex). The generation of stable clones overexpressing the alkaline phosphatase (AP) protein was as previously described (71).

Proliferation Assay

5,000 k-ras-transformed $Perk^{+/+}$ or $Perk^{-/-}$ MEFs were plated in a 24-well dish. Cells were counted by heamocytometer every 24hr for 5 days. Results are representative of three independent experiments counted in triplicate.

Constructs

The bicistronic vectors: βgal/EMCV/CAT (containing the viral EMCV IRES), βgal/Empty/CAT (Empty vector control), and hp-βgal/Empty/CAT (hairpin containing empty vector) were described previously (39, 96). The human VCIP 5'UTR was cloned into the XhoI site of the intercistronic region between the βgal and CAT cistrons in both the βgal/Empty/CAT and hp-βgal/Empty/CAT. The VCIP 5'UTR deletion constructs were assembled by site directed mutagenesis using Quikchange II XL Site-Directed Mutagenesis Kit (Stratagene, as per the manufacturer's instructions).

Hypoxia Treatments

All experiments were performed with exponentially growing cells. For all experiments, with the exception of polysome fractionation, cells were plated in 60-mm glass culture dishes at a density of ~$1x10^6$ cells/plate. After approximately 20 h, the culture dishes were placed in a

hypoxic culture chamber (MACS VA500 miroaerophillic workstation [Don Whitley Scientific, Shipley, United Kingdom]). Hypoxic conditions were achieved with 90% N_2, 5% CO_2, 5% H_2 (anaerobic grade gas) and palladium catalysts to scavenge trace oxygen.

Isolation of Polysomes and RNA

Polysome fractionation and RNA isolation were performed as previously described (9).

Microarray Analysis

Microarray analysis was performed as previously described (9). Briefly, RNA from the high molecular weight polysomes (fractions 6-10) were pooled from the normoxic samples (hereafter called 0hr poly) and from hypoxic samples (hereafter called 4hr poly). Prior to microarray analysis, RNA from the polysome fractions and the total RNA from the cytoplasmic lysates (0hr Total and 4hr Total) were purified using the RNeasy kit (Qiagen, Mississauga, Canada), as per manufacturer's instructions. Twenty micrograms of each RNA sample were processed according to manufacturer's standard protocol (Affymetrix; Santa Clara, CA, USA) and hybridized to an Affymetrix mouse 430_2 gene chip. Data was analyzed using Genespring software (Silicon Genetics; Redwood City, CA, USA).

Total Cellular Changes and Polysome Analysis

The analysis of Total cellular mRNA and polysome-associated mRNAs was performed as described previously (9). To identify genes that are preferentially translated in a Perk-dependent manner during hypoxic stress, we compared the mean signal intensities of the $Perk^{+/+}$ 0hr poly gene chip to the 4hr poly gene chip and the $Perk^{-/-}$ 0hr poly gene chip to the 4hr poly gene chip using a mean cut-off of 1.5-fold. Genes that demonstrated a concomitant increase in total mRNA expression (>2-fold change in the 4hr total gene chip relative to the 0hr total gene chip) were removed. Using Genespring software (Silicon Genetics), we used

Venn Diagrams to create a list of hypoxia-responsive translationally regulated candidates that were induced exclusively in the $Perk^{+/+}$ cells relative to the $Perk^{-/-}$ cells. Genes were further categorized based on known or proposed molecular function and sorted on the ratio of 4hr poly signal/ 0hr poly signal, used as a basis for interpreting the efficiency of translation during hypoxic stress.

Quantitative RT-PCR

The aforementioned total and polysomal RNA from hypoxic (4hr) and normoxic treated $Perk^{+/+}$ and $Perk^{-/-}$ cells was reverse transcribed (1μg RNA) in the presence of 40ng of VSV-M RNA (a viral transcript used as a control for RT efficiency and Q-PCR). Quantitative PCR was performed in triplicate to amplify all targets using the FastStart DNA Master SYBR Green I kit (Roche Diagnostics, Laval Canada, as per manufacturer's instructions) and the Roche Lightcycler thermocycler. Crossing points were converted to absolute quantities based on standard curves generated for each target amplicon. All target signals were subsequently normalized to VSV-M in order to correct for RT-PCR efficiency.

Primers used are listed below

mGADD34: forward ctgcaaggggctgataagag, reverse aggggtcagccttgttttct

mATF3: forward cagagcctggtgttgtgcta, reverse ggtgtcgtccatcctctgtt

mVCIP: forward cctcttctgcctcttcatgg, reverse gccacatacgggttctgagt

mGrb10: forward ctggctgacctggaagaaag, reverse tcagaaacactgcgcatagg

mHyou1: forward acctagagaagcgggagagg, reverse gcttgtccttcagcatcaca

mIGFBP2: forward acaacgagcagcaggagact, reverse cagaagcaagggaggttcag

mMMP13: forward atcctggccaccttcttctt, reverse tttctcggagcctgtcaact

mCol6a: forward cctgctcagccagtccttac, reverse gacttctcgggacactctcg

Q-PCR results are presented as the number of transcripts per μg of Total RNA or Polysomal RNA. Results from each transcript were normalized to an exogenous control mRNA (VSV-M).

β-Galactosidase and CAT analysis

Cells were washed in PBS and harvested in the CAT ELISA kit lysis buffer (Roche Molecular Biochemicals, as per manufacturer's instructions). β-Galactosidase enzymatic activity in cell extracts was determined as previously described (63). CAT levels were determined using the CAT ELISA kit (Roche Molecular Biochemicals, as per manufacturer's instructions). The relative IRES activity was determined as the ratio of CAT/βgal in a minimum of three independent experiments.

Measurement of Spurious Splicing and Cryptic Promoter Activity

Total RNA was isolated from U2OS cells transfected with the βgal/EMCV/CAT, βgal/Empty/CAT or βgal/VCIP/CAT reporter plasmids and reverse transcribed using SuperScript II (Invitrogen). Quantitative PCR was performed in triplicate to amplify all targets using the FastStart DNA Master SYBR Green I kit (Roche Diagnostics, Laval Canada, as per manufacturer's instructions) and the Roche Lightcycler thermocycler. Primer sequences are indicated below

βgal (5'-ACTATCCCGACCGCCTTACT-3'; 5'-CTGTAGCGGCTGATGTTGAA-3') and CAT (5'-GCGTGTTACGGTGAAAACCT-3'; 5'-GGGCGAAGAAGTTGTCCATA-3'), as described previously(Holcik et al. 2005 RNA).

Animals

Xenograft Tumor Model

Athymic Nu/Nu mice (Charles River Labs) were subcutaneously injected with $5x10^5$ transformed $Perk^{+/+}$ and $Perk^{-/-}$ MEFs or HT.29Puro and HT.29PerkΔC cells in 100μl of PBS. Tumors were monitored daily. Final tumor volumes were determined following tumor resection based on the formula V=length x width x depth.

Biodegradable Polymer Matrix

Porous polylactic acid (PLA) sponges were a gift of Dr. D. Mooney (Harvard) and were prepared as previously described (67). The day prior to implantation, sponges were soaked in 100% ethanol for 2h followed by two washes in PBS. Sponges were soaked overnight in PBS prior to embedding of cells.

Tumor/Endothelial cell sponge implants

Prior to sponge transplantation, $9x10^5$ HDMEC overexpressing alkaline phosphatase (AP) cells and $1x10^5$ $Perk^{+/+}$ or $Perk^{-/-}$ k-ras transformed MEFs were resuspended in 18μl of a 1:1 mixture of growth factor-reduced Matrigel (Collaborative Biomedical Products, Cambridge, Massachusetts) and allowed to adsorb into the prepared sponges. The sponges were incubated for 30min at 37°C to allow for the gelation of Matrigel. Nude mice were anesthetized with Isofluorane and one sponge was implanted subcutaneously in the dorsal region of each mouse. Twenty-one days after transplantation, the mice were sacrificed and the implants were retrieved. The implants were fixed overnight in 10% buffered formalin at room temperature. Sponges were cut in half and one half was stained for alkaline phosphatase. Unstained sections were paraffin embedded for subsequent histologic evaluation.

Staining for Alkaline Phosphatase

Following fixation, sponges were washed three times in PBS at room temperature and once in PBS at 65°C for 30min to inactivate any endogenous phosphatase activity. This was followed by a wash in AP buffer (100nM Tris HCl, pH 8.5, 100mM NaCl, 50nM MgCl2) for 10min at room temperature. The sponge slices were stained in a solution of BCIP/NBT (5-bromo-4-chloro-3-indolyl-phosphate/nitroblue tetrazolium chloride; SIGMA) overnight at room temperature in the dark. The reaction was stopped with 20mM EDTA in PBS and the slices were embedded in paraffin for histologic evaluation. Four micron sections were obtained, counterstained with Eosin, and visualized using an Olympus BX50 light microscope. Pictures were captured with a Nikon Coolpix 100 digital camera.

Statistics

Unless otherwise noted, data are reported as the mean ± standard deviations. Statistical significance was determined using a Student's t test where appropriate and p values less than 0.05 were considered significant.

Results

Perk contributes to tumor growth and angiogenesis in vivo.

Inactivation of ISR signaling by mutations in the ER kinase Perk (dn-PerkΔC, Perk-/- MEFs) and the translation initiation factor eIF2α (eIF2α^{S51A}) impairs cell survival and results in diminished tumor growth in vivo, suggesting the presence of Perk can increase the ability of transformed MEFs to survive and adapt to the tumor microenvironment (7). To examine the contribution of Perk to these processes we used *in vivo* model systems: Perk$^{+/+}$ and Perk$^{-/-}$ k-ras transformed MEFs were injected subcutaneously in the hind limb of nude mice. Measurements of tumor volumes were determined after tumor resection and demonstrate that Perk$^{+/+}$ tumors were, on average, 16x larger than Perk$^{-/-}$ tumors (Perk$^{+/+}$ 493.4±88.7, Perk$^{-/-}$ 30.8±15.8; $p<0.001$) (Figure 1B). Interestingly, we observed upon tumor dissection that Perk$^{-/-}$ tumors appeared to have severe limitations in their ability to stimulate angiogenesis (Figure 1A). While Perk$^{+/+}$ tumors developed rapidly and became highly vascularized, tumors that lacked Perk remained as small, pale, poorly vascularized nodules (Figure 1A: Top left panel vs Top right panel). A number of Perk$^{-/-}$ tumors demonstrated severe hemorrhage in a confined area containing the tumor (Figure 1D). However, upon resection, these tumors were also small in size and appeared poorly vascularized. Similar observations were made previously in nude mice implanted with HT29 cells expressing a dominant negative mutant allele of Perk (Koumenis, unpublished observations). Whether the growth of Perk$^{-/-}$ tumors is solely limited by an increase in their apoptotic index, as previously suggested, or if a compromised ability to induce adaptive pathways, including angiogenesis, have a measurable effect on tumor growth, had not yet been elucidated prior to this study. In vitro growth kinetics demonstrated that k-ras transformed Perk$^{-/-}$ MEFs displayed similar if

not advantageous growth kinetics compared to $Perk^{+/+}$ MEFs (Figure 1C), therefore differences in tumor growth are not due to differences in *in vitro* proliferation rates. We would thus hypothesize that the differential response of $Perk^{+/+}$ and $Perk^{-/-}$ cells to the tumor microenvironment influences their survival, growth, and adaptive potential.

Perk affects endothelial cell survival and vessel formation in vivo

In order to study how Perk expression modulates angiogenesis and affects tumor growth, we used a mouse model of angiogenesis in which PLA sponges seeded with k-ras transformed $Perk^{+/+}$ or $Perk^{-/-}$ cells along with AP-HDMECs, were subcutaneously implanted in nude mice. Perk expression resulted in a higher intra-tumoral vascular density of AP-expressing human microvessels (Figure 2A and 2B). Interestingly, the microenvironment provided by the $Perk^{-/-}$ tumors resulted in significantly fewer functional AP-expressing human microvessels (Figure 2B). Although AP-HDMEC cells formed tubule structures, the endothelial cells remained cuboidal in shape and the centers of many of these tubules remained filled with other AP-HDMEC cells (Figure 2A), suggesting that the consequence of disrupting Perk signaling within the tumor microenvironement results in disrupted angiogenic signals that prevent the appropriate organization and maturation of HDMECs into functional vessels (Figure 2B). This account is further supported by the repeated observation that masses of red blood cells, in the absence of any discernable vessels, can be seen permeating the tumor matrix, perhaps due to leaky and incomplete vascular assembly (Figure 2A green arrows) along with our observation that $Perk^{-/-}$ tumors are frequently highly hemorrhagic (Figure 1D). These studies suggest that the tumor microenvironment provided in a Perk expressing tumor can promote endothelial cell survival and vascular maturation

A

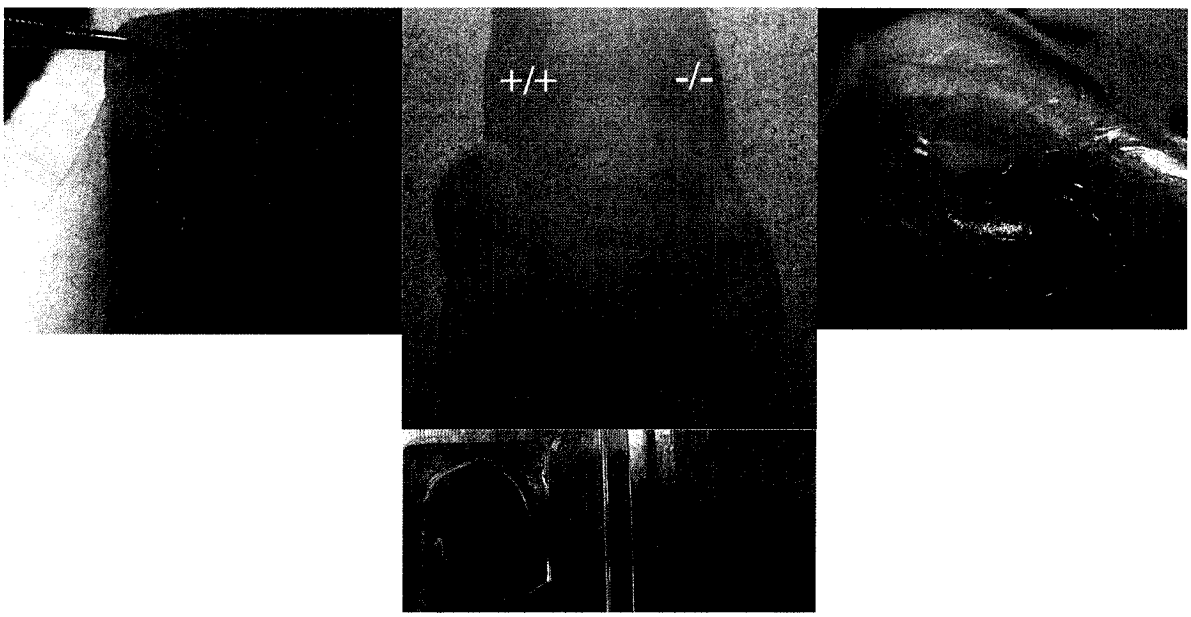
+/+
-/-

B

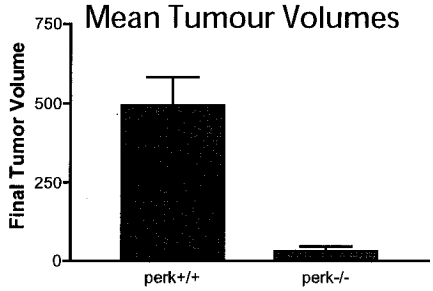
Mean Tumour Volumes
Final Tumor Volume
750
500
250
0
perk+/+
perk-/-

C

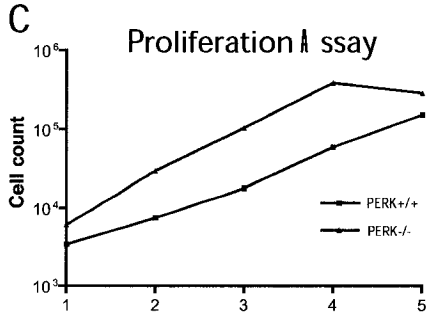
Proliferation Assay
Cell count
10^6
10^5
10^4
10^3
1
2
3
4
5
PERK+/+
PERK-/-

D

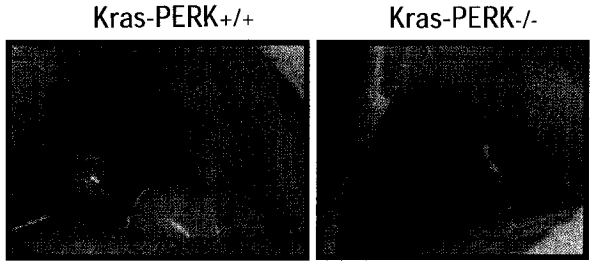
Kras-PERK+/+
Kras-PERK-/-

Figure 1: Perk affects tumor growth and angiogenesis in vivo

(A) Middle frame; Representative nude mouse injected with $Perk^{+/+}$ K-Ras MEFs (left flank) and $Perk^{-/-}$ K-Ras MEFs (right flank) with $5x10^5$ cells/site, at sacrifice. The dissected tumors are displayed below. Top Frame (Left and Right): Photograph of $Perk^{+/+}$ (left) and $Perk^{-/-}$ (right) tumors during dissection. Note the number of vessels migrating towards the $Perk^{+/+}$ (left) tumor compared to the $Perk^{-/-}$ (right) tumor.

(B) Final tumor volumes from 7 animals at sacrifice 23-41days following subcutaneous inoculation of tumor cells (mean±s.e.m)

(C) Growth rates of K-Ras transformed $Perk^{+/+}$ and $Perk^{-/-}$ MEFs in vitro (n=3).

(D) Three representative photographs from Nude mice at sacrifice following a subcutaneous injected of $5x10^5$ Kras transformed $Perk^{+/+}$ (top panel) or $Perk^{-/-}$ MEFs (bottom panel). Note the hemorrhagic pocket surrounding the $Perk^{-/-}$ tumors. Upon dissection, tumors within these blood filled pockets remained small, pale nodules.

A

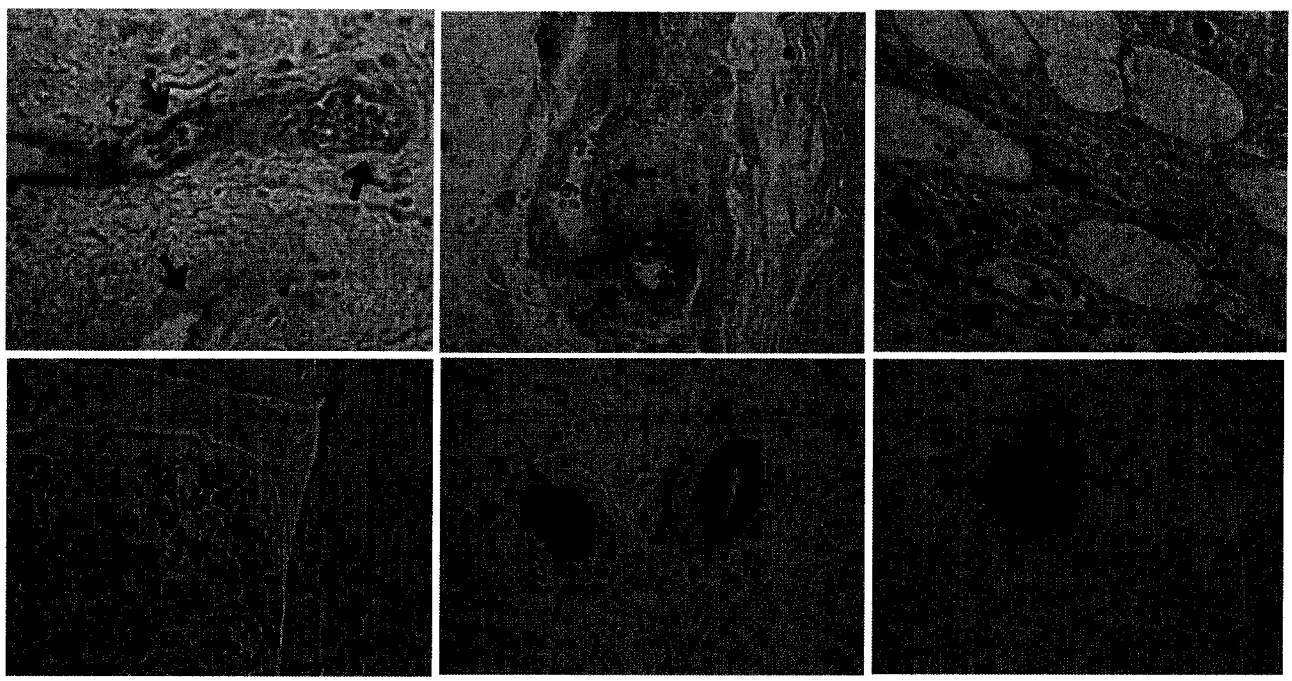
Perk+/+
Perk-/-

B

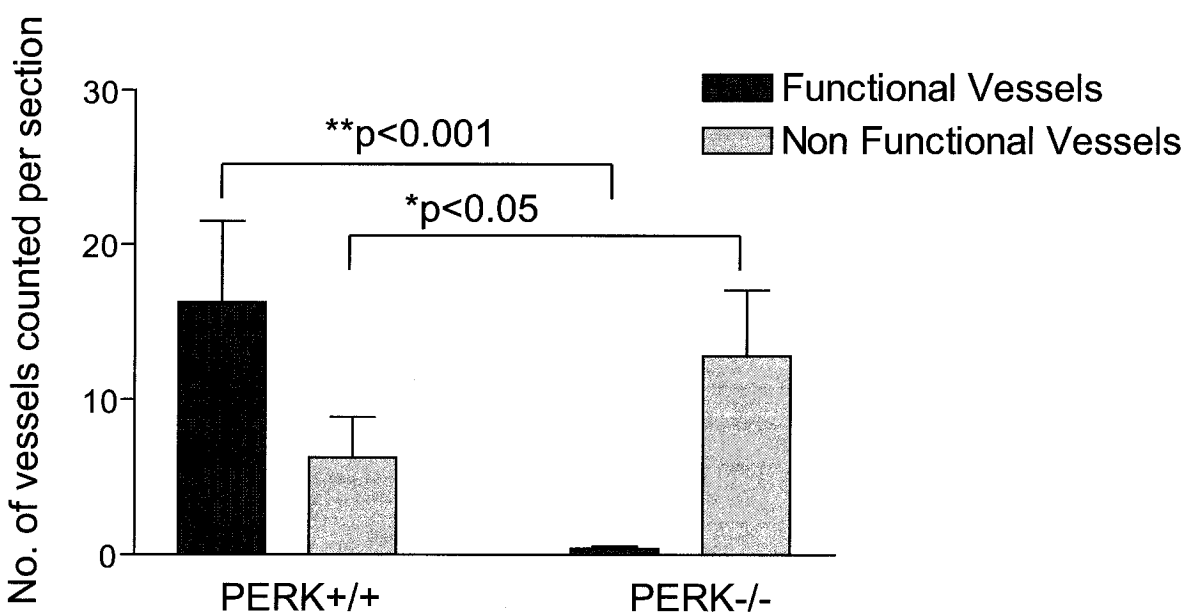
No. of vessels counted per section
30
20
10
0
**p<0.001
*p<0.05
Functional Vessels
Non Functional Vessels
PERK+/+
PERK-/-

Figure 2: Perk affects microvessel formation *in vivo*

A) Paraffin embedded AP stained sponges were sectioned (4μm), Eosin counterstained, and visualized by light microscopy. *Top panel*: Representative pictures from $Perk^{+/+}$ and AP-HDMEC inoculated matrigel/sponge implants. *Bottom panel*: Representative pictures from $Perk^{-/-}$ and AP-HDMEC inoculated matrigel/sponge implants. Blank arrows indicate AP expressing functional vessels as designated by the presence of red blood cells within the vessel. Black arrowheads demonstrate non-functional vessels as designated by the cuboidal shape of the AP-expressing endothelial cells. Green arrows indicate hemorrhagic red blood cell infiltration. All pictures were taken at 40X magnification.

B) The number of functional and non-functional vessels per section was quantified by visualization under 40X magnification with a light microscope. The bars represent the mean ± S.E.M. from three $Perk^{+/+}$ and four $Perk^{-/-}$ containing sponges measured from three serial sections.

resulting in functional vessel formation, tumor growth, and ultimately in the development of hypoxia tolerance.

Microarray Analysis of Polysome-bound mRNAs reveal a role for Perk in the translational regulation of angiogenic genes during hypoxic stress

We performed a microarray analysis on polysome-associated $Perk^{+/+}$ and $Perk^{-/-}$ SV40 immortalized MEFs in order to identify a cohort of genes that are translationally regulated by Perk which may play an essential role in the adaptive response to hypoxic stress. We isolated mRNAs from the high molecular weight polysomes (Fractions 6-10) and total cellular mRNAs from SV40 immortalized $Perk^{+/+}$ and $Perk^{-/-}$ MEFS exposed to normoxia or severe hypoxia (4hr, <0.01%) (Note: for brevity, hypoxia in the text denotes severe hypoxia). The optical density polysome profiles are shown in Figure 3 and demonstrate a significant inhibition in protein synthesis following hypoxic stress, as evidenced by a reduction in polysome-associated mRNAs and by the accumulation of free mRNA and rRNA, with a considerable increase in the monosome peak. Although $Perk^{-/-}$ cells demonstrate an inhibition in translation during hypoxic stress, this response is notably stronger in $Perk^{+/+}$ cells, which demonstrate a more significant decrease in polysome-associated messages (Figure 3; compare $Perk^{+/+}$ 4hr polysomes to $Perk^{-/-}$ 4hr polysomes). This observation has been reported by several groups (7, 59), which substantiates an essential role for Perk in the regulation of translation initiation during acute hypoxic stress. We used microarray analysis to compare the gene expression profiles from total cellular mRNAs and polysome-associated mRNAs from both the $Perk^{+/+}$ and $Perk^{-/-}$ SV40 transformed MEFs. We tailored our analysis to identify genes that displayed a hypoxia and Perk dependent increase in their translational efficiency as determined by their induced

presence in the polysomes without a large change in total cellular mRNA levels. Successful candidates displayed an induced polysome-association in $Perk^{+/+}$ cells without a concomitant induction in the total cytoplasmic mRNA pool, while polysome-associated gene expression in $Perk^{-/-}$ cells remained unchanged or decreased in response to hypoxic stress (Supplemental Figure S2). Additionally, we sought genes that were translationally repressed by hypoxic stress in $Perk^{+/+}$ cells and demonstrated translational-induction in $Perk^{-/-}$ cells. Genes that met these requirements were functionally clustered and are displayed in Table 1.

Data from our microarray substantiated the observations made in the $Perk^{-/-}$ tumors, as our analysis identified the Perk-dependent differential regulation of a cohort of pro-angiogenic genes. Therefore, disruption of Perk within the tumor microenvionment may result in aberrant angiogenic signals from multiple pathways thereby contributing to the development of poorly vascularized tumors. Notably, many of the genes identified by this analysis have been implicated in multiple pathways involved in tumor angiogenesis including cell-cell adhesion, matrix remodeling and ECM proteolysis.

VCIP and other angiogenic factors are efficiently translated during hypoxic stress in $Perk^{+/+}$ cells

We used quantitative real-time PCR (Q-PCR) to verify the translational regulation of 6 candidate genes identified by our microarray analysis (Figures 4, 5, and S1). Q-PCR values were normalized to an internal control, vesicular stomatitis virus RNA encoding the M protein (VSV-M), added exogenously to each RT reaction. With the exception of VCIP, translationally regulated array candidates demonstrated a re-distribution into the polysome-fraction without a concomitant increase in the amount of mRNA in the total lystate (Figures 5 and S1). Our initial microarray analysis demonstrated a modest increase in the steady-state

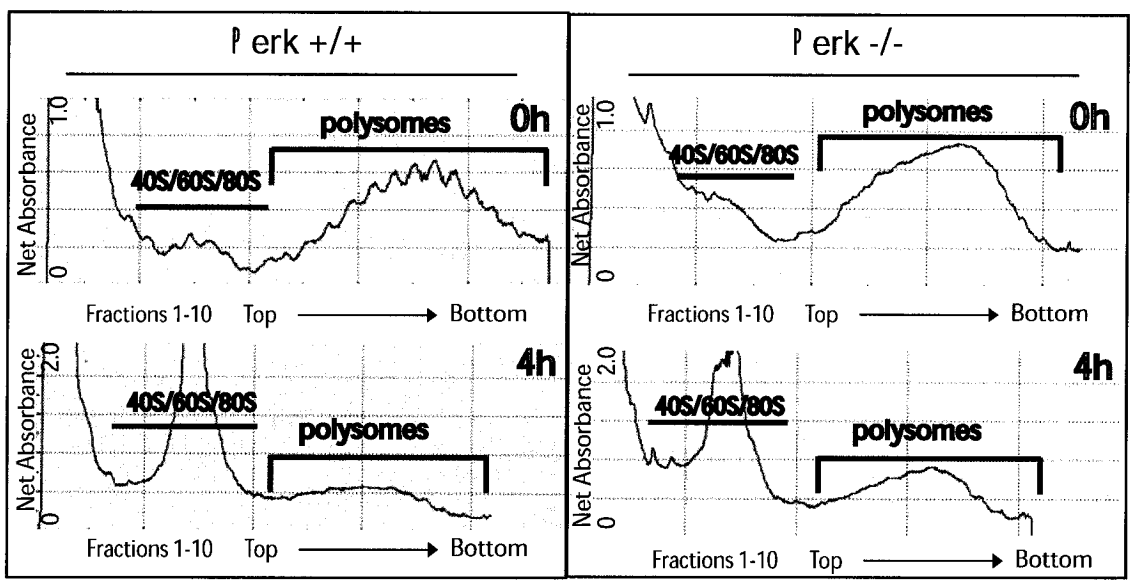
P erk +/+
P erk -/-
0h
4h
polysomes
40S/60S/80S
Net Absorbance
1.0
2.0
0
Fractions 1-10
Top
Bottom

Figure 3: Translational inhibition in response to hypoxic stress is reduced in Perk$^{-/-}$ MEFs

Polysome Profiles (Abs at 254nm) in cell lysates fractionated by sucrose density ultracentrifugation. SV40 immortalized Perk$^{+/+}$ and Perk$^{-/-}$ cells were exposed to hypoxic stress for 4hrs or left untreated (0hr). Cells were treated with cycloheximide (100μg/mL) (37°C, 3min) and lysed in a Triton X-100 buffer (4°C). Cell lysates were layered on a 10ml continuous sucrose gradient (10-50%), ultracentrifuged in an SW-41 rotor 39K for 90min. The position of the polysomes and ribosomal subunits is indicated. The increase in monosome-bound transcripts and ribosomal subunits combined with the decrease in polysomes apparent in the hypoxia treated cells is indicative of decreased protein translation.

Table 1: PERK dependent - Translationally regulated genes

Function	PERK+/+ Translational Induction	PERK+/+ Transcriptional Induction	PERK-/- Translational Induction	PERK-/- Transcriptional Induction	Gene Name	
Regulation of cell growth	3.9	1.9	*abs*	*abs*	Igfbp2: insulin-like growth factor binding protein 2	[83]
	3.2	1.5	1.5	1.2	Nov: Nephroblastoma overexpressed gene	
Blood vessel formation	4.1	2.0	1.0	2.0	VCIP: VEGF and type I collagen inducible protein	[42]
Cell adhesion	2.9	0.9	0.8	1.1	D7Ertd458e: Poliovirus receptor	
	2.4	0.7	*abs*	*abs*	Thbs2: thrombospondin 2	[10, 19]
	3.6	1.4	*abs*	*abs*	cspg2: chondroitin sulfate proteoglycan 2 (versican)	[13]
	2.0	0.8	0.8	0.9	col6a3: procollagen, type VI, alpha 3	[86]
	2.4	0.8	*abs*	*abs*	col12a1: collagen, type XII, alpha 1	
	0.9	0.3	2.0	2.0	EEMP1: EGF-containing fibulin-like extracellular matrix protein 1	[49]
Collagen catabolism	2.1	0.4	*abs*	*abs*	mmp13: matrix metalloproteinase 13	[1]
	1.1	1.1	3.2	2.8	TIMP3: Tissue inhibitor of metalloproteinase3	[78]
Regulation of transcription	2.2	0.9	1.0	1.5	Aebp1: AE binding protein 1	
Ephrin Receptor Activity	*abs*	*abs*	2.6	0.7	EphA4: Ephrin Receptor A4	[99]
Protein Trasportation/ Folding	2.5	1.5	*abs*	*abs*	ptprm: protein tyrosine phosphatase receptor type M	
	2.2	1.4	1.1	1.9	Rrbp1: ribosome binding protein 1	
	2.1	1.1	0.9	1.5	hyou1: hypoxia up-regulated 1 (ORP150)	[73]
	2.8	1.0	0.9	1.0	slitl2: slit-like 2	
	2.1	0.7	1.4	2.0	plod1: procollagen-lysine 1 2-oxoglutarate 5-dioxygenase 1	
	2.1	1.2	1.4	1.0	lamp2:lysosomal membrane glycoprotein 2	
Transporter Activity	2.0	0.3	0.7	0.8	aqp1: aquaporin 1	
Signal transduction	2.1	1.5	1.3	0.7	Grb10: growth factor receptor bound protein 10	[68]
	2.5	1.0	1.0	3.7	pdgfrb: platelet-derived growth factor receptor beta	
	2.4	0.8	*abs*	*abs*	stmn2: stathmin-like 2	
Unknown	4.6	*abs*	*abs*	*abs*	dcn: decorin	
	2.5	1.0	0.5	2.1	zfp503: zinc finger protein 503	
	2.1	0.9	0.7	0.8	tnc: tenascin C	
	2.1	1.5	0.6	0.8	crlf1: cytokine receptor-like factor 1	

Table 1: Perk-dependent Translationally Regulated Genes

Results of microarray analysis to identify transcripts that were exclusively associated with high molecular weight polysomes in SV40 immortalized $Perk^{+/+}$ MEFs following an acute response to hypoxic stress (4hr). Genespring 5.0 software was used to compare the relative expression of polysome-bound mRNAs from $Perk^{+/+}$ and $Perk^{-/-}$ MEFs following acute normoxia (0poly) or hypoxia (4poly) treated cells. Genes that were exclusively induced >1.5-fold in the polysomes of $Perk^{+/+}$ MEFs (+/+ poly 4/0) and showed either a decrease or no significant change in their polysome-association in $Perk^{-/-}$ MEFs (-/- poly4/0). Candidates that demonstrated less than a 2fold change in total cellular mRNA (+/+Total 4/0) were considered for further analysis. These genes were functionally clustered and subsets of these genes are represented in this table. Candidates with a described role in angiogenesis are referenced in red.

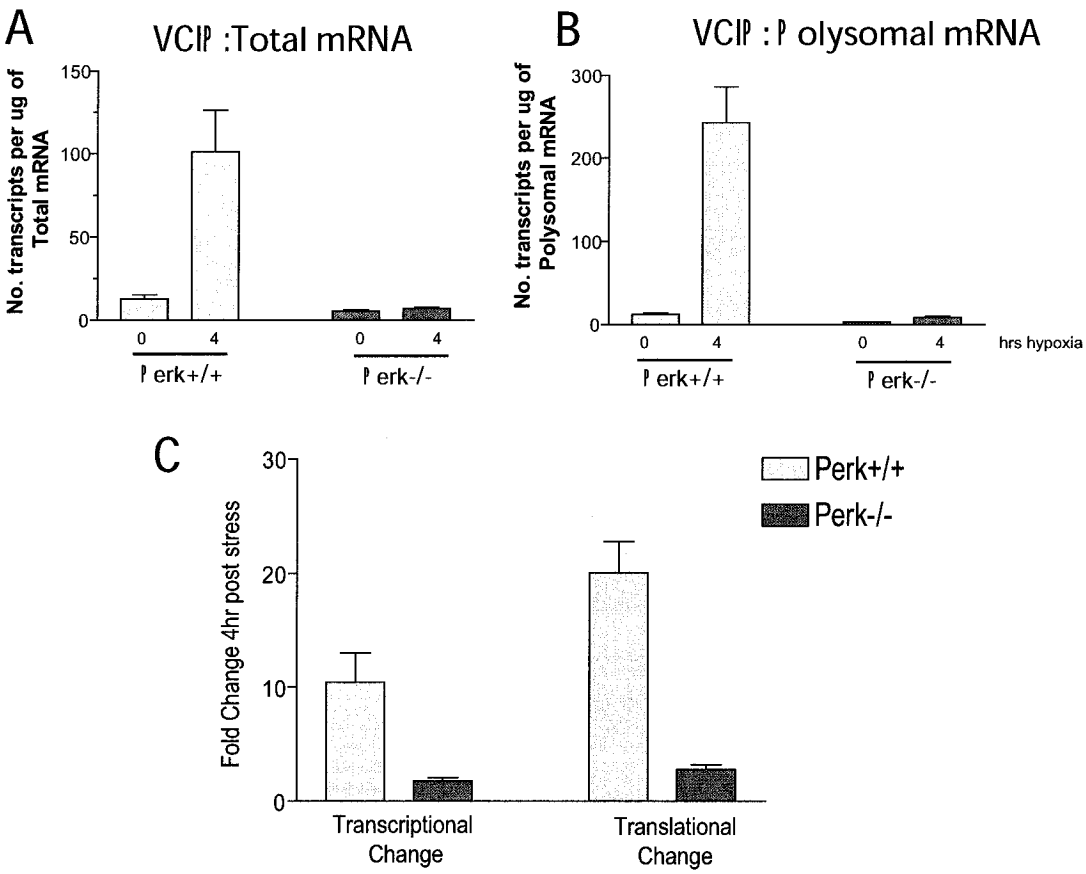
A
VCIP :Total mRNA
No. transcripts per ug of Total mRNA
150
100
50
0
0
4
0
4
P erk+/+
P erk-/-
B
VCIP : P olysomal mRNA
No. transcripts per ug of Polysomal mRNA
300
200
100
0
0
4
0
4
hrs hypoxia
P erk+/+
P erk-/-
C
Fold Change 4hr post stress
30
20
10
0
Perk+/+
Perk-/-
Transcriptional Change
Translational Change

Figure 4: VCIP mRNA is more efficiently translated during hypoxia in Perk$^{+/+}$ cells

(A) *Total mRNA expression is unaffected by hypoxia.* Total RNA was isolated prior to sucrose gradient fractionation from hypoxia treated (4hr) or normoxic (0hr) SV40 immortalized Perk$^{+/+}$ and Perk$^{-/-}$ cells, reverse transcribed and quantified by real-time PCR. The quantities of each transcript are described as the number of transcripts isolated per μg of Total RNA. Each sample was independently normalized to a spiked internal control. Q-PCR analysis was replicated in triplicate. Results are representative of the average ± S.E.M of three independent experiments

(B) *VCIP transcripts are enriched in the polysomes of Perk$^{+/+}$ cells during hypoxia.* High molecular weight polysomes from hypoxia treated (4hr) or normoxic (0hr) SV40 immortalized Perk$^{+/+}$ and Perk$^{-/-}$ cells were pooled (fractions 6-10), reverse transcribed and quantified by real-time PCR. The quantities of each transcript are described as the number of transcripts isolated per μg of polysomal RNA. Each sample was independently normalized to a spiked internal control. Q-PCR analysis was repeated in triplicate. Results are representative of the average ± S.E.M of three independent experiments.

(C) *Perk+/+ cells demonstrate induced translation of VCIP during hypoxia.* The transcriptional fold change was plotted as the number of VCIP transcripts isolated per μg of Total RNA from hypoxia treated (4hr) vs normoxic (0hr) cytoplasmic lysates. The translational fold change was plotted as the number of VCIP transcripts isolated per μg of Polysomal RNA from hypoxia treated (4hr) vs normoxic (0hr) lysates.

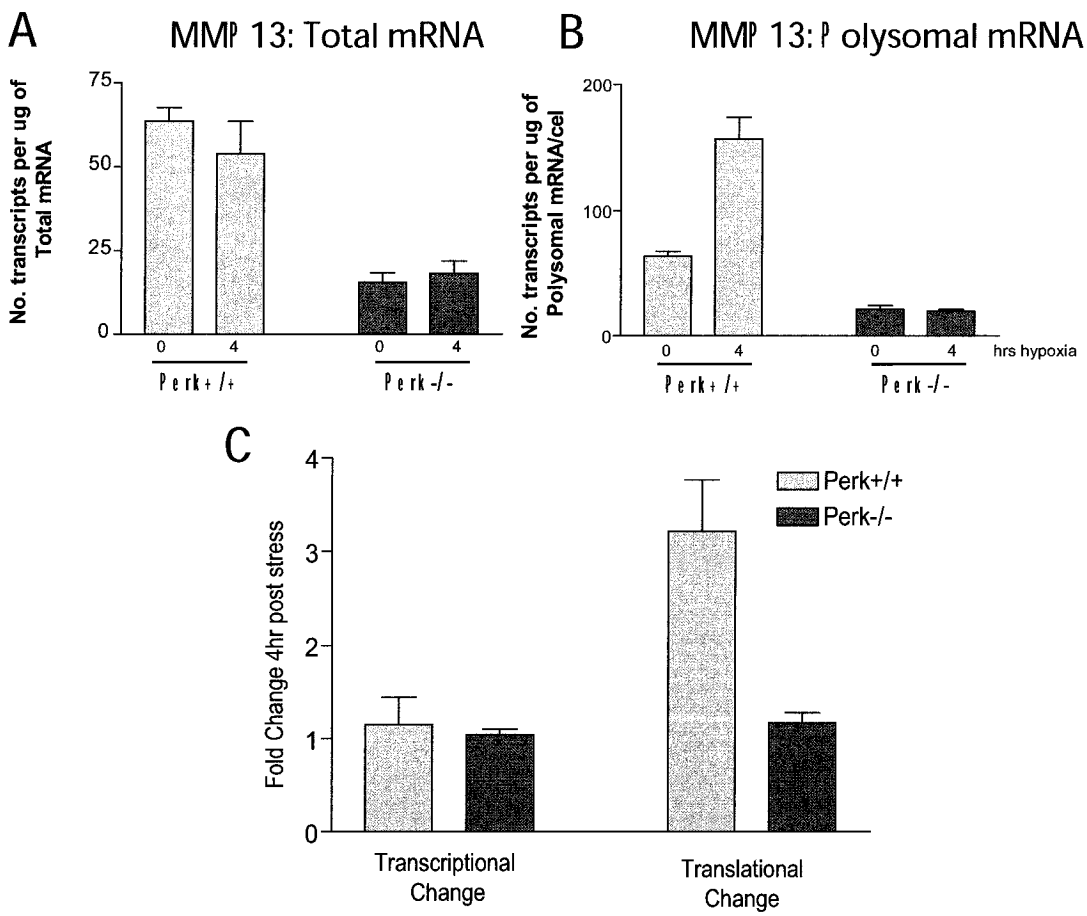
A
MMP 13: Total mRNA
No. transcripts per ug of Total mRNA
75
50
25
0
0
4
0
4
Perk+/+
Perk-/-
B
MMP 13: Polysomal mRNA
No. transcripts per ug of Polysomal mRNA/cel
200
100
0
0
4
0
4
hrs hypoxia
Perk+/+
Perk-/-
C
Fold Change 4hr post stress
4
3
2
1
0
Perk+/+
Perk-/-
Transcriptional Change
Translational Change

Figure 5: MMP13 mRNA is more efficiently translated during hypoxia in Perk$^{+/+}$ cells

(A) *Total mRNA expression is unaffected by hypoxia.* Total RNA was isolated prior to sucrose gradient fractionation from hypoxia treated (4hr) or normoxic (0hr) SV40 immortalized Perk$^{+/+}$ and Perk$^{-/-}$ cells, reverse transcribed and quantified by real-time PCR. The quantities of each transcript are described as the number of transcripts isolated per μg of Total RNA. Each sample was independently normalized to a spiked internal control. Q-PCR analysis was replicated in triplicate. Results are representative of the average ± S.E.M of three independent experiments

(B) *MMP13 transcripts are enriched in the polysomes of Perk$^{+/+}$ cells during hypoxia.* High molecular weight polysomes from hypoxia treated (4hr) or normoxic (0hr) SV40 immortalized Perk$^{+/+}$ and Perk$^{-/-}$ cells were pooled (fractions 6-10), reverse transcribed and quantified by real-time PCR. The quantities of each transcript are described as the number of transcripts isolated per μg of polysomal RNA. Each sample was independently normalized to a spiked internal control. Q-PCR analysis was repeated in triplicate. Results are representative of the average ± S.E.M of three independent experiments.

(C) *Perk$^{+/+}$ cells demonstrate induced translation of MMP13 during hypoxia.* The transcriptional fold change was plotted as the number of MMP13 transcripts isolated per μg of Total RNA from hypoxia treated (4hr) vs normoxic (0hr) cytoplasmic lysates. The translational fold change was plotted as the number of MMP13 transcripts isolated per μg of Polysomal RNA from hypoxia treated (4hr) vs normoxic (0hr) lysates.

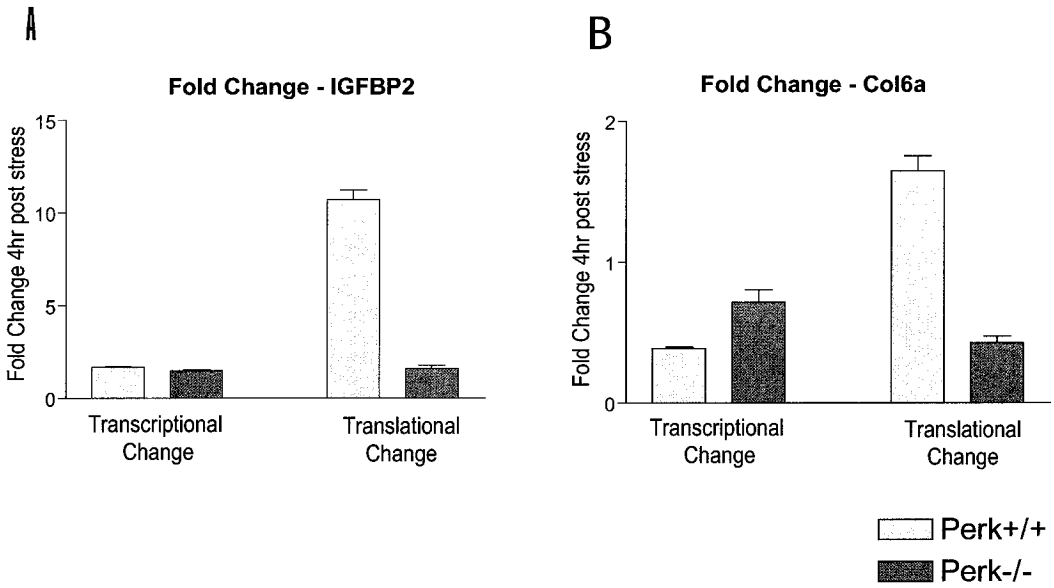
A
Fold Change - IGFBP2
Fold Change 4hr post stress
15
10
5
0
Transcriptional Change
Translational Change
B
Fold Change - Col6a
Fold Change 4hr post stress
2
1
0
Transcriptional Change
Translational Change
Perk+/+
Perk-/-

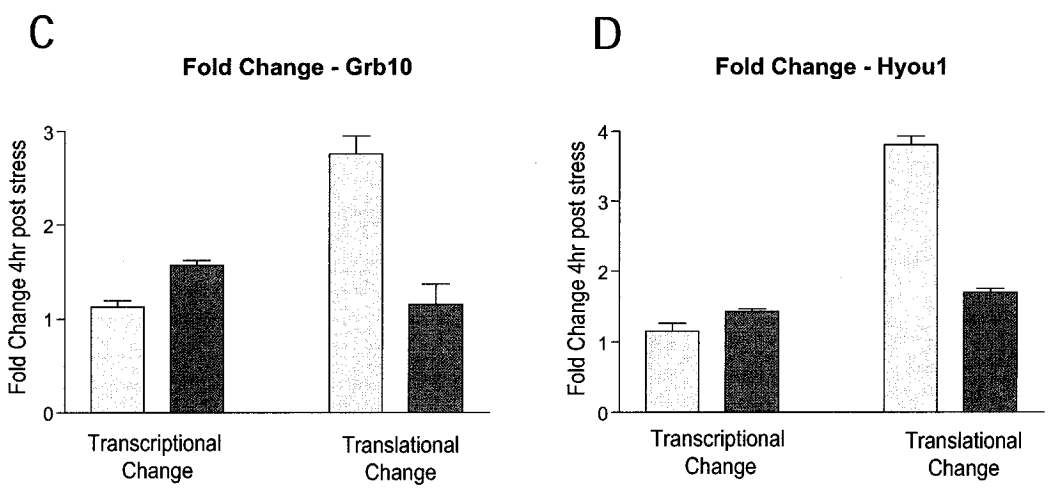
C
Fold Change - Grb10
Fold Change 4hr post stress
3
2
1
0
Transcriptional Change
Translational Change
D
Fold Change - Hyou1
Fold Change 4hr post stress
4
3
2
1
0
Transcriptional Change
Translational Change

Supplemental Figure S1: Perk-dependent Translationally Regulated Genes

A-D) $Perk^{+/+}$ cells demonstrate induced translation of IGFBP2, Col6a, Grb10, and Hyou1 during hypoxic stress. The transcriptional fold change was plotted as the number of transcripts isolated per mg of Total RNA from hypoxic (4hr) vs normoxic (0hr) cytoplasmic lysates. The translational fold change was plotted as the number of transcripts isolated per μg of Polysomal RNA from hypoxic (4hr) vs normoxic (0hr) lysates.

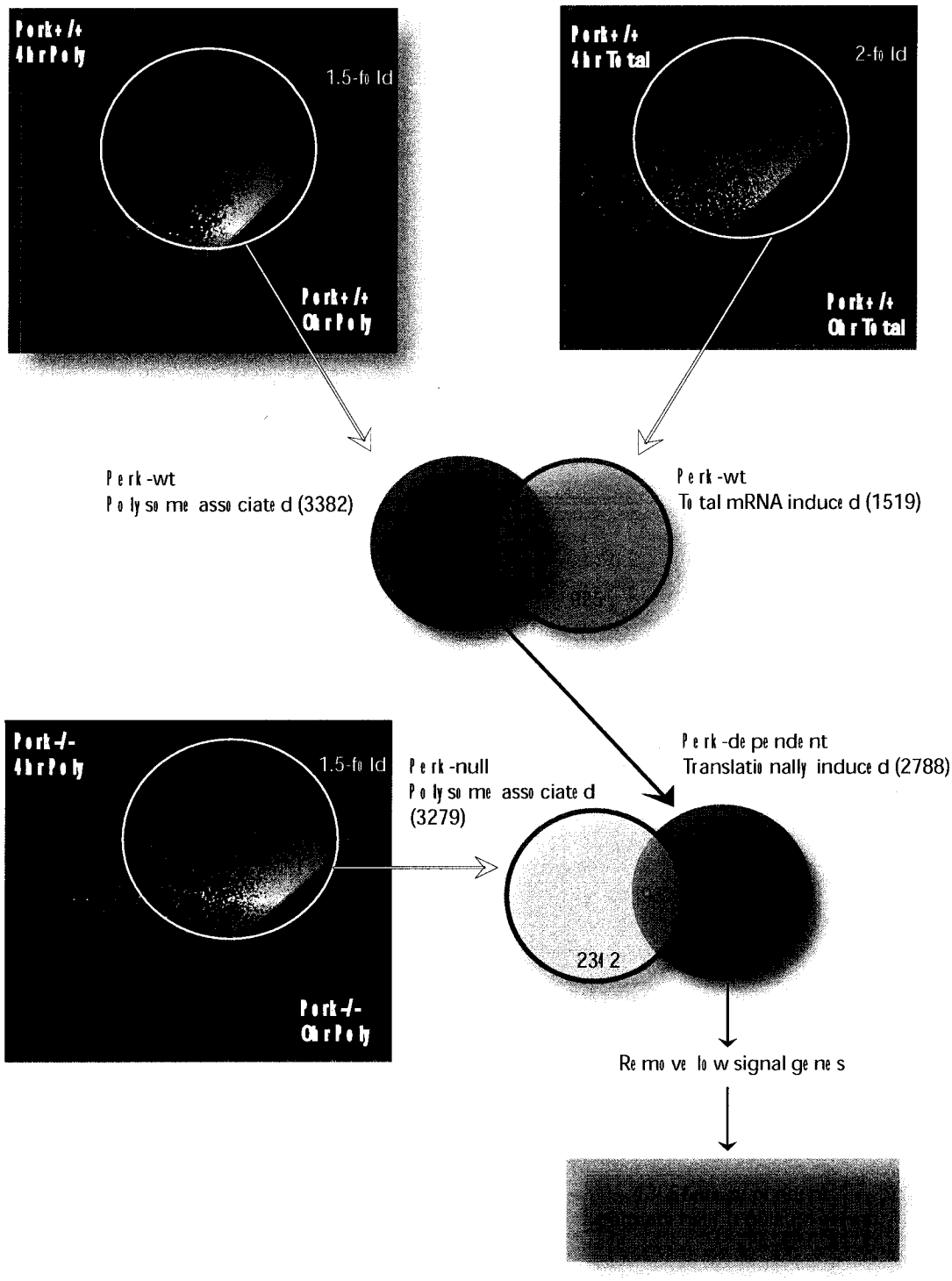
Perk+/+
4hr Poly
1.5-fold
Perk+/+
Ctr Poly
Perk+/+
4hr Total
2-fold
Perk+/+
Ctr Total
Perk-wt
Polysome associated (3382)
Perk-wt
Total mRNA induced (1519)
Perk-/-
4hr Poly
1.5-fold
Perk-null
Polysome associated
(3279)
Perk-dependent
Translationally induced (2788)
2312
Perk-/-
Ctr Poly
Remove low signal genes

Supplemental Figure S2: Strategy for determining Perk-dependent translationally regulated candidates in response to hypoxic stress

Using Genespring software we identified by scatter plot a list of genes that were induced >1.5-fold during stress in the Perk+/+ polysome arrays and a list of genes that were induced >2-fold during stress in the Perk+/+ total arrays. Using Venn Diagrams we removed genes that were induced >2-fold in the total cytoplasmic lysates from genes that demonstrated a translational increase. We identified by scatter plot a list of genes that were induced >1.5-fold during stress in the Perk-/- polysome arrays. Using Venn Diagrams we removed genes that demonstrated an increase in the translation in both Perk+/+ and Perk-/- arrays, keeping genes that demonstrated a Perk-dependent translational induction in response to hypoxic stress without a concomitant increase in total cyplasmic mRNAs. The remaining genes were further filtered for quality control, removing candidates with signals close to background noise.

levels of VCIP mRNA and a 4-fold increase in the polysome-associated mRNAs in $Perk^{+/+}$ cells upon hypoxic stress. Upon validation by Q-PCR we noted a 10-fold difference in steady-state levels (Figure 4A; Compare 0h vs 4h in $Perk^{+/+}$ and $Perk^{-/-}$, Figure 4C), and a 20-fold translational induction in VCIP expression exclusively in $Perk^{+/+}$ cells (Figure 4B; Compare 0h vs 4h in $Perk^{+/+}$ and $Perk^{-/-}$, Figure 4C). It has been reported that VCIP exhibits a strong transcriptional induction in response to growth factors and cytokines in endothelial cells and epidermoid carcinomas (42); however, to our knowledge, this is the first report describing the post-transcriptional regulation of VCIP. Remarkably, $Perk^{-/-}$ cells were incapable of eliciting either a transcriptional or translational induction in VCIP expression in response to hypoxic stress (Figure 4). Similarly, $Perk^{+/+}$ cells demonstrated a differential translational induction of other genes involved in the regulation of angiogenesis, including MMP13, a metalloprotease that has been implicated in tumor invasion. The translational induction of MMP13 is evidenced by the recruitment of its mRNAs to the polysomes exclusively in $Perk^{+/+}$ cells in response to hypoxic stress (Figure 5B; compare 0h vs 4h in $Perk^{+/+}$ vs $Perk^{-/-}$) without a concomitant increase in total cellular mRNAs (Figure 5A; 0h vs 4h). Other validated candidates demonstrated similar translational induction in the absence of changes in total cellular mRNAs including Hyou1, Grb10, IGFBP2, and Col6a (Supplementary Figure S1). Only 5.4 % of the well-represented genes on the microarray demonstrated any translational dependence on Perk expression (Genes induced >1.5-fold in the polysome fractions exclusively in $Perk^{+/+}$ cells without a concomitant induction in the total mRNA >2-fold relative to the number of total genes that demonstrated reliable signal by microarray; 1254/25055, Table 1). However, not all hypoxia induced genes demonstrated a dependence on Perk expression, including ATF3 (Figure 6). Both $Perk^{+/+}$ and $Perk^{-/-}$ cells

demonstrated a strong transcriptional (Figure 4A, 4C) and translational (Figure 6B, 6C) induction in ATF3 expression during hypoxic stress. We previously demonstrated that ATF3 responded to hypoxic stress by an increase in total cellular mRNA and by an increase in its polysome-association (Blais 2004); this study however, demonstrates that induction of ATF3 in response to hypoxic stress is not dependent on Perk expression, a finding that has been corroborated by Gardner *et al.* (submitted).

As expected, large changes in steady-state mRNA levels in response to hypoxic stress were largely independent of Perk. We did observe, however, a reduced transcriptional (2-fold) and translational (3-fold) induction in the expression of CHOP/GADD153 in $Perk^{-/-}$ MEFs, which correlated with the reduced transcriptional induction of Myd116 (Gadd34) and CA6, two downstream targets of CHOP/GADD153 (Table 2). Previously, we demonstrated that hypoxic stress resulted in a substantial induction in CHOP expression (7), an observation that appears to be dependent on the activation of two UPR responsive transcription factors, ATF4 (31) and ATF3 (46). The observation that CHOP expression was residually induced in $Perk^{-/-}$ MEFS suggests perhaps that ATF3 plays some role in the regulation of CHOP during hypoxic stress. Additionally, we noted a 7-fold and 8-fold difference between $Perk^{+/+}$ and $Perk^{-/-}$ cells, in the expression of metallothioneins 1 and 2 (MT1 and MT2), two members of a family of stress-induced proteins that play a critical role in protecting cells against metal toxicity and oxidants. The transcriptional induction of MT1 in response to hypoxia has been previously described (69). More recently Bi *et al.* described the activation of MT1 transcription upon the inhibition of protein synthesis with CHX (8), suggesting a connection between the regulation of translation and the transcriptional induction of genes involved in the adaptive response to stress.

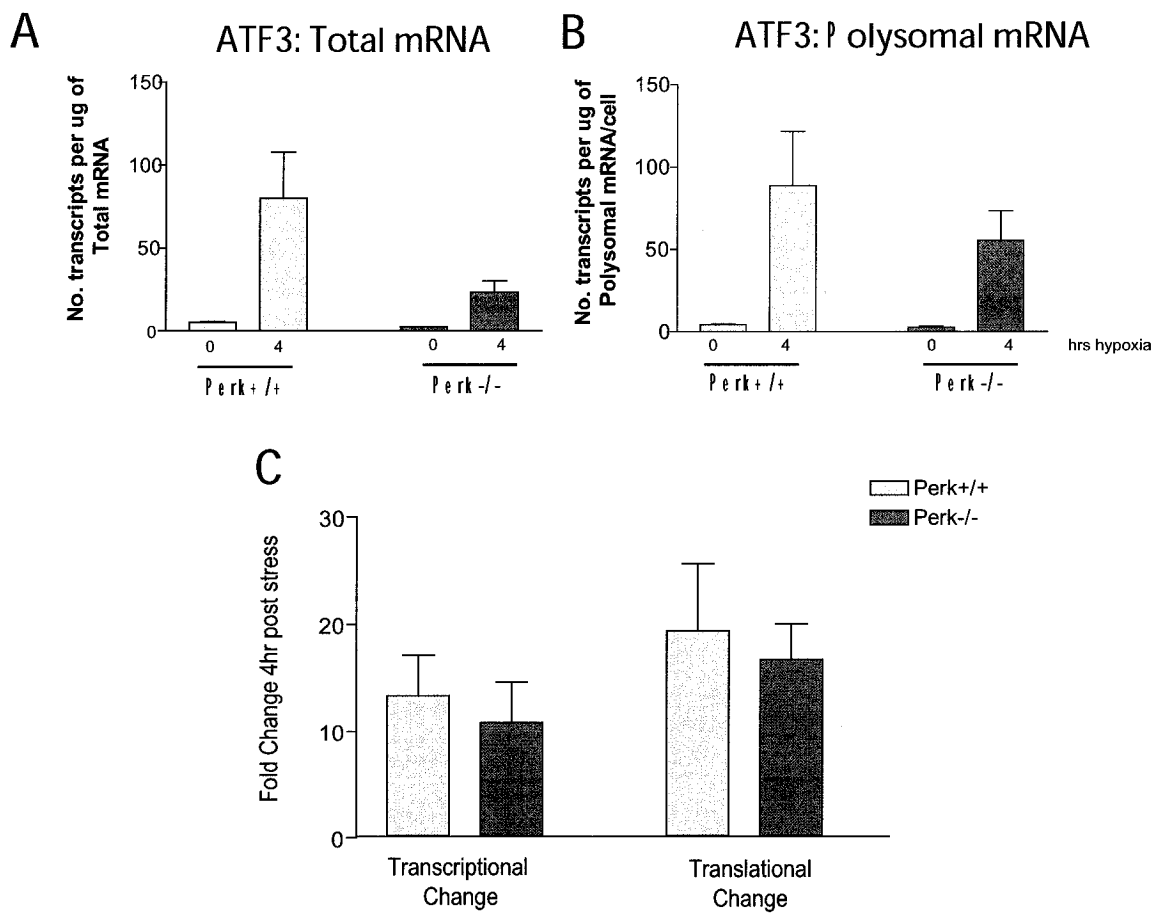
A
ATF3: Total mRNA
No. transcripts per ug of Total mRNA
150
100
50
0
0
4
0
4
Perk+/+
Perk-/-
B
ATF3: Polysomal mRNA
No. transcripts per ug of Polysomal mRNA/cell
150
100
50
0
0
4
0
4
hrs hypoxia
Perk+/+
Perk-/-
C
Perk+/+
Perk-/-
Fold Change 4hr post stress
30
20
10
0
Transcriptional Change
Translational Change

Figure 6: ***Transcription and translation of ATF3 mRNA is not dependent on Perk activity during hypoxia.***

(A) *ATF3 Total mRNA expression is induced by hypoxic stress.* Total RNA was isolated prior to sucrose gradient fractionation from hypoxia treated (4hr) or normoxic (0hr) SV40 immortalized $Perk^{+/+}$ and $Perk^{-/-}$ cells, reverse transcribed and quantified by real-time PCR. The quantities of each transcript are described as the number of transcripts isolated per μg of Total RNA. Each sample was independently normalized to a spiked internal control. Q-PCR analysis was replicated in triplicate. Results are representative of the average ± S.E.M of three independent experiments

(B) *ATF3 transcripts are enriched in the polysomes of $Perk^{+/+}$ and $Perk^{-/-}$ cells during hypoxia.* High molecular weight polysomes from hypoxia treated (4hr) or normoxic (0hr) SV40 immortalized $Perk^{+/+}$ and $Perk^{-/-}$ cells were pooled (fractions 6-10), reverse transcribed and quantified by real-time PCR. The quantities of each transcript are described as the number of transcripts isolated per μg of polysomal RNA. Each sample was independently normalized to a spiked internal control. Q-PCR analysis was repeated in triplicate. Results are representative of the average ± S.E.M of three independent experiments.

(C) *$Perk^{+/+}$ and $Perk^{-/-}$ cells demonstrate induced transcription and translation of ATF3 during hypoxia.* The transcriptional fold change was plotted as the number of ATF3 transcripts isolated per μg of Total RNA from hypoxia treated (4hr) vs normoxic (0hr) cytoplasmic lysates. The translational fold change was plotted as the number of VCIP transcripts isolated per μg of Polysomal RNA from hypoxia treated (4hr) vs normoxic (0hr) lysates.

Table 2: Hypoxia induced; Perk-independent - Total Cellular Changes

Function	Transcriptional Fold Change *Perk+/+*	*Perk-/-*	Gene Name
Angiogenesis	7.9	5.8	VEGF A [83-85]
	4.9	3.1	adrenomedullin 2 [86-88]
	4.7	4.4	Heme oxygenase 1 [89]
	3.6	2.2	angiopoietin-like 6
	3.6	3.3	ephrin B2 [90]
	1.8	2.4	angiomotin
NO mediated	22.1	3.3	metallothionein 1 [32-33]
	18.7	2.4	metallothionein 2 [32-33]
UPR	13.8	15.4	hsp1A
	10.1	26.6	hsp1A
	4.5	6.3	hsp1
	3.5	4.4	hsp70
	6.3	2.2	Myd116 (Gadd34) [7]
	1.9	2.5	DnaJ (Hsp40) homolog
	11.5	6.0	Ddit3 (CHOP) [7,15,91]
Regulation of Transcription	15.6	18.6	ATF3 [7, 102]
	3.0	2.0	ATF5
	4.8	2.5	Max dimerization protein
	3.4	1.8	Max protein
Metabolism	8.6	2.6	CA6
	6.3	1.9	endothelial cell growth factor 1
	3.2	5.2	adenylate kinase 4 [92, 93]
	2.2	1.9	aldehyde dehydrogenase 2 [94]
	2.0	2.0	6-phosphofructo-2-kinase/fructorse-2, 6-biphosphatase3
	2.0	2.2	phosphoglucomutase 2
	3.4	4.0	hexokinase 2 [95, 96]
	2.2	2.7	pyruvate carboxylase [97]
	3.0	1.8	asparagine synthetase
Response to DNA Damage	10.9	5.6	DNA-damage-inducible transcript 3
	6.9	4.8	GADD45a [101]
	5.1	8.3	DNA-damage-inducible transcript 4
Apoptosis	4.8	2.5	Max-dimerization protein
	3.4	18.6	NIP3 [98-100]
	2.5	2.8	BCL2-like 11 (apoptosis facilitator)
mRNA processing and Translation	2.2	2.5	cytoplasmic polyadenylation element binding protein 4
	2.1	1.9	dual specificity phosphatase 3

Table 2: Total Cellular mRNA Changes in Gene Expression During Hypoxia.

Results of Affymetrix MG430_2 microarray analysis used to identify steady state changes in gene expression during hypoxia. Genespring 5.0 software was used to compare $Perk^{+/+}$ and $Perk^{-/-}$ 4total to 0total RNA to determine gene changes induced >2fold. Genes were functionally clustered and referenced if previously identified in the literature. Only named genes are included in this list, ESTs were omitted.

The 5'UTR of VCIP mediates internal initiation

Previous reports have established that VCIP gene expression is induced by growth factors and cytokines (42); however, the contribution of post-transcriptional regulation on VCIP expression had not yet been addressed. To ascertain if VCIP might be regulated in a similar manner to ATF4, through inhibitory uORFs in its 5'UTR, we searched the human VCIP 5'UTR and other mammalian orthologs for conserved uORFs and consistently found only one uORF present at the extreme 5' region of its 5'UTR. Unlike ATF4, which has two conserved uORFs in its 5'UTR and is negatively regulated by the second uORF that causes read through of the canonical start codon (60, 92), we found no evidence for this mechanism of regulation in the VCIP 5'UTR. Interestingly, when we performed a sequence analysis of mammalian VCIP 5'UTRs, we noticed significant sequence homology between the human VCIP 5'UTR and other mammalian species (Figure 7A). As hypoxic stress results in reduced cap-dependent translation initiation (4, 16, 50, 59, 91), internal ribosome recruitment to the VCIP 5'UTR may provide an alternative explanation to its translational induction during hypoxic stress. To test if VCIP contained an active IRES element we cloned its 5'UTR into a βgal/CAT bicistronic vector (Figure 7B). This construct is transcribed as a single capped mRNA with a short intercistronic sequence separating the 5'βgal cistron (beta-galactosidase) and the 3'CAT cistron (Chloramphenicol Acetyl Transferase). Translation of βgal is regulated by cap-dependent translation whereas CAT translation can only be initiated by a *bona fide* IRES element capable of initiating cap-independent translation. The viral EMCV IRES cloned into the bicistronic vector was used as a positive control whereas the empty bicistronic vector was included as a negative control.

In addition, we created deletion mutants within the VCIP 5'UTR to help define the region(s) of IRES activity (Figure 7B). Significant CAT activity was detected in extracts from cells transfected with the βgal/VCIP/CAT or βgal/EMCV/CAT bicistronic constructs. As expected, no CAT expression was detected in cell extracts from βgal/Empty/CAT transfected cells (Figure 8A). Additionally, a small stem-loop structure was cloned upstream of the βgal cistron in the βgal/VCIP/CAT vector. This stem-loop structure creates an obstacle to the scanning ribosome thereby inhibiting cap-dependent translation. Significant CAT expression was detected in lysates from cells transfected with the HP-βgal /VCIP/CAT expression vector (Figure 9A) in the absence of any measurable βgal activity suggesting that the VCIP 5'-UTR mediates the production of CAT independent of βgal as would be expected if an IRES element were present. Deletion constructs were created based on the homology pattern observed across species within the 5'UTR of VCIP (Figure 7A). No homology was observed within the regions of 1-140 bp, similarly CAT activity was ablated in this construct as compared to the empty vector control, suggesting that alone, this sequence does not contain an IRES sequence. Most of the homology identified within the 5'UTR spanned the sequence between 140-380 bp although CAT activity was only marginally active in this construct. Interestingly, only when the sequences 1-140 bp were added to the sequences spanning 140-380 bp was significant IRES activity observed (Figure 8A) suggesting a modular composition of the VCIP IRES. To ensure that VCIP IRES activity could not be explained by spurious splicing or cryptic promoter activity we compared the quantities of βgal and CAT cistrons of the bi-cistronic mRNA by Q-PCR. The βgal/CAT bicistronic vector is transcribed as a single mRNA, thus the ratio of βgal/CAT cistrons should equal 1. In the event that splicing or cryptic promoter activity is present within the 5'UTR of VCIP,

A

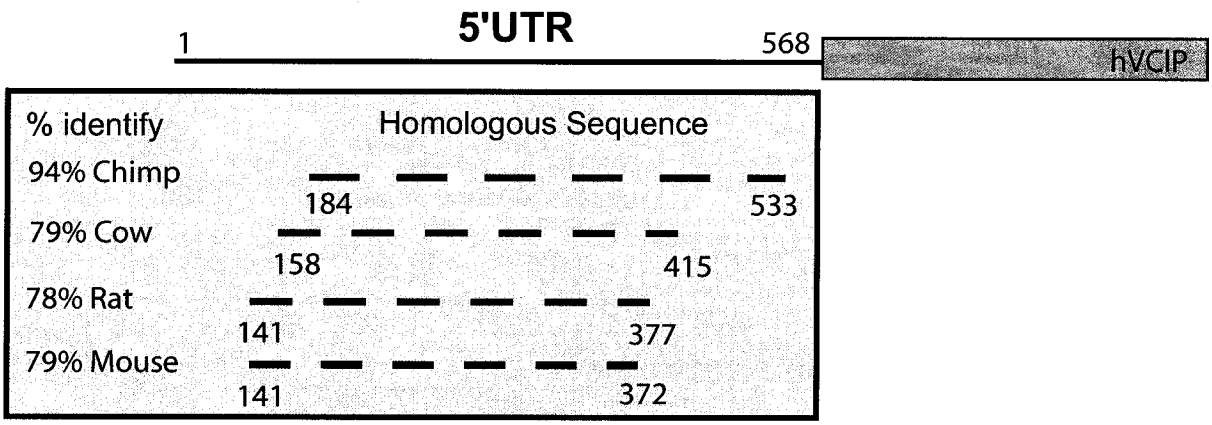
5'UTR
1
568
hVCIP
% identify
Homologous Sequence
94% Chimp
184
533
79% Cow
158
415
78% Rat
141
377
79% Mouse
141
372

B

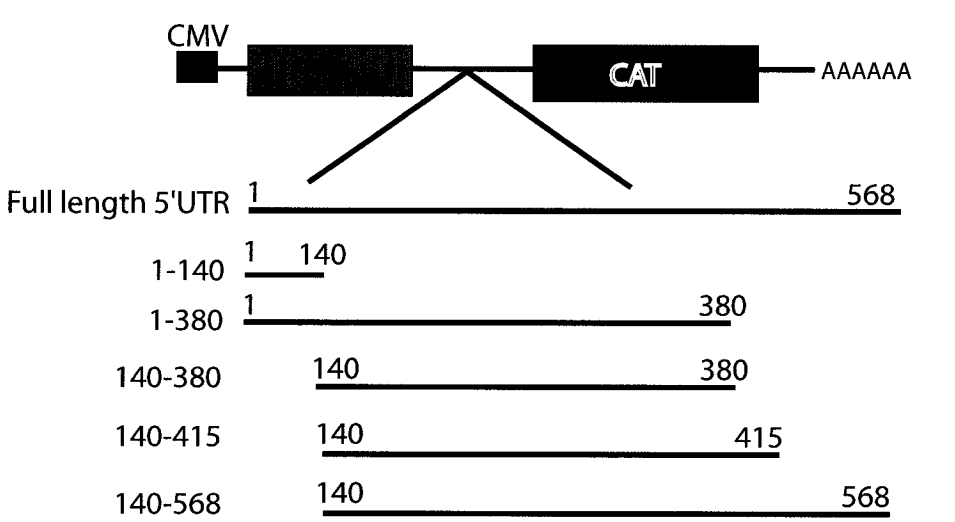
Constructs in gal/CATbicistronic vector
CMV
CAT
AAAAAA
Full length 5'UTR
1
568
1-140
1
140
1-380
1
380
140-380
140
380
140-415
140
415
140-568
140
568

Figure 7: VCIP 5'UTR is highly conserved

A) VCIP 5'UTR displays high conservation among several mammalian species. The various species are identified on the left with their percent identity to the human VCIP 5'UTR indicated. A dashed line specifies the areas within the 5' UTR that share high homology with the human sequence.

B) A schematic of the various VCIP 5'UTR deletion constructs cloned into the βgal/CAT bicistronic vector.

CAT transcripts would be transcribed independently from βgal, thus the quantity of CAT mRNA would exceed that of βgal mRNA which could explain increased CAT activity in the absence of βgal expression. Q-PCR measurements demonstrated no differences in the proportion of βgal to CAT cistron RNA from cells transfected with either the EMCV, Empty, or VCIP bicistronic vectors (Figure 9B) indicating that CAT activity measured in the VCIP bicistronic vector resulted from a *bona fide* cellular IRES within the 5'UTR.

IRES Activity Is Maintained during Hypoxia:

To assess whether the putative VCIP IRES could function in a bicistronic context under hypoxic conditions, we transfected U2OS cells with βgal/EMCV/CAT or βgal/VCIP/CAT and placed these cells under normoxic or hypoxic conditions and expression of βgal and CAT activity were measured in cell extracts. We observed that the CAT/βgal activity decreased approximately 25% in cells transfected with the βgal/EMCV/CAT vector (Figure 8B). This effect is likely an overestimation of the true CAT/βgal activity due to the extreme stability of both βgal and CAT proteins, most probably EMCV IRES activity and global protein translation are similarly diminished in response to hypoxic stress. In contrast the CAT/βgal activity measured in cells transfected with the βgal/VCIP/CAT construct remained high, suggesting the VCIP IRES remains efficiently translated during hypoxic stress despite the substantial inhibition that occurs in protein translation. Moreover, U2OS cells co-transfected with the βgal/VCIP/CAT vector and a stress-inducible luciferase reporter fused to the 5'UTR of ATF4 demonstrate preferential association with polysomes during hypoxic stress (Supplemental Figure S3) providing supporting evidence for the preferential translation of VCIP during hypoxic stress.

A

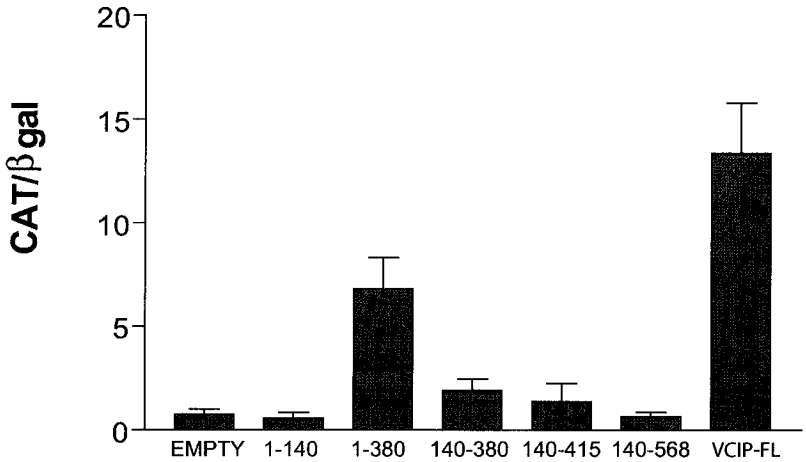
CAT/βgal
20
15
10
5
0
EMPTY
1-140
1-380
140-380
140-415
140-568
VCIP-FL

B

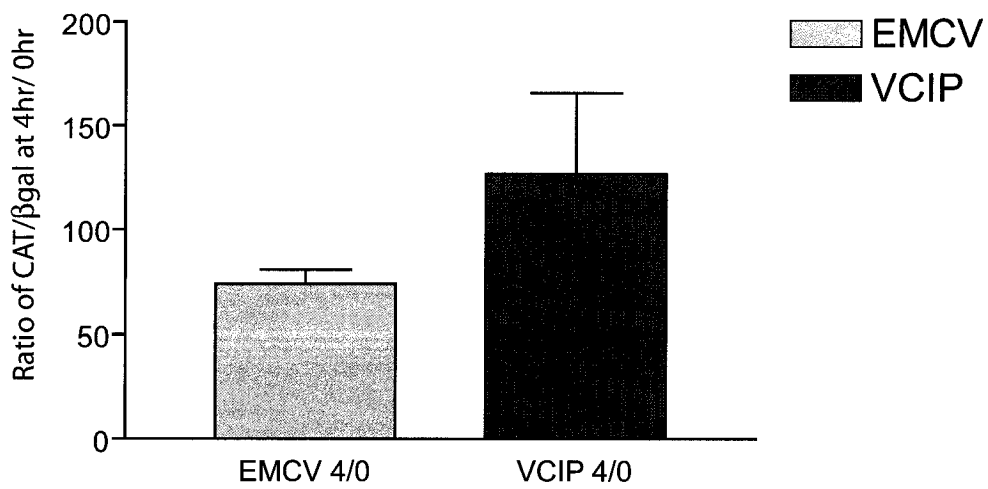
Ratio of CAT/βgal at 4hr/ 0hr
200
150
100
50
0
EMCV 4/0
VCIP 4/0
EMCV
VCIP

Figure 8: VCIP 5'UTR contains a functional IRES

A) U2OS cells were transfected with βgal/Empty/CAT control vector, The full length VCIP 5'UTR (VCIP FL), or various constructs containing portions of the VCIP 5'UTR cloned into the bicistronic βgal/CAT expression construct. The IRES activity is expressed as the CAT activity divided by the βgal activity measured in cell lysates taken 24hr post-transfection. The error bars represent the average ± S.E.M from 4-8 independent experiments.

B) U2OS cells were transfected with either the βgal/EMCV/CAT or βgal/VCIP/CAT bicistronic plasmids. Cells were either treated with hypoxia for 4hrs or left untreated, 24hrs post-transfection and the relative IRES activity was determined for each IRES element. Measurements represent the ratio of CAT/βgal activity at 4hr hypoxia/ CAT/βgal activity at 0hr. The bars represent the average ± S.E.M from 3-5 independent experiments.

A

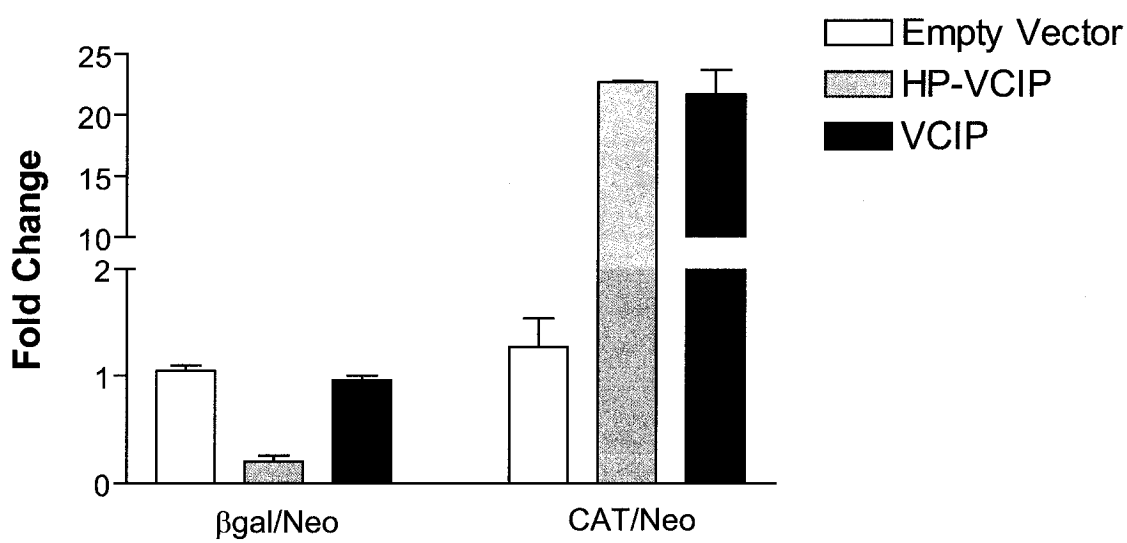
Empty Vector
HP-VCIP
VCIP
Fold Change
25
20
15
10
2
1
0
βgal/Neo
CAT/Neo

B

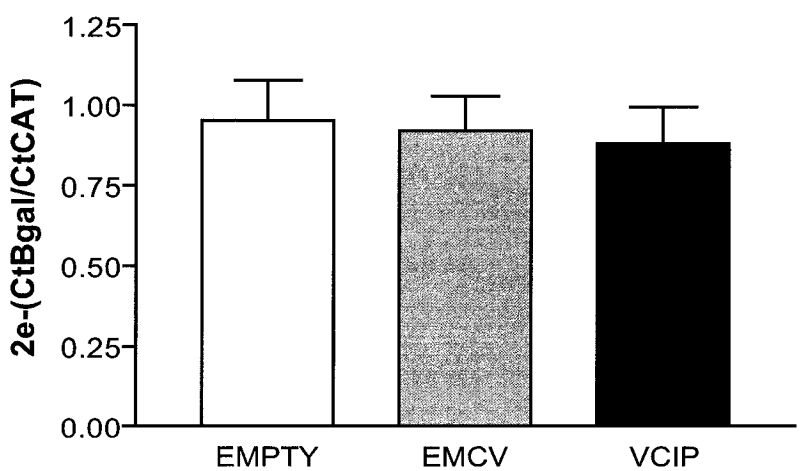
2e-(CtBgal/CtCAT)
1.25
1.00
0.75
0.50
0.25
0.00
EMPTY
EMCV
VCIP

Figure 9: VCIP 5'UTR does not contain cryptic promoter activity or evidence of spurious splicing

A) U2OS cells were transfected with the βgal/EMPTY/CAT, βgal/VCIP/CAT, or HP-βgal/VCIP/CAT bicistronic plasmids. βgal and CAT activity was measured in cell lysates taken 24hr post-transfection and were normalized to the number of transfected cells based on Neomycin activity. Reported βgal and CAT activities are expressed relative to measurements obtained for βgal/EMPTY/CAT. Bars represent the average ± S.E.M from 3 independent experiments.

B) Quantitative RT-PCR was performed on total RNA isolated from U2OS cells transfected with βgal/EMCV/CAT, βgal/Empty/CAT, or βgal/VCIP/CAT bicistronic plasmids. Q-PCR reactions were carried out to quantify the number of βgal and CAT cistrons expressed in each plasmid. The CAT/βgal ratio was calculated as 2-[Ct(CAT)-Ct(βgal)]. The bars represent the mean ± S.E.M. from 6-7 independent experiments performed in triplicate.

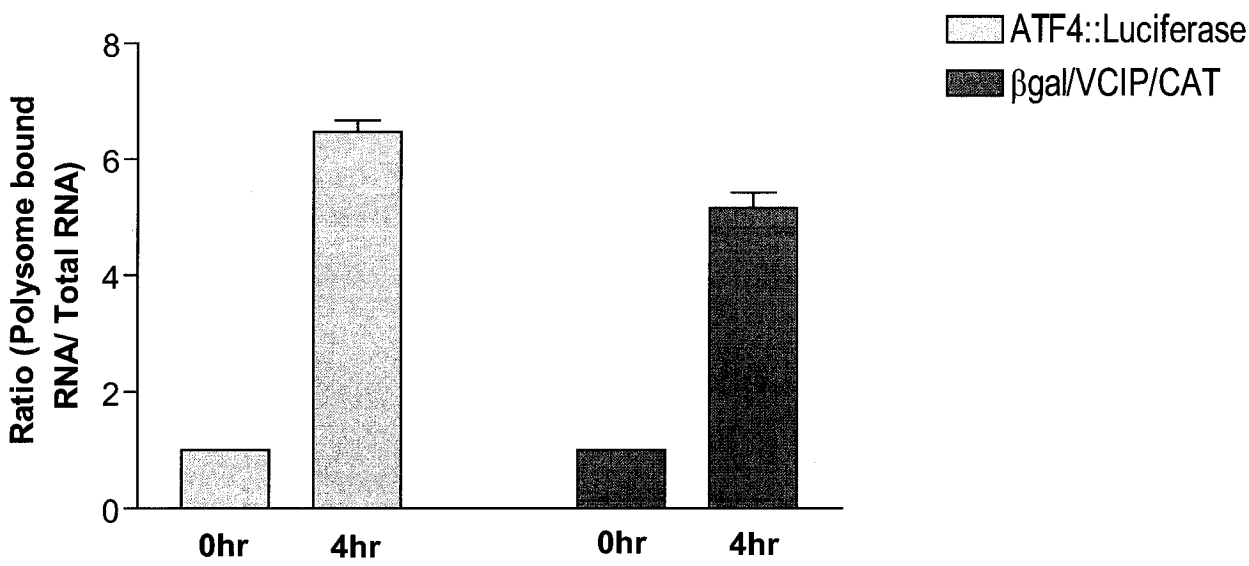
ATF4::Luciferase
βgal/VCIP/CAT
Ratio (Polysome bound RNA/ Total RNA)
8
6
4
2
0
0hr
4hr
0hr
4hr

Supplemental Figure S3: VCIP IRES is preferentially recruited to the polysomes during hypoxic stress.

U2OS cells were co-transfected the bgal/VCIP/CAT bicistronic vector and a stress inducible ATF4 5'UTR luciferase fusion vector. Twenty-four hours post-transfection, transfected U2OS cells were placed in an anaerobic chamber for 4 hrs or left untreated. Cytoplasmic lysates were fractionated by sucrose gradient sedimentation and total and polysomal RNA isolated was reverse transcribed in the presence of an external control (VSV-M). The data represent the ratio of Luciferase or CAT mRNAs associated with the polysomes and total cytoplasmic lysates following 0h and 4h of hypoxic stress. Results are normalized to normoxic controls and represent the average +/- SEM of three individual samples.

Discussion

Tumor cell tolerance to hypoxia is an important determinant of the level of hypoxia which can be sustained within a given cell. This intrinsic property drives an adaptive response that results in increased cell survival during periods of heightened cellular stress and can elicit resistance to anticancer therapies. Recently, stress tolerant cell lines were generated by means of repeated cycles of hypoxia and reoxygenation. Weinmann *et al.* established that hypoxia resistant cell lines demonstrated cross-resistance to apoptosis induced by etoposide and UV irradiation (98). Additionally, stress tolerant tumor cell lines generated by Yao *et al.* were more invasive, and when injected subcutaneously into nude mice, resulted in faster growing tumours that demonstrated increased intratumoral angiogenesis (100).

The rapid and sustained inhibition of protein translation during hypoxic stress is thought to be one mechanism utilized by cells to promote hypoxia tolerance. The coordinated inhibition of protein translation, an energy costly mechanism, is one energy conserving strategy exploited by the cell when ATP levels are limited. Global translation inhibition is achieved upon activation of the ISR through the phosphorylation of eIF2α by the ER resident kinase Perk (51). The luminal domain of Perk is negatively regulated by the ER chaperone BiP/Grp78, which maintains Perk in its inactive state in unstressed cells (6). During ER stress, the accumulation of unfolded proteins within the ER promotes the dissociation of BiP from the luminal domain of Perk, to assist in protein folding. This dissociation results in the activation of Perk through oligomerization and trans-autophosphorylation of the cytoplasmic kinase domain (34). Similar to ER stress, hypoxia results in the activation of Perk and phosphorylation of eIF2α (51) resulting in the attenuation of translation initiation and the paradoxical translational induction of ATF4 (9). ATF4 activates the induction of

downstream UPR genes including CHOP, BiP, and GADD34 (7, 9). The mechanism of Perk activation however, has not yet been elucidated. Activation of the ISR constitutes one arm of a larger coordinated program called the Unfolded Protein Response (UPR). Hypoxic stress similarly results in the activation of other branches of the UPR including the activation of another ER transmembrane protein, IRE-1 (82). The role of hypoxic stress in the activation of the UPR has recently been thoroughly reviewed (52).

Perk has been implicated in promoting cell survival and adaptation in response to a variety of environmental stresses including ER stress (31, 33) and hypoxia (7, 9, 51). In response to hypoxic stress, $Perk^{-/-}$ MEFs not only exhibit attenuated phosphorylation of eIF2α and reduced inhibition of protein synthesis, but also reduced survival both *in vitro* and *in vivo*. Tumors derived from cells with a compromised ISR ($Perk^{-/-}$ MEFs, HT29 cells expressing dnPerkΔC, and cells expressing an unphosphorylatable knock-in mutant $eIF2\alpha^{S51A}$) demonstrate reduced tumor cell viability and result in smaller tumor growth when compared to tumors with an intact ISR (7).

A growing number of studies now support the idea that mechanisms that regulate global mRNA translation can simultaneously control the translation of individual genes necessary for cell survival and adaptation during stress (7, 9, 50). We previously demonstrated through a collective analysis of data generated by microarray of polysome-associated mRNAs during prolonged hypoxic stress, the Perk dependent translational-regulation of ATF4, an important mediator of the ISR (9). Similar analyses have been previously employed to identify translationally regulated genes involved in the host cell response to poliovirus infection (48), T-cell activation (65), VHL expression (26), oncogenic signalling through Ras and Akt (79), and more recently in a time course of hypoxic stress (50). The exact role that Perk plays in

the progression of hypoxia tolerance however, has not been fully elucidated. A previous microarray study identified several Perk dependent transcriptionally induced changes in gene expression in an immortalized mouse hippocampal model for oxidative glutamanergic toxicity (61); however, large scale analysis of Perk mediated changes in translation had not been completed prior to this study. Our analysis revealed the Perk-dependent preferential translation of a wide variety of pro-angiogenic genes, indicating that Perk may play a fundamental role in the translational regulation of a complex process that regulates the development of hypoxia tolerance through multiple pathways. It seems unlikely that any single gene product regulated by Perk will be solely responsible for the control of tumour angiogenesis in response to hypoxic stress, but rather by the orchestrated expression of many complementary gene products. In this study we examined how one of our validated candidates VCIP, an $\alpha_5\beta_1$ and $\alpha_v\beta_3$ integrin binding protein, is regulated at the translational level. The critical importance of VCIP gene function during angiogenesis is underscored by the observation that anti-VCIP antibodies block bFGF and VEGF induced capillary morphogenesis (97) and that mouse embryos lacking the VCIP gene die between day E7-10.5, and demonstrate abnormal vascular development (20). The pro-angiogenic growth factors, bFGF and VEGF are capable of eliciting a strong transcriptional induction in VCIP gene expression however the post-transcriptional regulation of VCIP had not been previously investigated. Our data establish that hypoxic stress in the absence of exogenous growth factors can initiate a 10-fold induction in the steady state levels of VCIP transcripts. Moreover, VCIP mRNAs demonstrated a 20-fold translational induction as determined by their increased association with polysomes following hypoxic stress, suggesting VCIP expression is regulated by both transcriptional and post-transcriptional mechanisms. The

VCIP 5'UTR is unusually long (568bp) and surprisingly highly conserved across mammalian species. Unlike ATF4, the VCIP 5'UTR did not contain multiple conserved uORFs; therefore, the mechanism utilized to maintain its preferential translation during hypoxic stress is not likely due to ribosome shunting or re-initiation. Instead, our data support the presence of an active IRES element within its 5'UTR, which may in part explain its preferential translation when global translation is largely inhibited. Using deletion constructs of the hVCIP 5'UTR, we were able to determine that the VCIP IRES element is present between 1-380 bp. Removing the first 1-140 bp from this construct, however, abolishes any IRES activity despite our observation that the sequence between 1-140 bp alone does not contain any IRES activity, suggesting that this sequence is necessary to determine the optimal secondary structure of the VCIP RNA for IRES mediated translation. Numerous studies have identified hypoxia responsive genes that employ IRES elements to maintain their translational priority during stress, including PDGF (5), HIF1α (54), VEGF (66, 90), BiP (62), TIE-2 (74), and ODC (77). The importance of IRES mediated translation is revealed by the observation that mRNAs that contain IRES elements encode proteins that play important roles in cell growth, proliferation, differentiation, and in the regulation of apoptosis; cellular programs that are often usurped by malignant cells (40). This suggests that IRES mediated translation may be an important mechanism utilized by the cell to maintain and induce gene expression in order to mediate cellular adaptation and cell viability when faced with stressful microenvironments. A possible connection between eIF2α phosphorylation and IRES translation has also been proposed. The activities of cat1, PDGF2, VEGF and c-myc have been shown to increase either during differentiation or in response to various cellular stresses that increase the phosphorylation of eIF2α (21, 27). The mechanism

for eIF2α phosphorylation mediated IRES expression is not clear, as the phosphorylation of eIF2α results in the inhibition of ternary complex formation, a requirement for the initiation of all cellular mRNAs, including those that are regulated by cap-independent mechanisms. Whether eIF2α(p) sensitive IRES elements require specific *trans*-acting factors to mediate their translational activation during cellular stress has not been elucidated, but could help to explain their dependence on the phosphorylation of eIF2α. Alternatively, mRNAs with IRES elements may compete with other cellular mRNAs for the limited translational machinery to ensure their translational priority during times of reduced protein synthesis. Another explanation includes the possibility that eIF2α is not the only substrate of the Perk kinase and that in fact other molecules may be modulated by direct Perk phosphorylation. Interestingly, in response to ER stress, eIF2α^{S51A} cells failed to induce approximately one-third of the genes that are normally induced by ER stress (61), suggesting Perk is capable of mediating eIF2α independent gene regulation. Recently, the bzip transcription factor Nrf2 was identified as a second Perk substrate (17). In response to Perk activation, Nrf2 is phosphorylated by Perk which promotes its dissociation from Keap1 thereby facilitating its translocation to the nucleus where it binds and activates the transcription of antioxidant genes (93, 94). Aberrant Nrf2 regulation may help to explain why cells experience increased oxidative stress in the absence of Perk. Whether the translational regulation of the cohort of pro-angiogenic genes discussed here are predominantly regulated by eIF2α phosphorylation or whether they represent novel targets of Perk phosphorylation remains to be investigated.

The significance of Perk's role in regulating the translation of pro-angiogenic genes is emphasized by our observation that a wide variety of angiogenic genes involved in different braches of the angiogenic response demonstrated increased polysome-association following

hypoxic stress. Included in the Q-PCR validated candidates is a matrix metalloproteinase, MMP13. MMP mediated extra-cellular matrix and basement membrane dissolution is an essential event for endothelial cell activation, migration and capillary formation. More recent studies have implicated MMP expression in earlier steps of tumor evolution including the stimulation of cell proliferation and modulation of angiogenesis (23, 24). The hMMP13 gene was originally identified in breast carcinoma and its expression has since been related to other malignancies (25). Expression of hMMP13 has also been linked to the progression of rheumatoid arthritis (RA) in the synovial membrane, a disease that shares common features with tumor invasion (58). Remarkably, hMMP13 transcripts are translationally silenced by the interaction of its 3'UTR and the nucleo-cytoplasmic shuttling protein TIAR (15); to our knowledge however, we are the first to describe the translational induction of MMP13 during hypoxic stress. VCIP may be similarly regulated as it has been demonstrated to contain an unusually long 3'UTR (>2Kb). We found it to contain two 15-LOX-DICE (15-lipoxygenase differentiation control element) sequences. The CU-rich 15-LOX-DICE element is one of the best characterized 3'UTR control elements (80). Translational inhibition is mediated by the formation of a binary complex between the 15-LOX-DICE element and KH domain proteins hnRNP E1 and K. Minimally, two 15-LOX-DICE elements are required to confer translational repression of a transcript and 2-4 repetitions per transcript is average. However, as many as 31 repetitions have been identified in a single 3'UTR (quail myelin protein mRNA) (80). In light of this observation, we are currently undertaking efforts to determine if the 3' and 5'-UTRs of VCIP mutually regulate its post-transcriptional expression under aerobic and hypoxic conditions.

What is the physiological role for Perk in the translational regulation of these proteins in the development of hypoxia tolerance? Cells with a compromised ISR pathway demonstrate severe sensitivity to hypoxia (51) and pharmacological agents that promote ER stress (33). Our studies corroborated findings from Bi *et al.*, as tumors derived from transformed $Perk^{-/-}$ MEFs are smaller than their wildtype counterparts. Furthermore, we made the observation that these tumors remained pale in color, and did not appear to recruit angiogenic vessels as did wild-type tumors. In a mouse model of angiogenesis where tumor cells were co-cultured with AP-expressing human microdermal endothelial cells, we made the observation that the tumor microenvironment imparted by $Perk^{-/-}$ cells resulted in abortive angiogenesis. Inappropriate levels of the constellation of ligands and receptors required during vessel maturation can result in the production of abnormal vessels. Maturation requires the recruitment of mural cells, the generation of an extracellular matrix and specialization of the vessel wall for structural support (44). Expression of PDGF-B and ligation to its receptor (PDGFR-β) is required for the recruitment of pericyte progenitor cells and eventual onset of vessel maturation (14, 44). The significance of PDGF-B during angiogenesis is underscored by the observation that PDGF-B deficient mice die *in utero* at day E7.5 due to the inability to assemble mature vasculature in several organs (36, 44, 56, 57, 88). Furthermore, PDGF expression has been demonstrated to decrease over the progression of vessel maturation, indicating its requirement during the onset of maturation. Similar to hypoxic stress, cellular differentiation results in the inhibition of global protein synthesis which correlates with the phosphorylation of eIF2α. Gerlitz *et al.* have demonstrated that IRES-mediated translation of PDGF during differentiation is dependent on the phosphorylation of eIF2α (27). Although we were unable to detect any changes in PDGF expression by microarray, our analysis did

reveal a Perk-dependent 2.6-fold induction in the translational efficiency of its receptor, PDGFR-β; whereas its expression in $Perk^{-/-}$ MEFs was undetected relative to background (data not shown). Also critical for vessel formation and stabilization are the Tie receptors (Tie1 and Tie2). As mentioned previously, Tie2 is preferentially translated by an IRES element within its 5'UTR during hypoxic stress, however, whether IRES activity is dependent on eIF2α -phosphorylation has not yet been determined.

Taken together, our data support the notion that Perk serves to fine-tune the translational efficiency of a subset of pro-angiogenic mRNAs during the course of hypoxic stress. Importantly, the inability to signal through Perk resulted in smaller tumor growth due in part to disregulated angiogenic signals that produced non-functional blood vessels. We propose that the translational regulation conferred by Perk in response to acute hypoxic stress represents a critical aspect in the development of hypoxia tolerance and in tumor growth. Results from this study further support the notion that Perk remains an attractive target for novel anti-cancer therapies.

Acknowledgments

JB was supported by a CIHR-CGS doctoral award. This work was supported by a grant from the National Cancer Institute of Canada (to JCB). Work done by DR and HPH was supported by NIH grants ES08681 and DK47119. MH is a CIHR New Investigator.

References

1. **Ala-aho, R., and V. M. Kahari.** 2005. Collagenases in cancer. Biochimie **87:**273-86.
2. **Ameri, K., E. M. Hammond, C. Culmsee, M. Raida, D. M. Katschinski, R. H. Wenger, E. Wagner, R. J. Davis, T. Hai, N. Denko, and A. L. Harris.** 2006. Induction of activating transcription factor 3 by anoxia is independent of p53 and the hypoxic HIF signalling pathway. Oncogene.
3. **Ameri, K., C. E. Lewis, M. Raida, H. Sowter, T. Hai, and A. L. Harris.** 2004. Anoxic induction of ATF-4 through HIF-1-independent pathways of protein stabilization in human cancer cells. Blood **103:**1876-82.
4. **Arsham, A. M., J. J. Howell, and M. C. Simon.** 2003. A novel hypoxia-inducible factor-independent hypoxic response regulating mammalian target of rapamycin and its targets. J Biol Chem **278:**29655-60.
5. **Bernstein, J., O. Sella, S. Y. Le, and O. Elroy-Stein.** 1997. PDGF2/c-sis mRNA leader contains a differentiation-linked internal ribosomal entry site (D-IRES). J Biol Chem **272:**9356-62.
6. **Bertolotti, A., Y. Zhang, L. M. Hendershot, H. P. Harding, and D. Ron.** 2000. Dynamic interaction of BiP and ER stress transducers in the unfolded-protein response. Nat Cell Biol **2:**326-32.
7. **Bi, M., C. Naczki, M. Koritzinsky, D. Fels, J. Blais, N. Hu, H. Harding, I. Novoa, M. Varia, J. Raleigh, D. Scheuner, R. J. Kaufman, J. Bell, D. Ron, B. G. Wouters, and C. Koumenis.** 2005. ER stress-regulated translation increases tolerance to extreme hypoxia and promotes tumor growth. Embo J **24:**3470-81.
8. **Bi, Y., G. X. Lin, L. Millecchia, and Q. Ma.** 2006. Superinduction of metallothionein I by inhibition of protein synthesis: role of a labile repressor in MTF-1 mediated gene transcription. J Biochem Mol Toxicol **20:**57-68.
9. **Blais, J. D., V. Filipenko, M. Bi, H. P. Harding, D. Ron, C. Koumenis, B. G. Wouters, and J. C. Bell.** 2004. Activating transcription factor 4 is translationally regulated by hypoxic stress. Mol Cell Biol **24:**7469-82.
10. **Bornstein, P., T. R. Kyriakides, Z. Yang, L. C. Armstrong, and D. E. Birk.** 2000. Thrombospondin 2 modulates collagen fibrillogenesis and angiogenesis. J Investig Dermatol Symp Proc **5:**61-6.
11. **Brown, J. M., and A. J. Giaccia.** 1998. The unique physiology of solid tumors: opportunities (and problems) for cancer therapy. Cancer Res **58:**1408-16.
12. **Bruick, R. K.** 2000. Expression of the gene encoding the proapoptotic Nip3 protein is induced by hypoxia. Proc Natl Acad Sci U S A **97:**9082-7.
13. **Cattaruzza, S., M. Schiappacassi, A. Ljungberg-Rose, P. Spessotto, D. Perissinotto, M. Morgelin, M. T. Mucignat, A. Colombatti, and R. Perris.** 2002. Distribution of PG-M/versican variants in human tissues and de novo expression of isoform V3 upon endothelial cell activation, migration, and neoangiogenesis in vitro. J Biol Chem **277:**47626-35.
14. **Cho, H., T. Kozasa, C. Bondjers, C. Betsholtz, and J. H. Kehrl.** 2003. Pericyte-specific expression of Rgs5: implications for PDGF and EDG receptor signaling during vascular maturation. Faseb J **17:**440-2.
15. **Chua, P. K., M. E. Melish, Q. Yu, R. Yanagihara, K. S. Yamamoto, and V. R. Nerurkar.** 2003. Elevated levels of matrix metalloproteinase 9 and tissue inhibitor of metalloproteinase 1 during the acute phase of Kawasaki disease. Clin Diagn Lab Immunol **10:**308-14.
16. **Connolly, E., S. Braunstein, S. Formenti, and R. J. Schneider.** 2006. Hypoxia inhibits protein synthesis through a 4E-BP1 and elongation factor 2 kinase pathway controlled by mTOR and uncoupled in breast cancer cells. Mol Cell Biol **26:**3955-65.
17. **Cullinan, S. B., D. Zhang, M. Hannink, E. Arvisais, R. J. Kaufman, and J. A. Diehl.** 2003. Nrf2 is a direct PERK substrate and effector of PERK-dependent cell survival. Mol Cell Biol **23:**7198-209.
18. **Damert, A., M. Machein, G. Breier, M. Q. Fujita, D. Hanahan, W. Risau, and K. H. Plate.** 1997. Up-regulation of vascular endothelial growth factor expression in a rat glioma is conferred by two distinct hypoxia-driven mechanisms. Cancer Res **57:**3860-4.
19. **de Fraipont, F., A. C. Nicholson, J. J. Feige, and E. G. Van Meir.** 2001. Thrombospondins and tumor angiogenesis. Trends Mol Med **7:**401-7.

20. **Escalante-Alcalde, D., L. Hernandez, H. Le Stunff, R. Maeda, H. S. Lee, C. Jr Gang, V. A. Sciorra, I. Daar, S. Spiegel, A. J. Morris, and C. L. Stewart.** 2003. The lipid phosphatase LPP3 regulates extra-embryonic vasculogenesis and axis patterning. Development **130:**4623-37.
21. **Fernandez, P. M., S. O. Tabbara, L. K. Jacobs, F. C. Manning, T. N. Tsangaris, A. M. Schwartz, K. A. Kennedy, and S. R. Patierno.** 2000. Overexpression of the glucose-regulated stress gene GRP78 in malignant but not benign human breast lesions. Breast Cancer Res Treat **59:**15-26.
22. **Firth, J. D., B. L. Ebert, C. W. Pugh, and P. J. Ratcliffe.** 1994. Oxygen-regulated control elements in the phosphoglycerate kinase 1 and lactate dehydrogenase A genes: similarities with the erythropoietin 3' enhancer. Proc Natl Acad Sci U S A **91:**6496-500.
23. **Folgueras, A. R., A. M. Pendas, L. M. Sanchez, and C. Lopez-Otin.** 2004. Matrix metalloproteinases in cancer: from new functions to improved inhibition strategies. Int J Dev Biol **48:**411-24.
24. **Freije, J. M., M. Balbin, A. M. Pendas, L. M. Sanchez, X. S. Puente, and C. Lopez-Otin.** 2003. Matrix metalloproteinases and tumor progression. Adv Exp Med Biol **532:**91-107.
25. **Freije, J. M., I. Diez-Itza, M. Balbin, L. M. Sanchez, R. Blasco, J. Tolivia, and C. Lopez-Otin.** 1994. Molecular cloning and expression of collagenase-3, a novel human matrix metalloproteinase produced by breast carcinomas. J Biol Chem **269:**16766-73.
26. **Galban, S., J. Fan, J. L. Martindale, C. Cheadle, B. Hoffman, M. P. Woods, G. Temeles, J. Brieger, J. Decker, and M. Gorospe.** 2003. von Hippel-Lindau protein-mediated repression of tumor necrosis factor alpha translation revealed through use of cDNA arrays. Mol Cell Biol **23:**2316-28.
27. **Gerlitz, G., R. Jagus, and O. Elroy-Stein.** 2002. Phosphorylation of initiation factor-2 alpha is required for activation of internal translation initiation during cell differentiation. Eur J Biochem **269:**2810-9.
28. **Graeber, T. G., C. Osmanian, T. Jacks, D. E. Housman, C. J. Koch, S. W. Lowe, and A. J. Giaccia.** 1996. Hypoxia-mediated selection of cells with diminished apoptotic potential in solid tumours. Nature **379:**88-91.
29. **Greijer, A. E., P. van der Groep, D. Kemming, A. Shvarts, G. L. Semenza, G. A. Meijer, M. A. van de Wiel, J. A. Belien, P. J. van Diest, and E. van der Wall.** 2005. Up-regulation of gene expression by hypoxia is mediated predominantly by hypoxia-inducible factor 1 (HIF-1). J Pathol **206:**291-304.
30. **Griffin, J. L., C. Rae, R. M. Dixon, G. K. Radda, and P. M. Matthews.** 1998. Excitatory amino acid synthesis in hypoxic brain slices: does alanine act as a substrate for glutamate production in hypoxia? J Neurochem **71:**2477-86.
31. **Harding, H. P., I. Novoa, Y. Zhang, H. Zeng, R. Wek, M. Schapira, and D. Ron.** 2000. Regulated translation initiation controls stress-induced gene expression in mammalian cells. Mol Cell **6:**1099-108.
32. **Harding, H. P., H. Zeng, Y. Zhang, R. Jungries, P. Chung, H. Plesken, D. D. Sabatini, and D. Ron.** 2001. Diabetes mellitus and exocrine pancreatic dysfunction in perk-/- mice reveals a role for translational control in secretory cell survival. Mol Cell **7:**1153-63.
33. **Harding, H. P., Y. Zhang, A. Bertolotti, H. Zeng, and D. Ron.** 2000. Perk is essential for translational regulation and cell survival during the unfolded protein response. Mol Cell **5:**897-904.
34. **Harding, H. P., Y. Zhang, and D. Ron.** 1999. Protein translation and folding are coupled by an endoplasmic-reticulum-resident kinase. Nature **397:**271-4.
35. **Harding, H. P., Y. Zhang, H. Zeng, I. Novoa, P. D. Lu, M. Calfon, N. Sadri, C. Yun, B. Popko, R. Paules, D. F. Stojdl, J. C. Bell, T. Hettmann, J. M. Leiden, and D. Ron.** 2003. An integrated stress response regulates amino acid metabolism and resistance to oxidative stress. Mol Cell **11:**619-33.
36. **Hellstrom, M., M. Kalen, P. Lindahl, A. Abramsson, and C. Betsholtz.** 1999. Role of PDGF-B and PDGFR-beta in recruitment of vascular smooth muscle cells and pericytes during embryonic blood vessel formation in the mouse. Development **126:**3047-55.
37. **Hochachka, P. W., L. T. Buck, C. J. Doll, and S. C. Land.** 1996. Unifying theory of hypoxia tolerance: molecular/metabolic defense and rescue mechanisms for surviving oxygen lack. Proc Natl Acad Sci U S A **93:**9493-8.
38. **Hockel, M., K. Sclenger, H. Hamm, P. G. Knapstein, R. Hohenfellner, and H. P. Rosler.** 1996. Five-year experience with combined operative and radiotherapeutic treatment of recurrent gynecologic tumors infiltrating the pelvic wall. Cancer **77:**1918-33.

39. **Holcik, M., C. Lefebvre, C. Yeh, T. Chow, and R. G. Korneluk.** 1999. A new internal-ribosome-entry-site motif potentiates XIAP-mediated cytoprotection. Nat Cell Biol **1**:190-2.
40. **Holcik, M., N. Sonenberg, and R. G. Korneluk.** 2000. Internal ribosome initiation of translation and the control of cell death. Trends Genet **16**:469-73.
41. **Humtsoe, J. O., R. A. Bowling, Jr., S. Feng, and K. K. Wary.** 2005. Murine lipid phosphate phosphohydrolase-3 acts as a cell-associated integrin ligand. Biochem Biophys Res Commun **335**:906-19.
42. **Humtsoe, J. O., S. Feng, G. D. Thakker, J. Yang, J. Hong, and K. K. Wary.** 2003. Regulation of cell-cell interactions by phosphatidic acid phosphatase 2b/VCIP. Embo J **22**:1539-54.
43. **Iyer, N. V., L. E. Kotch, F. Agani, S. W. Leung, E. Laughner, R. H. Wenger, M. Gassmann, J. D. Gearhart, A. M. Lawler, A. Y. Yu, and G. L. Semenza.** 1998. Cellular and developmental control of O2 homeostasis by hypoxia-inducible factor 1 alpha. Genes Dev **12**:149-62.
44. **Jain, R. K.** 2003. Molecular regulation of vessel maturation. Nat Med **9**:685-93.
45. **Jiang, B. H., J. Z. Zheng, S. W. Leung, R. Roe, and G. L. Semenza.** 1997. Transactivation and inhibitory domains of hypoxia-inducible factor 1alpha. Modulation of transcriptional activity by oxygen tension. J Biol Chem **272**:19253-60.
46. **Jiang, H. Y., S. A. Wek, B. C. McGrath, D. Lu, T. Hai, H. P. Harding, X. Wang, D. Ron, D. R. Cavener, and R. C. Wek.** 2004. Activating transcription factor 3 is integral to the eukaryotic initiation factor 2 kinase stress response. Mol Cell Biol **24**:1365-77.
47. **Jogi, A., J. Vallon-Christersson, L. Holmquist, H. Axelson, A. Borg, and S. Pahlman.** 2004. Human neuroblastoma cells exposed to hypoxia: induction of genes associated with growth, survival, and aggressive behavior. Exp Cell Res **295**:469-87.
48. **Johannes, G., M. S. Carter, M. B. Eisen, P. O. Brown, and P. Sarnow.** 1999. Identification of eukaryotic mRNAs that are translated at reduced cap binding complex eIF4F concentrations using a cDNA microarray. Proc Natl Acad Sci U S A **96**:13118-23.
49. **Klenotic, P. A., F. L. Munier, L. Y. Marmorstein, and B. Anand-Apte.** 2004. Tissue inhibitor of metalloproteinases-3 (TIMP-3) is a binding partner of epithelial growth factor-containing fibulin-like extracellular matrix protein 1 (EFEMP1). Implications for macular degenerations. J Biol Chem **279**:30469-73.
50. **Koritzinsky, M., M. G. Magagnin, T. van den Beucken, R. Seigneuric, K. Savelkouls, J. Dostie, S. Pyronnet, R. J. Kaufman, S. A. Weppler, J. W. Voncken, P. Lambin, C. Koumenis, N. Sonenberg, and B. G. Wouters.** 2006. Gene expression during acute and prolonged hypoxia is regulated by distinct mechanisms of translational control. Embo J **25**:1114-25.
51. **Koumenis, C., C. Naczki, M. Koritzinsky, S. Rastani, A. Diehl, N. Sonenberg, A. Koromilas, and B. G. Wouters.** 2002. Regulation of protein synthesis by hypoxia via activation of the endoplasmic reticulum kinase PERK and phosphorylation of the translation initiation factor eIF2alpha. Mol Cell Biol **22**:7405-16.
52. **Koumenis, C., and B. G. Wouters.** 2006. "Translating" tumor hypoxia: unfolded protein response (UPR)-dependent and UPR-independent pathways. Mol Cancer Res **4**:423-36.
53. **Ladoux, A., and C. Frelin.** 2000. Coordinated Up-regulation by hypoxia of adrenomedullin and one of its putative receptors (RDC-1) in cells of the rat blood-brain barrier. J Biol Chem **275**:39914-9.
54. **Lang, K. J., A. Kappel, and G. J. Goodall.** 2002. Hypoxia-inducible factor-1alpha mRNA contains an internal ribosome entry site that allows efficient translation during normoxia and hypoxia. Mol Biol Cell **13**:1792-801.
55. **Lee, P. J., B. H. Jiang, B. Y. Chin, N. V. Iyer, J. Alam, G. L. Semenza, and A. M. Choi.** 1997. Hypoxia-inducible factor-1 mediates transcriptional activation of the heme oxygenase-1 gene in response to hypoxia. J Biol Chem **272**:5375-81.
56. **Leveen, P., M. Pekny, S. Gebre-Medhin, B. Swolin, E. Larsson, and C. Betsholtz.** 1994. Mice deficient for PDGF B show renal, cardiovascular, and hematological abnormalities. Genes Dev **8**:1875-87.
57. **Lindahl, P., B. R. Johansson, P. Leveen, and C. Betsholtz.** 1997. Pericyte loss and microaneurysm formation in PDGF-B-deficient mice. Science **277**:242-5.
58. **Lindy, O., Y. T. Konttinen, T. Sorsa, Y. Ding, S. Santavirta, A. Ceponis, and C. Lopez-Otin.** 1997. Matrix metalloproteinase 13 (collagenase 3) in human rheumatoid synovium. Arthritis Rheum **40**:1391-9.

59. **Liu, L., T. P. Cash, R. G. Jones, B. Keith, C. B. Thompson, and M. C. Simon.** 2006. Hypoxia-induced energy stress regulates mRNA translation and cell growth. Mol Cell **21**:521-31.
60. **Lu, P. D., H. P. Harding, and D. Ron.** 2004. Translation reinitiation at alternative open reading frames regulates gene expression in an integrated stress response. J Cell Biol **167**:27-33.
61. **Lu, P. D., C. Jousse, S. J. Marciniak, Y. Zhang, I. Novoa, D. Scheuner, R. J. Kaufman, D. Ron, and H. P. Harding.** 2004. Cytoprotection by pre-emptive conditional phosphorylation of translation initiation factor 2. Embo J **23**:169-79.
62. **Macejak, D. G., and P. Sarnow.** 1991. Internal initiation of translation mediated by the 5' leader of a cellular mRNA. Nature **353**:90-4.
63. **MacGregor, G. R., Nolan, G. P., Fiering, S., Roederer, M., and Herzenberg, L. A. .** 1991. Use of E. coli lacZ (b-Galactosidase) as a reporter gene. Humana Press Inc., , Clifton NJ.
64. **Mathupala, S. P., A. Rempel, and P. L. Pedersen.** 2001. Glucose catabolism in cancer cells: identification and characterization of a marked activation response of the type II hexokinase gene to hypoxic conditions. J Biol Chem **276**:43407-12.
65. **Mikulits, W., B. Pradet-Balade, B. Habermann, H. Beug, J. A. Garcia-Sanz, and E. W. Mullner.** 2000. Isolation of translationally controlled mRNAs by differential screening. Faseb J **14**:1641-52.
66. **Miller, D. L., J. A. Dibbens, A. Damert, W. Risau, M. A. Vadas, and G. J. Goodall.** 1998. The vascular endothelial growth factor mRNA contains an internal ribosome entry site. FEBS Lett **434**:417-20.
67. **Mooney, D. J., K. Sano, P. M. Kaufmann, K. Majahod, B. Schloo, J. P. Vacanti, and R. Langer.** 1997. Long-term engraftment of hepatocytes transplanted on biodegradable polymer sponges. J Biomed Mater Res **37**:413-20.
68. **Murdaca, J., C. Treins, M. N. Monthouel-Kartmann, R. Pontier-Bres, S. Kumar, E. Van Obberghen, and S. Giorgetti-Peraldi.** 2004. Grb10 prevents Nedd4-mediated vascular endothelial growth factor receptor-2 degradation. J Biol Chem **279**:26754-61.
69. **Murphy, B. J., G. K. Andrews, D. Bittel, D. J. Discher, J. McCue, C. J. Green, M. Yanovsky, A. Giaccia, R. M. Sutherland, K. R. Laderoute, and K. A. Webster.** 1999. Activation of metallothionein gene expression by hypoxia involves metal response elements and metal transcription factor-1. Cancer Res **59**:1315-22.
70. **Nguyen, S. V., and W. C. Claycomb.** 1999. Hypoxia regulates the expression of the adrenomedullin and HIF-1 genes in cultured HL-1 cardiomyocytes. Biochem Biophys Res Commun **265**:382-6.
71. **Nor, J. E., M. C. Peters, J. B. Christensen, M. M. Sutorik, S. Linn, M. K. Khan, C. L. Addison, D. J. Mooney, and P. J. Polverini.** 2001. Engineering and characterization of functional human microvessels in immunodeficient mice. Lab Invest **81**:453-63.
72. **O'Rourke, J. F., C. W. Pugh, S. M. Bartlett, and P. J. Ratcliffe.** 1996. Identification of hypoxically inducible mRNAs in HeLa cells using differential-display PCR. Role of hypoxia-inducible factor-1. Eur J Biochem **241**:403-10.
73. **Ozawa, K., Y. Tsukamoto, O. Hori, Y. Kitao, H. Yanagi, D. M. Stern, and S. Ogawa.** 2001. Regulation of tumor angiogenesis by oxygen-regulated protein 150, an inducible endoplasmic reticulum chaperone. Cancer Res **61**:4206-13.
74. **Park, E. H., J. M. Lee, J. D. Blais, J. C. Bell, and J. Pelletier.** 2005. Internal translation initiation mediated by the angiogenic factor Tie2. J Biol Chem **280**:20945-53.
75. **Pettersen, E. O., N. O. Juul, and O. W. Ronning.** 1986. Regulation of protein metabolism of human cells during and after acute hypoxia. Cancer Res **46**:4346-51.
76. **Price, B. D., and S. K. Calderwood.** 1992. Gadd45 and Gadd153 messenger RNA levels are increased during hypoxia and after exposure of cells to agents which elevate the levels of the glucose-regulated proteins. Cancer Res **52**:3814-7.
77. **Pyronnet, S., L. Pradayrol, and N. Sonenberg.** 2000. A cell cycle-dependent internal ribosome entry site. Mol Cell **5**:607-16.
78. **Qi, J. H., Q. Ebrahem, and B. Anand-Apte.** 2003. Tissue inhibitor of metalloproteinases-3 and Sorsby fundus dystrophy. Adv Exp Med Biol **533**:97-105.
79. **Rajasekhar, V. K., A. Viale, N. D. Socci, M. Wiedmann, X. Hu, and E. C. Holland.** 2003. Oncogenic Ras and Akt signaling contribute to glioblastoma formation by differential recruitment of existing mRNAs to polysomes. Mol Cell **12**:889-901.

80. **Reimann, I., A. Huth, H. Thiele, and B. J. Thiele.** 2002. Suppression of 15-lipoxygenase synthesis by hnRNP E1 is dependent on repetitive nature of LOX mRNA 3'-UTR control element DICE. J Mol Biol **315:**965-74.
81. **Reisdorph, R., and R. Lindahl.** 2001. Aldehyde dehydrogenase 3 gene regulation: studies on constitutive and hypoxia-modulated expression. Chem Biol Interact **130-132:**227-33.
82. **Romero-Ramirez, L., H. Cao, D. Nelson, E. Hammond, A. H. Lee, H. Yoshida, K. Mori, L. H. Glimcher, N. C. Denko, A. J. Giaccia, Q. T. Le, and A. C. Koong.** 2004. XBP1 is essential for survival under hypoxic conditions and is required for tumor growth. Cancer Res **64:**5943-7.
83. **Russo, V. C., B. S. Schutt, E. Andaloro, S. I. Ymer, A. Hoeflich, M. B. Ranke, L. A. Bach, and G. A. Werther.** 2005. Insulin-like growth factor binding protein-2 binding to extracellular matrix plays a critical role in neuroblastoma cell proliferation, migration, and invasion. Endocrinology **146:**4445-55.
84. **Scheuner, D., B. Song, E. McEwen, C. Liu, R. Laybutt, P. Gillespie, T. Saunders, S. Bonner-Weir, and R. J. Kaufman.** 2001. Translational control is required for the unfolded protein response and in vivo glucose homeostasis. Mol Cell **7:**1165-76.
85. **Schmidt-Kastner, R., C. Aguirre-Chen, T. Kietzmann, I. Saul, R. Busto, and M. D. Ginsberg.** 2004. Nuclear localization of the hypoxia-regulated pro-apoptotic protein BNIP3 after global brain ischemia in the rat hippocampus. Brain Res **1001:**133-42.
86. **Sherman-Baust, C. A., A. T. Weeraratna, L. B. Rangel, E. S. Pizer, K. R. Cho, D. R. Schwartz, T. Shock, and P. J. Morin.** 2003. Remodeling of the extracellular matrix through overexpression of collagen VI contributes to cisplatin resistance in ovarian cancer cells. Cancer Cell **3:**377-86.
87. **Shweiki, D., A. Itin, D. Soffer, and E. Keshet.** 1992. Vascular endothelial growth factor induced by hypoxia may mediate hypoxia-initiated angiogenesis. Nature **359:**843-5.
88. **Soriano, P.** 1994. Abnormal kidney development and hematological disorders in PDGF beta-receptor mutant mice. Genes Dev **8:**1888-96.
89. **Sowter, H. M., P. J. Ratcliffe, P. Watson, A. H. Greenberg, and A. L. Harris.** 2001. HIF-1-dependent regulation of hypoxic induction of the cell death factors BNIP3 and NIX in human tumors. Cancer Res **61:**6669-73.
90. **Stein, I., A. Itin, P. Einat, R. Skaliter, Z. Grossman, and E. Keshet.** 1998. Translation of vascular endothelial growth factor mRNA by internal ribosome entry: implications for translation under hypoxia. Mol Cell Biol **18:**3112-9.
91. **Tinton, S. A., and P. M. Buc-Calderon.** 1999. Hypoxia increases the association of 4E-binding protein 1 with the initiation factor 4E in isolated rat hepatocytes. FEBS Lett **446:**55-9.
92. **Vattem, K. M., and R. C. Wek.** 2004. Reinitiation involving upstream ORFs regulates ATF4 mRNA translation in mammalian cells. Proc Natl Acad Sci U S A **101:**11269-74.
93. **Venugopal, R., and A. K. Jaiswal.** 1996. Nrf1 and Nrf2 positively and c-Fos and Fra1 negatively regulate the human antioxidant response element-mediated expression of NAD(P)H:quinone oxidoreductase1 gene. Proc Natl Acad Sci U S A **93:**14960-5.
94. **Venugopal, R., and A. K. Jaiswal.** 1998. Nrf2 and Nrf1 in association with Jun proteins regulate antioxidant response element-mediated expression and coordinated induction of genes encoding detoxifying enzymes. Oncogene **17:**3145-56.
95. **Vihanto, M. M., J. Plock, D. Erni, B. M. Frey, F. J. Frey, and U. Huynh-Do.** 2005. Hypoxia up-regulates expression of Eph receptors and ephrins in mouse skin. Faseb J **19:**1689-91.
96. **Warnakulasuriyarachchi, D., S. Cerquozzi, H. H. Cheung, and M. Holcik.** 2004. Translational induction of the inhibitor of apoptosis protein HIAP2 during endoplasmic reticulum stress attenuates cell death and is mediated via an inducible internal ribosome entry site element. J Biol Chem **279:**17148-57.
97. **Wary, K. K., and J. O. Humtsoe.** 2005. Anti-lipid phosphate phosphohydrolase-3 (LPP3) antibody inhibits bFGF- and VEGF-induced capillary morphogenesis of endothelial cells. Cell Commun Signal **3:**9.
98. **Weinmann, M., V. Jendrossek, D. Guner, B. Goecke, and C. Belka.** 2004. Cyclic exposure to hypoxia and reoxygenation selects for tumor cells with defects in mitochondrial apoptotic pathways. Faseb J **18:**1906-8.
99. **Wimmer-Kleikamp, S. H., and M. Lackmann.** 2005. Eph-modulated cell morphology, adhesion and motility in carcinogenesis. IUBMB Life **57:**421-31.

100. **Yao, K., J. A. Gietema, S. Shida, M. Selvakumaran, X. Fonrose, N. B. Haas, J. Testa, and P. J. O'Dwyer.** 2005. In vitro hypoxia-conditioned colon cancer cell lines derived from HCT116 and HT29 exhibit altered apoptosis susceptibility and a more angiogenic profile in vivo. Br J Cancer **93:**1356-63.

101. **Yasuda, S., S. Arii, A. Mori, N. Isobe, W. Yang, H. Oe, A. Fujimoto, Y. Yonenaga, H. Sakashita, and M. Imamura.** 2004. Hexokinase II and VEGF expression in liver tumors: correlation with hypoxia-inducible factor 1 alpha and its significance. J Hepatol **40:**117-23.

102. **Zhang, P., B. McGrath, S. Li, A. Frank, F. Zambito, J. Reinert, M. Gannon, K. Ma, K. McNaughton, and D. R. Cavener.** 2002. The PERK eukaryotic initiation factor 2 alpha kinase is required for the development of the skeletal system, postnatal growth, and the function and viability of the pancreas. Mol Cell Biol **22:**3864-74.

APPENDIX B:
INTERNAL TRANSLATION INITIATION MEDIATED BY THE ANGIOGENIC FACTOR TIE2

Contribution to the Collaboration

Our contribution to this manuscript is represented in Figure 1. Cell culture and hypoxic exposure of Huvec cells to hypoxic stress was performed by J.Blais. Polysome-fractionation studies of Huvec cells in response to normoxic and hypoxic treatment and RNA isolation was performed by J.Blais. The written contribution to this manuscript, as required in the results section, materials and methods and figure legend, was written by J. Blais and edited by Dr. J. Pelletier.

Summary

The authors of this paper delineate the translational regulation of a pro-angiogenic protein required for blood vessel maturation in response to hypoxic stress. They demonstrate during hypoxic stress that protein synthesis is dramatically inhibited and while most genes are subjected to a decrease in their translational efficiency, the efficiency of Tie2 translation is maintained. They attribute this translational regulation, at least in part, to a novel cellular IRES element within the 5'UTR of Tie2 that is capable of initiating cap-independent translation and thereby maintain its translational priority under unfavorable conditions.

THE JOURNAL OF BIOLOGICAL CHEMISTRY
© 2005 by The American Society for Biochemistry and Molecular Biology, Inc.

Vol. 280, No. 22, Issue of June 3, pp. 20945–20953, 2005
Printed in U.S.A.

Internal Translation Initiation Mediated by the Angiogenic Factor Tie2*

Received for publication, November 10, 2004, and in revised form, March 8, 2005
Published, JBC Papers in Press, March 31, 2005, DOI 10.1074/jbc.M412744200

Eun-Hee Park‡§, Joseph M. Lee‡, Jaime D. Blais¶, John C. Bell¶, and Jerry Pelletier‡‖

From the ‡Department of Biochemistry and ‖McGill Cancer Center, McGill University, Montreal, Quebec H3G 1Y6, Canada and the ¶Ottawa Regional Cancer Centre Research Laboratories, Ottawa, Ontario K1H 8L6, Canada

Tie2 is an endothelium-specific receptor tyrosine kinase required for normal blood vessel maturation. We report that Tie2 mRNA translation is maintained under hypoxic conditions. To identify the mechanism responsible for this, we undertook structure/function analysis of the Tie2 5′-untranslated region (UTR). Transcription start site mapping indicates the existence of a several mRNA isoforms containing unusually long 5′-UTRs (>350 nucleotides) with five upstream open reading frames. We find internal ribosome binding activity that allows the Tie2 mRNA to initiate in a cap-independent fashion. Our data provide a framework for understanding how Tie2 mRNA is translated despite a cumbersome structured 5′-UTR and how its production is secured under unfavorable environmental conditions.

Angiogenesis is an essential step in allowing tumors to grow beyond 1–2 mm in diameter (1). Although the vasculature of most adult tissues is quiescent, during embryogenesis or in pathological conditions such as cancer, a pro-angiogenic setting is established. At least two families of growth factors, vascular endothelial growth factor (VEGF)[1] and the angiopoietins, are required for this process. VEGF mediates its effects through VEGFR-1/Flt-1 and VEGFR-2/Flk-1/KDR, two endothelial receptors implicated as central regulators of the vascular system under both normal and abnormal physiological conditions (2–5). VEGF expression is stimulated under hypoxic conditions by the transcription factor hypoxia-inducible factor-1 (HIF-1), which regulates a large range of physiological responses as a consequence of reduced oxygen availability (6, 7).

The angiopoietins belong to a second family of angiogenic factors essential for blood vessel maturation. Angiopoietin-1 (Ang-1) is an agonist of endothelial cell tyrosine kinase receptor Tie2/tek (8). Studies with Tie2 null mice indicate that the angiopoietin/Tie2 signaling system plays a role in the later steps of angiogenesis (9). Consistent with a central role for Tie2 in angiogenesis, germ line-activating mutations in humans are associated with vascular dysmorphogenesis (10). Additionally, the naturally occurring Tie2 antagonist, Ang-2, disrupts angiogenesis *in vivo* (11). Blocking Tie2 activation with recombinant Ang-2 significantly inhibits tumor growth (12) and is associated with activation of apoptosis (13), possibly due to disruption of Akt signaling (14). Hence, studies aimed at better defining the regulation of Tie2 expression are important in assessing anti-angiogenic therapeutic avenues.

In addition to profound transcriptional effects (6, 7), exposure of cells to hypoxia attenuates protein synthesis by decreasing translation initiation (15, 16). Two main steps of initiation are targets for regulation, either 43 S ribosomal complex formation (by affecting eIF2 phosphorylation status (17)) or the mRNA/ribosome binding step (18). Ribosome recruitment in eukaryotes can occur by two mechanisms, a cap-dependent process and by internal ribosome recruitment. Cap-dependent recruitment occurs through eIF4F-mediated recognition of the m^7G-cap structure and involves binding of the 43 S preinitiation complex near the mRNA 5′-end, followed by scanning to the appropriate AUG start codon (18). Barriers to the scanning process, such as mRNA secondary structure and uORFs, impinge in a negative fashion on the translational efficiency of a mRNA species. The cap dependence of an mRNA is thought to be a function of 5′-cap-proximal secondary structure; hence mRNAs with reduced secondary structure will have reduced dependence on eIF4F for initiation, whereas those with increased secondary structure are more dependent on eIF4F for initiation (19, 20). Internal ribosome recruitment allows an mRNA to bypass the cap-dependent initiation requirement for eIF4F. These different mechanisms of initiation provide a layer of gene regulation by which expression of specific mRNAs can be maintained or altered independent of others. Although hypoxia exerts inhibitory effects on cap dependent ribosome binding (16), several mRNAs implicated in angiogenesis remain efficiently translated, including VEGF (21–24), HIF-1α (25), and Tie2 (this report). Whereas VEGF and HIF-1α achieve this by recruiting ribosomes internally to an IRES, the issue of how Tie2 is able to circumvent this translational block has not been addressed previously. Herein, we present functional studies that identify the presence of an IRES element within the Tie2 5′-UTR, highlighting the complexities of Tie2 expression at the level of translation.

EXPERIMENTAL PROCEDURES

Cell Lines, Transfections, and Hypoxia Treatment—Primary human umbilical vein endothelial cells (HUVECs) were purchased from Clonetics (Walkersville, MD) and maintained in endothelial growth medium-2 supplemented with growth factors, 2% fetal bovine serum, 50 μg/ml gentamicin, and 50 μg/ml amphotericin according to the manufacturer's instructions.

DNA transfections into primary HUVECs were performed using

* This work was supported by Grant MOP-11354 from the Canadian Institutes of Health Research (CIHR) (to J. P.). The costs of publication of this article were defrayed in part by the payment of page charges. This article must therefore be hereby marked "*advertisement*" in accordance with 18 U.S.C. Section 1734 solely to indicate this fact.

§ Supported by a K. M. Hunter/CIHR doctoral research award.

** CIHR Senior Investigator. To whom correspondence should be addressed: McIntyre Medical Sciences Bldg., Rm. 810, 3655 Promenade Sir William Osler, McGill University, Montreal, Quebec H3G 1Y6, Canada. Tel.: 514-398-2323; Fax: 514-398-7384; E-mail: jerry.pelletier@mcgill.ca.

[1] The abbreviations used are: VEGF, vascular endothelial growth factor; HIF, hypoxia-inducible factor; Ang, angiopoietin; IRES, internal ribosome entry site; UTR, untranslated region; HUVEC, human umbilical vein endothelial cell; EMCV, encephalomyocarditis virus; ORF, open reading frame; uORF, upstream ORF; RT, reverse transcriptase; nt, nucleotide; ODC, ornithine decarboxylase; RACE, rapid amplification of cDNA ends; RPA, RNase protection assay.

Lipofectin (Invitrogen), as specified by the manufacturer. Briefly, 1.5–1.8 × 10^5 cells were seeded per 10-cm^2 plate and grown in endothelial growth medium-2 supplemented with 2% fetal bovine serum. Cells were harvested 24 h post-transfection and luciferase activities measured using the dual-luciferase reporter assay system (Promega, Madison, WI). Transient RNA transfections were performed using the cationic lipid reagent, DMRIE-C (Invitrogen). Approximately 1.8 × 10^6 HUVECs were seeded per 10-cm^2 plate 24 h prior to transfection. Cells were then transfected with 20 μg of capped and polyadenylated mRNA and harvested 8 h post-transfection. Transfections were performed in duplicate and repeated three times. For polysome analysis and RNA isolation, extracts prepared from HUVECs grown under hypoxia (>0.01% O_2) and normoxia (20% O_2) for 16 h were fractionated by velocity sedimentation on 10–50% sucrose gradients. All experiments with HUVECs were performed between passages two and five.

Primer Extension—Human placental poly(A)$^+$ or total RNA was obtained from Clontech (Palo Alto, CA). Total RNA from HUVECs was isolated using TRIzol (Invitrogen) according to the manufacturer's suggested protocol. Oligonucleotides were end-labeled with [γ-^{32}P]ATP (3000 Ci/mmol; PerkinElmer Life Sciences) using T4 polynucleotide kinase and purified after separation on 8% denaturing polyacrylamide gels. A mixture of 2.5 μg of mRNA or 25 μg of total RNA and 2 × 10^5 cpm of the primer was annealed at 65 °C for 15 min. The extension reaction was performed using SuperScript II (Invitrogen) according to the manufacturer's instructions. Extension products were separated on an 8% denaturing gel and the products visualized by autoradiography.

RNase Protection Assay—Templates for riboprobe synthesis were prepared by subcloning a 244-bp fragment containing the hTie2 5′-flanking sequence (−467 to −224) into the pBluescript II KS(+) plasmid (Stratagene, La Jolla, CA) to create hTie2UP-Ribo15/pKSII. [α-^{32}P]UTP (800 Ci/mmol) was used with the MAXIscript *in vitro* transcription kit (Ambion, Austin, TX) to generate riboprobes from the XhoI-linearized hTie2UP-Ribo15/pKSII. The radiolabeled cRNA was purified by 8% denaturing gel electrophoresis, followed by elution for 12 h at 37 °C in 0.5 M ammonium acetate, 1 mM EDTA, 0.2% SDS. The efficiency of labeling was determined by scintillation counting, and 1 × 10^5 cpm of each labeled riboprobe were used per reaction. RNase protection assays were performed using the RPAIII system (Ambion) according to the manufacturer's instructions. Briefly, the labeled riboprobe was hybridized to 5 μg of human placental poly(A)$^+$ for 16 h at 42 °C. Following hybridization, unprotected single-stranded RNA was digested with a mixture of RNase A (2.5 units/ml) plus RNase T1 (100 units/ml). The resulting protected products were separated on an 8% denaturing polyacrylamide gel and visualized by autoradiography.

Sucrose Gradients and Polysome Analysis—Polysome analyses were performed on HUVECs at 70% confluence. Cells were treated with 0.1 mg/ml cyclohexamide for 3 min and harvested in lysis buffer (15 mM Tris-HCl (pH 7.4), 300 mM NaCl, 15 mM $MgCl_2$, 1% Triton X-100, 0.1 mg/ml cyclohexamide, 333.3 units/ml RNase inhibitor (Ambion)) at 4 °C. After a brief centrifugation, the extract was layered on 10–50% sucrose gradients in buffer (15 mM Tris-HCl (pH 7.4), 300 mM NaCl, 15 mM $MgCl_2$). Gradients were centrifuged at 39,000 rpm for 1.5 h at 4 °C, and fractions were collected across the gradient and snap-frozen in liquid nitrogen. Total RNA or RNA from the indicated pooled fractions following sucrose gradient centrifugation was isolated using TRIzol.

Generation of Monocistronic and Bicistronic Constructs—The generation of bicistronic constructs was based on pRΔDEF (26). First, a fragment corresponding to the hTie2 5′-UTR was generated by PCR amplification of the hTie2 5′-UTR cDNA and subcloned into pGL3-BASIC (Promega). In the second step, the fragments containing hTie2 5′-UTR and amino-terminal coding region of firefly luciferase were introduced into pRΔDEF by replacing the ΔEMCV 5′-UTR and the first 121-bp of firefly luciferase. Bicistronic constructs containing a stable stem-loop structure (TAR(+III) element (27)) were generated by inserting the stem-loop element 232 bp upstream of the *Renilla* coding region of the above-mentioned bicistronic constructs. For all of the recombinant constructs generated in this study in which a reporter was placed downstream of uORF5, its AUG codon was placed in-frame with the predicted Tie2 AUG codon embedded in uORF5. The accuracy of all constructs was confirmed by sequencing.

Real-time Reverse Transcriptase (RT)-PCR Analysis—Relative expression levels were assessed using a 200–300-ng RNA sample by real-time, one-step RT-PCR using the Roche Diagnostics LightCycler instrument and the Roche Diagnostics LightCycler RNA master SYBR green I kit according to the manufacturer's instruction. The level of 28 S rRNA was used as a reference value for quantitation within samples to determine the relative amounts of specific mRNA. The sequences of oligonucleotides used for RT-PCR are available on request.

Northern Blot Analysis—Total RNA was isolated following transfection with bicistronic reporters. Following extraction of RNA with TRIzol, 21 μg of total RNA was loaded onto a 1% formaldehyde-agarose gel, separated by electrophoresis, and transferred to a nylon membrane. Hybridization was in ExpressHyb hybridization solution (BD Biosciences) at 68 °C with a ~400-nt firefly luciferase-specific ^{32}P-labeled probe. Autoradiography of the membrane was performed at −80 °C with film (Kodak X-Omat) to visualize the radioactive signal.

Metabolic Labeling with [^{35}S]Methionine—HUVECs were plated at 2.7 × 10^5 cells per 150-mm plate and incubated for 24 h, followed by a further 12–36-h incubation under either normoxic or hypoxic conditions. Cells were then washed with phosphate-buffered saline and incubated in methionine-free RPMI 1640 medium (Sigma) supplemented with 10% fetal calf serum and [^{35}S]methionine (PerkinElmer Life Sciences) 4 h prior to harvesting. Cells were washed three times with phosphate-buffered saline and harvested in lysis buffer (25 mM HEPES (pH 7.4), 137 mM NaCl, 10% glycerol, 2.5 mM EDTA, 2.5 mM EGTA, 0.5% Triton X-100, 5 mM β-mercaptoethanol, 2 μg/ml aprotinin, 2 μg/ml leupeptin, 2 μg/ml pepstatin A). The cell lysates (500 μg of total protein) were precleared with protein G-Sepharose and immunoprecipitations performed with anti-Tie2 (Santa Cruz Biotechnology, Inc., Santa Cruz, CA), anti-β-actin antibodies (Abcam Inc., Cambridge, MA), and anti-ornithine decarboxylase (ODC) (Sigma) antibodies, respectively. The immunoprecipitates were then subjected to SDS-PAGE, followed by fluorography. Experiments were performed twice at least in triplicate.

RESULTS

Tie2 mRNA Is Translated under Hypoxic Conditions—To assess the translational behavior of Tie2 mRNA under hypoxic conditions, we monitored its distribution across polysomes from normoxic and hypoxic treated primary HUVECs (Fig. 1). Under hypoxic conditions, there is a reduction in polysomes accompanied by an apparent increase in amount of free ribosomal subunits (Fig. 1*A*), as reported previously (23, 25) and consistent with a reduction in protein synthesis associated with this physiological treatment. Quantitative RT-PCR from fractions collected from the bottom or top half of the polysomes (N/H-4 and N/H-3, respectively), as well as from the top of the gradient (N/H-1) and the region containing the ribosomal subunits (N/H-2), revealed that the distribution of Tie2 and VEGR mRNAs remain unchanged when cells are transferred from normoxic to hypoxic conditions (Fig. 1*B*). In contrast, the vast majority of β-actin mRNA appears in heavy polysomes under normoxic conditions (N-4) and redistributes to lighter fractions (H-3, H-2, H-1) when HUVECs are transferred to hypoxia (Fig. 1*B*). This is similar to what has been reported previously for β-actin mRNA redistribution when cells are exposed to hypoxia (25, 28). We also assessed the change in polysome distribution of a second mRNA encoding ODC. Translation of this transcript is generally cap-dependent (29, 30), except during mitosis (31). As the majority of cells in our experiment were not in mitosis (<5%), we expect ODC to behave as a cap-dependent transcript. The majority of ODC mRNA from HUVECs under normoxic growth conditions was in N-2 or heavy polysomes (N-4). Upon exposure of HUVECs to hypoxia, the majority of the mRNA in the N-4 fraction shifted to lighter polysomes (H-3). These results are consistent with a reduction in cap-dependent protein synthesis associated with hypoxia (23, 25). Like other reports documenting mRNA redistribution among polysomes during hypoxia, we do not observe a complete disaggregation of β-actin (25, 28) or ODC mRNA into free mRNA (Fig. 1*B*), despite an apparent flattening of the polysome peak (Fig. 1*A*). We attribute this to the relative insensitivity of using spectrophotometry to monitor polysomes and suspect that there is some residual polysomes in the hypoxia-treated samples.

To assess Tie2 protein levels under hypoxic conditions, we performed Western blot analysis on total protein isolated from HUVECs (Fig. 2*A*). HIF-2α protein was detected only in extracts prepared from hypoxic cells confirming activation of the hypoxic response (Fig. 2*A*). In this Western blot analysis, an-

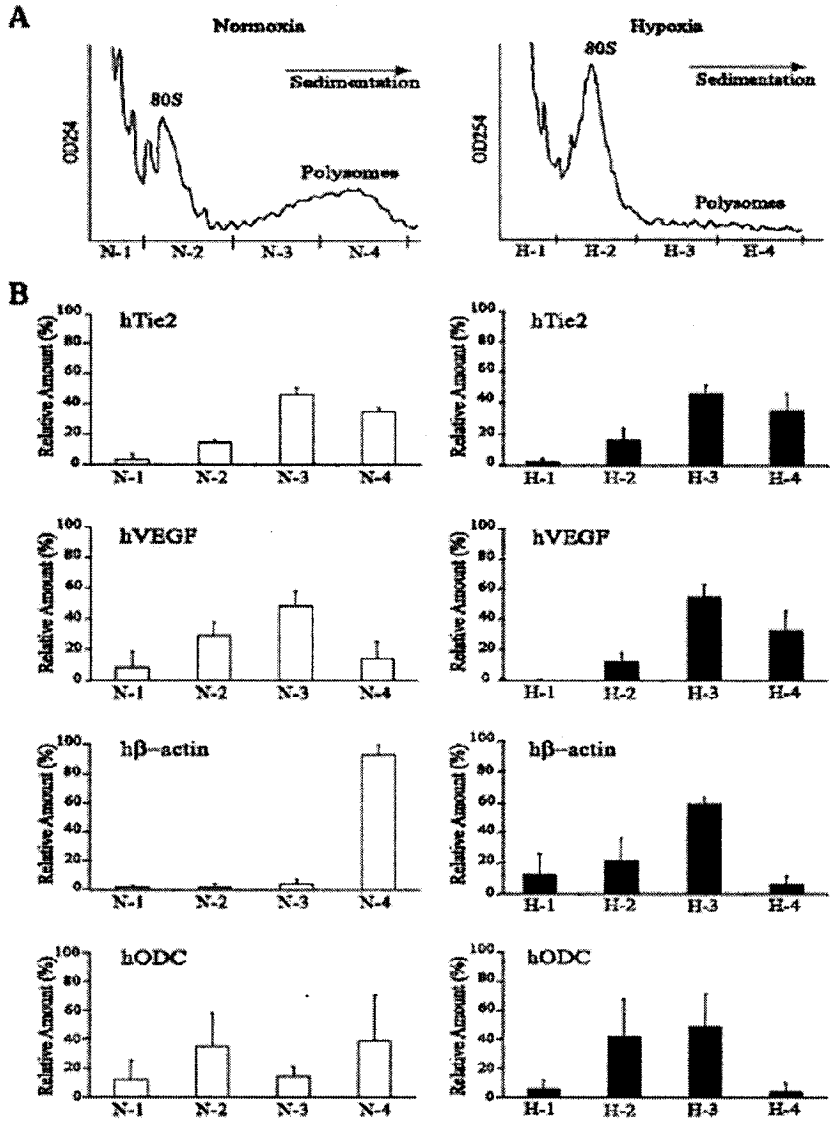

FIG. 1. **Effect of hypoxia on Tie2 expression in HUVECs.** *A*, A_{254} profile of polysomes obtained from HUVECs under normoxic or hypoxic conditions. *B*, RNA was purified from the indicated pooled fractions in *A* and quantified using real-time RT-PCR. For each gene, the relative amount of each pooled fraction was calculated as a percentage of its total in the polysomes. The results are an average of three independent experiments, and the standard deviations are shown. Primers used for quantitative RT-PCR of the hTie2 transcript were hTie2-(443–423) (5′-GATGAATTGCGAGATGGATAGGGCTTGAG-3′) (targeting nts −257 to −285) and hTie2UP-5′2 (5′-ACCTTCCACAGTTCCAGAAAGGAG-3′) (targeting nts +43 to +66).

ti-H3 histone was used as a loading control for HIF-2α (Fig. 2*A*). Consistent with the polysome profiling results (Fig. 1), Tie2 protein was present in both normoxic and hypoxic treated cells (Fig. 2*A*). (In this experiment, a nonspecific band labeled with an *asterisk* is used as a loading control for Tie2.) Tie2 protein was actively translated under both normoxic and hypoxic conditions as assessed by metabolic labeling of HUVECs followed by immunoprecipitation with anti-Tie2 antibodies (Fig. 2*B*). In contrast, synthesis of β-actin and ODC was significantly decreased after exposure of HUVECs to hypoxic stress (Fig. 2*B*). To gauge the extent to which translation in HUVECs is suppressed by hypoxia, we measured the rate of [^{35}S]methionine incorporation into newly synthesized proteins in HUVECs under normoxic or hypoxic conditions (Fig. 2*C*). Under hypoxic conditions, protein synthesis is reduced by 85% in HUVECs, in comparison with HUVECs under normoxic or reoxygenated conditions following hypoxic stress (Fig. 2*C*). Taken together these results indicate that translation of Tie2 mRNA is resistant to the reduction in protein synthesis accompanied by hypoxic treatement of HUVECs.

The levels of Tie2, VEGF, and β-actin mRNAs in total RNA isolated from HUVECs were also measured by quantitative RT-PCR (Fig. 2*D*). VEGF mRNA levels increased 70-fold in response to hypoxia, whereas those of β-actin decreased ~4-fold (Fig. 2*D*). These results are consistent with previously reported effects of hypoxia on VEGF and β-actin gene expres-

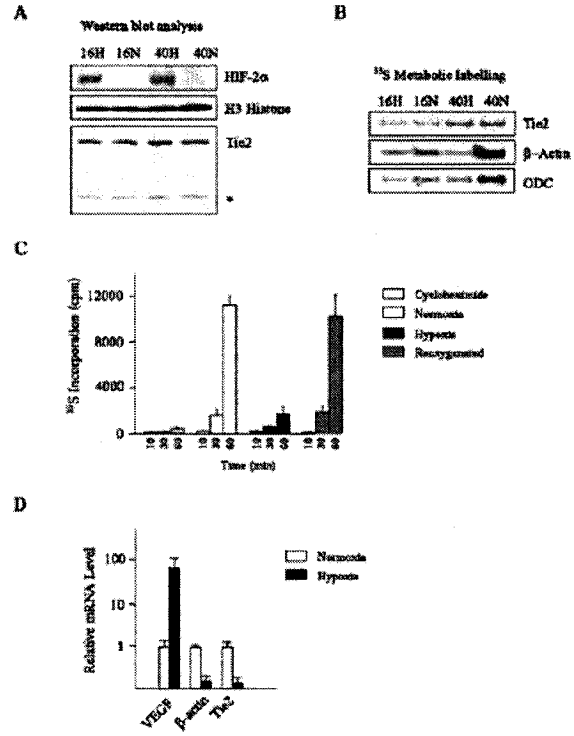

FIG. 2. **Tie2 protein production is maintained under hypoxic conditions.** *A*, Tie2 protein expression in HUVECs exposed to hypoxia (*H*; 1% O_2) or normoxia (*N*; 20% O_2) for 16 and 40 h. *Upper panel*, Western blot analysis performed using polyclonal anti-HIF-2α (Novus Biologicals, Inc., Littleton, CO) antibodies. *Middle panel*, Western blot analysis performed using histone H3 antisera (Cell Signaling, Beverly, MA). *Lower panel*, Western blot analysis performed using anti-Tie2 (Santa Cruz Biotechnology, Inc.) antibodies. A nonspecific band (indicated by an *asterisk*) was used as a loading control. *B*, metabolic labeling of Tie2 under hypoxic conditions. HUVECs were metabolically labeled with [^{35}S]methionine under normoxia (*N*) or hypoxia (*H*) and immunoprecipitated with anti-Tie2 or anti-β-actin antisera. Immunoprecipiates were resolved by SDS-PAGE and visualized by fluorography. *C*, metabolic labeling using [^{35}S]methionine in HUVECs under conditions of normoxia, hypoxia, or reoxygenation. HUVEC cells were preincubated for 40 h under hypoxia or normoxia or incubated for 40 h under hypoxia, followed by 1 h of normoxia (reoxygenated). Radiolabeled methionine incorporation under normoxia is also presented in the presence of 20 μg/ml cycloheximide. Cells were incubated in the presence of [^{35}S]methionine for 10, 30, or 60 min, then immediately harvested. Trichloroacetic acid precipitation of cell lysates was performed in duplicate and used to determine the incorporation of [^{35}S]methionine into protein. Each measurement was normalized with respect to total protein as determined by the Lowry protein assay (51). The results represent the average of three independent experiments performed, and the *error bars* denote the error of the mean. *D*, total RNA was isolated from cells and used as template for real-time RT-PCR. The relative mRNA amounts were normalized to the abundance of the 28 S rRNA and averaged for three independent experiments.

sions (32–34). Under hypoxic conditions, Tie2 mRNA levels decreased ~4-fold, consistent with the results reported by Mandriota and Pepper (35).

Mapping the Human Tie2 5′-Untranslated Region—In an attempt to understand how Tie2 translation is maintained under hypoxic stress, during a time when overall cap-dependent protein synthesis is attenuated, we undertook a structure/function approach to mapping of the Tie2 5′-UTR. The transcription start sites of the human Tie2 mRNA have been previously defined using 5′-RACE and primer extension (36). The results suggested the presence of 10 transcription initiation sites situated from 269 to 414 nucleotides upstream of the initiator AUG codon (37). However from this report, it is not possible to assess which sites were detected by primer extension *versus* those identified by 5′-RACE. We re-mapped the transcription initiation sites in the human Tie2 mRNA to identify transcription start sites. Primer extension analysis was performed with three oligonucleotides (hTie2-UP-6, hTie2-UP-7, hTie2-UP-1), which together span the entire length of the Tie2 5′-UTR (Fig. 3*A*). No specific products were visualized with hTie2-UP-6 or hTie2-UP-7, indicating that these likely reside too far downstream of the transcription start site(s). However, two distinct extension products were obtained with hTie2-UP-1 (Fig. 3*B*). These fragments map to nts −372 and −377 of the Tie2 5′-UTR (Fig. 3*D*, encased within *gray boxes*).

To complement the primer extension results and determine whether we could detect the same start sites, we performed RNase protection experiments. The probe used extended from −467 to −224 (Fig. 3*D*, generated by primers hTie2-UP-4 and hTie2-UP-5). Two major protected fragments of 127 and 149 nucleotides were observed (Fig. 3*C*). These mapped to positions −372 and −350 of the Tie2 5′-UTR (Fig. 3*D*). We note that the start site at nucleotide −350 may have been missed in the primer extension analysis, due to high background in this size range of the gel (Fig. 3*C*). Taken together, the RNase protection and primer extension results indicate that a major Tie2 transcription site lies at nucleotide −372. This site also lies within 2 nucleotides of the identified murine Tie2 transcription initiation site (37). Sequence analysis of over 300 5′-RACE PCR products demonstrated sequence contiguity with the Tie2 genomic DNA sequence, indicating the absence of a frequent splicing event within the Tie2 5′-UTR.[2] Hence, the Tie2 mRNA isoforms identified here contain several features predicted to be inhibitory to a cap-dependent initiation mechanism, notably a lengthy 5′-UTR (372 nts), five uORFs, and an AUG codon embedded with the last uORF (Fig. 3*D*). In this report, we further characterize the translational properties of the −372 isoform.

The Tie2 5′-UTR Mediates Internal Initiation—One mechanism by which Tie2 could be efficiently translated under hypoxic conditions (Fig. 2*B*), a situation that reduces cap-dependent translation initiation (16, 26), would be if Tie2 translation proceeded by internal ribosome recruitment to the 5′-UTR. To test this, the Tie2 5′-UTR was positioned within the intercistronic spacer between the firefly and *Renilla* luciferase coding regions (Fig. 4*A*). We also generated a construct in which all uAUGs had been removed by mutating AUG to UUG, to assess their potential contribution to IRES activity (Fig. 4*A*). As a negative control for these experiments, we utilized a deletion mutant of the EMCV 5′-UTR that does not support internal ribosome binding (Fig. 4*A*, construct Ren/ΔEMC/FF). The length of the ΔEMC sequence is ~440 bp, similar to the size of the Tie2 5′-UTR used in these experiments (372 bp). In addition, we generated constructs in which the human immunodeficiency virus TAR element (TAR(+III)) was positioned upstream of *Renilla* luciferase. This allowed us to probe whether firefly luciferase expression was independent of *Renilla* expression and not a consequence of ribosome reinitation (Fig. 4*A*). The stable secondary structure of this element ($\Delta G = -49.9$ kcal/mol) is expected to act as a physical barrier to 5′-end-mediated initiation and decrease expression of the *Renilla* luciferase protein (27).

Transfection experiments with HUVECs revealed that expression vectors containing the TAR(+III) element upstream of the *Renilla* luciferase initiation codon displayed a ~5-fold re-

[2] E.-H. Park and J. Pelletier, unpublished data.

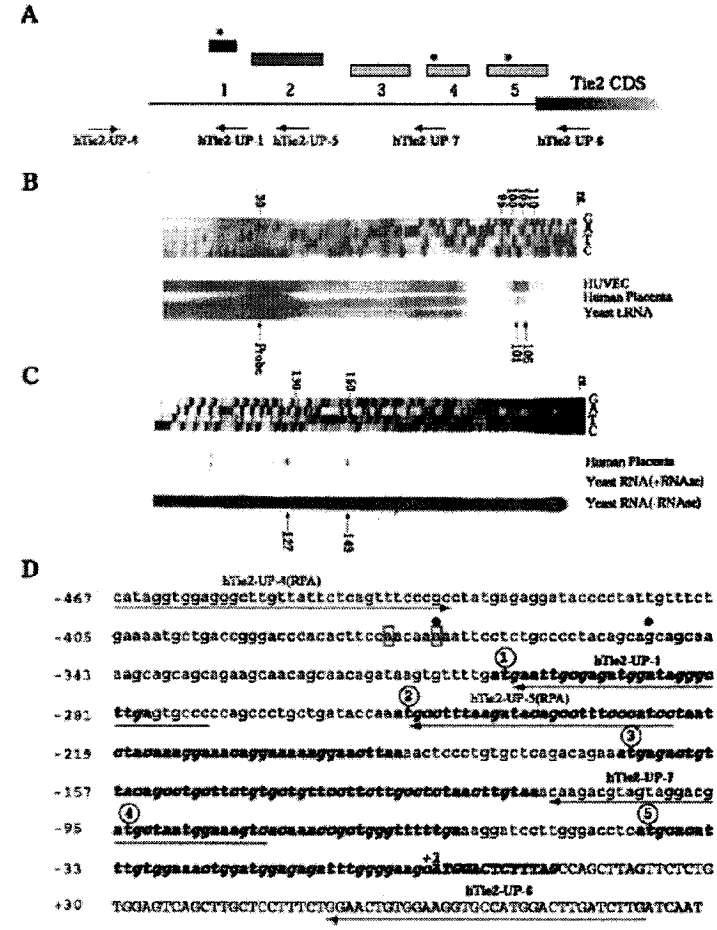

FIG. 3. **Determination of the transcription start site(s) of human Tie2 mRNA.** *A*, schematic representation of the human Tie2 5′-UTR. The uORFs are depicted as well as their relative reading frames by different shades of *gray*. *Asterisks* above an uORF indicates the presence of an internal AUG, in-frame with the uORF initiator AUG. *B*, mapping of the transcription start sites of the human Tie2 gene by primer extension. Total RNA from HUVECs, human placental poly(A)$^+$ RNA, and yeast tRNA were analyzed using oligonucleotide hTie2-UP-1 as a primer. Sequencing reactions were used as molecular markers. The two major products (*arrows*) terminate at adenosine residues and are encased in the *gray boxes* in *D*. The smaller products observed from the human placenta mRNA preparations were not reproducibly seen among different experiments. *C*, RNase protection mapping of the human Tie2 mRNA. The RNase protection assay (RPA) of human placental poly(A)$^+$ RNA or yeast RNA was performed as described under "Experimental Procedures." Sequencing reactions were used as molecular markers. The *arrows* indicate the size and position of migration of the protected fragments. *D*, nucleotide sequence upstream of the human Tie2 initiation codon. The Tie2 translation start codon is designated as +1, and five uORFs are indicated in *bold* and *italics*. The locations of the oligonucleotides used for primer extension and RPA are shown. The transcription start sites determined by primer extension and RPA are indicated by *gray boxes* and *gray circles* above the nucleotide, respectively.

duction in *Renilla* luciferase activity relative to the constructs lacking this stem-loop barrier (Fig. 4*B*, compare *lanes 1–3* to *lanes 4–6*). Very low levels of firefly luciferase activity were detectable from cells transfected with Ren/ΔEMC/FF or TAR(+III)/Ren/ΔEMC/FF, since the ΔEMC 5′-UTR does not allow for efficient reinitiation or for internal ribosome recruitment (Fig. 4*B*, *lanes 1* and *4*). However, significant and comparable firefly luciferase activities were detected in extracts from cells transfected with Ren/Tie2/FF and TAR(+III)/Ren/Tie2/FF (Fig. 4*B*, compare *lane 2* with *lane 5*) or with Ren/Tie2ΔuAUG/FF and TAR(+III)/Ren/Tie2ΔuAUG/FF (Fig. 4*B*, compare *lane 3* with *lane 6*). These results indicate that the Tie2 5′-UTR mediates the production of firefly luciferase independent of *Renilla* luciferase, as would be expected if an IRES was present.

IRES Activity Is Maintained during Hypoxia—One function of the Tie2 IRES might be to maintain efficient translation during hypoxia (Fig. 1). To assess whether the putative Tie2 IRES could function in a bicistronic context under hypoxic conditions, we transfected HUVECs with Ren/ΔEMC/FF or Ren/Tie2ΔAUG/FF and placed these cells under normoxic or hypoxic conditions (Fig. 4*C*). Luciferase activities were then measured in cell extracts. We observed that the relative *Renilla* luciferase activity decreased ~2-fold when cells were exposed to hypoxia (Fig. 4*C*). This effect is likely an underestimation of the true decrease in protein synthesis, since it relies on measuring enzyme activity, some of which will be already present prior to the start of hypoxic treatment. Expression of the firefly luciferase cistron was increased slightly under hypoxic conditions in Ren/Tie2ΔuAUG/FF (Fig. 4*C*). The hypoxic/normoxic ratio indicates that the potential Tie2 IRES activity was even slightly stimulated under hypoxic conditions (Fig. 4*C*). These results indicate that the putative Tie2 IRES is functional during hypoxic treatment.

Northern blot analysis indicates that bicistronic transcripts produced *in vivo* from Ren/ΔEMC/FF, Ren/Tie2/FF, and Ren/Tie2ΔAUG/FF were of comparable quality (Fig. 4*D*). No major degradation product was visible that could account for the differential expression of firefly luciferase from Ren/Tie2/FF and Ren/Tie2ΔAUG/FF, relative to Ren/ΔEMC/FF (Fig. 4*B*).

Another alternative interpretation for the observed results would be the existence of cryptic splice sites upstream of the firefly luciferase coding region that could eliminate a portion, or all of, the upstream *Renilla* sequences. Subsequent translation of a spliced transcript could then lead to increased firefly luciferase levels, without the need to invoke the existence of an IRES. As a test for this, we performed RT-PCR on total RNA isolated from HUVECs that had been transfected with Ren/Tie2/FF or Ren/Tie2ΔuAUG/FF (Fig. 5*A*). PCR primers were designed that targeted the 5′-UTR of *Renilla* and within the firefly luciferase coding region (Fig. 5*A*, *left panel*). A single DNA product was obtained following RT-PCR of RNA from transfected cells and corresponds in size to the expected full-length PCR product encompassing the *Renilla* ORF and Tie2

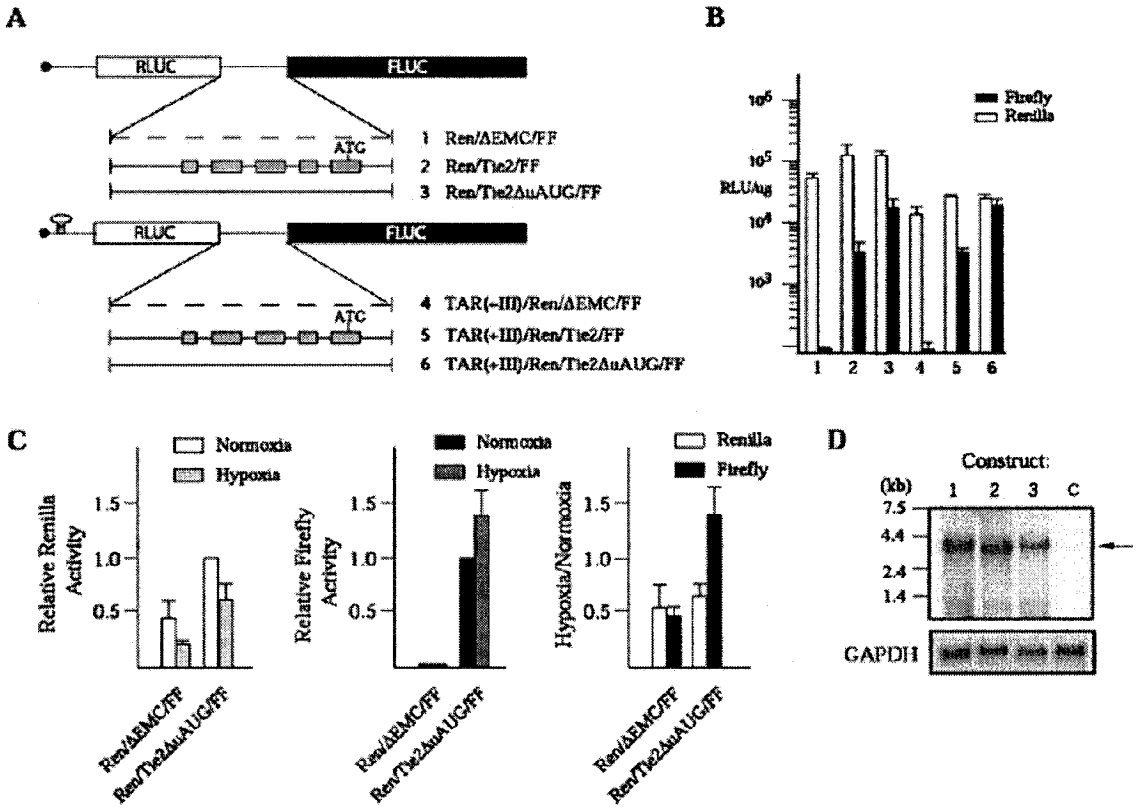

FIG. 4. **The Tie2 5′-UTR mediates internal initiation *in vivo*. *A*,** schematic representation of bicistronic constructs containing the Tie2 5′-UTR in the intercistronic region. The *Renilla* and firefly luciferase ORFs are denoted by a *white* and *black box*, respectively. The stem-loop structure upstream of the *Renilla* ORF in the TAR(+III) construct series represents the human immunodeficiency virus TAR element. *B*, quantitation of luciferase activities following DNA transfection into HUVECs. The relative light units per microgram of protein extract are denoted for both the *Renilla* and firefly luciferase proteins. The construct number is indicated below the *x* axis. The results represent the average of three independent experiments performed, and the *error bars* denote the error of the mean. *C*, quantitation of *Renilla* luciferase activities obtained from transfected cells exposed to normoxia or hypoxia. Luciferase activities were determined, normalized to the protein content of each extract, then set relative to the value obtained for Ren/Tie2ΔAUG/FF under normoxic conditions. Ratios of the hypoxic to normoxic values are also calculated and plotted. Values plotted are the average of three independent experiments with the standard error presented. *D*, Northern blot of RNA isolated from transfected HUVECs and probed for firefly luciferase. The nature of the construct is indicated above the panel and corresponds to the numbering scheme used in *A*. The *arrowhead* indicates the position of migration of the bicistronic mRNA, and the *bottom panel* is the same blot reprobed with glyceraldehyde-3-phosphate dehydrogenase (*GAPDH*), to account for possible variations in loading.

5′-UTR (~1.7 kbp) (Fig. 5*A*). PCR products were not observed when reverse transcriptase was omitted from the RT-PCR (Fig. 5*A*). From this experiment, no evidence of splicing was obtained as assessed by the lack of smaller PCR products (whose amplification should be favored during the PCR) (Fig. 5*A*).

To ensure that the results obtained in Fig. 4 were not due to the presence of a cryptic promoter within the Tie2 5′-UTR, we generated expression vectors in which the Tie2 5′-UTR was placed upstream of the firefly luciferase gene in a promoterless plasmid backbone (Fig. 5*B*). A firefly reporter construct containing SV40 promoter (SV40/Luc) was used as a positive control. Transfection of these reporter constructs into HUVECs showed that pGL-Basic (negative control) and hTie2/Luc constructs produced similar levels of low luciferase activity (Fig. 5*C*). On the other hand, SV40/Luc yielded over 100 times higher luciferase activity compared with hTie2/Luc and pGL-Basic (Fig. 5*C*). These results indicate the absence of a detectable cryptic promoter activity within the Tie2 5′-UTR.

To confirm and extend these results, we performed a series of mRNA transfection experiments. We generated capped and polyadenylated mRNAs from bicistronic constructs containing: (i) the EMCV 5′-UTR with the deleted IRES (negative control), (ii) the poliovirus IRES (positive control), and (iii) the Tie2 5′-UTR containing or lacking all uAUGs (Fig. 6*A*). Following transfection of mRNAs into HUVECs, firefly and *Renilla* production was assessed by Western blotting (Fig. 6*B*) or by measuring luciferase activities (Fig. 6*C*). Western blotting experiments revealed that production of *Renilla* luciferase was similar among the four transfected mRNA species, whereas the levels of firefly luciferase differed among expression constructs (Fig. 6*B*). No firefly luciferase was observed from cells transfected with TAR(+III)/Ren/ΔEMC/FF (*lane 3*), consistent with the absence of an IRES in this construct. In contrast, transfection of TAR(+III)/Ren/Polio/FF mRNA into HUVECs produced high levels of firefly luciferase (*lane 4*). Firefly luciferase was also detectable from cells transfected with TAR(+III)/Ren/Tie2/FF and TAR(+III)/Ren/Tie2ΔuAUG/FF mRNAs, with slightly more being produced from the construct lacking uAUGs (Fig. 6*B*, compare *lane 1* with *lane 2*).

These results were confirmed by monitoring *Renilla* and firefly luciferase activities (Fig. 6*C*). The FF/Ren ratio obtained from HUVECs transfected with TAR(+III)/Ren/Polio/FF mRNA was ~100-fold greater than that obtained from cells transfected with TAR(+III)/Ren/ΔEMC/FF mRNA, consistent with the presence of an IRES in the former transcript (Fig. 6*C*). The FF/Ren ratio of TAR(+III)/Ren/Tie2ΔuAUG/FF trans-

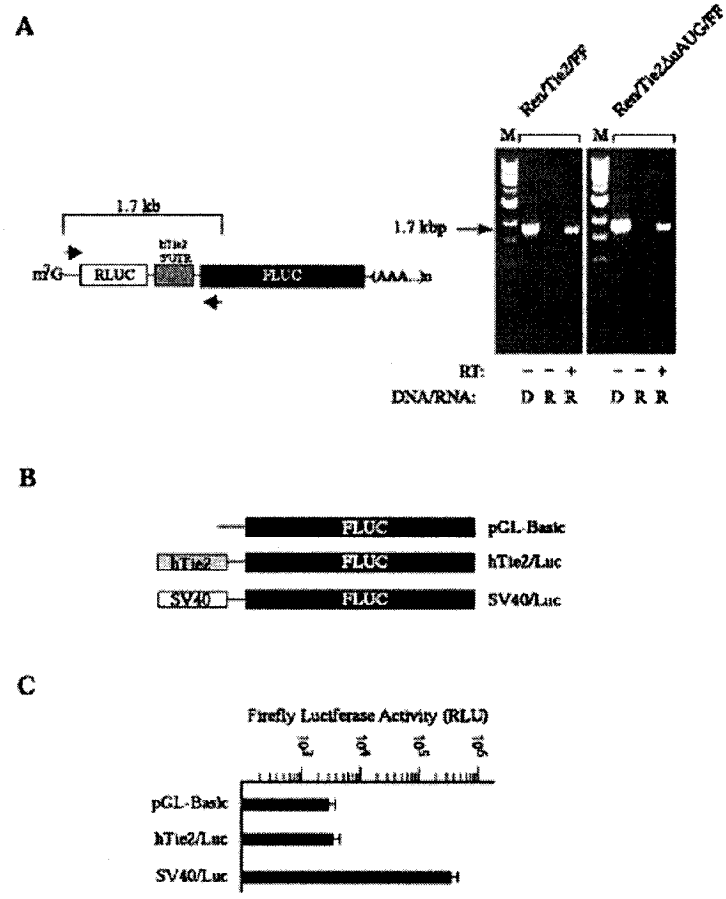

FIG. 5. **Absence of cryptic splicing within the Tie2 5′-UTR.** *A*, RT-PCR analysis of total RNA isolated from transfected HUVECs. PCRs were performed from plasmid DNA (*lanes* labeled *D*) as positive controls. RT-PCRs were performed from RNA in which RT was added (+) or omitted (−). The expected size of the PCR products is indicated. Molecular size markers (*M*) are 1-kbp ladders from New England Biolabs. The location of the PCR primers used in this amplification are schematically shown. *B*, assessing promoter activity of the Tie2 5′-UTR. Schematic representation of constructs used to test for cryptic promoter activity within the Tie2 5′-UTR is shown. The firefly luciferase ORF is denoted by a *black box*. The pGL-Basic vector (Promega) lacks a defined active promoter. The Tie2 5′-UTR (nts −372 to +69) was placed upstream of the firefly luciferase gene. SV40/Luc contains the SV40 promoter driving transcription of the firefly luciferase gene and was used as a positive control. *C*, HUVECs were transfected with pGL-Basic, hTie2/Luc, or SV40/Luc in conjunction with the plasmid pRL-CMV (Promega). Lysates were prepared from the cells following transfection, and luciferase activities were measured. The relative light units per microgram of protein extract are shown for the firefly luciferase protein. To account for variations in transfection efficiency, firefly luciferase activity was normalized to that of *Renilla* luciferase. The results represent the average of three independent experiments performed in duplicate, and the *error bars* denote the error of the mean.

fected cells was ~8-fold higher than that of the negative control. These results indicate that the observed Tie2 IRES activity is RNA-dependent and not due to the presence of a cryptic promoter. TAR(+III)/Ren/Tie2/FF exhibited ~3-fold lower FF/Ren ratio than that detected with TAR(+III)/Ren/Tie2ΔuAUG/FF, further suggesting that the uORFs within the Tie2 5′-UTR negatively affect IRES-mediated translation (see "Discussion").

DISCUSSION

The angiopoietin-Tie2 signaling pathway plays an important role in the development of normal and tumor vasculature. Tie2 expression is elevated in human cancers (breast, ovarian, hepatocellular, glioblastoma) with expression being localized in "vascular hot spots" at the leading edge of invasive tumors (reviewed by Peters *et al.* (38)). Conflicting reports have been presented regarding changes in Tie2 protein and mRNA levels during hypoxia. Increases in Tie2 protein expression have been reported to parallel increases in Tie2 mRNA levels (39–41). In contrast, Mandriota and Pepper (35) have reported decreased Tie2 mRNA levels during hypoxia, and Lin *et al.* (42) indicated unchanged Tie2 protein levels under hypoxia. The reasons for these discrepancies are not clear but may reflect response differences to hypoxia among the different cell lines. In our hands, Tie2 mRNA levels decrease as a consequence of hypoxia treatment (Fig. 2*D*) with protein production continuing at levels comparable with those observed during normoxia (Fig. 2*B*). Our study indicates that Tie2 protein production is secured under hypoxic conditions (Fig. 2*B*), when general translation is reduced.

The presence of an IRES within the Tie2 5′-UTR provides an explanation for how this mRNA is able to escape the reduction in translation imposed by hypoxia. Exposure of cells to hypoxic conditions has been shown to be associated with a decrease in cap-dependent translation as a result of increased formation of the eIF4E/4E-BP1 inhibitory complex (16, 43). In addition, increased phosphorylation of eIF2α associated with hypoxia also contributes to decreased general protein synthetic rates but increases the production of a specific set of mRNAs (15). The idea that the Tie2 IRES allows an escape from translation repression during hypoxia is supported by our experiments in which the Tie2 IRES activity was maintained, and even slightly stimulated, under hypoxic conditions (Fig. 4*C*).

The Tie2 mRNA 5′-UTR contains five uORFs, an unusually high number for a eukaryotic transcript (Fig. 3*D*). The primer combination used to assess the polysome distribution of the hTie2 mRNA in Fig. 1*B* spanned five uORFs and the first 60 nucleotides following the initiation codon (Fig. 3*D*). Our quantitative RT-PCR results demonstrate that the Tie2 transcript obtained using these primers is associated with polysomes under both normoxic and hypoxic conditions, indicating that translating Tie2 mRNA contains this complex 5′-UTR with its five uORFs. We note that in both DNA and RNA transfections, expression of firefly luciferase is increased when all of the Tie2 uAUGs are deleted (Figs. 4*B* and 6). A simple interpretation of these results is that some (or all) of the uORFs reside between the IRES and the initiator ATG and are encountered by the internally initiated ribosome. This could have the consequence

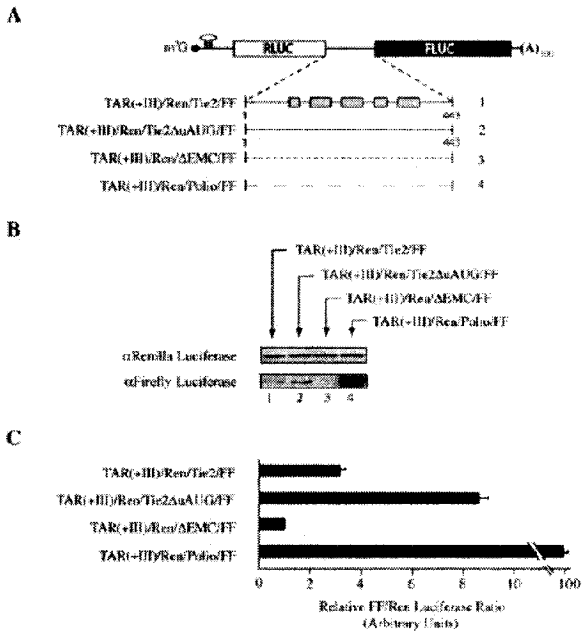

FIG. 6. **Messenger RNA transfection into HUVEC cells.** *A*, schematic representation of mRNA species used in mRNA transfections. *B*, Western blot analysis of extracts from HUVECs transfected with bicistronic mRNAs shown in *A*. Cell lysates were analyzed by immunoblotting with anti-*Renilla* luciferase and anti-firefly luciferase antisera. The nature of the transfected mRNA is indicated above the lanes. *C*, luciferase activities were measured from HUVEC lysates following RNA transfection. The relative FF/Ren ratio obtained for each mRNA contruct is shown. The ratio of the negative control, TAR(+III)/Ren/ΔEMC/FF, was arbitrarily set to 1. The results represent the average of three independent experiments performed in duplicate, and the *error bars* denote the error of the mean.

of reducing translation initiation, due to ribosomes dropping off during re-initiation, or bypassing the initiation codon of the major ORF, due to an inability to re-acquire a ternary complex.

Another possibility for the role of the Tie2 uORFs in translation initiation could be to simply prevent the majority of ribosomes that have initiated by a cap-dependent mechanism from reaching the Tie2 initiation codon, thereby acting as a damper to prevent 5′-end-mediated initiation from interfering with IRES activity on the Tie2 mRNA template. Alternatively, the structure of the Tie2 IRES may be dynamically affected by scanning ribosomes. In this situation, ribosomes initiated in a cap-dependent fashion could affect Tie2 5′-UTR secondary structure and impact on IRES function. Such a model has been implicated in the function of the cat-1 IRES, where disruption of RNA-RNA interactions between the 5′- and 3′-end of an IRES prevents inducible internal initiation. The cat-1 IRES activity is restored upon inhibition of 5′-end mediation initiation (44). Whether a similar scenario occurs on the Tie2 IRES needs to be experimentally addressed and may indicate that translation initiation on the Tie2 mRNA is more dynamic and complex than expected.

Our findings indicate that Tie2 belongs to a class of mRNA transcripts harboring IRES activity to circumvent the reduction of protein synthesis imposed during hypoxic stress. Other mRNAs in this category include c-*myc* (45–48), *HIF-1α* (25), and *VEGF* (21–24). The presence of IRESs in the 5′-UTRs of two mRNAs encoding major angiogenic factors (*VEGF* and *Tie2*) suggest that this translation initiation mechanism plays an important role in the control of angiogenesis. The advantage of IRES-dependent expression during this process might be to allow specific gene expression during a time when global translation is reduced. We would expect that additional genes whose expressions are maintained during hypoxia represent excellent candidates for harboring IRESs. Additionally, the Tie2/angiopoietin-1 signaling system has been implicated in regulating quiescence of hematopoietic stem cells in the bone marrow niche (49). Tie2 expression needs to be maintained during quiescence, a physiological state associated with reduced protein synthesis (50). Hence, the Tie2 IRES described herein may serve to circumvent the translation block imposed by quiescence to keep Tie2 protein levels constant.

Acknowledgments—We thank the anonymous reviewers for their helpful comments in improving the manuscript.

REFERENCES

1. Risau, W. (1997) *Nature* **386**, 671–674
2. Carmeliet, P., Ferreira, V., Breier, G., Pollefeyt, S., Kieckens, L., Gertsenstein, M., Fahrig, M., Vandenhoeck, A., Harpal, K., Eberhardt, C., Declercq, C., Pawling, J., Moons, L., Collen, D., Risau, W., and Nagy, A. (1996) *Nature* **380**, 435–439
3. Ferrara, N., Carver-Moore, K., Chen, H., Dowd, M., Lu, L., O'Shea, K. S., Powell-Braxton, L., Hillan, K. J., and Moore, M. W. (1996) *Nature* **380**, 439–442
4. Shalaby, F., Rossant, J., Yamaguchi, T. P., Gertsenstein, M., Wu, X. F., Breitman, M. L., and Schuh, A. C. (1995) *Nature* **376**, 62–66
5. Griffioen, A. W., and Molema, G. (2000) *Pharmacol. Rev.* **52**, 237–268
6. Maxwell, P. H., Pugh, C. W., and Ratcliffe, P. J. (2001) *Curr. Opin. Genet. Dev.* **11**, 293–299
7. Semenza, G. L. (2002) *Trends Mol. Med.* **8**, S62–S67
8. Suri, C., Jones, P. F., Patan, S., Bartunkova, S., Maisonpierre, P. C., Davis, S., Sato, T. N., and Yancopoulos, G. D. (1996) *Cell* **87**, 1171–1180
9. Dumont, D. J., Gradwohl, G., Fong, G. H., Puri, M. C., Gertsenstein, M., Auerbach, A., and Breitman, M. L. (1994) *Genes Dev.* **8**, 1897–1909
10. Vikkula, M., Boon, L. M., Carraway, K. L., 3rd, Calvert, J. T., Diamonti, A. J., Goumnerov, B., Pasyk, K. A., Marchuk, D. A., Warman, M. L., Cantley, L. C., Mulliken, J. B., and Olsen, B. R. (1996) *Cell* **87**, 1181–1190
11. Maisonpierre, P. C., Suri, C., Jones, P. F., Bartunkova, S., Wiegand, S. J., Radziejewski, C., Compton, D., McClain, J., Aldrich, T. H., Papadopoulos, N., Daly, T. J., Davis, S., Sato, T. N., and Yancopoulos, G. D. (1997) *Science* **277**, 55–60
12. Lin, P., Buxton, J. A., Acheson, A., Radziejewski, C., Maisonpierre, P. C., Yancopoulos, G. D., Channon, K. M., Hale, L. P., Dewhirst, M. W., George, S. E., and Peters, K. G. (1998) *Proc. Natl. Acad. Sci. U. S. A.* **95**, 8829–8834
13. Jones, N., Voskas, D., Master, Z., Sarao, R., Jones, J., and Dumont, D. J. (2001) *EMBO Rep.* **2**, 438–446
14. Papapetropoulos, A., Fulton, D., Mahboubi, K., Kalb, R. G., O'Connor, D. S., Li, F., Altieri, D. C., and Sessa, W. C. (2000) *J. Biol. Chem.* **275**, 9102–9105
15. Koumenis, C., Naczki, C., Koritzinsky, M., Rastani, S., Diehl, A., Sonenberg, N., Koromilas, A., and Wouters, B. G. (2002) *Mol. Cell. Biol.* **22**, 7405–7416
16. Arsham, A. M., Howell, J. J., and Simon, M. C. (2003) *J. Biol. Chem.* **278**, 29655–29660
17. Clemens, M. J. (2001) *J. Cell. Mol. Med.* **5**, 221–239
18. Gingras, A. C., Raught, B., and Sonenberg, N. (1999) *Annu. Rev. Biochem.* **68**, 913–963
19. Gebrke, L., Auron, P. E., Quigley, G. J., Rich, A., and Sonenberg, N. (1983) *Biochemistry* **22**, 5157–5164
20. Svitkin, Y. V., Pause, A., Haghighat, A., Pyronnet, S., Witherell, G., Belsham, G. J., and Sonenberg, N. (2001) *RNA (N. Y.)* **7**, 382–394
21. Huez, I., Creancier, L., Audigier, S., Gensac, M. C., Prats, A. C., and Prats, H. (1998) *Mol. Cell. Biol.* **18**, 6178–6190
22. Akiri, G., Nahari, D., Finkelstein, Y., Le, S. Y., Elroy-Stein, O., and Levi, B. Z. (1998) *Oncogene* **17**, 227–236
23. Stein, I., Itin, A., Einat, P., Skaliter, R., Grossman, Z., and Keshet, E. (1998) *Mol. Cell. Biol.* **18**, 3112–3119
24. Miller, D. L., Dibbens, J. A., Damert, A., Risau, W., Vadas, M. A., and Goodall, G. J. (1998) *FEBS Lett.* **434**, 417–420
25. Lang, K. J., Kappel, A., and Goodall, G. J. (2002) *Mol. Biol. Cell* **13**, 1792–1801
26. Johannes, G., Carter, M. S., Eisen, M. B., Brown, P. O., and Sarnow, P. (1999) *Proc. Natl. Acad. Sci. U. S. A.* **96**, 13118–13123
27. Parkin, N. T., Cohen, E. A., Darveau, A., Rosen, C., Haseltine, W., and Sonenberg, N. (1988) *EMBO J.* **7**, 2831–2837
28. Gorlach, A., Camenisch, G., Kvietikova, I., Vogt, L., Wenger, R. H., and Gassmann, M. (2000) *Biochim. Biophys. Acta* **1493**, 125–134
29. Rousseau, D., Kaspar, R., Rosenwald, I., Gehrke, L., and Sonenberg, N. (1996) *Proc. Natl. Acad. Sci. U. S. A.* **93**, 1065–1070
30. Seidel, E. R., and Ragan, V. L. (1997) *Br. J. Pharmacol.* **120**, 571–574
31. Pyronnet, S., Pradayrol, L., and Sonenberg, N. (2000) *Mol. Cell* **5**, 607–616
32. Shweiki, D., Itin, A., Soffer, D., and Keshet, E. (1992) *Nature* **359**, 843–845
33. Forsythe, J. A., Jiang, B. H., Iyer, N. V., Agani, F., Leung, S. W., Koos, R. D., and Semenza, G. L. (1996) *Mol. Cell. Biol.* **16**, 4604–4613
34. Levy, A. P., Levy, N. S., Wegner, S., and Goldberg, M. A. (1995) *J. Biol. Chem.* **270**, 13333–13340
35. Mandriota, S. J., and Pepper, M. S. (1998) *Circ. Res.* **83**, 852–859
36. Hewett, P. W., Daft, E. L., and Murray, J. C. (1998) *Biochem. Biophys. Res. Commun.* **252**, 546–551
37. Fadel, B. M., Boutet, S. C., and Quertermous, T. (1998) *Biochem. J.* **330**, 335–343

38. Peters, K. G., Kontos, C. D., Lin, P. C., Wong, A. L., Rao, P., Huang, L., Dewhirst, M. W., and Sankar, S. (2004) *Recent Prog. Horm. Res.* 59, 51–71
39. Park, Y. S., Kim, N. H., and Jo, I. (2003) *Microvasc. Res.* 65, 125–131
40. Willam, C., Koehne, P., Jurgensen, J. S., Grafe, M., Wagner, K. D., Bachmann, S., Frei, U., and Eckardt, K.-U. (2000) *Circ. Res.* 87, 370–377
41. Christensen, R. A., Fujikawa, K., Madore, R., Oettgen, P., and Varticovski, L. (2002) *J. Cell. Biochem.* 85, 505–515
42. Lin, S., Shyu, K. G., Lee, C. C., Wang, B. W., Chang, C. C., Liu, Y. C., Huang, F. Y., and Chang, H. (2002) *Biochem. Biophys. Res. Commun.* 296, 710–715
43. Tinton, S. A., and Buc-Calderon, P. M. (1999) *FEBS Lett.* 446, 55–59
44. Yaman, I., Fernandez, J., Liu, H., Caprara, M., Komar, A. A., Koromilas, A. E., Zhou, L., Snider, M. D., Scheuner, D., Kaufman, R. J., and Hatzoglou, M. (2003) *Cell* 113, 519–531
45. Johannes, G., and Sarnow, P. (1998) *RNA (N. Y.)* 4, 1500–1513
46. Nanbru, C., Prats, A. C., Droogmans, L., Defrance, P., Huez, G., and Kruys, V. (2001) *Oncogene* 20, 4270–4280
47. Stoneley, M., Paulin, F. E., Le Quesne, J. P., Chappell, S. A., and Willis, A. E. (1998) *Oncogene* 16, 423–428
48. Nanbru, C., Lafon, I., Audigier, S., Gensac, M. C., Vagner, S., Huez, G., and Prats, A. C. (1997) *J. Biol. Chem.* 272, 32061–32066
49. Arai, F., Hirao, A., Ohmura, M., Sato, H., Matsuoka, S., Takubo, K., Ito, K., Koh, G. Y., and Suda, T. (2004) *Cell* 118, 149–161
50. Hofmann, G. E., and Hand, S. C. (1994) *Proc. Natl. Acad. Sci. U. S. A.* 91, 8492–8496
51. Lowry, O. H., Rosebrough, N. J., Farr, A. L., and Randall, R. J. (1951) *J. Biol. Chem.* 193, 265–275

APPENDIX C:
INTERNAL RIBOSOME ENTRY SITE-MEDIATED TRANSLATION OF APAF-1 BUT NOT XIAP, IS REGULATED DURING UV-INDUCED CELL DEATH

Contribution to the Collaboration

Our contribution to this manuscript is represented in Figure 6. We provided the siRNAs to PERK and performed the troubleshooting experiments required to obtain a substantial inhibition in PERK expression. Primers to amplify PERK by Q-PCR were provided and proper experimental conditions determined by J.Blais. The data presented in Panel B was completed by J Blais. Written contribution to this manuscript in the appropriate areas of the results section, figure legend, and material and methods, were written by J. Blais and edited by Dr. M Holcik.

Summary

The authors of this paper investigated the translational regulation of two known apoptotic proteins in response to UVC irradiation. In response to UVC irradiation, protein synthesis is inhibited and an increase in cell death is observed, due in part to the translational induction of the pro-apoptotic protein APAF-1. Importantly, $PERK^{-/-}$ MEFs demonstrate increased sensitivity to UV-induced cell death. This finding correlates with the observation that $PERK^{-/-}$ MEFs, cells expressing dn-PERKΔC and siRNA mediated knock-down of endogenous PERK, demonstrate higher APAF-1 IRES activity following UVC irradiation than wildtype MEFs, suggesting that PERK may act as a negative regulator of UV-mediated cell death. Moreover, activity of APAF-1 IRES activity is not impacted by the expression of $eIF2\alpha^{S51A}$, suggesting eIF2α phosphorylation may not be the only important cellular target regulated by PERK.

THE JOURNAL OF BIOLOGICAL CHEMISTRY VOL. 281, NO. 22, pp. 15155–15163, June 2, 2006

Internal Ribosome Entry Site-mediated Translation of Apaf-1, but Not XIAP, Is Regulated during UV-induced Cell Death*[S]

Received for publication, October 18, 2005, and in revised form, March 13, 2006 Published, JBC Papers in Press, April 4, 2006, DOI 10.1074/jbc.M511319200

Nicoleta Hosszu Ungureanu[‡], Mireille Cloutier[‡], Stephen M. Lewis[‡], Naomi de Silva[‡], Jaime D. Blais[§], John C. Bell[§], and Martin Holcik[‡1]

From the [‡]Apoptosis Research Center, Children's Hospital of Eastern Ontario, Ottawa, Ontario K1H 8L1 and the [§]Ottawa Health Research Institute, Ottawa, Ontario K1H 8L6, Canada

Components of the cellular translation machinery are targets of caspase-mediated cleavage during apoptosis that correlates with the inhibition of protein synthesis, which accompanies apoptosis. Paradoxically, protein synthesis is required for apoptosis to occur in many experimental settings. Previous studies showed that two proteins that regulate apoptosis by controlling caspase activity, XIAP and Apaf-1, are translated by a unique, cap-independent mechanism mediated by an internal ribosome entry site (IRES) that is used preferentially under conditions in which normal cap-dependent translation is repressed. We investigated the regulation of XIAP and Apaf-1 following UVC irradiation. We show that UVC irradiation leads to the inhibition of translation and cell death. Furthermore, IRES-mediated translation of Apaf-1, but not XIAP, is enhanced by UVC irradiation, and this increase in Apaf-1 translation correlated with cell death. The enhanced Apaf-1 IRES-mediated translation is caspase-independent but is negatively modulated by the eIF2α kinase protein kinase RNA-like endoplasmic reticulum kinase. These data suggest that progression of UV-induced apoptosis requires IRES-mediated translation of Apaf-1 to ensure continuous levels of Apaf-1 despite an overall suppression of protein synthesis.

Normal cellular functions require complex control of cellular homeostasis, and apoptosis plays an essential role in this process. In this context, apoptosis is a cellular stress response that serves to eliminate cells that are too damaged to maintain their proper function. UV light is a common type of environmental stress that causes DNA damage and induces apoptosis in mammalian cells by engaging the mitochondrial branch of apoptotic signaling pathway (1). This pathway of apoptosis requires the release of cytochrome *c* from mitochondria into the cytoplasm, where it binds to the adaptor protein Apaf-1, triggering the formation of the apoptosome (2). Formation of the apoptosome results in the stepwise activation of caspases-9 and -3 that, in turn, cleave intracellular substrates leading to the final demise of the cell (3). The assembly of the apoptosome and autoactivation of caspase-9 represent critical events in the mitochondrial apoptotic pathway, and Apaf-1 plays a central role in this process. Conversely, XIAP,[2] the most potent member of the IAP (inhibitor of apoptosis protein) family, also associates with the apoptosome to prevent both the activation and activity of caspase-3 (4). Thus, both Apaf-1 and XIAP play critical but opposing roles in the regulation of the activity of the apoptosome.

Previous studies have underlined the importance of Apaf-1 and XIAP in regulating UV-induced apoptosis. It was shown that increased Apaf-1 protein levels correlate with increased sensitivity to UV-induced apoptosis (5–7). For example, T cells from Apaf-1 knock-out mice (5), as well as Apaf-1-deficient K562 and CEM leukemic cells (6), all exhibited increased resistance to UV-induced apoptosis. In contrast, restoration of Apaf-1 protein levels by transient transfection restored the sensitivity of leukemic cells to UV-induced apoptosis (6). On the other hand, increased XIAP protein levels conferred resistance of MCF-7 cells to UV-induced apoptosis (8).

Given the importance of Apaf-1 and XIAP proteins in the control of the cellular response to UV irradiation, it is important to understand the mechanisms involved in regulating the expression of both of these proteins. Cells generally respond to environmental stress stimuli by inhibiting global translation. In contrast, a small proportion of mRNAs containing IRES (internal ribosome entry sequence) elements within their 5′-untranslated region (UTR) are refractory to this inhibition and continue to be efficiently translated (9). UV irradiation was shown to inhibit protein synthesis by inducing phosphorylation of the translation initiation factor eIF2α by either the PERK (10) or GCN2 (11, 12) eIF2α kinases. Interestingly, both Apaf-1 and XIAP contain IRES elements within their respective 5′-UTRs and exhibit distinct modes of regulation (13, 14). However, the regulation of Apaf-1 or XIAP translation during UV irradiation-induced apoptosis has not been explored.

In the present study we investigated the regulation of Apaf-1 and XIAP expression during UV stress. We found that UV irradiation inhibits protein synthesis and triggers dose-dependent cell death in 293T cells. However, Apaf-1 protein levels are significantly enhanced following UV irradiation. This paradox is explained by the translational induction of Apaf-1 expression mediated by the Apaf-1 IRES element in response to UV irradiation, which is refractory to UV-mediated inhibition of global protein synthesis. In contrast, translation of XIAP was inhibited to the same extend as global protein synthesis. We further found that the translation of Apaf-1 is independent of the phosphorylation status of eIF2α but is modulated by the eIF2α kinase PERK both *in vitro* and *in vivo*.

* This work was supported in part by grants from the Canadian Institutes of Health Research (CIHR), Premier's Research Excellence Award, and the Canada Foundation for Innovation, Ontario Research and Development Challenge Fund. The costs of publication of this article were defrayed in part by the payment of page charges. This article must therefore be hereby marked "*advertisement*" in accordance with 18 U.S.C. Section 1734 solely to indicate this fact.

[S] The on-line version of this article (available at http://www.jbc.org) contains supplementary Fig. 1S.

[1] A CIHR New Investigator. To whom correspondence should be addressed: Apoptosis Research Center, Children's Hospital of Eastern Ontario, 401 Smyth Rd., Ottawa, Ontario K1H 8L1, Canada. Tel.: 613-738-3207; Fax: 613-738-4833; E-mail: martin@rmgcheo.med.uottawa.ca.

[2] The abbreviations used are: XIAP, inhibitor of apoptosis protein; RPA, ribonuclease protection assay; CAT, chloramphenicol acetyltransferase; IRES, internal ribosome entry site; UTR, untranslated region; PERK, protein kinase RNA-like endoplasmic reticulum kinase; GCN2, general control non-derepressible-2; z-VAD-fmk, benzyloxycarbonyl-VAD-fluoromethyl ketone; ELISA, enzyme-linked immunosorbent assay; siRNA, small interference RNA; RT, revere transcription; eIF2α, α-subunit of initiation factor 2; ER, endoplasmic reticulum; MEF, mouse embryonic fibroblast.

EXPERIMENTAL PROCEDURES

Cell Culture and Transfection Reagents—Mouse embryonic fibroblasts from PERK-null ($PERK^{-/-}$) or PERK wild-type ($PERK^{+/+}$) mice were maintained in Dulbecco's modified Eagle's medium (Wisent Inc.) supplemented with heat-inactivated 10% fetal calf serum, 2 mM L-glutamine, 1% antibiotics (100 units/ml penicillin-streptomycin), 1% essential amino acids, and 0.01% β-mercaptoethanol. Human embryonic kidney (293T) cells were maintained in standard conditions in Dulbecco's modified Eagle's medium supplemented with heat-inactivated 10% fetal calf serum, 2 mM L-glutamine, and 1% antibiotics (100 units/ml penicillin-streptomycin). Transient transfection and co-transfection were done using Lipofectamine Plus reagent (Invitrogen) according to the manufacturer's protocol. Briefly, cells were seeded at a density of 3×10^5 cells/ml in 6-well plates coated with poly-D-lysine (5 μg/ml) and were transfected 24 h later in serum-free Opti-MEM medium (Invitrogen) with 2 μg of DNA and 4 μl of lipid per well. The transfection mixture was replaced 4 h later with fresh Dulbecco's modified Eagle's medium supplemented with 10% fetal calf serum, 2 mM glutamine, and 1% antibiotics. Co-transfections of 293T cells were done as described above except that 1 μg of bicistronic plasmid was combined with 1 μg of expression vector.

Plasmids—The bicistronic vectors pβgal/hUTR/CAT (containing the human XIAP IRES) and pβgal/Apaf-1/CAT (containing the Apaf-1 IRES) were described previously (15, 16). The expression vectors for the FLAG-tagged GCN2 wild-type and the dominant-negative mutant GCN2 K → M (containing a point mutation that destroys the kinase activity of GCN2), the *myc*-tagged PERK wild-type and the *T7*-tagged PERKΔC expression vector (containing the coding sequence of the luminal domain of PERK), the *myc*-tagged IRE1b wild-type and the dominant-negative IRE1bΔC expression vector (containing the coding sequence of the luminal domain of IRE1b), and the eIF2α wild-type and eIF2α S51A mutant (containing a point mutation that prevents the phosphorylation of eIF2α) were kindly provided by Drs. R. Wek, S. Wu, and D. Ron and were previously described (10, 17).

UV Irradiation—Cells were irradiated at room temperature in fresh medium with a 30-watt UVC light source (254 nm). The intensity of UVC light was measured prior to each experiment with a UVX radiometer (UVP Inc., Upland, CA). Transfected cells were irradiated 24 h post-transfection as described above. For the z-VAD-fmk experiments the cells were pre-treated with z-VAD-fmk (100 μM) or Me_2SO for 2 h before UVC treatment and for 24 h post UVC treatment. Cell viability was determined 24 h following UVC irradiation using the Vi-Cell cell viability analyzer (Beckman Coulter).

Analysis of Global Protein Synthesis—Both control and UV-irradiated cells were labeled with [^{35}S]methionine (200 μCi/ml, Amersham Biosciences) for 1 h in methionine/cysteine-free minimal essential medium (Invitrogen) in which L-cysteine was added to a final concentration of 63 mg/liter. Cells were harvested in ice-cold phosphate-buffered saline and lysed for 20 min at 4 °C in radioimmune precipitation assay buffer (15 Nonidet P-40, 1% sodium deoxycholate, 0.1% SDS, 0.15 M NaCl, 0.01 M sodium phosphate, pH 7.2, 2 mM EDTA, 0.1 mM phenylmethylsulfonyl fluoride) containing 10 μg/ml each of aprotinin, pepstatin A, and leupeptin (all from Sigma). The lysates were then centrifuged at 14,000 × *g* for 10 min, and supernatants were collected. Protein concentration in the supernatant was determined by using a protein assay kit (Bradford Assay, Bio-Rad), and equal amounts of protein samples were separated by 10% SDS-PAGE. The total proteins were visualized by Coomassie Brilliant Blue (R-250) staining, and the ^{35}S incorporation was visualized by autoradiography.

Western Blot Analysis—Cells were harvested in ice-cold phosphate-buffered saline, and cell extracts were prepared in radioimmune precipitation assay buffer as described above. Equal amounts of protein samples were separated by 10% SDS-PAGE and analyzed by Western blotting. The antibodies used were as follows: mouse monoclonal anti-FLAG M2 (Stratagene), mouse monoclonal anti-*c*-Myc (Sigma), mouse monoclonal anti-T7 (Novagen), rabbit monoclonal anti-eIF2α (Cell Signaling Technology), rabbit monoclonal anti-phospho eIF2α (Ser-51, Cell Signaling Technology), rabbit polyclonal anti-XIAP (Ægera), mouse monoclonal anti-Actin (Sigma), rat monoclonal anti-Apaf-1 (Chemicon), rabbit polyclonal anti-CREB2/ATF4 (Santa Cruz Biotechnology), and mouse monoclonal anti-processed caspase 3 (Cell Signaling Technology). The antibodies were used at the manufacturer's suggested dilutions, and conditions were followed by secondary antibody (horseradish peroxidase-conjugated sheep anti-mouse or anti-rabbit IgG, Amersham Biosciences). Antibody complexes were detected using the ECL plus Western blotting detection system (Amersham Biosciences). If quantification of protein data was required the Western blots were performed as described above, but the secondary antibody used was Alexa Fluor 680 goat anti-mouse, anti-rat, or anti-rabbit IgG (LI-Cor Inc.). Antibody complexes were then detected and quantified using the Odyssey Infrared Imaging system (LI-Cor Inc.).

β-Galactosidase and CAT Analysis—Cells were briefly washed in ice-cold phosphate-buffered saline and harvested in the CAT ELISA kit lysis buffer (Roche Molecular Biochemicals) according to the protocol provided by the manufacturer. β-Galactosidase enzymatic activity in cell extracts was spectrophotometrically determined using *o*-nitrophenyl-β-D-galacotpyranoside (18). The CAT levels were determined using the CAT ELISA kit (Roche Molecular Biochemicals) and the protocol provided by the manufacturer. The relative IRES activity was determined as a ratio of CAT/β-galactosidase in three independent experiments performed in triplicates. All data are shown as an average ± S.D. of three independent experiments performed in triplicates.

RNA Interference—293T cells were transfected in a 6-well plate with control siRNA (CY3-labeled, U47296, Dharmacon) or with a PERK-targeting Smartpool (M-004883-01, Dharmacon) using RNAiFect (Qiagen) as per the manufacturer's instructions. The cells were replated on the next day, and the levels of PERK message were assessed by quantitative RT-PCR 72 h post-transfection. For detection of Apaf-1 IRES activity, the PERK or control siRNA transfected cells were transfected the day following siRNA transfection with the Apaf-1 bicistronic plasmid pβgal/Apaf-1/CAT. The UVC irradiation and β-galactosidase and CAT analyses were performed as described above.

Ribonuclease Protection Assay—Total RNA was isolated from UVC-treated or control cells with TRIzol reagent (Invitrogen) and treated with 1 unit of DNase I. The ^{32}P-labeled antisense RNA probes spanning 162 nucleotides of the XIAP 5′-UTR (coordinates 0 to −162), the complete Apaf-1 5′-UTR, or human glyceraldehyde-3-phosphate dehydrogenase (BD Pharmingen) were synthesized using the MaxiScript T7 transcription kit (Ambion) and gel-purified. RPA analyses were performed using the RPA III kit (Ambion) and the protocol provided by the manufacturer. Briefly, 10 μg of total RNA was hybridized overnight at 42 °C with 5×10^4 cpm of high specific activity probe and then digested with an RNase A/RNase T1 mix. The digested samples were ethanol-precipitated and separated on a denaturing polyacrylamide gel. The protected fragments were visualized by x-ray film and quantified on a Bio-Rad Model GS-670 imaging densitometer.

Quantitative RT-PCR—Total RNA was isolated from UVC-treated or control cells that were previously transfected with the pβgal/Apaf-1/CAT reporter plasmid as described above. For quantitative RT-PCR,

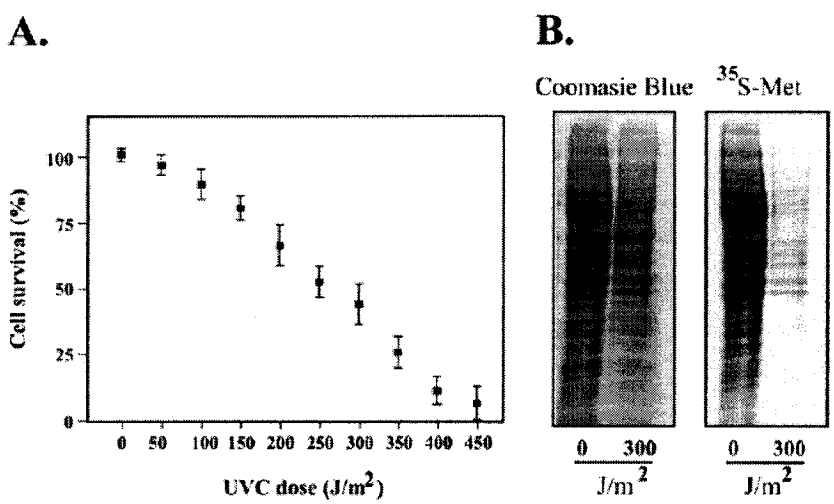

FIGURE 1. **UVC irradiation induces cell death and inhibits nascent protein synthesis.** *A*, 293T cells were treated with the indicated doses of UVC irradiation, and cell viability was determined 24 h later as described under "Experimental Procedures." Each data point represents the average ± S.D. determined from three independent experiments performed in triplicate. *B*, UVC treated or untreated 293T cells were pulse-labeled with [^{35}S]Met for 1 h, and total cell extracts (30 μg/lane) were resolved by 10% SDS-PAGE as described under "Experimental Procedures." The protein gel was then stained with Coomassie Blue R-250 to detect total proteins, followed by autoradiography to visualize newly synthesized proteins.

reverse transcription was carried out using the First-Strand cDNA Synthesis kit (Amersham Biosciences) with NotI-d(T)$_{18}$ primers. The quantitative PCR was performed using the QuantiTect SYBR green PCR kit (Qiagen) and analyzed on an ABI Prism 7000 sequence detection system using the ABI Prism 7000 SDS Software. Quantitative PCRs were carried out to detect β-galactosidase (5′-ACTATCCCGACCGCCTTACT-3′ and 5′-CTGTAGCGGCTGATGTTGAA-3′) and CAT (5′-GCGTGTTACGGTGAAAACCT-3′ and 5′-GGGCGAAGAAGTTGTCCATA-3′) as described previously (19). The primers for detection of PERK were as follows: forward, 5′-CTCACAGGCAAAGGAAGGAG-3′, and reverse, 5′-AACAACTCCAAAGCCACCAC-3′.

RESULTS

UV Irradiation Induces Cell Death and Inhibits Protein Synthesis—To investigate the regulatory mechanism of UVC-induced cell death, we first determined the sensitivity of 293T cells to UVC irradiation. Twenty-four hours after exposure to increasing doses of UVC the percentage of surviving 293T cells was determined by viable cell count using the Beckman Coulter Vi-Cell 1.01 cell viability analyzer. UVC irradiation was found to induce cell death in a dose-dependent manner, with 50% cell survival at a UVC dose of 300 J/m^2 and only 10% survival at 450 J/m^2 (Fig. 1*A*). The 300 J/m^2 dose was therefore chosen for subsequent experiments.

We next asked whether the exposure of 293T cells to UVC irradiation also inhibits protein synthesis in 293T cells as have been shown previously for other cell lines (10–12). UVC-irradiated 293T cells were metabolically labeled with [^{35}S]Met, and protein lysates were analyzed by SDS-PAGE followed by Coomassie Blue staining and autoradiography. These analyses revealed that protein synthesis was substantially reduced in the UVC-irradiated cells compared with non-irradiated 293T cells (Fig. 1*B*), confirming that UV irradiation inhibits protein synthesis in 293T cells.

Apaf-1 but Not XIAP Protein Expression Is Induced by UVC Irradiation and Is Necessary for UV-induced Cell Death—We next investigated whether UV irradiation affects the expression of Apaf-1 and XIAP, two proteins involved in the regulation of UV-mediated cell death. When compared with the corresponding expression of endogenous Apaf-1 and XIAP in non-irradiated 293T cells, the expression of Apaf-1 increased significantly in UVC-irradiated cells, whereas the expression of XIAP was slightly reduced (Fig. 2*A*). When we examined the RNA samples isolated from treated and untreated cells by RPA analysis we noted that the levels of Apaf-1 mRNA did not change in response to UVC irradiation (Fig. 2*B*). This suggests that the observed increase in Apaf-1 protein levels following UVC irradiation could be due to translational up-regulation of Apaf-1.

It has been demonstrated previously that IRES-dependent translation is preferentially employed during conditions of cellular stress (13–15, 20). Because both the Apaf-1 and XIAP mRNAs have IRES elements within their 5′-UTRs, we examined the effect of UVC irradiation on the activity of Apaf1 and XIAP IRES elements. To study IRES-mediated translation exclusively, we used the previously described bicistronic pβgal/CAT reporter plasmid that has the β-galactosidase gene and chloramphenicol acetyltransferase gene as first and second cistrons, respectively, with the IRES to be tested inserted between the two cistrons (15). In this system, expression of the second cistron (CAT) is dependent on IRES activity. Bicistronic reporter plasmids carrying either the Apaf1 IRES or the XIAP IRES were transfected into 293T cells, and IRES-dependent translation of CAT was determined 24 h after treatment with increasing doses of UVC irradiation (Fig. 2*C*). The activity of the XIAP IRES (as measured by CAT expression) was inhibited to the same extend as global protein synthesis (measured by β-galactosidase expression). In sharp contrast, the activity of the Apaf-1 IRES paralleled the increase in UVC dose, with a 5-fold increase in activity at an UVC dose of 200 J/m^2, and an 8-fold increase in activity at 450 J/m^2 (Fig. 2*C* and Table 1).

It is formally possible that the observed induction of Apaf-1 IRES activity is due to transcriptional induction, cryptic promoter activity, or spurious splicing of the bicistronic RNA transcript (βgal/Apaf-1/CAT) produced from the pβgal/Apaf-1/CAT plasmid, thus altering the ratio of CAT protein to β-galactosidase protein. We therefore determined the effect of UVC irradiation on the integrity of the βgal/Apaf-1/CAT bicistronic RNA transcript using quantitative RT-PCR as described previously (19). Total RNA was isolated 24 h post-UVC irradiation and subjected to quantitative RT-PCR of the Apaf-1 bicistronic mRNA, and this confirmed that the increase in Apaf-1 IRES activity was not due to transcriptional induction, cryptic promoter activity, or spurious splicing of the bicistronic mRNA (Fig. 2*D*).

The results presented above demonstrate that increasing doses of UVC irradiation induce Apaf-1 IRES-dependent translation that correlates with a loss of viability in 293T cells. These data are in agreement

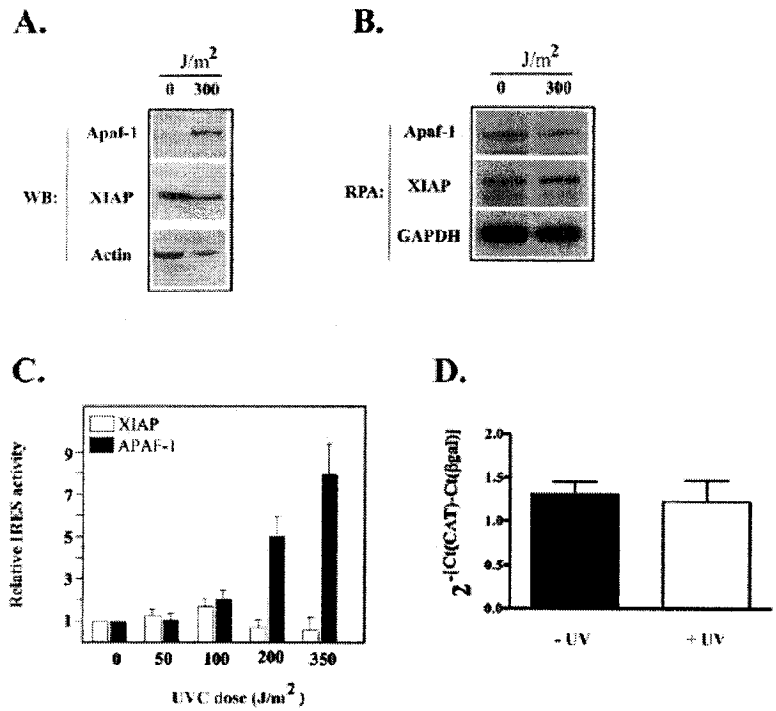

FIGURE 2. **UVC induces the expression of Apaf-1 but not XIAP via IRES-mediated translation.** *A*, 293T cells were treated with the indicated doses of UVC irradiation, total protein lysates were prepared 24 h later and resolved by 10% SDS-PAGE. Endogenous expression of Apaf-1 and XIAP proteins was determined by Western blot analyses using antibodies against Apaf-1 and XIAP, respectively. The expression of β-actin in both UVC-treated and untreated cells was used as a control. *B*, ribonuclease protein assay (RPA) of Apaf-1, XIAP, and glyceraldehyde-3-phosphate dehydrogenase mRNAs in treated and untreated cells (same as *A*). *C*, 293T cells were transiently transfected with the XIAP or Apaf-1 IRES bicistronic reporter constructs and the effect of UVC irradiation on XIAP (*white bars*) and Apaf-1 IRES (*black bars*) translation were determined 24 h later by measuring the β-galactosidase and CAT activities as described under "Experimental Procedures." The relative IRES activity in non-irradiated cells was set as 1 for each construct. The *bars* represent the average ± S.D. determined from three independent experiments performed in triplicates. *D*, quantitative RT-PCR was performed on DNase I-treated total RNA isolated from 293T cells transfected with Apaf-1 IRES bicistronic plasmids. The RNA was isolated and reverse transcribed as described under "Experimental Procedures." The quantitative real-time RT-PCR was performed using the QuantiTect SYBR green RT-PCR kit (Qiagen) and analyzed on an ABI Prism 7000 sequence detection system using the ABI Prism 7000 SDS Software. Quantitative PCR reactions were carried out to detect the β-galactosidase and CAT cistrons of the bicistronic mRNA. The CAT/β-galactosidase ratio was calculated as $2^{-[Ct(CAT)-Ct(\beta gal)]}$. The *bars* represent the mean ± S.E. of three experiments.

TABLE 1

UVC irradiation enhances Apaf-1 IRES-mediated translation but not cap-dependent or XIAP IRES-dependent translation

Construct[a]	β-Galactosidase[b]	CAT[b]	Relative IRES activity[c]
Apaf-1 (0 J/m²)	0.184 (±0.031)	0.213 (±0.049)	1.157
Apaf-1 (450 J/m²)	0.105 (±0.023)	1.021 (±0.093)	9.724
XIAP (0 J/m²)	0.210 (±0.038)	2.173 (±0.098)	10.347
XIAP (450 J/m²)	0.098 (±0.029)	0.638 (±0.078)	6.518

[a] Cells were transfected with the indicated plasmids and exposed to 0 or 450 J/m² UVC 24 h post-transfection as described under "Experimental Procedures."
[b] β-Galactosidase (cap-dependent) and CAT (IRES-dependent) levels were determined 24 h post-UV irradiation as described under "Experimental Procedures" and are shown per 1 μg of total protein.
[c] Relative IRES activity was determined as CAT/β-galactosidase.

with previously published findings that repression of Apaf-1 expression using small interfering RNA (siRNA) to Apaf-1 (21), or by deletion of the Apaf-1 gene (5–7) resulted in the suppression of UV-induced apoptosis. Conversely, restoration of Apaf-1 protein levels resensitized cells to UV-induced apoptosis (6). Taken together, these data suggest that continued translation of Apaf-1 afforded by the Apaf-1 IRES element is required for cell death induced by UVC irradiation.

UVC-mediated Induction of Apaf-1 Is Caspase-independent—We previously demonstrated that the activation of caspases is required for the stimulation of Apaf1 IRES activity in etoposide-treated cells (13). To determine if Apaf-1 IRES activity is regulated by the same mechanism during UVC-induced cellular stress, 293T cells were transfected with either the Apaf-1 IRES or XIAP IRES bicistronic plasmids, treated with the broad-range caspase inhibitor z-VAD-fmk, and then irradiated. As shown in Fig. 3*A*, pre-treatment of cells with z-VAD-fmk had no effect on the induction of Apaf1 IRES activity following UVC irradiation, although it was sufficient to inhibit caspase-3 cleavage (Fig. 3*B*). These data suggest that the induction of Apaf-1 IRES activity by UVC irradiation is caspase-independent.

UVC-mediated Induction of Apaf-1 Is Independent of eIF2α Phosphorylation Status, but Is Modulated by PERK—Previous studies have shown that diverse cellular stresses can stimulate the IRES-mediated translation of some mRNAs via a mechanism that requires transient phosphorylation of the α-subunit of initiation factor 2 (eIF2α) (22). Recently, two distinct eIF2α kinases, GCN2 and PERK, were implicated in the phosphorylation of eIF2α and the consequent inhibition of protein synthesis during UVC irradiation (10–12). We therefore investigated whether GCN2, PERK, or phosphorylation of eIF2α are involved in the modulation of Apaf-1 IRES activity by UVC irradiation. To test the requirement for GCN2, 293T cells were co-transfected with each of the bicistronic constructs containing the XIAP IRES and Apaf-1 IRES and one of the following expression vectors: pCI, FLAG-GCN2, or FLAG-GCN2K→M, a catalytically inactive dominant-negative GCN2 mutant. The expression of GCN2 or GCN2K→M had the expected effect on the phosphorylation status of eIF2α (Fig. 4*A*). The relative IRES activities of

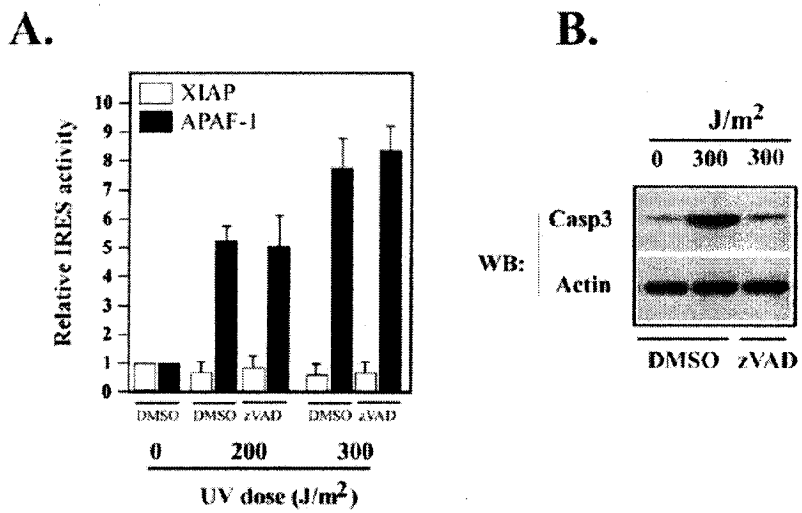

FIGURE 3. **UVC-mediated induction of Apaf-1 IRES activity is independent of caspase activation.** *A*, 293T cells were transiently transfected with either Apaf-1 IRES or XIAP IRES containing bicistronic plasmids. 24 h following transfection the cells were pre-treated with z-VAD-fmk (100 μM) for 2 h and then exposed to the indicated doses of UVC irradiation. Cell lysates were prepared 24 h post irradiation as described under "Experimental Procedures," and the IRES activity was determined. The relative IRES activity in the non-irradiated cells was set as 1 for each IRES. The *bars* represent the average ± S.D. determined from three independent experiments performed in triplicates. *B*, the activity of z-VAD-fmk was verified by Western blot analysis using antibodies against cleaved caspase-3.

XIAP and Apaf-1 IRESs were then determined in both UVC-treated and untreated cells. XIAP IRES activity did not change in response to UVC irradiation regardless of the GCN2 expression vector used (Fig. 4*B*). Similarly, 293T cells co-transfected with the Apaf-1 bicistronic plasmid and either of the GCN2 expression plasmids did not exhibit any changes in Apaf-1 IRES activity following UVC irradiation (Fig. 4*B*). These results indicate that UVC-induced Apaf-1 IRES activity is independent of GCN2 activity.

To determine whether PERK plays a role in Apaf-1 IRES activity following UVC irradiation, 293T cells were co-transfected with each of the bicistronic constructs containing the XIAP IRES and Apaf-1 IRES and one of the following vectors: pCI, *myc*-PERK, or T7-PERKΔC, a catalytically inactive dominant-negative PERK mutant. Again, the expression of PERK or PERKΔC had the expected effect on the phosphorylation status of eIF2α (Fig. 4*C*). Twenty-four hours post-transfection, cells were UVC-irradiated. We observed that XIAP IRES activity was not affected by the overexpression of either PERK or its inactive mutant, PERKΔC, in UVC-irradiated 293T cells (Fig. 4*D*). In contrast, overexpression of the dominant negative PERKΔC mutant resulted in a significant increase in the UVC-mediated induction of Apaf-1 IRES activity when compared with the control vector (Fig. 4*D*). We determined the effect of PERKΔC overexpression on the integrity of the βgal/Apaf-1/CAT bicistronic RNA transcript using quantitative RT-PCR. Total RNA was isolated 24 h post-UVC irradiation and subjected to quantitative RT-PCR. As shown in Fig. 4*E*, the ratio of CAT and β-galactosidase transcripts was unchanged in PERKΔC-transfected cells treated with UVC as compared with non-irradiated cells. These data confirm that the integrity of the bicistronic RNA transcript produced from the pβgal/Apaf-1/CAT reporter plasmid is not affected by PERKΔC overexpression, and therefore spurious splicing did not contribute to the apparent Apaf-1 IRES activity.

It is possible that overexpression of the PERK dominant-negative mutant PERKΔC has an inadvertent effect on IRE1, another ER-resident- and ER-stress-activated protein, which results in the observed changes in Apaf-1 IRES activity. Although this notion is unlikely, we nevertheless wanted to test this possibility. Thus, 293T cells were co-transfected with the bicistronic constructs containing the Apaf-1 IRES and one of the following expression vectors: pCI, myc-IRE1b, or myc-IRE1bΔC, a dominant negative IRE1b mutant. The overexpression of IRE1b or IRE1bΔC had no effect on the Apaf-1 IRES activity following UVC irradiation (supplementary Fig. 1S). These results indicate that the effect of PERKΔC on UVC-induced Apaf-1 IRES activity is not mediated through inadvertent inhibition of IRE1b.

Because activation of both GCN2 and PERK results in the phosphorylation of eIF2α, one possible mechanism explaining how PERKΔC could modulate Apaf-1 IRES activity is via the phosphorylation of eIF2α. To directly test this hypothesis, 293T cells were co-transfected with the Apaf-1 IRES or XIAP IRES bicistronic plasmids and a plasmid expressing either eIF2α or eIF2αS51A, a non-phosphorylatable mutant of eIF2α. We observed that overexpression of either eIF2α or eIF2αS51A did not alter the Apaf-1 IRES activity following UVC irradiation (Fig. 5*A*), although the levels of eIF2α phosphorylation were significantly higher in eIF2α- than in eIF2αS51A-transfected cells (Fig. 5*B*).

Taken together, these results suggest that the induction of Apaf-1 IRES activity by UVC irradiation is independent of the phosphorylation status of eIF2α. Furthermore, the expression of the dominant-negative catalytically inactive mutant of PERK increases the activity of the Apaf-1 IRES following UV stress, suggesting that PERK may function as a negative regulator of Apaf-1 IRES-mediated translation.

To further verify the notion that PERK plays a role in Apaf-1 IRES activity we utilized siRNA-mediated knock-down of PERK. 293T cells were transfected either with control or PERK-targeting siRNA and the efficiency of knock-down was determined in transfected cells by quantitative RT-PCR to be ~90% (Fig. 6*A*). To functionally confirm that PERK levels were lowered sufficiently, control or PERK siRNA-transfected cells were exposed to thapsigargin (1 μM), an inducer of ER stress, for 2 h, and the levels of ATF4 were determined by Western blot analysis (Fig. 6*B*). ATF4/CREB2 is a transcription factor that is translationally induced in a PERK-dependent manner in response to ER stress (23). Indeed, upon PERK depletion, we observed a significant reduction in ATF4 in thapsigargin-treated cells, thus confirming our ability to sufficiently reduce PERK levels. To determine the effect of PERK knock-down on Apaf-1 IRES activity we transfected the control or PERK siRNA-transfected cells with the Apaf-1 IRES bicistronic reporter plasmid and exposed the cells to UVC irradiation. We observed that in PERK siRNA-transfected cells the activity of Apaf-1 IRES was significantly enhanced in response to UVC (Fig. 6*C*). However, the extent of Apaf-1 IRES activation was not as great as that observed with PERKΔC co-expression. This is likely due to the fact that we were only able to

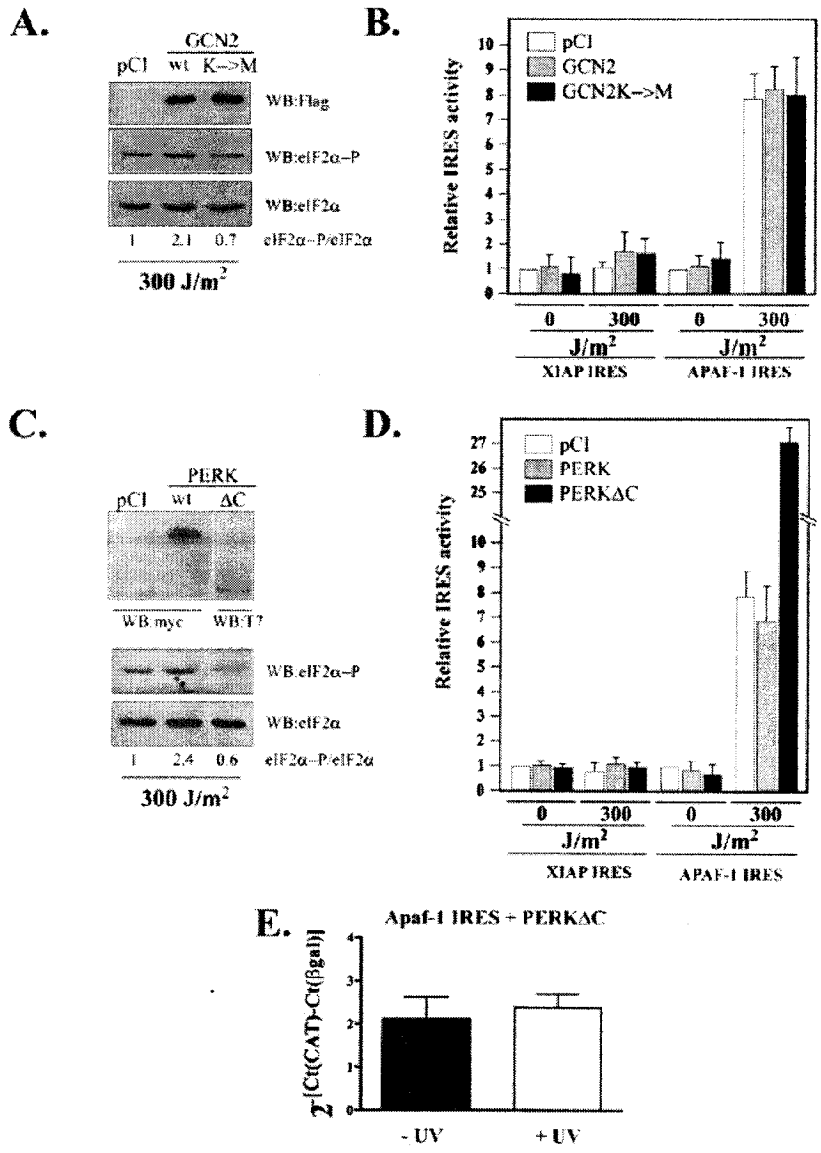

FIGURE 4. **PERK kinase but not GCN2 kinase regulates UVC-mediated induction of Apaf-1 IRES activity.** *A*, 293T cells were co-transfected with either Apaf1 or XIAP IRES-containing bicistronic plasmids and FLAG-GCN2 or FLAG-GCN2K→M expressing vector, and the expression levels of FLAG-GCN2 and FLAG- GCN2K→M proteins were determined by Western blot analysis using the anti-FLAG antibodies. The levels of eIF2α phosphorylation were determined in UVC-irradiated cells (300 J/m²) using the anti-eIF2α and anti-phospho-eIF2α antibodies, respectively, 3 h post-UVC irradiation. The levels of eIF2α and phosphorylated eIF2α were determined using LI-COR Odyssey (version 1.1), and the ratio of eIF2α-P/eIF2α is shown *below* the blot. *B*, co-transfected cells (as in *A*) were irradiated with 300 J/m² UVC 24 h post-transfection, and the relative IRES activity was determined 24 h after UVC irradiation for each IRES as described under "Experimental Procedures." The IRES activity in pCI-transfected, non-irradiated cells was set as 1. The *bars* represent the average ± S.D. of three independent experiments performed in triplicates. *C*, 293T cells were co-transfected with either Apaf1 or XIAP IRES-containing bicistronic plasmids and myc-PERK- or T7-PERKΔC-expressing vector. Expression levels of myc-PERK and T7-PERKΔC proteins were determined by Western blot analysis using the anti-myc or anti-T7 antibodies. The levels of eIF2α phosphorylation were determined in UVC-irradiated cells (300 J/m², as in *A*). *D*, co-transfected cells (as in *C*) were irradiated with 300 J/m² UVC 24 h post-transfection and the relative IRES activity was determined 24 h after UVC irradiation for each IRES as described under "Experimental Procedures." The IRES activity in pCI transfected, non-irradiated cells was set as 1. The *bars* represent the average ± S.D. of three independent experiments performed in triplicates. *E*, quantitative RT-PCR was performed on DNase I-treated total RNA isolated from 293T cells co-transfected with Apaf-1 IRES bicistronic plasmid and T7-PERKΔC-expressing vector. The RNA was isolated and reverse transcribed as described under "Experimental Procedures." The quantitative real-time RT-PCR was performed using the QuantiTect SYBR green RT-PCR kit (Qiagen) and analyzed on an ABI Prism 7000 sequence detection system using the ABI Prism 7000 SDS software. Quantitative PCR reactions were carried out to detect the β-galactosidase and CAT cistrons of the bicistronic mRNA. The CAT/β-galactosidase ratio was calculated as $2^{-[Ct(CAT)-Ct(\beta gal)]}$. The *bars* represent the mean ± S.E. of three experiments.

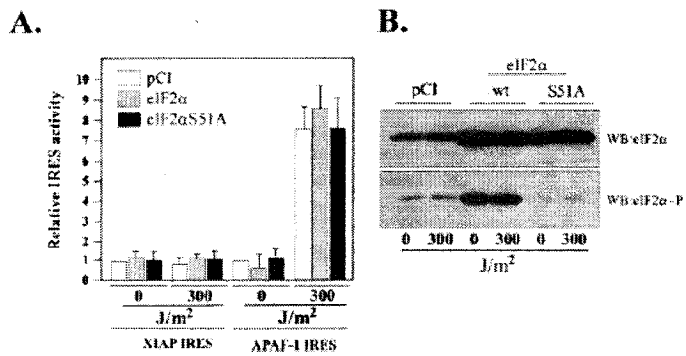

FIGURE 5. **UVC-mediated induction of Apaf-1 IRES activity is independent of the phosphorylation of eIF2α.** *A*, 293T cells were co-transfected with either Apaf-1 or XIAP IRES-containing bicistronic plasmids and eIF2α- or eIF2αS51A-expressing vector. Cells were irradiated with 300 J/m² UVC 24 h post-transfection, and the relative IRES activity was determined 24 h after UVC irradiation for each IRES as described under "Experimental Procedures." The IRES activity in pCI-transfected, non-irradiated cells was set as 1. The *bars* represent the average ± S.D. of three independent experiments performed in triplicates. *B*, expression levels of eIF2α and eIF2αS51A proteins and their level of phosphorylation were determined by Western blot analysis using the anti-eIF2α and anti-phospho-eIF2α antibodies.

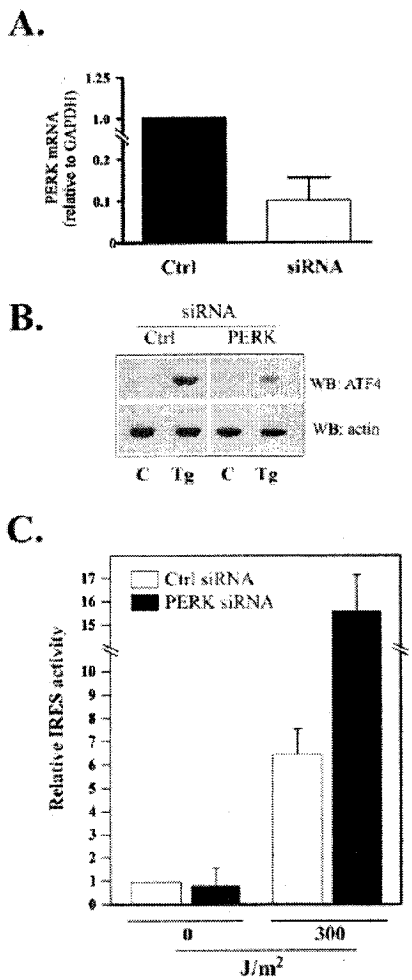

FIGURE 6. **PERK kinase regulates UVC-mediated induction of Apaf-1 IRES activity.** *A*, the levels of PERK mRNA (relative to glyceraldehyde-3-phosphate dehydrogenase (*GAPDH*)) in 293T cells transiently transfected with control or PERK-targeting siRNAs were determined by quantitative RT-PCR analysis. The relative expression of PERK in control siRNA-transfected cells was set as 1. The *bars* represent the average ± S.D. of two independent experiments analyzed in triplicates. *B*, the functional consequence of PERK down-regulation was verified by determining the levels of ATF4 in control and PERK siRNA-treated cells exposed to thapsigargin (*Tg*, 1 μM) or Me_2SO control. Actin was used as a control of equal loading. *C*, 293T cells were transfected with control or PERK siRNAs and re-transfected with Apaf1 IRES-containing bicistronic plasmid 24 h later. Cells were irradiated with 300 J/m^2 UVC 24 h after a second transfection, and the relative IRES activity was determined 24 h after UVC irradiation as described under "Experimental Procedures." The IRES activity in control siRNA-transfected, non-irradiated cells was set as 1. The *bars* represent the average ± S.D. of two independent experiments performed in triplicates.

reduce PERK levels by ~90%, and the remaining PERK may be sufficient to negatively regulate Apaf-1 IRES activity to some degree. In contrast, overexpression of the PERKΔC dominant-negative mutant likely inhibits nearly all endogenous PERK. Nevertheless, these data strongly suggest that PERK may function as a negative regulator of Apaf-1 IRES-mediated translation.

PERK-null Cells Exhibit Increased Levels of Apaf-1 and Enhanced Sensitivity to UVC—To examine the *in vivo* role of PERK in Apaf-1 IRES-mediated translation following UVC irradiation, we compared the expression of Apaf-1 in mouse embryonic fibroblasts (MEFs) deleted for PERK (PERK$^{-/-}$) to the corresponding level of Apaf-1 expression in normal MEF cells (PERK$^{+/+}$). Western blot analysis revealed that the basal level of Apaf-1 in PERK$^{-/-}$ cells is 3- to 4-fold higher than the level of Apaf-1 expression in PERK$^{+/+}$ cells (Fig. 7*A*). Similarly, the induction of the Apaf-1 expression following exposure to UVC irradiation was greatly enhanced in the PERK$^{-/-}$ cells (Fig. 7*A*). Moreover, the increased level of Apaf-1 protein in the PERK$^{-/-}$ cells correlated with enhanced sensitivity of the PERK-null cells to UVC irradiation (Fig. 7*B*). These findings suggest that PERK might function as a negative regulator of Apaf-1 translation *in vivo*, and thus a negative regulator of Apaf-1 mediated cell death following UVC irradiation.

DISCUSSION

To gain insight into the control of UVC-induced cell death, the present study aimed to investigate the mechanisms that regulate expression of two proteins involved in the control of apoptosis, the anti-apoptotic protein XIAP, and the pro-apoptotic protein Apaf-1. Importantly, XIAP and Apaf-1 play opposing roles in the regulation of apoptosis. Whereas Apaf-1 is essential for the formation of the apoptosome and consequent activation of the caspase cascade, XIAP is a potent intrinsic inhibitor of caspases (19, 23). In addition, both Apaf-1 and XIAP are found associated with the apoptosome (4), suggesting that their coordinated function is required for the fine tuning of the apoptotic response. To date, many studies have been conducted to determine the involvement of the XIAP and Apaf-1 proteins in cell survival regulation during UV-induced cellular stress. It was demonstrated that an increase in XIAP protein levels parallels a decrease in sensitivity to UV-induced apoptosis (8). Moreover, overexpression of XIAP inhibited UV-induced cell death in MCF-7 cells (8). Similarly, the levels of XIAP protein decreased in keratinocytes exposed to increasing doses of UVB irradiation (24). Conversely, it was shown that an increase in Apaf-1 protein levels parallels an increase in sensitivity to UV-induced apoptosis (5–7, 21). Lassus *et al.* (21) showed that repression of Apaf-1 expression using siRNA to Apaf-1 resulted in the prevention of UV-induced apoptosis in IMR90E1A cells. Furthermore, T cells from Apaf-1 knock-out mice (5), as well as the Apaf-1-deficient K562 and CEM leukemic cell lines (6, 7), all exhibited increased resistance to UV-induced apoptosis. Restoration of Apaf-1 protein levels by transient transfection of the Apaf-1-deficient leukemic cells with an Apaf-1 plasmid resensitized these cells to UV-induced apoptosis (6). Taken together, these findings provide substantial evidence for the importance of the antagonistic roles of XIAP and Apaf-1 proteins in regulating UV-induced apoptosis.

The regulation of XIAP and Apaf-1 expression during UV-induced cellular stress, however, has not been investigated. Interestingly, both XIAP and Apaf-1 mRNAs are translated by a cap-independent mechanism facilitated by IRES elements located in their respective 5′-UTRs. It emerged recently that the IRES mechanism is utilized preferentially during conditions when normal cap-dependent translation initiation is compromised (9, 25, 26). These conditions include diverse cellular stress, differentiation, mitosis, and apoptosis. In fact, while only a small fraction of cellular mRNAs contain IRES elements in their respective 5′-UTRs, the majority of these elements are found in genes involved in the control of cell growth, proliferation, and survival (9, 25–27).

UV radiation inhibits nascent protein synthesis (10–12). Paradoxically, protein synthesis is required for UVC-induced cell death in 293T cells, because treatment of cells with the protein synthesis inhibitor cycloheximide significantly protects cells from UVC-induced death (data not shown). We and others have shown previously that IRES-mediated translation escapes the control mechanisms that regulate cap-dependent translation during cellular stress (13, 14, 20, 22, 28, 29). We

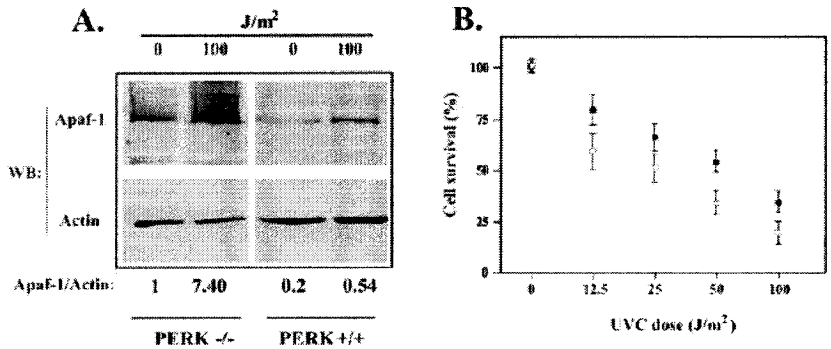

FIGURE 7. **PERK-null mouse embryonic fibroblasts have increased levels of Apaf-1 and are more sensitive to UV irradiation.** *A*, the expression of Apaf-1 in MEFs deleted for PERK (*PERK*$^{-/-}$), compared with its expression in normal MEF cells (*PERK*$^{+/+}$) was determined by Western blot analysis in both UVC-irradiated and control cells using anti-Apaf-1 monoclonal antibodies. The amount of Apaf-1 relative to actin is shown below the blot. The relative expression of Apaf-1 in PERK$^{+/+}$ non-irradiated cells was set as 1. A representative blot is shown. *B*, MEF PERK$^{+/+}$ (*black squares*) and MEF PERK$^{-/-}$ (*white squares*) cells were treated with indicated doses of UVC irradiation, and the cell viability was determined 24 h later as described under "Material and Methods." Each *point* represents the average ± S.D. determined from three independent experiments performed in triplicates.

have also demonstrated that IRES-mediated translation of pro-survival proteins is activated during transient stress conditions, whereas IRES-mediated translation of pro-death proteins is activated during severe apoptotic conditions (13). Thus, we hypothesized that low dose (sublethal) UVC irradiation would result in an increase in XIAP IRES activity, whereas high dose (lethal) UVC irradiation would be accompanied by an increase in Apaf-1 IRES-mediated translation. Contrary to what we expected, exposure to various doses of UVC did not result in significant changes in XIAP IRES activity or XIAP protein levels. However, we observed that increasing doses of UVC irradiation resulted in an increase in Apaf-1 IRES activity, paralleled by an increase of the endogenous Apaf-1 protein. This increase in Apaf-1 protein synthesis was observed despite the general cessation of protein synthesis evoked by UVC irradiation. Thus, during UV stress, Apaf-1 IRES activity and the corresponding increase in Apaf-1 protein levels is required for cell death. Our finding that increasing doses of UVC irradiation do not affect XIAP IRES activity, but significantly increase the activity of the Apaf-1 IRES, points to the distinct regulation of IRES-mediated translation during cellular stress, which we previously suggested (13, 30).

We have previously demonstrated the activation of Apaf-1 IRES activity during etoposide-induced cell death (13). We further showed that Apaf-1 IRES activation is caspase-dependent and is mediated by the caspase-cleaved fragments of the eIF4G translation initiation factor family members eIF4GI and p97/DAP5/NAT1 (13). Surprisingly, the UVC-mediated induction of Apaf-1 IRES activity does not appear to be caspase-dependent, because z-VAD-fmk treatment of cells prior to UVC irradiation did not affect Apaf-1 IRES-mediated translation. This suggests that cells may have evolved distinct regulatory pathways to regulate expression of apoptotic proteins in response to divergent physiological stresses.

It has been demonstrated that some, but not all, IRES elements are regulated by the phosphorylation of the eukaryotic initiation factor eIF2α (22, 31). Because eIF2α is phosphorylated in response to UV stress (10–12), we investigated the involvement of eIF2α in UVC-induced Apaf-1 IRES activity. The phosphorylation of eIF2α is important for the control of cap-dependent translation, because an increase in phosphorylation of eIF2α attenuates formation of the ternary complex, resulting in a reduction in global protein synthesis rates (32). The phosphorylation of eIF2α during UV stress is facilitated by two eIF2α kinases, GCN2 (11) and PERK (10). Our results indicate that eIF2α phosphorylation is not required for UVC-mediated induction of Apaf-1 IRES activity, because the overexpression of the wild-type or the non-phosphorylatable mutant of eIF2α did not affect Apaf-1 IRES activity following irradiation. Furthermore, activation of the GCN2 kinase is also not required, because the overexpression of a wild-type or a catalytically inactive dominant-negative mutant GCN2 did not affect Apaf-1 IRES activity following UV irradiation. Surprisingly, however, although Apaf-1 IRES activity following UV irradiation was not affected by the overexpression of the PERK kinase, Apaf-1 IRES activity was considerably increased by the overexpression of the PERK dominant-negative catalytically inactive mutant PERKΔC or in cells with depleted PERK levels. The involvement of PERK in the regulation of Apaf-1 expression was further confirmed in PERK-null MEFs that exhibit increased levels of Apaf-1 and display enhanced susceptibility to UVC-mediated death.

Our findings support the hypothesis that there exists specific regulatory mechanisms that control translation of distinct IRES elements in response to cellular stress (9, 13, 22, 30). In addition, we provide the first evidence that enhanced Apaf-1 IRES-mediated translation assures the continued expression of the Apaf-1 protein during UV stress. This increase in Apaf-1 IRES activity is required for cell death following UVC irradiation. Although the exact molecular mechanism that induces Apaf-1 IRES-mediated translation following UVC irradiation needs to be further investigated, we show that Apaf-1 IRES activity is negatively regulated by the PERK kinase. PERK is the primary kinase involved signal transduction during endoplasmic reticulum stress and unfolded protein response (33). In this context, the regulation of Apaf-1 during endoplasmic stress and endoplasmic stress-induced apoptosis warrants further examination.

Acknowledgments—We thank the members of our laboratory for useful discussion. We are grateful to Drs. David Ron and Shiyong Wu for the gifts of GCN2, GCN2K-M, PERK, PERKΔC, IRE1b, IRE1bΔC, eIF2α, and eIF2αS51A expression vectors.

REFERENCES

1. Bossy-Wetzel, E., Newmeyer, D. D., and Green, D. R. (1998) *EMBO J.* 17, 37–49
2. Zou, H., Li, Y., Liu, X., and Wang, X. (1999) *J. Biol. Chem.* 274, 11549–11556
3. Adams, J. M., and Cory, S. (2002) *Curr. Opin. Cell Biol.* 14, 715–720
4. Bratton, S. B., Walker, G., Srinivasula, S. M., Sun, X. M., Butterworth, M., Alnemri, E. S., and Cohen, G. M. (2001) *EMBO J.* 20, 998–1009
5. Yoshida, H., Kong, Y. Y., Yoshida, R., Elia, A. J., Hakem, A., Hakem, R., Penninger, J. M., and Mak, T. W. (1998) *Cell* 94, 739–750
6. Jia, L., Srinivasula, S. M., Liu, F. T., Newland, A. C., Fernandes-Alnemri, T., Alnemri, E. S., and Kelsey, S. M. (2001) *Blood* 98, 414–421
7. Fu, W. N., Bertoni, F., Kelsey, S. M., McElwaine, S. M., Cotter, F. E., Newland, A. C., and Jia, L. (2003) *Oncogene* 22, 451–455
8. Srinivasula, S. M., Ahmad, M., Fernandes-Alnemri, T., and Alnemri, E. S. (1998) *Mol. Cell* 1, 949–957
9. Holcik, M., Sonenberg, N., and Korneluk, R. G. (2000) *Trends Genet.* 16, 469–473
10. Wu, S., Hu, Y., Wang, J.-L., Chatterjee, M., Shi, Y., and Kaufman, R. J. (2002) *J. Biol. Chem.* 277, 18077–18083
11. Deng, J., Harding, H. P., Raught, B., Gingras, A. C., Berlanga, J. J., Scheuner, D., Kaufman, R. J., Ron, D., and Sonenberg, N. (2002) *Curr. Biol.* 12, 1279–1286
12. Jiang, H. Y., and Wek, R. C. (2005) *Biochem. J.* 385, 371–380

13. Nevins, T. A., Harder, Z. M., Korneluk, R. G., and Holcik, M. (2003) *J. Biol. Chem.* **278**, 3572–3579
14. Henis-Korenblit, S., Shani, G., Sines, T., Marash, L., Shohat, G., and Kimchi, A. (2002) *Proc. Natl. Acad. Sci. U. S. A.* **99**, 5400–5405
15. Holcik, M., Lefebvre, C. A., Yeh, C., Chow, T., and Korneluk, R. G. (1999) *Nat. Cell Biol.* **1**, 190–192
16. Holcik, M., Gordon, B. W., and Korneluk, R. G. (2003) *Mol. Cell. Biol.* **23**, 280–288
17. Fernandez, J., Bode, B., Koromilas, A., Diehl, J. A., Krukovets, I., Snider, M. D., and Hatzoglou, M. (2002) *J. Biol. Chem.* **277**, 11780–11787
18. MacGregor, G. R., Nolan, G. P., Fiering, S., Roederer, M., and Herzenberg, L. A. (1991) in *Methods in Molecular Biology* (Murray, E. J., and Walker, J. M., eds) pp. 217–235, Humana Press Inc., Clifton, NJ
19. Holcik, M., Graber, T., Lewis, S. M., Lefebvre, C. A., Lacasse, E., and Baird, S. (2005) *RNA* **11**, 1605–1609
20. Warnakulasuriyarachchi, D., Cerquozzi, S., Cheung, H. H., and Holcik, M. (2004) *J. Biol. Chem.* **279**, 17148–17157
21. Lassus, P., Opitz-Araya, X., and Lazebnik, Y. (2002) *Science* **297**, 1352–1354
22. Fernandez, J., Yaman, I., Sarnow, P., Snider, M. D., and Hatzoglou, M. (2002) *J. Biol. Chem.* **277**, 19198–19205
23. Holcik, M., and Korneluk, R. G. (2001) *Nat. Rev. Mol. Cell Biol.* **2**, 550–556
24. Takasawa, R., and Tanuma, S. (2003) *Apoptosis* **8**, 291–299
25. Holcik, M., and Sonenberg, N. (2005) *Nat. Rev. Mol. Cell Biol.* **6**, 318–327
26. Hellen, C. U., and Sarnow, P. (2001) *Genes Dev.* **15**, 1593–1612
27. Holcik, M. (2004) *Curr. Cancer Drug Targets* **4**, 299–311
28. Fernandez, J., Lopez, A. B., Wang, C., Mishra, R., Zhou, L., Yaman, I., Snider, M. D., and Hatzolgou, M. (2003) *J. Biol. Chem.* **278**, 50000–50009
29. Fernandez, I., Yaman, I., Mishra, R., Merrick, W. C., Snider, M. D., Lamers, W. H., and Hatzoglou, M. (2001) *J. Biol. Chem.* **276**, 12285–12291
30. Lewis, S. M., and Holcik, M. (2005) *Cell Death Differ.* **12**, 547–553
31. Gerlitz, G., Jagus, R., and Elroy-Stein, O. (2002) *Eur. J. Biochem.* **269**, 2810–2819
32. Hinnebusch, A. G. (2000) in *Translation Control of Gene Expression*, 2nd Ed. (Sonenberg, N., Hershey, J. W. B., and Mathews, M. B., eds) pp. 185–243, Cold Spring Harbor Laboratory Press, Cold Spring Harbor, NY
33. Harding, H. P., Zhang, Y., and Ron, D. (1999) *Nature* **397**, 271–274

4. DISCUSSION

It is generally accepted that tumor hypoxia is an impediment to current anti-cancer therapy due in large part to the ability of malignancies to adapt and survive in unfavorable tumor microenvironments. The aim of this thesis was to identify cellular pathways that mediate the development of hypoxia tolerance using microarray analysis of polysome-associated mRNAs following hypoxic stress. In response to hypoxic stress, a rapid, sustained, and reversible inhibition of protein synthesis, among other energy conserving strategies, is observed. This process is mediated at least in part due to the phosphorylation of eIF2α by the ER resident kinase, PERK. Despite the severe inhibition in translation, a small fraction of mRNAs continue to be translated. We hypothesized that amongst these mRNAs, a subset of transcripts required for cellular adaptation and continued cell viability would be preferentially translated during hypoxic stress. The strategy to assess polysome-associated mRNAs by microarray, instead of total cellular mRNAs, facilitated the discovery of genes that are translationally regulated in response to hypoxia instead of relying on steady state changes in total mRNA expression, which may or may not correlate with an increase in their efficiencies of translation. A genome wide assessment of the effects of hypoxia on translational control has permitted several main discoveries.

i) Polysome analysis of HeLa cells following prolonged exposure (16h) to severe hypoxic stress, revealed the PERK-dependent preferential translation of an important mediator of the ISR, ATF4. Combined with our findings that numerous genes involved in the UPR demonstrated transcriptional and translational induction during stress, suggests that hypoxia might signal through the ER resulting in the induction of genes necessary for the adaptive response to stress.

ii) Inactivation of the ISR in cells results in their increased sensitivity to hypoxic stress both *in vitro* and *in vivo*, supporting our findings that translational regulation of important ISR genes is required for the development of hypoxia tolerance. Moreover, tumors derived from mutant cell lines incapable of activating the ISR, are smaller, display increased apoptosis, and appear less vascularized, than tumors derived from wildtype cells.

iii) Microarray analysis of polysome-associated mRNAs in $PERK^{+/+}$ and $PERK^{-/-}$ MEFs in response to acute (4hr) hypoxic stress implicate PERK in the translational regulation of a cohort of pro-angiogenic genes including VCIP, an integrin binding protein that promotes cellular adhesion. This finding was supported by observations made in a mouse model of angiogenesis that the microenvironment provided by $PERK^{-/-}$ transformed MEFs results in fewer functional blood vessels and an increase in the number of aberrant malformed vessels, due perhaps, to abortive angiogenic signals.

iv) VCIP and Tie2, two pro-angiogenic genes that demonstrate preferential translation in response to hypoxic stress, contain active IRES elements within their 5'UTRs. Translational regulation of VCIP appears to be positively regulated by PERK as $PERK^{-/-}$ MEFs fail to mobilize VCIP mRNAs into the polysomes upon hypoxic stress. Interestingly, PERK negatively regulates the IRES activity of pro-apoptotic APAF-1 in response to UV-induced cell death, suggesting that phosphorylation of eIF2α and global attenuation of translation initiation may represent only one of PERK's known roles in the cellular response to stress. Future studies will be required to fully elucidate PERK's role in the regulation of IRES mediated translational regulation.

Despite our improved understanding of the importance of translational regulation to the cellular response to hypoxic stress, numerous questions remain. These unresolved subjects and the direction of future research in the field of tumor hypoxia are discussed.

4.1 The Biological Response to Hypoxic Stress

4.1.1 Apoptosis

Exposure of cells to hypoxic stress results in a rapid and sustained inhibition in protein synthesis that is regulated in part through the phosphorylation of eIF2α by the ER resident kinase, PERK [115]. Translational inhibition in response to hypoxia is fully reversible upon reoxygenation and appears to be independent of HIF1 function as $HIF1^{-/-}$ MEFs demonstrate comparable levels of eIF2α phosphorylation in response to hypoxic stress [115]. Phosphorylation of eIF2α and the resulting translational attenuation leads to the paradoxical translational induction of ATF4, an important mediator of the ISR [91]. ATF4 transcriptionally activates genes that help to attenuate the ISR (GADD34 and BiP) [91, 96] and in the event of uncontrolled cellular stress, cell death pathways are activated in part through the ATF4-dependent transcriptional activation of CHOP/Gadd153 [91, 108]. Although the apoptotic response to hypoxic stress has not been fully elucidated, cells experiencing prolonged periods of ER stress undergo programmed cell death initiated from the ER. Cells with a compromised UPR are substantially more sensitive to ER stress, presumable due to the continued accumulation of misfolded proteins, a process termed "proteotoxicity" [88, 116]. The exact apoptotic mechanisms that are initiated in the ER have not been

completely elucidated, however strong evidence supports that Ca^{2+} release from ER stores and the subsequent activation of a caspase cascade mediates cell death in response to ER stress [67, 117-119]. Numerous pathways have been implicated in the apoptotic response to cellular stress, including the ISR which results in the induction of CHOP expression. CHOP leads to the depletion of cellular glutathione and an increase in ROS production in the ER, due in part to the transcriptional induction of ERO1α, an ER oxidase [105, 109]. Inhibition of ERO1α reduces the accumulation of ROS during ER stress leading to cytoprotection. A strong transcriptional and translational induction in CHOP expression also occurs in response to hypoxic stress [67, 68]. Moreover, ATF4 and CHOP protein expression were noted in hypoxic areas of human tumor biopsy samples [67]. The knockdown of CHOP by siRNA transfection results in an increase in the cellular resistance to severe hypoxic stress (Blais; unpublished observations). Similar observations have been made in $CHOP^{-/-}$ MEFs in response to ER stress however, $CHOP^{-/-}$ mice do not demonstrate increased sensitivity to lethal doses of tunicamycin [108] suggesting that other proapoptotic pathways are important to the cellular response to stress.

Another crucial activator of ER-induced apoptosis is the Bcl-2 family of proteins. Traditionally thought to be localized to the mitochondrial membrane, a pool of endogenous Bcl-2 has been demonstrated to reside in the ER membrane [120]. Expression of an ER-targeted variant of Bcl-2 (Bcl-cb5) protects cells from ER stress induced apoptosis presumably by maintaining the pro-apoptotic BH3 only proteins, Bax and Bak, in their inactive conformation [121-123]. ER stress-

induces the oligomerization and activation of Bax and Bak, resulting in Ca^{2+} release from the ER and the induction of cell death [121, 122]. Studies using $Bax^{-/-}$ /$Bak^{-/-}$ MEFs have demonstrated exceptional resistance to ER stress [124, 125], implicating Bax and Bak as major regulators of stress induced apoptosis. Interestingly, it has been demonstrated that Bcl-2 is negatively regulated by CHOP [105], suggesting that, indirectly, CHOP may play a role in mediating the activation of a pro-apoptotic caspase cascade. Although the precedence for Bax/Bak mediated apoptosis has been set for ER stress, their importance in mediating hypoxia-induced apoptosis has not been elucidated. Considering the importance of the UPR in the cellular adaptive response to hypoxia and the parallels observed between the two pathways thus far, one might hypothesize similar findings will be observed in response to prolonged periods of hypoxic stress. Whether the increased sensitivity of $PERK^{-/-}$ cells to hypoxic stress might be explained in part due to increased Bax/Bak activation has not been determined, however preliminary data demonstrates that expression of the ER-targeted Bcl-2 (Bcl-cb5) in $PERK^{-/-}$ MEFs partially rescues their overt sensitivity to hypoxic stress (Koumenis, unpublished observations). The use of $Bak^{-/-}$, $Bax^{-/-}$ and $Bax^{-/-}$ /$Bak^{-/-}$ MEFs in future studies could assist in addressing their roles in mediating the apoptotic response to hypoxic stress

The activation of caspase-12, a murine proapoptotic cysteine protease associated with the ER membrane, plays a critical role in ER stress [73, 126, 127] and hypoxic stress-induced apoptosis [67]. In a recent study it was demonstrated that cells which were incapable of eliciting the UPR, undergo apoptosis more readily, exhibit higher levels of activated caspase-12 and -3 and elevated levels of

PARP cleavage in response to hypoxia compared to cells with an intact UPR [67]. Alhough caspase-12 may play a role in the activation of a caspase cascade, alone it is not sufficient to significantly impact the apoptotic response, as caspase-12$^{-/-}$ MEFs demonstrated equal sensitivity to hypoxic stress as their wildtype counterpart [67]. Moreover, with few exceptions, human caspase-12 is presumed functionally inactive due to the presence of a premature stop codon and a loss of function mutation [128], suggesting the described role of caspase-12 in the apoptotic response to ER or hypoxic stress may only be relevant to mouse models. Recent studies have described that the human complements to caspase-12 may be caspases-2/7 [129] and caspase-4 [130]. In one study, the identification of a subpopulation of caspase-2 in ER-enriched microsomal fractions was demonstrated to act as a proximal activator of ER-induced cell death [129]. Findings that ER stress, but not other forms of cellular stress (UV irradiation, etoposide or staurosporine), result in the activation of ER localized caspase-4 suggest it may play a key role in ER stress-induced apoptosis in humans [130]. The roles of caspase-2 and -4 in hypoxia-induced cell death however, have not been determined.

Together, deregulated apoptotic signaling pathways help to explain the increased sensitivity of PERK$^{-/-}$ cells to hypoxic stress as well as reduced tumor growth observed when injected into nude mice [67, 68, 115]. Consistent with this notion, hypoxic regions within PERK$^{-/-}$ tumors demonstrate significant overlap with activated caspase-3 [67], indicating that the growth of PERK$^{-/-}$ tumors is limited, in part, by their overt sensitivity to hypoxic stress.

4.1.2 Translational Induction of Angiogenic Genes

Our recent findings that PERK regulates the translational efficiency of a cohort of pro-angiogenic genes suggests that $PERK^{-/-}$ tumors may experience limited growth and development due not only to their increased apoptotic potential but additionally due to aberrant angiogenic signals resulting in less vascularized tumors. Tumor growth and development require the ability to induce cell proliferation, evade the activation of cell death pathways, and activate angiogenic pathways to recruit blood vessel growth from the surrounding stroma, to increase the delivery of necessary oxygen and nutrients. VEGF is one of the most important angiogenic growth factors in tumor angiogenesis due to its ability to induce endothelial cell proliferation. The importance of VEGF in vascular development was revealed upon deletion of the VEGF gene in mice; an embryonic lethal phenotype due to the complete lack of vascular development [131]. VEGF expression is rapidly and reversibly induced by hypoxic stress [132] due in part to the presence of HRE sequences within its 5' and 3'flanking regions that convey transcriptional activation by HIF1 [133]. VEGF protein expression is further regulated by posttranscriptional mechanisms including increased mRNA stability [35, 36, 134] and increased translational efficiency through IRES mediated translational initiation [37-39].

The translational efficiency of a given mRNA is influenced by both positive and negative regulatory elements within their respective 5' and 3'UTRs. The importance of UTRs in the regulation of posttranscriptional gene expression is exemplified by findings that these regions are often highly conserved and have been proposed to act as sensors of environmental stress [135]. Functional IRES

elements are estimated to occur in as many as 3-5% of all cellular transcripts [47]. The importance of IRES mediated translation is revealed by the observation that mRNAs that contain IRES elements encode proteins that play important roles in cell growth, proliferation, differentiation, and in the regulation of apoptosis; cellular programs that are often usurped by malignant cells [60]. The identification of active IRES elements in several hypoxia responsive genes including HIF-1α [54], BiP [97], ODC [57], and the pro-angiogenic genes, VEGF [37], TIE2 [56] **(Appendix B)**, PDGF [136], and more recently, VCIP (Blais JD, submitted **Chapter 3**), underscores the importance of IRES mediated translational regulation of critical genes involved in signaling pathways that influence the cellular adaptive response to stress. Together with findings that PERK regulates the translational induction of VCIP, at least in part, by IRES-mediated translational initiation during hypoxic stress, and the recent connection between eIF2α phosphorylation and IRES translation of other cellular transcripts implies that perhaps PERK may play a critical role in stress-induced translational regulation. It is largely accepted that phosphorylation of eIF2α results in a global inhibition in translation initiation, how PERK and/or eIF2α phosphorylation mediate the cap-independent IRES activity of particular transcripts has not been elucidated. One explanation may be that these particular IRES elements are better able to compete for available translational machinery and hence ensure their translational priority in times of reduced protein synthesis.

Alternatively, the PERK-dependent expression of auxiliary cellular proteins that may be induced during hypoxia may be required for efficient IRES-mediated

translation of particular IRES-containing transcripts. Several IRES *trans*-acting factors (ITAFs) have been implicated in IRES-mediated translation and, thus far, their requirement appears to be IRES specific [137].

Another explanation includes the possibility that eIF2α is not a unique PERK substrate. In response to ER stress, eIF2α^{S51A} cells failed to induce approximately one-third of the genes that are normally induced by ER stress [92], suggesting PERK is capable of mediating eIF2α independent gene regulation. Recently, the bzip transcription factor Nrf2 was identified as a second PERK substrate [138]. In response to PERK activation, Nrf2 translocates to the nucleus where it binds and activates the transcription of antioxidant genes [139, 140]. Aberrant Nrf2 regulation may help to explain why cells experience increased oxidative stress in the absence of PERK. Recently, the IRES-mediated translational regulation of pro-apoptotic APAF-1 was determined to be negatively regulated by PERK in response to UV-induced cell death (**Appendix C**). Protein synthesis is rapidly inhibited in response to UV-irradiation due to the phosphorylation of eIF2α by PERK [141] and/or GCN2 [142, 143]. However the translational activation of a subset of proteins is required for apoptosis to occur, including a critical regulator of the apoptosome, APAF-1 [144, 145]. The translational efficiency of APAF-1 mRNAs is maintained due to the presence of an active IRES element within its 5'UTR [146, 147]. The ATP-dependent aggregation of APAF-1 results in the formation of the apoptosome and activation of a caspase cascade following cytochrome-c release from the mitochondria. This culminates in the activation of cell death through the sequential activation of caspase-9 and caspase-3. Consistent

with these findings, T-cells from APAF-$1^{-/-}$ mice [83] and APAF-1 deficient K562 and CEM leukemic cells exhibit enhanced resistance to UV-induced apoptosis [144]. In the study from Ungureanu *et al.* (**Appendix C**), $PERK^{-/-}$ MEFs demonstrated an increased sensitivity to UV-irradiation which correlated with a 3-4-fold induction in APAF-1 IRES activity [148]. Expression of a dominant negative catalytically inactive PERK (dn-PERKΔC) or siRNA mediated knock-down of endogenous PERK, resulted in similar findings, suggesting that PERK negatively regulates APAF-1 during UV-irradiation [148]. Expression of $eIF2\alpha^{S51A}$, an unphosphorylatable mutant of eIF2α, however, did not result in increased APAF-1 IRES activity [148]. This suggests that phosphorylation of eIF2α and induction of the ISR is not the only important cellular target subject to PERK regulation and demonstrates the need for continued research in this field to fully elucidate the pathways that are regulated by PERK during cellular stress.

4.1.3 Implications for Tumor Growth

We hypothesized that genes important to the adaptive response to hypoxia would demonstrate a translational advantage during hypoxic stress. Through two independent analyses of data generated by microarray analysis of polysome-associated mRNAs, we have identified two critical adaptive pathways that appear to be regulated by PERK; (i) the ISR arm of the UPR; (ii) the translational induction of a cohort of pro-angiogenic genes. Adaptation and cell viability are influenced by the induction of the ISR during hypoxic stress, as cells with a compromised UPR exhibit increased apoptosis both *in vitro* and *in vivo*. Tumors cells with abrogated PERK activity ($PERK^{-/-}$ MEFs and HT29 colorectal

carcinoma cells expressing dn-PERKΔC) as well as cells with abrogated eIF2α phosphorylation (eIF2α^{S51A}, HT29 colorectal carcinoma cells expressing a COOH-truncated mutant of GADD34) display significantly reduced clonogenic survival compared to their corresponding wildtype cells (Bi 2005 and Koumenis unpublished observations). These findings have been substantiated *in vivo* as transformed cells with an intact PERK-eIF2α signaling pathway form tumors that grow faster and appear better vascularized than tumors derived from cells with abrogated PERK signaling (PERK$^{-/-}$, PERKdnΔC) or eIF2α phosphorylation (eIF2α^{S51A} cells) [67] (Blais JD, submitted **Chapter 3**), suggesting that the differential response of these cells to the tumor microenvironment must play a critical role in tumor development. Using a mouse model of angiogenesis, we discovered that the PERK$^{-/-}$ tumor microenvironment influenced the increased formation of non-functional, atypical vessels and resulted in the formation of fewer functional vessels than the microenvironment provided by the PERK$^{+/+}$ tumors. Taken with findings that PERK influences the translational regulation of a cohort of pro-angiogenic genes suggests that part of the PERK-dependent adaptive response may include the regulation of tumor angiogenesis; a process currently accepted to be largely HIF1 dependent. What has yet to be determined is whether PERK$^{-/-}$ tumors remain small and poorly vascularized due only to their increased sensitivity to hypoxic stress, which arises early in tumor development, or alternatively, due to inappropriate or incomplete angiogenic signaling that results in limited tumor growth and development. Likely, a combination of a decreased apoptotic threshold to ER stress and disregulated promotion of tumor angiogenesis

will help to explain the limited growth of $PERK^{-/-}$ tumors. Preliminary data suggests that over-expression of the ER-targeted Bcl-2 (bcl-cb5) in $PERK^{-/-}$ MEFs partially rescues their heightened sensitivity to hypoxic stress, therefore future mouse models might include comparing the growth and development of k-ras transformed $PERK^{-/-}$ MEFs stably expressing bcl-cb5 to wildtype cells. The observation of limited tumor growth in $PERK^{-/-}$/bcl-cb5 expressing cells would suggest that the impaired adaptive response in $PERK^{-/-}$ cells is mediated, at least in part, by the translational inhibition of pro-angiogenic genes in response to hypoxia.

4.2 Biological Models of Tumorigenesis

4.2.1 Targeting the UPR

Tumor hypoxia presents a substantial problem to therapeutics efforts and is currently viewed as a selective pressure that selects for more aggressive and metastatic tumors. Cumulative evidence supports findings that hypoxia activates the UPR as a mechanism of cellular adaptation and promotes tumor growth and increased resistance to chemotherapeutic agents [149]. However, activation of the UPR in hypoxic tumors may provide a unique opportunity for tumor-specific targeted therapies. One strategy to target the UPR in cancer cells is by developing small molecule inhibitors to target PERK or IRE1. While no specific inhibitors have been identified, screening of small molecule libraries for inhibitors to PERK and IRE1 could prove to be a fruitful avenue for future research. An alternative approach would be to target tumor cells that demonstrate an overactive UPR with pharmacological agents that further induce ER stress. It seems reasonable to

hypothesize that tumor cells that utilize the UPR as an adaptive pathway could be forced past their tolerance level and into apoptosis by subjecting these cells to additional ER stress. This approach could be useful in the treatment of multiple myeloma, a disease that relies heavily on the UPR for continued cell viability (*see below*).

4.2.2 Targeting multiple myeloma by combination therapy

Both normal and malignant plasma cells produce and secrete large amounts of immunoglobulins (Igs). This requires a well-developed ER with abundant molecular chaperones to facilitate proper protein folding and export. Activation of the unfolded protein response (UPR) is vital for maintaining proper folding of Igs in plasma cells [150]. XBP-1 is necessary for plasma cell differentiation [151], and only the spliced XBP-1 species can reconstitute Ig secretion [152]. Furthermore, studies have demonstrated abundant expression of XBP-1 in myelomas suggesting a pivotal role for the UPR in plasma cell malignancies [151]. Agents that target the proteasome, a proteolytic complex responsible for the degradation of ubiquitinated proteins, have demonstrated therapeutic efficacy in the treatment of multiple myeloma [153, 154]. Proteasome inhibitors have been demonstrated to simultaneously induce ER stress and suppress the UPR by inhibiting the activity of IRE1, and hence XBP-1 mRNA splicing, thereby preventing an effective UPR and initiating cell death. Inactivation of PERK signaling may likewise render multiple myeloma (MM) cells sensitive to cell death by compromising the UPR, as activity of the ISR maintains XBP-1 mRNA levels [79]. We would therefore predict that MM cells treated with PERK inhibitors would be hypersensitive to additive treatments with proteasome inhibitors such as MG-132 or PS-341 (Velcade). This

may prove to be a potent therapeutic combination for the treatment of other tumors, such as adenocarcinomas of the prostate, breast and ovary that also originate from secretory cells.

4.2.3 Mouse models of human multiple myeloma

Tassone *et al.* recently developed a novel *in* vivo multiple myeloma (MM) model by engrafting the interleukin 6 (IL-6)-dependent human MM cell line INA-6 into severe combined immunodeficiency (SCID) mice previously given implants of a human fetal bone chip (SCID-hu mice). Both the level of soluble human IL-6 receptor (shuIL-6R) in murine serum and fluorescence imaging of host animals served as sensitive indicators of tumor growth. Due to the presence of the human microenvironment, evaluation of anticancer therapeutics in this model is likely to yield information predictive of their activity in MM patients. Amendment of mouse models of human MM could facilitate the evaluation of novel therapeutics including potential PERK inhibitors alone and in combination with other MM treatment regiments including proteasome inhibitors.

4.3 Conclusions

Control of mRNA translation is an important cellular response to hypoxia. Despite our improved understanding of the regulation of translation and the pathways involved in the promotion of hypoxia tolerance, several questions remain to be addressed by future studies

i) To gain a better understanding of the cellular response to stress, we will need to determine if a predominant mechanism of translational regulation occurs in

response to stress and to what degree the control of mRNA translation during hypoxia might be altered in cancer.

ii) In order to exploit the tumor microenvironment for the discovery of novel anti-cancer therapeutics, the pro-apoptotic signaling pathways that mediate cell death will need to be clearly elucidated.

iii) Likewise, a better understanding of the pathways that help to regulate the angiogenic response could expedite the discovery of novel anti-angiogenic therapies that could contribute to the arrested growth and development of malignancies.

The work presented here reveals the importance of PERK and the ISR in promoting hypoxia tolerance and cytoprotection during periods of hypoxic stress. Furthermore, these studies demonstrate the potential of using microarray technology to assay the cellular proteome to identify key pathways in the cellular response to hypoxia. The potential to exploit the UPR offers a novel approach to target the very stresses that hinder existing anti-tumor treatments.

5. REFERENCES

1. Thomlinson, R.H. and L.H. Gray, *The histological structure of some human lung cancers and the possible implications for radiotherapy.* Br J Cancer, 1955. **9**(4): p. 539-49.
2. Vaupel, P. and M. Hoeckel, *Predictive power of the tumor oxygenation status.* Adv Exp Med Biol, 1999. **471**: p. 533-9.
3. Nordsmark, M., et al., *Prognostic value of tumor oxygenation in 397 head and neck tumors after primary radiation therapy. An international multi-center study.* Radiother Oncol, 2005. **77**(1): p. 18-24.
4. Nordsmark, M., M. Overgaard, and J. Overgaard, *Pretreatment oxygenation predicts radiation response in advanced squamous cell carcinoma of the head and neck.* Radiother Oncol, 1996. **41**(1): p. 31-9.
5. Brizel, D.M., et al., *Oxygenation of head and neck cancer: changes during radiotherapy and impact on treatment outcome.* Radiother Oncol, 1999. **53**(2): p. 113-7.
6. Rofstad, E.K., et al., *Hypoxia-induced treatment failure in advanced squamous cell carcinoma of the uterine cervix is primarily due to hypoxia-induced radiation resistance rather than hypoxia-induced metastasis.* Br J Cancer, 2000. **83**(3): p. 354-9.
7. Tannock, I.F. and D.G. Warr, *Unconventional therapies for cancer: a refuge from the rules of evidence?* Cmaj, 1998. **159**(7): p. 801-2.
8. Durand, R.E., *The influence of microenvironmental factors during cancer therapy.* In Vivo, 1994. **8**(5): p. 691-702.
9. Teicher, B.A., J.S. Lazo, and A.C. Sartorelli, *Classification of antineoplastic agents by their selective toxicities toward oxygenated and hypoxic tumor cells.* Cancer Res, 1981. **41**(1): p. 73-81.
10. Batchelder, R.M., et al., *Oxygen dependence of the cytotoxicity of the enediyne anti-tumour antibiotic esperamicin A1.* Br J Cancer Suppl, 1996. **27**: p. S52-6.
11. Pettersen, E.O. and T. Lindmo, *Inhibition of cell-cycle progression by acute treatment with various degrees of hypoxia: modifications induced by low concentrations of misonidazole present during hypoxia.* Br J Cancer, 1983. **48**(6): p. 809-17.
12. Sciandra, J.J. and J.R. Subjeck, *Heat shock proteins and protection of proliferation and translation in mammalian cells.* Cancer Res, 1984. **44**(11): p. 5188-94.
13. Graeber, T.G., et al., *Hypoxia induces accumulation of p53 protein, but activation of a G1-phase checkpoint by low-oxygen conditions is independent of p53 status.* Mol Cell Biol, 1994. **14**(9): p. 6264-77.

14. Sutherland, R.M., et al., *Resistance to adriamycin in multicellular spheroids.* Int J Radiat Oncol Biol Phys, 1979. **5**(8): p. 1225-30.
15. Comerford, K.M., et al., *Hypoxia-inducible factor-1-dependent regulation of the multidrug resistance (MDR1) gene.* Cancer Res, 2002. **62**(12): p. 3387-94.
16. Graeber, T.G., et al., *Hypoxia-mediated selection of cells with diminished apoptotic potential in solid tumours.* Nature, 1996. **379**(6560): p. 88-91.
17. Reynolds, T.Y., S. Rockwell, and P.M. Glazer, *Genetic instability induced by the tumor microenvironment.* Cancer Res, 1996. **56**(24): p. 5754-7.
18. Hockel, M., et al., *Five-year experience with combined operative and radiotherapeutic treatment of recurrent gynecologic tumors infiltrating the pelvic wall.* Cancer, 1996. **77**(9): p. 1918-33.
19. Hanahan, D. and R.A. Weinberg, *The hallmarks of cancer.* Cell, 2000. **100**(1): p. 57-70.
20. Ivan, M., et al., *HIFalpha targeted for VHL-mediated destruction by proline hydroxylation: implications for O2 sensing.* Science, 2001. **292**(5516): p. 464-8.
21. Jaakkola, P., et al., *Targeting of HIF-alpha to the von Hippel-Lindau ubiquitylation complex by O2-regulated prolyl hydroxylation.* Science, 2001. **292**(5516): p. 468-72.
22. Iyer, N.V., et al., *Cellular and developmental control of O2 homeostasis by hypoxia-inducible factor 1 alpha.* Genes Dev, 1998. **12**(2): p. 149-62.
23. Ryan, H.E., J. Lo, and R.S. Johnson, *HIF-1 alpha is required for solid tumor formation and embryonic vascularization.* Embo J, 1998. **17**(11): p. 3005-15.
24. Jiang, B.H., et al., *Transactivation and inhibitory domains of hypoxia-inducible factor 1alpha. Modulation of transcriptional activity by oxygen tension.* J Biol Chem, 1997. **272**(31): p. 19253-60.
25. Maxwell, P.H., et al., *Hypoxia-inducible factor-1 modulates gene expression in solid tumors and influences both angiogenesis and tumor growth.* Proc Natl Acad Sci U S A, 1997. **94**(15): p. 8104-9.
26. Giatromanolaki, A., et al., *Relation of hypoxia inducible factor 1 alpha and 2 alpha in operable non-small cell lung cancer to angiogenic/molecular profile of tumours and survival.* Br J Cancer, 2001. **85**(6): p. 881-90.
27. Schindl, M., et al., *Overexpression of hypoxia-inducible factor 1alpha is associated with an unfavorable prognosis in lymph node-positive breast cancer.* Clin Cancer Res, 2002. **8**(6): p. 1831-7.

28. Birner, P., et al., *Overexpression of hypoxia-inducible factor 1alpha is a marker for an unfavorable prognosis in early-stage invasive cervical cancer.* Cancer Res, 2000. **60**(17): p. 4693-6.
29. Zagzag, D., et al., *Expression of hypoxia-inducible factor 1alpha in brain tumors: association with angiogenesis, invasion, and progression.* Cancer, 2000. **88**(11): p. 2606-18.
30. Zhong, H., et al., *Increased expression of hypoxia inducible factor-1alpha in rat and human prostate cancer.* Cancer Res, 1998. **58**(23): p. 5280-4.
31. Zhong, H., et al., *Overexpression of hypoxia-inducible factor 1alpha in common human cancers and their metastases.* Cancer Res, 1999. **59**(22): p. 5830-5.
32. Kondo, K., et al., *Inhibition of HIF is necessary for tumor suppression by the von Hippel-Lindau protein.* Cancer Cell, 2002. **1**(3): p. 237-46.
33. Wong, M.P., et al., *Vascular endothelial growth factor is up-regulated in the early pre-malignant stage of colorectal tumour progression.* Int J Cancer, 1999. **81**(6): p. 845-50.
34. Salven, P., P. Heikkila, and H. Joensuu, *Enhanced expression of vascular endothelial growth factor in metastatic melanoma.* Br J Cancer, 1997. **76**(7): p. 930-4.
35. Levy, N.S., et al., *Hypoxic stabilization of vascular endothelial growth factor mRNA by the RNA-binding protein HuR.* J Biol Chem, 1998. **273**(11): p. 6417-23.
36. Dibbens, J.A., et al., *Hypoxic regulation of vascular endothelial growth factor mRNA stability requires the cooperation of multiple RNA elements.* Mol Biol Cell, 1999. **10**(4): p. 907-19.
37. Stein, I., et al., *Translation of vascular endothelial growth factor mRNA by internal ribosome entry: implications for translation under hypoxia.* Mol Cell Biol, 1998. **18**(6): p. 3112-9.
38. Miller, D.L., et al., *The vascular endothelial growth factor mRNA contains an internal ribosome entry site.* FEBS Lett, 1998. **434**(3): p. 417-20.
39. Akiri, G., et al., *Regulation of vascular endothelial growth factor (VEGF) expression is mediated by internal initiation of translation and alternative initiation of transcription.* Oncogene, 1998. **17**(2): p. 227-36.
40. Kraggerud, S.M., J.A. Sandvik, and E.O. Pettersen, *Regulation of protein synthesis in human cells exposed to extreme hypoxia.* Anticancer Res, 1995. **15**(3): p. 683-6.

41. Koritzinsky, M., et al., *Gene expression during acute and prolonged hypoxia is regulated by distinct mechanisms of translational control.* Embo J, 2006. **25**(5): p. 1114-25.
42. Nielsen, F.C. and J. Christiansen, *Posttranscriptional regulation of insulin-like growth factor II mRNA.* Scand J Clin Lab Invest Suppl, 1995. **220**: p. 37-46.
43. Rosenwald, I.B., et al., *Transient inhibition of protein synthesis induces expression of proto-oncogenes and stimulates resting cells to enter the cell cycle.* Cell Prolif, 1995. **28**(12): p. 631-44.
44. Sheets, M.D., et al., *The 3'-untranslated regions of c-mos and cyclin mRNAs stimulate translation by regulating cytoplasmic polyadenylation.* Genes Dev, 1994. **8**(8): p. 926-38.
45. Novoa, I., et al., *Stress-induced gene expression requires programmed recovery from translational repression.* Embo J, 2003. **22**(5): p. 1180-7.
46. Rajasekhar, V.K., et al., *Oncogenic Ras and Akt signaling contribute to glioblastoma formation by differential recruitment of existing mRNAs to polysomes.* Mol Cell, 2003. **12**(4): p. 889-901.
47. Johannes, G. and P. Sarnow, *Cap-independent polysomal association of natural mRNAs encoding c-myc, BiP, and eIF4G conferred by internal ribosome entry sites.* Rna, 1998. **4**(12): p. 1500-13.
48. Ruggero, D. and P.P. Pandolfi, *Does the ribosome translate cancer?* Nat Rev Cancer, 2003. **3**(3): p. 179-92.
49. Clemens, M.J. and U.A. Bommer, *Translational control: the cancer connection.* Int J Biochem Cell Biol, 1999. **31**(1): p. 1-23.
50. Donze, O., et al., *Abrogation of translation initiation factor eIF-2 phosphorylation causes malignant transformation of NIH 3T3 cells.* Embo J, 1995. **14**(15): p. 3828-34.
51. Lazaris-Karatzas, A. and N. Sonenberg, *The mRNA 5' cap-binding protein, eIF-4E, cooperates with v-myc or E1A in the transformation of primary rodent fibroblasts.* Mol Cell Biol, 1992. **12**(3): p. 1234-8.
52. Arsham, A.M., J.J. Howell, and M.C. Simon, *A novel hypoxia-inducible factor-independent hypoxic response regulating mammalian target of rapamycin and its targets.* J Biol Chem, 2003. **278**(32): p. 29655-60.
53. Jang, S.K., et al., *A segment of the 5' nontranslated region of encephalomyocarditis virus RNA directs internal entry of ribosomes during in vitro translation.* J Virol, 1988. **62**(8): p. 2636-43.
54. Lang, K.J., A. Kappel, and G.J. Goodall, *Hypoxia-inducible factor-1alpha mRNA contains an internal ribosome entry site that allows efficient translation during normoxia and hypoxia.* Mol Biol Cell, 2002. **13**(5): p. 1792-801.

55. Macejak, D.G. and P. Sarnow, *Internal initiation of translation mediated by the 5' leader of a cellular mRNA.* Nature, 1991. **353**(6339): p. 90-4.
56. Park, E.H., et al., *Internal translation initiation mediated by the angiogenic factor Tie2.* J Biol Chem, 2005. **280**(22): p. 20945-53.
57. Pyronnet, S., L. Pradayrol, and N. Sonenberg, *A cell cycle-dependent internal ribosome entry site.* Mol Cell, 2000. **5**(4): p. 607-16.
58. Fernandez, J., et al., *Regulation of internal ribosome entry site-mediated translation by eukaryotic initiation factor-2alpha phosphorylation and translation of a small upstream open reading frame.* J Biol Chem, 2002. **277**(3): p. 2050-8.
59. Gerlitz, G., R. Jagus, and O. Elroy-Stein, *Phosphorylation of initiation factor-2 alpha is required for activation of internal translation initiation during cell differentiation.* Eur J Biochem, 2002. **269**(11): p. 2810-9.
60. Holcik, M., N. Sonenberg, and R.G. Korneluk, *Internal ribosome initiation of translation and the control of cell death.* Trends Genet, 2000. **16**(10): p. 469-73.
61. Berry, M.J., et al., *Mechanism of interferon action. Purification and substrate specificities of the double-stranded RNA-dependent protein kinase from untreated and interferon-treated mouse fibroblasts.* J Biol Chem, 1985. **260**(20): p. 11240-7.
62. Cherkasova, V.A. and A.G. Hinnebusch, *Translational control by TOR and TAP42 through dephosphorylation of eIF2alpha kinase GCN2.* Genes Dev, 2003. **17**(7): p. 859-72.
63. Chen, J.J. and I.M. London, *Regulation of protein synthesis by heme-regulated eIF-2 alpha kinase.* Trends Biochem Sci, 1995. **20**(3): p. 105-8.
64. Harding, H.P., Y. Zhang, and D. Ron, *Protein translation and folding are coupled by an endoplasmic-reticulum-resident kinase.* Nature, 1999. **397**(6716): p. 271-4.
65. Frerichs, K.U., et al., *Suppression of protein synthesis in brain during hibernation involves inhibition of protein initiation and elongation.* Proc Natl Acad Sci U S A, 1998. **95**(24): p. 14511-6.
66. Paschen, W. and J. Doutheil, *Disturbance of endoplasmic reticulum functions: a key mechanism underlying cell damage?* Acta Neurochir Suppl, 1999. **73**: p. 1-5.
67. Bi, M., et al., *ER stress-regulated translation increases tolerance to extreme hypoxia and promotes tumor growth.* Embo J, 2005. **24**(19): p. 3470-81.
68. Blais, J.D., et al., *Activating transcription factor 4 is translationally regulated by hypoxic stress.* Mol Cell Biol, 2004. **24**(17): p. 7469-82.

69. Jordan, R., et al., *Replication of a cytopathic strain of bovine viral diarrhea virus activates PERK and induces endoplasmic reticulum stress-mediated apoptosis of MDBK cells.* J Virol, 2002. **76**(19): p. 9588-99.
70. Su, H.L., C.L. Liao, and Y.L. Lin, *Japanese encephalitis virus infection initiates endoplasmic reticulum stress and an unfolded protein response.* J Virol, 2002. **76**(9): p. 4162-71.
71. Gow, A., C.M. Southwood, and R.A. Lazzarini, *Disrupted proteolipid protein trafficking results in oligodendrocyte apoptosis in an animal model of Pelizaeus-Merzbacher disease.* J Cell Biol, 1998. **140**(4): p. 925-34.
72. Gu, F., et al., *Protein-tyrosine phosphatase 1B potentiates IRE1 signaling during endoplasmic reticulum stress.* J Biol Chem, 2004. **279**(48): p. 49689-93.
73. Rao, R.V., et al., *Coupling endoplasmic reticulum stress to the cell death program. Mechanism of caspase activation.* J Biol Chem, 2001. **276**(36): p. 33869-74.
74. Kaneko, M. and Y. Nomura, *ER signaling in unfolded protein response.* Life Sci, 2003. **74**(2-3): p. 199-205.
75. Sargsyan, E., M. Baryshev, and S. Mkrtchian, *The physiological unfolded protein response in the thyroid epithelial cells.* Biochem Biophys Res Commun, 2004. **322**(2): p. 570-6.
76. Zhang, K. and R.J. Kaufman, *Signaling the unfolded protein response from the endoplasmic reticulum.* J Biol Chem, 2004. **279**(25): p. 25935-8.
77. Tirasophon, W., et al., *The endoribonuclease activity of mammalian IRE1 autoregulates its mRNA and is required for the unfolded protein response.* Genes Dev, 2000. **14**(21): p. 2725-36.
78. Iwawaki, T., et al., *Translational control by the ER transmembrane kinase/ribonuclease IRE1 under ER stress.* Nat Cell Biol, 2001. **3**(2): p. 158-64.
79. Calfon, M., et al., *IRE1 couples endoplasmic reticulum load to secretory capacity by processing the XBP-1 mRNA.* Nature, 2002. **415**(6867): p. 92-6.
80. Shen, X., et al., *Complementary signaling pathways regulate the unfolded protein response and are required for C. elegans development.* Cell, 2001. **107**(7): p. 893-903.
81. Yoshida, H., et al., *XBP1 mRNA is induced by ATF6 and spliced by IRE1 in response to ER stress to produce a highly active transcription factor.* Cell, 2001. **107**(7): p. 881-91.

82. Ruegsegger, U., J.H. Leber, and P. Walter, *Block of HAC1 mRNA translation by long-range base pairing is released by cytoplasmic splicing upon induction of the unfolded protein response.* Cell, 2001. **107**(1): p. 103-14.
83. Yoshida, H., et al., *Identification of the cis-acting endoplasmic reticulum stress response element responsible for transcriptional induction of mammalian glucose-regulated proteins. Involvement of basic leucine zipper transcription factors.* J Biol Chem, 1998. **273**(50): p. 33741-9.
84. Yamamoto, K., et al., *Differential contributions of ATF6 and XBP1 to the activation of endoplasmic reticulum stress-responsive cis-acting elements ERSE, UPRE and ERSE-II.* J Biochem (Tokyo), 2004. **136**(3): p. 343-50.
85. Ye, J., et al., *ER stress induces cleavage of membrane-bound ATF6 by the same proteases that process SREBPs.* Mol Cell, 2000. **6**(6): p. 1355-64.
86. Chen, X., J. Shen, and R. Prywes, *The luminal domain of ATF6 senses endoplasmic reticulum (ER) stress and causes translocation of ATF6 from the ER to the Golgi.* J Biol Chem, 2002. **277**(15): p. 13045-52.
87. Harding, H.P., et al., *An integrated stress response regulates amino acid metabolism and resistance to oxidative stress.* Mol Cell, 2003. **11**(3): p. 619-33.
88. Harding, H.P., et al., *Perk is essential for translational regulation and cell survival during the unfolded protein response.* Mol Cell, 2000. **5**(5): p. 897-904.
89. Vattem, K.M. and R.C. Wek, *Reinitiation involving upstream ORFs regulates ATF4 mRNA translation in mammalian cells.* Proc Natl Acad Sci U S A, 2004. **101**(31): p. 11269-74.
90. Lu, P.D., H.P. Harding, and D. Ron, *Translation reinitiation at alternative open reading frames regulates gene expression in an integrated stress response.* J Cell Biol, 2004. **167**(1): p. 27-33.
91. Harding, H.P., et al., *Regulated translation initiation controls stress-induced gene expression in mammalian cells.* Mol Cell, 2000. **6**(5): p. 1099-108.
92. Lu, P.D., et al., *Cytoprotection by pre-emptive conditional phosphorylation of translation initiation factor 2.* Embo J, 2004. **23**(1): p. 169-79.
93. Harding, H.P., et al., *Diabetes mellitus and exocrine pancreatic dysfunction in perk-/- mice reveals a role for translational control in secretory cell survival.* Mol Cell, 2001. 7(6): p. 1153-63.
94. Zhang, P., et al., *The PERK eukaryotic initiation factor 2 alpha kinase is required for the development of the skeletal system, postnatal growth,*

and the function and viability of the pancreas. Mol Cell Biol, 2002. **22**(11): p. 3864-74.
95. Delepine, M., et al., *EIF2AK3, encoding translation initiation factor 2-alpha kinase 3, is mutated in patients with Wolcott-Rallison syndrome.* Nat Genet, 2000. **25**(4): p. 406-9.
96. Novoa, I., et al., *Feedback inhibition of the unfolded protein response by GADD34-mediated dephosphorylation of eIF2alpha.* J Cell Biol, 2001. **153**(5): p. 1011-22.
97. Ma, Y. and L.M. Hendershot, *Delineation of a negative feedback regulatory loop that controls protein translation during endoplasmic reticulum stress.* J Biol Chem, 2003. **278**(37): p. 34864-73.
98. Srivastava, S.P., K.U. Kumar, and R.J. Kaufman, *Phosphorylation of eukaryotic translation initiation factor 2 mediates apoptosis in response to activation of the double-stranded RNA-dependent protein kinase.* J Biol Chem, 1998. **273**(4): p. 2416-23.
99. Haze, K., et al., *Mammalian transcription factor ATF6 is synthesized as a transmembrane protein and activated by proteolysis in response to endoplasmic reticulum stress.* Mol Biol Cell, 1999. **10**(11): p. 3787-99.
100. Shang, J. and M.A. Lehrman, *Discordance of UPR signaling by ATF6 and Ire1p-XBP1 with levels of target transcripts.* Biochem Biophys Res Commun, 2004. **317**(2): p. 390-6.
101. Bertolotti, A., et al., *Dynamic interaction of BiP and ER stress transducers in the unfolded-protein response.* Nat Cell Biol, 2000. **2**(6): p. 326-32.
102. Koong, A.C., et al., *The regulation of GRP78 and messenger RNA levels by hypoxia is modulated by protein kinase C activators and inhibitors.* Radiat Res, 1994. **138**(1 Suppl): p. S60-3.
103. Li, L.J., et al., *Establishment of a Chinese hamster ovary cell line that expresses grp78 antisense transcripts and suppresses A23187 induction of both GRP78 and GRP94.* J Cell Physiol, 1992. **153**(3): p. 575-82.
104. Wang, X.Z., et al., *Identification of novel stress-induced genes downstream of chop.* Embo J, 1998. **17**(13): p. 3619-30.
105. McCullough, K.D., et al., *Gadd153 sensitizes cells to endoplasmic reticulum stress by down-regulating Bcl2 and perturbing the cellular redox state.* Mol Cell Biol, 2001. **21**(4): p. 1249-59.
106. Friedman, A.D., *GADD153/CHOP, a DNA damage-inducible protein, reduced CAAT/enhancer binding protein activities and increased apoptosis in 32D c13 myeloid cells.* Cancer Res, 1996. **56**(14): p. 3250-6.

107. Oyadomari, S., et al., *Targeted disruption of the Chop gene delays endoplasmic reticulum stress-mediated diabetes.* J Clin Invest, 2002. **109**(4): p. 525-32.
108. Zinszner, H., et al., *CHOP is implicated in programmed cell death in response to impaired function of the endoplasmic reticulum.* Genes Dev, 1998. **12**(7): p. 982-95.
109. Marciniak, S.J., et al., *CHOP induces death by promoting protein synthesis and oxidation in the stressed endoplasmic reticulum.* Genes Dev, 2004. **18**(24): p. 3066-77.
110. Gazit, G., J. Lu, and A.S. Lee, *De-regulation of GRP stress protein expression in human breast cancer cell lines.* Breast Cancer Res Treat, 1999. **54**(2): p. 135-46.
111. Cai, J.W., et al., *Induction of glucose regulated proteins during growth of a murine tumor.* J Cell Physiol, 1993. **154**(2): p. 229-37.
112. Fernandez, P.M., et al., *Overexpression of the glucose-regulated stress gene GRP78 in malignant but not benign human breast lesions.* Breast Cancer Res Treat, 2000. **59**(1): p. 15-26.
113. Korabiowska, M., et al., *GADD153 is an independent prognostic factor in melanoma: immunohistochemical and molecular genetic analysis.* Histol Histopathol, 2002. **17**(3): p. 805-11.
114. Jamora, C., G. Dennert, and A.S. Lee, *Inhibition of tumor progression by suppression of stress protein GRP78/BiP induction in fibrosarcoma B/C10ME.* Proc Natl Acad Sci U S A, 1996. **93**(15): p. 7690-4.
115. Koumenis, C., et al., *Regulation of protein synthesis by hypoxia via activation of the endoplasmic reticulum kinase PERK and phosphorylation of the translation initiation factor eIF2alpha.* Mol Cell Biol, 2002. **22**(21): p. 7405-16.
116. Scheuner, D., et al., *Translational control is required for the unfolded protein response and in vivo glucose homeostasis.* Mol Cell, 2001. **7**(6): p. 1165-76.
117. Paschen, W., et al., *Depletion of neuronal endoplasmic reticulum calcium stores by thapsigargin: effect on protein synthesis.* J Neurochem, 1996. **67**(4): p. 1735-43.
118. Ferrari, D., et al., *Endoplasmic reticulum, Bcl-2 and Ca2+ handling in apoptosis.* Cell Calcium, 2002. **32**(5-6): p. 413-20.
119. Kaufman, R.J., et al., *The unfolded protein response in nutrient sensing and differentiation.* Nat Rev Mol Cell Biol, 2002. **3**(6): p. 411-21.
120. Ferri, K.F. and G. Kroemer, *Organelle-specific initiation of cell death pathways.* Nat Cell Biol, 2001. **3**(11): p. E255-63.

121. Zong, W.X., et al., *Bax and Bak can localize to the endoplasmic reticulum to initiate apoptosis.* J Cell Biol, 2003. **162**(1): p. 59-69.
122. Scorrano, L., et al., *BAX and BAK regulation of endoplasmic reticulum Ca2+: a control point for apoptosis.* Science, 2003. **300**(5616): p. 135-9.
123. Nutt, L.K., et al., *Bax and Bak promote apoptosis by modulating endoplasmic reticular and mitochondrial Ca2+ stores.* J Biol Chem, 2002. **277**(11): p. 9219-25.
124. Wang, N.S., et al., *Transient expression of wild-type or mitochondrially targeted Bcl-2 induces apoptosis, whereas transient expression of endoplasmic reticulum-targeted Bcl-2 is protective against Bax-induced cell death.* J Biol Chem, 2001. **276**(47): p. 44117-28.
125. Thomenius, M.J., et al., *Bcl-2 on the endoplasmic reticulum regulates Bax activity by binding to BH3-only proteins.* J Biol Chem, 2003. **278**(8): p. 6243-50.
126. Nakagawa, T., et al., *Caspase-12 mediates endoplasmic-reticulum-specific apoptosis and cytotoxicity by amyloid-beta.* Nature, 2000. **403**(6765): p. 98-103.
127. Yoneda, T., et al., *Activation of caspase-12, an endoplastic reticulum (ER) resident caspase, through tumor necrosis factor receptor-associated factor 2-dependent mechanism in response to the ER stress.* J Biol Chem, 2001. **276**(17): p. 13935-40.
128. Fischer, H., et al., *Human caspase 12 has acquired deleterious mutations.* Biochem Biophys Res Commun, 2002. **293**(2): p. 722-6.
129. Cheung, H.H., et al., *Involvement of caspase-2 and caspase-9 in endoplasmic reticulum stress-induced apoptosis: A role for the IAPs.* Exp Cell Res, 2006.
130. Hitomi, J., et al., *Involvement of caspase-4 in endoplasmic reticulum stress-induced apoptosis and Abeta-induced cell death.* J Cell Biol, 2004. **165**(3): p. 347-56.
131. Carmeliet, P., et al., *Abnormal blood vessel development and lethality in embryos lacking a single VEGF allele.* Nature, 1996. **380**(6573): p. 435-9.
132. Shweiki, D., et al., *Vascular endothelial growth factor induced by hypoxia may mediate hypoxia-initiated angiogenesis.* Nature, 1992. **359**(6398): p. 843-5.
133. Damert, A., et al., *Up-regulation of vascular endothelial growth factor expression in a rat glioma is conferred by two distinct hypoxia-driven mechanisms.* Cancer Res, 1997. **57**(17): p. 3860-4.

134. Levy, A.P., N.S. Levy, and M.A. Goldberg, *Post-transcriptional regulation of vascular endothelial growth factor by hypoxia.* J Biol Chem, 1996. **271**(5): p. 2746-53.
135. Spicher, A., et al., *Highly conserved RNA sequences that are sensors of environmental stress.* Mol Cell Biol, 1998. **18**(12): p. 7371-82.
136. Bernstein, J., et al., *PDGF2/c-sis mRNA leader contains a differentiation-linked internal ribosomal entry site (D-IRES).* J Biol Chem, 1997. **272**(14): p. 9356-62.
137. Martinez-Salas, E., et al., *Functional interactions in internal translation initiation directed by viral and cellular IRES elements.* J Gen Virol, 2001. **82**(Pt 5): p. 973-84.
138. Cullinan, S.B., et al., *Nrf2 is a direct PERK substrate and effector of PERK-dependent cell survival.* Mol Cell Biol, 2003. **23**(20): p. 7198-209.
139. Venugopal, R. and A.K. Jaiswal, *Nrf2 and Nrf1 in association with Jun proteins regulate antioxidant response element-mediated expression and coordinated induction of genes encoding detoxifying enzymes.* Oncogene, 1998. **17**(24): p. 3145-56.
140. Venugopal, R. and A.K. Jaiswal, *Nrf1 and Nrf2 positively and c-Fos and Fra1 negatively regulate the human antioxidant response element-mediated expression of NAD(P)H:quinone oxidoreductase1 gene.* Proc Natl Acad Sci U S A, 1996. **93**(25): p. 14960-5.
141. Wu, S., et al., *Ultraviolet light inhibits translation through activation of the unfolded protein response kinase PERK in the lumen of the endoplasmic reticulum.* J Biol Chem, 2002. **277**(20): p. 18077-83.
142. Deng, J., et al., *Activation of GCN2 in UV-irradiated cells inhibits translation.* Curr Biol, 2002. **12**(15): p. 1279-86.
143. Jiang, H.Y. and R.C. Wek, *GCN2 phosphorylation of eIF2alpha activates NF-kappaB in response to UV irradiation.* Biochem J, 2005. **385**(Pt 2): p. 371-80.
144. Jia, L., et al., *Apaf-1 protein deficiency confers resistance to cytochrome c-dependent apoptosis in human leukemic cells.* Blood, 2001. **98**(2): p. 414-21.
145. Fu, W.N., et al., *Role of DNA methylation in the suppression of Apaf-1 protein in human leukaemia.* Oncogene, 2003. **22**(3): p. 451-5.
146. Coldwell, M.J., et al., *Initiation of Apaf-1 translation by internal ribosome entry.* Oncogene, 2000. **19**(7): p. 899-905.
147. Henis-Korenblit, S., et al., *The caspase-cleaved DAP5 protein supports internal ribosome entry site-mediated translation of death proteins.* Proc Natl Acad Sci U S A, 2002. **99**(8): p. 5400-5.

148. Ungureanu, N.H., et al., *Internal ribosome entry site-mediated translation of Apaf-1, but not XIAP, is regulated during UV-induced cell death.* J Biol Chem, 2006. **281**(22): p. 15155-63.
149. Ranganathan, A.C., et al., *Functional coupling of p38-induced up-regulation of BiP and activation of RNA-dependent protein kinase-like endoplasmic reticulum kinase to drug resistance of dormant carcinoma cells.* Cancer Res, 2006. **66**(3): p. 1702-11.
150. Kwiatkowski, D.J. and B.D. Manning, *Tuberous sclerosis: a GAP at the crossroads of multiple signaling pathways.* Hum Mol Genet, 2005. **14 Spec No. 2**: p. R251-8.
151. Reimold, A.M., et al., *Plasma cell differentiation requires the transcription factor XBP-1.* Nature, 2001. **412**(6844): p. 300-7.
152. Iwakoshi, N.N., A.H. Lee, and L.H. Glimcher, *The X-box binding protein-1 transcription factor is required for plasma cell differentiation and the unfolded protein response.* Immunol Rev, 2003. **194**: p. 29-38.
153. Hideshima, T., P.G. Richardson, and K.C. Anderson, *Targeting proteasome inhibition in hematologic malignancies.* Rev Clin Exp Hematol, 2003. **7**(2): p. 191-204.
154. LeBlanc, R., et al., *Proteasome inhibitor PS-341 inhibits human myeloma cell growth in vivo and prolongs survival in a murine model.* Cancer Res, 2002. **62**(17): p. 4996-5000.

Curriculum Vitae - Jaime Blais (née St. Louis)

Faculty of Medicine - Biochemistry
Human Molecular Genetics
Ottawa Regional Cancer Center
501 Smyth Rd. 3rd Floor – North Wing
Ottawa, ON. K1H 8L6
Phone: (613) 737-7700 x 75403
Email: jblais@ohri.ca

Academic History

2000-Present	**University of Ottawa – Human Molecular Genetics (HMG)** **Ottawa Regional Cancer Centre/Cancer Research Group** Ottawa, Ontario PhD. Candidate *Supervisor*: Dr. John C. Bell
1996-2000	**Carleton University** Graduated with BSc. High Honours Honours Biochemistry *Supervisor*: Dr. Kathleen Gilmour

Awards

2006	**National Cancer Institute of Canada Fellowship (NCIC)** Post-Doctorate support for a three-year fellowship to be help at NYU under the supervision of Dr. David Ron.
2005	**Canadian Granduate Scholarship Doctoral Award (CIHR)** Post-Graduate support in the PhD. Program at the University of Ottawa. Administered through the CIHR Doctoral Research Award competition. Top candidates received a CGS award.
2005	**Ontario Graduate Scholarsip (OGS)** Post-Graduate support in the PhD Program at the University of Ottawa. Award was declined in preference for the CIHR-CGS award.
2005	**University of Ottawa: Excellence Award** Administered from Univeristy of Ottawa to students who have been awarded funding from an external agency.
2004	**Ontario Graduate Scholarship in Science and Technology** Post-Graduate support in the PhD. Program at the University of Ottawa. In colloboration with the Ottawa Regional Cancer Centre. *Fourth Year of Study - PhD*
2003	**Ontario Graduate Scholarship in Science and Technology** Post-Graduate support in the PhD. Program at University of Ottawa In collaboration with the Ottawa Regional Cancer Centre

Third Year of Study-PhD

2003 **University of Ottawa Graduate Admissions Scholarship – Transfer into the PhD program**

2001 **Ontario Graduate Scholarship in Science and Technology**
Post-Graduate support in the MSc. Program at University of Ottawa
In collaboration with the Ottawa Regional Cancer Centre
Second Year of Study-MSc

2000 **University of Ottawa Graduate Admissions Scholarship – MSc Program**

2000 **Ontario Graduate Scholarship in Science and Technology**
Post-Graduate support in the MSc. Program at University of Ottawa
In collaboration with Pro-Virus
First Year of Study-MSc

Educational Programs

2000-2005 **Let's Talk Science Program**
Student Volunteer
Organized by: Dr. B. Vanderhyden

2001-2004 **Rotary Club**
Student Volunteer
Organize a yearly lab tour involving interactive demonstrations with students from the Rotary Club.

Publications

1. **Blais JD**, Edge R, Falls T, Harding HP, Ron D, Addison C, Holcik M, Bell JC. (2006) PERK Signaling is Essential for Cellular Adaptation and Survival during Hypoxic Stress. *Manuscript in preparation.*

2. Nicoleta Hosszu Ungureanu, Mireille Cloutier, Stephen M Lewis, Naomi de Silva, **Jaime D. Blais**, John C. Bell, and Martin Holcik (2006) IRES-mediated translation of Apaf-1, but not XIAP, is regulated during UV-induced cell death. *JCB*: **E.pub** April 4, 2006.

3. **Blais JD**, Filipenko V, Bi M, Harding HP, Ron D, Koumenis C, Wouters BG, Bell JC. (2004) Activating Transcription Factor 4 is Translationally Regulated by Hypoxic Stress. *Mol Cell* Biol: **24** (17): 7469-82

4. Baltzis D, Qu L, **Blais JD**, Bell JC, Papadopoulou S, Koromilas A. (2004) Resistance to VSV Infection requires a functional cross-talk between the eIF2a kinases PERK and PKR. J Virol. **78**(23): 12747-61

5. Park EH, Lee JM, **Blais JD**, Bell JC, Pelletier J. (2005) Internal translation initiation mediated by the angiogenic factor Tie2. J Biol Chem. **280**(22): 20945-53.

6. Bi M, Naczki C, Koritzinsky M, Fels D, **Blais JD**, Harding H, Novoa I, Varia M, Raleigh J,Scheuner D, Kaufman RJ, Bell J, Ron D, Wouters B, Koumenis C. (2005) ER stress-regulated translation increases tolerance to extreme hypoxia and promotes tumor growth. EMBO J. **24**(19):3470-81.

Presentations

1. **Blais JD**, Bell JC. Cellular Adaptation to Hypoxia: An Integrated Stress Response (Invited Talk) Skirball Institute, NYU Medical Centre (July 8th , 2005) New York, NY. USA.

2. **Blais JD**, Filipenko V, Bell JC. Cellular Adaptation to Hypoxia: An Integrated Stress Response (Invited Talk) Bringham's Women's Hospital; Harvard (April 14th, 2005) Boston, MA. USA.

3. **Blais JD**, Filipenko V, Bi M, Harding HP, Ron D, Koumenis C, Wouters BG, Bell JC. Microarray Analysis of Polysomes Reveals ATF4 is Translationally Regulated by Hypoxic Stress. (Invited Talk) Ottawa Hospital Research Institute Research Symposia (Nov 9th, 2004) Ottawa, ON. Canada.

2. **St.Louis, J.D.**, (Poster Discussion Panel) American Association of Cancer Research, San Francisco, California, USA (April 6-10, 2002)

Abstracts

1. **Blais JD**, Edge R, Harding HP, Ron D, Bell JC. Cellular Adaptation to Hypoxia: An Integrated Stress Response (Abstract) Keystone Symposia Meeting: Hypoxia and Development (January 16-21, 2006) Breckenridge, CO.

2. **Blais JD**, Filipenko V, Bi M, Harding HP, Ron D, Koumenis C, Wouters BG, Bell JC. Microarray Analysis of Polysomes Reveals ATF4 is Translationally Regulated by Hypoxic Stress. (Abstract) Oncolytic Viruses as Cancer Therapeutics Conference (March 9th-13th, 2005) Banff, Calgary.

3. **Blais JD**, Filipenko V, Bi M, Harding HP, Ron D, Koumenis C, Wouters BG, Bell JC. Microarray Analysis of Polysomes Reveals ATF4 is Translationally Regulated by Hypoxic Stress. (Abstract) Coldspring Harbour Meeting: Translational Control (Sept 7^{th}-12^{th}, 2004) Long Island NY.

4. Park EH, Lee JM, **Blais JD**, Bell JC, Pelletier J. (2004) Characterization of the 5'UTR of the human TIE-2 mRNA. (Abstract) Coldspring Harbour Meeting: Translational Control (Sept 7^{th}-12^{th}, 2004) Long Island NY.

5. **Blais JD**, Filipenko V, Bi M, Harding HP, Ron D, Koumenis C, Wouters BG, Bell JC. Microarray Analysis of Polysomes Reveals ATF4 is Translationally Regulated by Hypoxic Stress. (Abstract) Keystone Symposia Meeting: Biology of Hypoxia (March 25-28^{th} 2004) Steamboat Springs CO.
6. **Blais J.D**., Wouters BG, Bell JC. Microarray Analysis of Polysomes Reveals ATF4 is Translationally Regulated by Hypoxic Stress. (Abstract) BioNorth Conference and Exhibition (November 2003) Ottawa On.

7. **St.Louis, J.D.,** Wouters, B.G., and Bell, J.C. Differential gene expression under normoxic and hypoxic conditions. (Abstract) American Association of Cancer Research, San Francisco, California, USA (April 6-10, 2002)

8. **St.Louis, J.D.,** and Bell, J.C. Differential gene expression under normoxic and hypoxic conditions. (Abstract) 8^{th} Annual Ottawa Life Sciences National Conference and Exhibition (November 5-7, 2001)

9. Wouters, B.G., Koritzinsky, M., **St.Louis J.,** Sonenberg, N., Bell,J., Chiu, R.K., and Petterson, E.O. Regulation of gene-expression during hypoxia by protein translation. (Abstract) Radiation Research Society Annual Meeting, San Juan, Puerto Rico (April 21-25, 2001)

10. **St.Louis, J.D**., and Gilmour, K.D. Investigating the buffering potential of blood plasma in bullhead catfish (Abstract) Ontario Biology Honours Conference, Peterborough, ON. (March 2000)

Training Courses

1. **Gene Spring** – Intermediate Course for the analysis of expression array data
   Silicon Genetics – Redwood City California (February 20-21, 2002)
   Details: Genome Installation, Experimental Data Import, Types of Normalization, Experimental Parameters, Experimental Interpretations, Creating Gene Lists, Expression Profile Correlations, Statistical Group Comparison, Biochemical Pathways.
2. **Gene Spring** – Advanced Course for the analysis of expression array data
   Silicon Genetics – Redwood City California (February 22, 2002)
   Details: Global Error Models Clustering Techniques Principal Components Analysis, Classification Inspector, Class Predictor, Data Mining, Homology Tables, Scripts.